

# **INTERACTIONS OF 45S5 BIOACTIVE GLASS WITH THE DENTINE-PULP COMPLEX**

by

**EISHA COMAR**

A thesis submitted to the University of Birmingham for the degree of  
DOCTOR OF PHILOSOPHY



**UNIVERSITY OF  
BIRMINGHAM**

Department of Oral Biology  
The School of Dentistry  
College of Medical and Dental Sciences  
University of Birmingham  
September 2013

UNIVERSITY OF  
BIRMINGHAM

**University of Birmingham Research Archive**

**e-theses repository**

This unpublished thesis/dissertation is copyright of the author and/or third parties. The intellectual property rights of the author or third parties in respect of this work are as defined by The Copyright Designs and Patents Act 1988 or as modified by any successor legislation.

Any use made of information contained in this thesis/dissertation must be in accordance with that legislation and must be properly acknowledged. Further distribution or reproduction in any format is prohibited without the permission of the copyright holder.

## ABSTRACT

The bioactive glass, 45S5, has been proposed for the treatment of dentine hypersensitivity due to its ability to physiochemically occlude dentinal tubules. However, its biological effects on the dentine-pulp complex require further elucidation. The aims of this study were to characterise the ionic dissolution products of bioactive glass and observe their effects on both pulpal cells and the dentine extracellular matrix. The ability of bioactive glass to release dentine matrix components (DMCs) in the presence of a physiological fluid, saline, was investigated. The bioactive glass-released DMCs were characterised biochemically and compared with those released by EDTA, a well-established extractant, using high-throughput proteomic techniques. Results revealed the differential solubilisation of a broad range of proteins, including growth factors and other bioactive molecules, many of which had not previously been identified in dentine. *In vitro* analysis of dental pulp cells exposed to DMCs released by bioactive glass in saline solution demonstrated a dose-dependent increase in cell proliferation, whilst the direct effects of the ionic dissolution products of bioactive glass were also stimulatory to OD-21 cells. The positive responses of cells to bioactive glass-released DMCs and its ionic dissolution products indicates exciting potential to harness bioactive approaches therapeutically for dentine tissue repair and regeneration.

## **Acknowledgements**

It has been a privilege to work with Professors Paul Cooper and Tony Smith; I would like to thank them for their guidance and for teaching me so much. I would also like to express my sincere appreciation to Dr Jonathan Earl, of GlaxoSmithKline Consumer Healthcare, for his continued support of my project, in addition to providing valuable opportunities for conferences and collaborations.

I am grateful to Setareh Monajem-Isfahani for teaching me analytical chemistry techniques and for staying behind to supervise me for all those late nights in the GSK labs! I am also thankful to Richard Langford at the Cavendish Laboratories, University of Cambridge, for facilitating the FIB-SEM work. Thank you to Phil Tomson for arranging the multiplex ELISA work, and Upen Patel for his collaborative efforts in obtaining the human dental pulp cells. I am grateful to Gay Smith, Susan Finney and Michelle Holder for their technical assistance and thank you also to the porters for often opening the entire hospital at weekends just for my experiments! I would also like to acknowledge GlaxoSmithKline Consumer Healthcare for their generous financial support, in addition to the BBSRC.

I am very lucky to have met and forged lifetime friendships with students past and present (Jen, Lisa, James, Erum, Joss, Rachel, Pip, Helen, Sonam, Phil, Upen, Martin). Deserved special mentions go to Jonathan Coffee Robinson for making me laugh every single day, Michael for being my junk food provider and image analysis encyclopaedia, and Owen – it has been a [insert appropriate adjective] journey that I will never forget! Thanks also to Pip and Dave for giving me a transient social life during my solitary write-up period!

Outside of the lab, I have been fortunate to have an extensive and devoted support network. My parents have always given me the best of everything and their motivation kept me going throughout. Noush – you have been there from day one, thank you for being the most supportive and understanding friend I could ever wish for. Will, we have come a long way from Adelphi (and Chicago Rock) thank you so much for your relentless support. Lastly - Priy, Marianne, Lou, Symi, Aman, Kal, Neiha - thank you all for being my inspiration.

## CONTENTS

TABLE OF FIGURES.....	viii
LIST OF TABLES .....	xii
LIST OF ABBREVIATIONS .....	xiv

<b>1.0 INTRODUCTION .....</b>	<b>1</b>
1.1 The Dentine-pulp Complex.....	1
1.1.1 Dentine .....	1
1.1.1.1 The Structure of Dentine.....	1
1.1.1.2 The Composition of Dentine .....	2
1.1.1.3 Types of Dentine .....	3
1.1.1.4 Species Differences in Dentine.....	7
1.1.1.5 Permeability of Dentine .....	8
1.1.1.5.1 Dentine Extracellular Matrix Components .....	10
1.1.1.5.1.1 Dentine Extracellular Matrix Molecules .....	11
1.1.1.5.1.2 Growth Factors and Cytokines in Dentine.....	13
1.1.1.5.1.3 Mobilisation and Release of DMCs.....	16
1.1.1.5.1.4 Role of Bioactive DMCs in Tissue Repair and Regeneration .....	18
1.1.2 The Dental Pulp .....	21
1.1.2.1 Cells of the Dental Pulp .....	22
1.1.2.1.1 Odontoblasts.....	22
1.1.2.1.2 Fibroblasts.....	24
1.1.2.1.3 Immunocompetent Cells .....	25
1.1.2.1.4 Dental Pulp Stem Cells.....	25
1.1.2.2 The Pulp Extracellular Matrix .....	26
1.1.3 Vascularisation and Innervation in the Dentine-pulp Complex .....	27
1.2 Dentine Hypersensitivity .....	28
1.2.1 Aetiology of Dentine Hypersensitivity.....	29
1.2.1.1 Lesion Localisation .....	29

1.2.1.2	Lesion Initiation .....	30
1.2.2	Mechanisms of Dentine Hypersensitivity.....	31
1.2.2.1	Odontoblastic Transduction Theory of Dentine Hypersensitivity.....	32
1.2.2.2	Neural Theory of Dentine Hypersensitivity.....	32
1.2.2.3	Hydrodynamic Theory of Dentine Hypersensitivity .....	32
1.2.3	Treatment of Dentine Hypersensitivity .....	35
1.3	Bioactive Glasses .....	36
1.3.1	Structure and Composition of 45S5 Bioactive Glass .....	37
1.3.2	Formation of the HCA Layer .....	38
1.3.3	Ionic Dissolution Products of Bioactive Glass.....	38
1.3.3.1	Ionic Dissolution Products of Bioactive Glass and Osteogenesis.....	39
1.3.3.2	Antibacterial Activity of Bioactive Glass.....	43
1.3.4	Development of Bioactive Glass for an Oral Care Product .....	44
1.3.5	NovaMin®: Evidence of Efficacy in Dentine Hypersensitivity .....	45
1.4	Project Aims.....	47
<b>2.0</b>	<b>MATERIALS AND METHODS .....</b>	<b>49</b>
2.1	Preparation of Dentine Matrix Components.....	49
2.1.1	Dental Tissue Isolation.....	49
2.1.2	Dentine Preparation and Processing.....	49
2.1.3	Materials for Extraction.....	51
2.1.3.1	Bioactive Glass.....	51
2.1.3.2	Saline Solution with Protease Inhibitors .....	51
2.1.4	Extraction of Dentine Matrix Components .....	51
2.1.5	pH Profile of Extraction Supernatants.....	51
2.1.6	Extraction Absorbance Profile .....	52
2.1.7	Dialysis of Extraction Solutions.....	52
2.1.8	Lyophilisation.....	52
2.1.9	Efficiency of Extraction .....	53
2.2	Characterisation of Extracted Dentine Matrix Components.....	53
2.2.1	Quantification of Glycosaminoglycans .....	53

2.2.2	Quantification of Total Non-collagenous Protein .....	53
2.2.3	TGF- $\beta$ 1 ELISA.....	55
2.2.4	One-dimensional Sodium Dodecyl Sulphate Polyacrylamide Gel Electrophoresis (1D-SDS PAGE) Analysis .....	57
2.2.5	Proteomics: In-gel Digestion .....	59
2.2.6	Proteomics: LC-MS/MS Experiment .....	61
2.2.7	Multiplex Sandwich ELISA Array .....	62
2.3	Cell Culture .....	64
2.3.1	Cell Culture Medium and Conditions .....	64
2.3.2	Sterile Phosphate-buffered Saline.....	64
2.3.3	Cell Counting.....	64
2.4	Cell Preparation and Isolation .....	65
2.4.1	Recovery of OD-21 Cells from Cryopreservation .....	65
2.4.2	Maintenance of Cell Cultures .....	65
2.4.3	Cryopreservation of OD-21 Cells .....	65
2.4.4	Human Dental Pulp Isolation.....	66
2.4.5	Explant-derived Dental Pulp Cells .....	66
2.5	Exposure of Cells to Experimental Conditions .....	67
2.5.1	Cellular Exposure to Bioactive Glass and its Dissolution Products .....	67
2.5.1.1	Preparation of Bioactive Glass-conditioned Medium.....	67
2.5.1.2	Exposure of Cells to Bioactive Glass Dissolution Products .....	67
2.5.2	Cellular Exposure to Dentine Matrix Components.....	67
2.5.2.1	Preparation of Dentine Matrix Component-supplemented Media.....	67
2.5.2.2	Exposure of Cells to Dentine Matrix Components.....	68
2.6	Functional Response Assays .....	69
2.6.1	MTT Assay for Metabolic Activity.....	69
2.6.2	Lactate Dehydrogenase Assay for Cytotoxicity .....	70
2.6.3	Assessment of Cell Behaviour Cultured on PET Thinsets.....	71
2.6.4	Cell Counting Using Image Analysis.....	71
2.6.4.1	Validation of Counting Cells Using Image Analysis .....	72
2.7	Histological Techniques .....	74

2.7.1	Histological Processing of Cultures on PET Thinsets.....	74
2.7.2	Histological Sectioning of PET Thinsets.....	74
2.7.3	Hematoxylin and Eosin Staining .....	75
2.7.4	Histomorphometric Analysis .....	76
2.7.4.1	Hunting Curve Analysis.....	76
2.8	Scanning Electron Microscopy (SEM) .....	77
2.8.1	SEM Analysis of Cells Cultured on Porous PET Thinsets .....	77
2.8.2	Dentine Disc Preparation for Scanning Electron Microscopy .....	77
2.8.2.1	Quantitative Analysis of Dentine Disc and PET Thinset SEM Images .....	78
2.8.3	Focussed Ion Beam-scanning Electron Microscopy Analysis of Cells Cultured on Porous PET Membranes .....	78
2.9	Microbiological Techniques.....	79
2.9.1	Bacterial Culture .....	79
2.9.2	Bacterial Turbidity Assay .....	79
2.10	Chemical Analysis of Bioactive Glass Dissolution .....	80
2.10.1	Inductively Coupled Plasma Atomic Emission Spectrometry.....	80
2.10.1.1	ICP-AES Instrument Operational Parameters .....	82
2.10.1.2	Dissolution of Bioactive Glass in Water .....	82
2.10.1.3	Dissolution of Bioactive Glass in DMEM .....	83
2.10.1.4	Bioactive Glass Dissolution in Saline Solution.....	83
2.11	Statistical Analysis .....	84
<b>3.0</b>	<b>RESULTS CHAPTER ONE .....</b>	<b>85</b>
3.1	Biochemical Analysis of Dentine Matrix Components Released by 45S5 Bioactive Glass.....	85
3.1.1	pH of Extraction Supernatants .....	86
3.1.2	Protein Release in Extraction Supernatants.....	87
3.1.3	Percentage Yields of DMCs Recovered.....	89
3.1.4	Characterisation of DMCs.....	90
3.1.4.1	Non-collagenous Protein Content of Extracted DMCs.....	90
3.1.4.2	Glycosaminoglycan Content of DMCs .....	91



3.1.4.3	Quantification of TGF- $\beta$ 1 in Extracted DMCs .....	92
3.1.4.4	One-dimensional Polyacrylamide Gel Electrophoresis Analysis of DMCs ..	93
<b>4.0</b>	<b>RESULTS CHAPTER TWO .....</b>	<b>99</b>
4.1	Elemental Analysis of Bioactive Glass Dissolution .....	99
4.1.1	pH of Supernatants Over 7-day Extraction.....	101
4.1.2	Bioactive Glass Dissolution in Extraction Supernatants .....	103
4.1.2.1	Calcium Ion Concentrations in Extraction Supernatants .....	103
4.1.2.2	Sodium Ion Concentrations in Extraction Supernatants.....	105
4.1.2.3	Phosphorous Ion Concentrations in Extraction Supernatants.....	107
4.1.2.4	Silicon Ion Concentrations in Extraction Supernatants.....	109
4.1.3	Comparison of Bioactive Glass Dissolution in dH <sub>2</sub> O and DMEM.....	111
4.1.3.1	pH of Bioactive Glass-conditioned dH <sub>2</sub> O and DMEM .....	111
4.1.3.2	Calcium Ion Concentrations in Bioactive Glass-conditioned dH <sub>2</sub> O and DMEM.....	112
4.1.3.3	Sodium Ion Concentrations in Bioactive Glass-conditioned dH <sub>2</sub> O and DMEM.....	114
4.1.3.4	Phosphorous Ion Concentrations in Bioactive Glass-conditioned dH <sub>2</sub> O and DMEM.....	116
4.1.3.5	Silicon Ion Concentrations in bioactive glass-conditioned dH <sub>2</sub> O and DMEM. .....	118
<b>5.0</b>	<b>RESULTS CHAPTER THREE .....</b>	<b>120</b>
5.1	Eukaryotic and Prokaryotic Cellular Responses to Bioactive Glass Dissolution Products and Bioactive Glass in Saline-released DMCs.....	120
5.1.1	Eukaryotic Response to Bioactive Glass Dissolution Products .....	121
5.1.1.1	Preliminary Analyses of Eukaryotic Cell Responses to Bioactive Glass Dissolution Products.....	121
5.1.1.2	Lactate Dehydrogenase Release from Cells Exposed to Bioactive Glass- conditioned DMEM .....	127
5.1.1.3	Growth of Cells Exposed to Bioactive Glass-conditioned DMEM .....	128

5.1.1.4	Metabolic Activity in Cells Exposed to Bioactive Glass-conditioned DMEM ..	129
5.1.1.5	Effects of Bioactive Glass Dissolution Products in Calcium-free DMEM...	131
5.1.2	Eukaryotic Cell Responses to DMCs .....	133
5.1.2.1	Preliminary Analyses of Eukaryotic Cellular Response to DMCs .....	133
5.1.2.2	Lactate Dehydrogenase Release from Cells Exposed to DMCs.....	135
5.1.2.3	Growth of Cells Exposed to DMCs.....	136
5.1.2.4	Metabolic Activity in Cells Exposed to DMCs.....	137
5.1.3	Prokaryotic Cell Responses to Bioactive Glass Dissolution Products.....	138
5.1.4	Prokaryotic Cell Responses to DMCs.....	140
<b>6.0</b>	<b>RESULTS CHAPTER FOUR .....</b>	<b>143</b>
6.1	Development of a Cell Culture Model to Study Peritubular Dentinogenesis .....	143
6.1.1	Physical Characterisation of PET Thininserts.....	144
6.1.2	Growth Profile of Cells Cultured on PET Thininserts.....	150
6.1.3	Substrate Comparison of OD-21 Cell Response to DMCs .....	153
6.1.4	Validation of Methods to Assess Cell Number .....	154
6.1.5	Counts for OD-21 Cells Cultured on PET Thininserts Using Image Analysis.....	159
6.1.6	Histomorphometric Analysis of Cells Cultured on PET Thininserts.....	160
6.1.7	Cellular Responses to DMCs .....	163
6.1.8	FIB-SEM Slice-and-view .....	166
<b>7.0</b>	<b>RESULTS CHAPTER FIVE .....</b>	<b>168</b>
7.1	Proteomic Analysis of Dentine Matrix Components .....	168
7.1.1	Proteins Identified in Dentine Matrix Components .....	175
7.1.1.1	Relatively Abundant Proteins Detected in DMCs .....	177
7.1.1.2	Ontological Analysis .....	179
7.1.1.3	Multiplex Sandwich ELISA Analysis .....	192
<b>8.0</b>	<b>DISCUSSION .....</b>	<b>195</b>
8.1	Bioactive Glass Dissolution .....	196

8.2	Effects of the Ionic Dissolution Products of Bioactive Glass on Dental Pulp Cells .	200
8.3	Antibacterial Activity of Bioactive Glass Ionic Dissolution Products .....	203
8.4	Effects of Bioactive Glass-released DMCs on <i>Streptococcus mutans</i> .....	204
8.5	Characterisation of Bioactive Glass in Saline-released DMCs .....	206
8.6	Proteomic Analysis of Dentine Matrix Components .....	208
8.7	Mechanisms for DMC Release .....	214
8.8	Effects of Bioactive Glass in Saline-released DMCs on Pulpal Cells .....	216
8.9	Characterisation of a Cell Culture Model to Study Peritubular Dentinogenesis....	217
<b>9.0</b>	<b>CONCLUSIONS .....</b>	<b>222</b>
<b>10.0</b>	<b>FUTURE WORK .....</b>	<b>224</b>
	<b>REFERENCES .....</b>	<b>226</b>

## TABLE OF FIGURES

### CHAPTER ONE: INTRODUCTION

<b>Figure 1.1</b> Histological section of the dentine-pulp complex. ....	2
<b>Figure 1.2</b> SEM micrograph of the fracture surface of human coronal dentine. ....	4
<b>Figure 1.3</b> Schematic representation of odontoblast dual-level of secretion. ....	6
<b>Figure 1.4</b> Micrograph of a carious lesion in cross-sectioned dentine. ....	11
<b>Figure 1.5</b> Schematic diagram of the formation of reactionary and reparative dentine .....	21
<b>Figure 1.6</b> Illustration of the hydrodynamic theory of dentine hypersensitivity. ....	34
<b>Figure 1.7</b> Schematic diagram of 45S5 bioactive glass. ....	37
<b>Figure 1.8</b> Overview of the biological impact of the ionic dissolution products of bioactive glass. ....	42
<b>Figure 1.9</b> Scanning electron micrographs of dentine. ....	46

### CHAPTER TWO: MATERIALS AND METHODS

<b>Figure 2.1</b> Photographic images of the preparation process for the extraction of DMCs. ....	50
<b>Figure 2.2</b> Representative calibration curve using chondroitin-4-sulphate as a standard. ....	54
<b>Figure 2.3</b> Representative calibration curve using a range of concentrations of NCPs. ....	55
<b>Figure 2.4</b> Representative calibration curve using TGF- $\beta$ 1 recombinant kit standards. ....	57
<b>Figure 2.5</b> Standard curve used to determine the MW of unknown proteins by SDS-PAGE. ....	59
<b>Figure 2.6</b> Schematic diagram to illustrate delivery of DMCs to cells via PET Thinerts. ....	69
<b>Figure 2.7</b> Images illustrating automated method of cell counting using Fiji. ....	73
<b>Figure 2.8</b> Representative calibration curve used for Inductively Coupled Plasma Analysis. ....	83

### CHAPTER THREE: RESULTS

<b>Figure 3.1</b> pH profiles of extraction supernatants throughout the 7-day extraction period. ....	87
<b>Figure 3.2</b> Absorbance profiles of extraction supernatants throughout extraction. ....	89
<b>Figure 3.3</b> Non-collagenous protein content in extracted DMCs. ....	91

<b>Figure 3.4</b> Glycosaminoglycan content in extracted DMCs. ....	92
<b>Figure 3.5</b> TGF- $\beta$ 1 content in lyophilised extracts.....	93
<b>Figure 3.6</b> Photographic image of a representative silver-stained SDS-PAGE gel. ....	95
<b>Figure 3.7</b> Automatic band detection of SDS-PAGE gel by GelAnalyzer software. ....	97

## CHAPTER FOUR: RESULTS

<b>Figure 4.1</b> Schematic diagram illustrating the extraction process.....	100
<b>Figure 4.2</b> pH profile of extraction supernatants, throughout a 7-day extraction period....	102
<b>Figure 4.3</b> Concentration of calcium ions detected in daily extraction supernatants.....	104
<b>Figure 4.4</b> Concentration of sodium ions detected in daily extraction supernatants .....	106
<b>Figure 4.5</b> Concentration of phosphorous ions detected in daily extraction supernatants . .....	108
<b>Figure 4.6</b> Concentration of silicon ions detected in daily extraction supernatants. ....	110
<b>Figure 4.7</b> Concentration of calcium ions detected by ICP-AES.....	113
<b>Figure 4.8</b> Concentration of sodium ions, detected by ICP-AES. ....	115
<b>Figure 4.9</b> Concentration of phosphorous ions, detected by ICP-AES. ....	117
<b>Figure 4.10</b> Concentration of silicon ions, detected by ICP-AES. ....	119

## CHAPTER FIVE: RESULTS

<b>Figure 5.1</b> Metabolic activity of cells following exposure to bioactive glass-conditioned DMEM.....	123
<b>Figure 5.2</b> Images of OD-21 cells exposed to bioactive glass-conditioned DMEM.....	125
<b>Figure 5.3</b> Images of human dental pulp cells exposed to bioactive glass-conditioned DMEM. .....	126
<b>Figure 5.4</b> Mean LDH release from OD-21 cultures at 48 hours .....	128
<b>Figure 5.5</b> OD-21 cell numbers following exposure to bioactive glass-conditioned DMEM.	129
<b>Figure 5.6</b> Metabolic activity per cell for OD-21 cells, following a 48 hour exposure to increasing concentrations of bioactive glass-conditioned DMEM.....	130
<b>Figure 5.7</b> OD-21 cell response to bioactive glass-conditioned calcium-free DMEM.....	132

<b>Figure 5.8</b> Metabolic activity of OD-21 cells exposed to DMCs. ....	134
<b>Figure 5.9</b> LDH release from OD-21 cells following exposure to DMCs. ....	136
<b>Figure 5.10</b> OD-21 cell numbers following exposure to bioactive glass-released DMCs.....	137
<b>Figure 5.11</b> Metabolic activity per cell of OD-21 cells exposed to DMCs. ....	138
<b>Figure 5.12</b> Effects of bioactive glass-conditioned PBS on <i>S. mutans</i> growth. ....	140
<b>Figure 5.13</b> Effects of EDTA-released DMCs on <i>S. mutans</i> growth. ....	141
<b>Figure 5.14</b> Effects of bioactive glass and saline-released DMCs on <i>S. mutans</i> . ....	142

## CHAPTER SIX: RESULTS

<b>Figure 6.1</b> Representative SEM image of etched dentine surface. ....	145
<b>Figure 6.2</b> Representative SEM image of PET Thinserts.....	146
<b>Figure 6.3</b> Comparison of the feret diameters of dentine tubules using manual and semi-automated measuring techniques. ....	148
<b>Figure 6.4</b> Comparison of feret diameters of dentine tubules and PET Thinsert pores. ....	149
<b>Figure 6.5</b> Comparison of the numbers of tubules or pores per unit area. ....	150
<b>Figure 6.6</b> Growth profiles of cells cultured on PET Thinserts and 12-well microplates. ....	152
<b>Figure 6.7</b> Comparison of the metabolic activities of OD-21 cells cultured on standard 12-well microplates and PET Thinserts surfaces in response to bioactive glass-released DMCs. ....	154
<b>Figure 6.8</b> Validation of the MTT assay to assess cell numbers. ....	157
<b>Figure 6.9</b> Validation of the use of ImageJ to assess cell numbers.....	158
<b>Figure 6.10</b> Comparison of cell numbers generated from an MTT assay standard curve with cell numbers determined by image analysis. ....	159
<b>Figure 6.11</b> Cell numbers, determined by image analysis, of OD-21s cultured in the presence and absence (control) of DMCs. ....	160
<b>Figure 6.12</b> Hunting Curve analysis to determine the number of histological sections required to gain a representative number of cells per unit area.....	161
<b>Figure 6.13</b> Representative histological cross-section of OD-21 cells cultured on PET Thinserts. ....	162

<b>Figure 6.14</b> Cell numbers per unit area of OD-21 cells cultured on PET Thinserts in response to DMCs. ....	164
<b>Figure 6.15</b> Numbers of cellular extensions per unit area of cells cultured on PET Thinserts in the presence and absence (control) of DMCs. ....	165
<b>Figure 6.16</b> Sequential FIB-SEM process used to observe OD-21 cells cultured on PET Thinserts in cross-section. ....	167

## CHAPTER SEVEN: RESULTS

<b>Figure 7.1</b> Venn diagram showing number of proteins detected in DMCs released by EDTA, saline solution and 10 mg/mL bioactive glass in saline solution.....	176
-------------------------------------------------------------------------------------------------------------------------------------------------------------------	-----

## LIST OF TABLES

### CHAPTER ONE: INTRODUCTION

<b>Table 1.1</b>	Gene families up-regulated by the ionic dissolution products of bioactive glass...	40
------------------	------------------------------------------------------------------------------------	----

### CHAPTER TWO: MATERIALS AND METHODS

<b>Table 2.1</b>	Proteins analysed by Quantibody human multiplex sandwich ELISA array. ....	63
<b>Table 2.2</b>	Absorption wavelengths used during ICP-AES. ....	81
<b>Table 2.3</b>	Instrument operational parameters used for inductively coupled plasma atomic emission spectrometry. ....	82

### CHAPTER THREE: RESULTS

<b>Table 3.1</b>	Percentage yields of DMCs recovered.....	90
<b>Table 3.2</b>	Summary of analysis of SDS-PAGE gel by GelAnalyzer software. ....	98

### CHAPTER FOUR: RESULTS

<b>Table 4.1</b>	pH of bioactive glass-conditioned dH <sub>2</sub> O and DMEM. ....	112
------------------	--------------------------------------------------------------------	-----

### CHAPTER FIVE: RESULTS

<b>Table 5.1</b>	pH values of bioactive glass-conditioned PBS. ....	139
------------------	----------------------------------------------------	-----

### CHAPTER FOUR: RESULTS

<b>Table 7.1</b>	Ten most abundant proteins detected in DMCs. ....	178
<b>Table 7.2</b>	Cellular components associated with saline-released DMCs. ....	180
<b>Table 7.3</b>	Cellular components associated with bioactive glass in saline -released DMCs. .	180
<b>Table 7.4</b>	Cellular components associated with EDTA-released DMCs. ....	181
<b>Table 7.5</b>	Biological processes associated with saline-released DMCs.....	184



<b>Table 7.6</b> Biological processes associated with bioactive glass in saline solution-released DMCs.....	185
<b>Table 7.7</b> Biological processes associated with EDTA-released DMCs.....	186
<b>Table 7.8</b> Molecular functions associated with saline-released DMCs.....	189
<b>Table 7.9</b> Molecular functions associated with bioactive glass in saline solution-released DMCs.....	190
<b>Table 7.10</b> Molecular functions associated with EDTA-released DMCs. ....	191
<b>Table 7.11</b> Multiplex ELISA analysis of bioactive glass and EDTA-released DMCs.....	194

## LIST OF ABBREVIATIONS

<b>1D-SDS PAGE</b>	One dimensional sodium dodecyl sulphate polyacrylamide gel electrophoresis
<b>ACTN1</b>	Actinin alpha 1
<b>ADF</b>	Adrenomedullin
<b>AGT</b>	Angiotensin
<b>AHSG</b>	$\alpha$ -2-Heremans Schmid-glycoprotein
<b>ATP5A1</b>	ATP synthase subunit alpha
<b>ATP5B</b>	ATP synthase, H <sup>+</sup> transporting, mitochondrial F1 complex, beta polypeptide
<b>BMP</b>	Bone morphogenetic protein
<b>Ca</b>	Calcium
<b>Ca(OH)<sub>2</sub></b>	Calcium hydroxide
<b>CaO</b>	Calcium oxide
<b>DCD</b>	Demcadin
<b>DEFA1</b>	Defensin alpha 1
<b>DEJ</b>	Dentine-enamel junction
<b>DGP</b>	Dentine glycoprotein
<b>dH<sub>2</sub>O</b>	Distilled water
<b>DMCs</b>	Dentine matrix components
<b>DMEM</b>	Dulbecco's modified minimum essential media
<b>DMMB</b>	Dimethylmethylene blue
<b>DPP</b>	Dentine phosphoprotein
<b>DPSCs</b>	Dental pulp stem cells
<b>DPT</b>	Dermatopontin

<b>DSP</b>	Dentine sialoprotein
<b>EDTA</b>	Ethylenediaminetetraacetic acid
<b>EGF</b>	Epidermal growth factor
<b>ELISA</b>	Enzyme-linked immunoabsorbent assay
<b>FCS</b>	Foetal calf serum
<b>FGF</b>	Fibroblast growth factor
<b>FIB-SEM</b>	Focussed ion beam scanning electron microscopy
<b>GAGs</b>	Glycosaminoglycans
<b>GM-CSF</b>	Granulocyte-macrophage colony-stimulating factor
<b>H&amp;E</b>	Hematoxylin and eosin
<b>HCA</b>	Carbonated hydroxyapatite
<b>HIST1H2BK</b>	Histone cluster 1 H2BK
<b>ICP-AES</b>	Inductively coupled plasma atomic emission spectrometry
<b>IDA</b>	Industrial denatured alcohol
<b>IDE</b>	Inner dental epithelium
<b>IGF</b>	Insulin-like growth factor
<b>IL</b>	Interleukins
<b>ITD</b>	Intertubular dentine
<b>kV</b>	Kilovolt
<b>LC-MS/MS</b>	Liquid chromatography-tandem mass spectrometry
<b>LDH</b>	Lactate dehydrogenase
<b>LGR1</b>	Leucine-rich alpha-2 glycoprotein
<b>LYZ</b>	Lysozyme renal amyloidosis
<b>M-CSF</b>	Macrophage colony-stimulating factor

<b>MMPs</b>	Matrix metalloproteinases
<b>MSN</b>	Moesin
<b>MTA</b>	Mineral trioxide aggregate
<b>MTT</b>	3-(4,5-dimethylthiazol-2-yl)-2,5-diphenyltetrazolium bromide
<b>Na</b>	Sodium
<b>Na<sub>2</sub>O</b>	Sodium oxide
<b>NCPs</b>	Non-collagenous proteins
<b>NGF</b>	Nerve growth factor
<b>OD-21s</b>	Murine-derived dental pulp cell line
<b>P</b>	Phosphorous
<b>P<sub>2</sub>O<sub>5</sub></b>	Phosphorus pentoxide
<b>PBS</b>	Phosphate buffered saline
<b>PDGF</b>	Platelet-derived growth factor
<b>PDGF</b>	Platelet-derived growth factor
<b>PET</b>	Polyethylene terephthalate
<b>PTD</b>	Peritubular dentine
<b>RGD</b>	Arginine-glycine-aspartic acid tripeptide
<b>S100A8</b>	S100 calcium binding protein A8
<b>SCAP</b>	Stem cells from the apical papilla
<b>SEM</b>	Scanning electron microscopy
<b>SHED</b>	Stem cells from human exfoliated deciduous teeth
<b>Si</b>	Silicon
<b>SIBLINGs</b>	Small Integrin-Binding Ligand N-linked Glycoproteins
<b>SiO<sub>2</sub></b>	Silicon dioxide

<b>SLRPs</b>	Small leucine-rich proteoglycans
<b>TGFB1</b>	TGF- $\beta$ 1 induced protein ig-h3
<b>TGF-<math>\beta</math></b>	Transforming growth factor-beta
<b>TIMP3</b>	Metalloproteinase inhibitor 3
<b>TNF-<math>\alpha</math></b>	Tumour necrosis factor-alpha
<b>VCL</b>	Vinculin
<b>VEGF</b>	Vascular endothelial growth factor
<b>WMTA</b>	White mineral trioxide aggregate

## **1.0 INTRODUCTION**

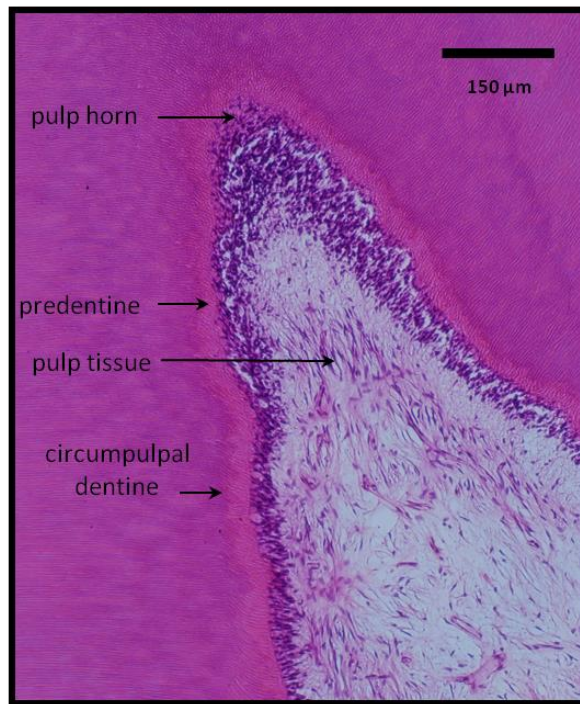
### **1.1 The Dentine-pulp Complex**

The dentine-pulp complex is comprised of the vital soft pulp tissue encased within the hard mineralised dentine (see Figure 1.1). The pulp and the dentine are considered as a complex, coupled developmentally and functionally. Although there is an abundance of both embryological and clinical evidence that both tissues function as an integrated unit, the term 'dentine-pulp complex' has also been challenged as an oversimplification by Goldberg and Lasfargues (1995). These authors do not dispute the common ancestry and relationship between the dentine and pulp, but believe they are very distinct tissues with their own properties. Nonetheless, it is clear that there is an intimate relationship between the dentine and pulp functionally.

#### **1.1.1 Dentine**

##### **1.1.1.1 The Structure of Dentine**

Dentine is a mineralised tissue, which constitutes the majority of the tooth and is phylogenetically believed to be derived from bone (Linde and Goldberg, 1993). It is characterised by densely packed dentinal tubules that traverse its thickness, containing cytoplasmic extensions of the formative cells for dentine – the odontoblasts. Odontoblast cell bodies are aligned against a layer of an unmineralised matrix, predentine, forming the peripheral boundary of the dental pulp (see Figure 1.1) (Linde, 1984).



**Figure 1.1 Histological section of the dentine-pulp complex.**

Image displays the pulp horn of a human third molar, stained with hematoxylin and eosin (H&E). The scale bar represents 150 μm. Image courtesy of Susan Finney and Phillip Tomson (personal communication).

#### **1.1.1.2 The Composition of Dentine**

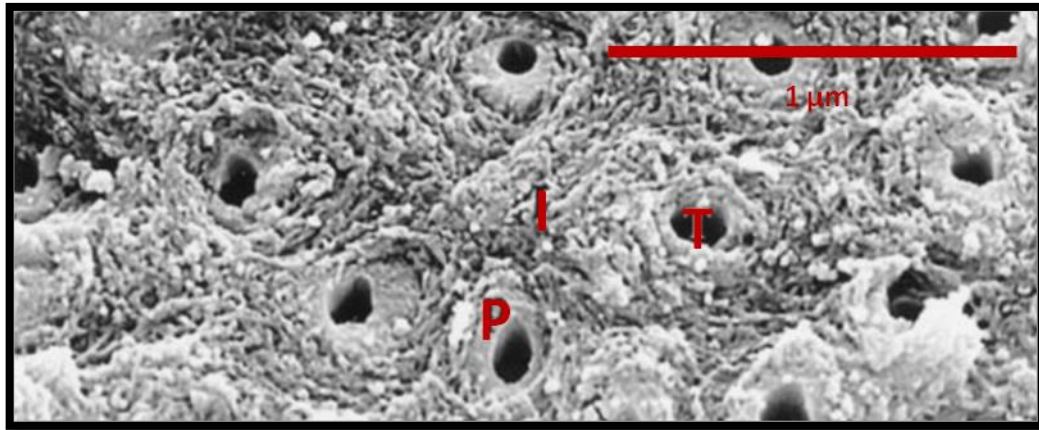
Dentine is comprised of water, inorganic and organic content. The inorganic phase is largely hydroxypatite, whereas the organic matrix comprises of collagen, non-collagenous proteins, proteoglycans, glycosaminoglycans, lipids and citrate (Linde, 1984). The inorganic mineral phase constitutes approximately 70 % by weight, whilst the organic component and water form 18 % and 12 %, respectively. The values by volume differ from those by weight due to the variation in specific gravity of the three components. Therefore, measuring dentine by

volume yields values of 50 % for inorganic content, 30 % for the organic phase and 20 % for water (Linde and Goldberg, 1993).

#### **1.1.1.3 Types of Dentine**

The structure of dentine is complex, involving several types of morphologically different tissue, which relate to the activity of odontoblasts throughout their life cycle. *Primary dentine* is rapidly produced at a rate of approximately 4 µm per day during development for tooth formation, and constitutes the majority of the dentine mass (Schour and Hoffman, 1939). The outermost layer of primary dentine, situated immediately beneath the enamel, is known as *mantle dentine* and is formed first by polarising relatively immature odontoblasts, which are yet to develop junctional complexes and have multiple processes (Linde and Goldberg, 1993). The remainder of primary dentine is termed *circumpulpal dentine* and is subdivided into *intertubular dentine* and *peritubular dentine* (Figure 1.2).





**Figure 1.2 SEM micrograph of the fracture surface of human coronal dentine.**

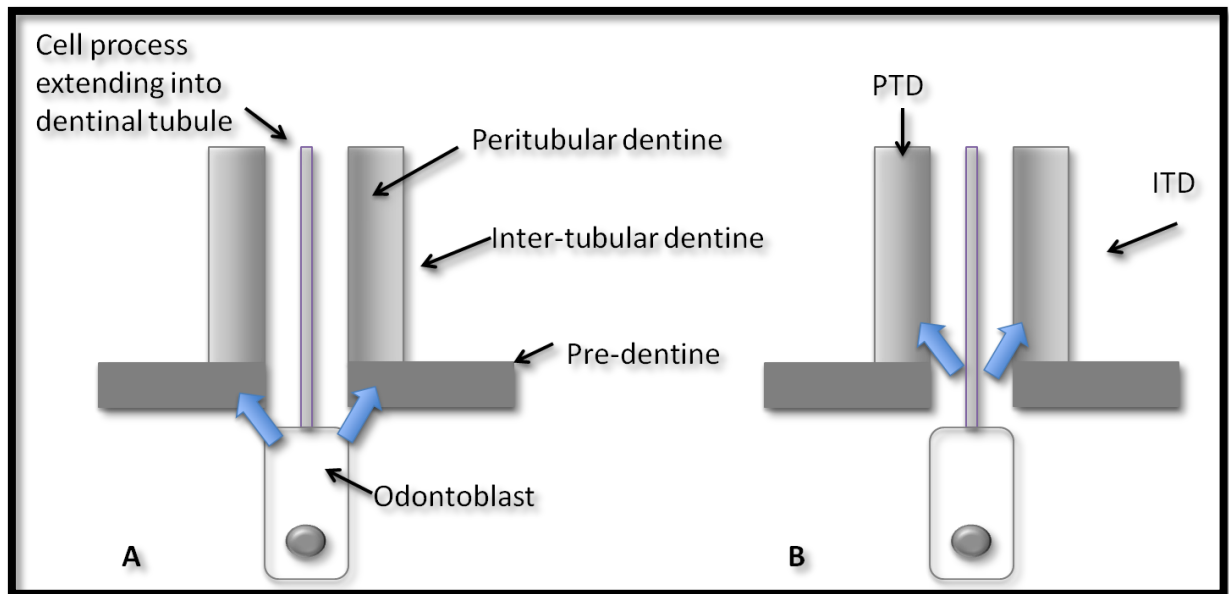
The dentinal tubules (T) are surrounded by peritubular dentine (P) and the intermediate space occupied by intertubular dentine (I). (*Image adapted from Weiner et al., 1999*).

In most species, peritubular dentine is located immediately around the tubular lumen and is sometimes referred to as *intratubular dentine*, perhaps reflecting its continuing deposition throughout life and gradual occlusion of the tubules. In mantle dentine, peritubular dentine is largely absent due to incomplete terminal differentiation of the odontoblasts, whereas a gradual thickening occurs with increasing distance from the dentine-enamel junction (DEJ). As the peritubular dentine thickens, the density of tubules per unit area also increases (Pashley, 1996; Zaslansky *et al.*, 2006).

In human teeth, peritubular dentine is clearly demarcated from intertubular dentine morphologically. It forms a hypermineralised sheath around the dentinal tubules and is devoid of collagen. Peritubular dentine contains magnesium and carbonate which account for its high solubility, and the absence of fibrous structures in peritubular dentine makes it a challenge to study after demineralisation (Linde and Goldberg, 1993). In contrast,

intertubular dentine (which is the predominant secretory product of odontoblasts) is comprised of 90 % type I collagen (Goldberg *et al.*, 2011). Earlier studies have reported differences in mineral between intertubular and peritubular dentine (Schroeder and Frank, 1985), whereas more recent investigations have demonstrated that the nature, organisation and size of the mineral phase between both types of dentine exhibit minimal differences (Weiner *et al.*, 1999; Magne *et al.*, 2002; Gotliv and Veis, 2007).

Peritubular dentine formation is a continuing process throughout life, however, the mechanisms responsible for its secretion and deposition remain unclear. Linde and Goldberg (1993) proposed that the reason for this being poorly understood is that a good experimental model to study peritubular dentine formation has yet to be identified. However, Linde hypothesised that dual-levels of secretion from the cell take place (see Figure 1.3) (Linde, 1989). Indeed, it was suggested that secretion from the odontoblast body gives rise to the unmineralised predentine and subsequently intertubular dentine, while secretion from the odontoblast process generates the more highly mineralised peritubular dentine (Linde, 1989). This perhaps also provides an explanation for the continuing increase in thickness of peritubular dentine throughout life.



**Figure 1.3 Schematic representation of odontoblast dual-level of secretion.**

**A)** Secretion by the odontoblast cell body of the main structural components (i.e. collagen and proteoglycans) into predentine, ultimately leading to the formation of intertubular dentine (ITD). **B)** Secretion by the odontoblasts cell process of matrix components at the mineralisation front, giving rise to the peritubular dentine (PTD).

Primary dentine is continuously formed during tooth development until two landmark events occur: the tooth is deemed functional and the root apex is closed, reflecting the completion of crown and root formation in the tooth (Linde and Goldberg, 1993). Odontoblasts subsequently form *secondary dentine* on the pulpal aspect of the primary dentine, at a relatively reduced rate of approximately 0.4  $\mu\text{m}$  per day throughout the life of the tooth. An irregularity in the smooth S-shaped structure has been reported in coronal secondary dentine, and it is thought that this may be a result of the transition from primary to secondary dentine (Linde, 1984). Understanding of the secretory activity of odontoblasts is currently relatively limited, but recent data following the transition between primary and

secondary dentinogenesis have been informative and have enabled elucidation of changes that occur in the odontoblast transcriptome (Simon *et al.*, 2009). The amount of secondary dentine present within a tooth is also thought to be an indicator of age and consequently, has forensic application (Paewinsky *et al.*, 2005).

In response to stimuli, often involving trauma or disease, *tertiary dentine* is formed and may be classified as either *reactionary* or *reparative dentine* (see Section 1.1.1.5.1.4). Triggers for tertiary dentine may include chemical irritants, trauma, caries, restorative procedures and attrition. The morphology of tertiary dentine can be distinct from physiological dentine and may be irregular with cell inclusions (Linde and Goldberg, 1993).

Between the mineralised tissue and the dental pulp on the formative surface lies a layer of dentine known as *predentine*. This is an unmineralised dentine matrix, which is largely comprised of collagen and this will eventually be mineralised to form mature dentine. Predentine is present throughout the lifetime of the tooth, although it is constantly replaced (Linde, 1984). The continuous secretion of predentine by the odontoblasts occurs concomitantly with the transformation of older predentine into mineralised dentine, resulting in a relatively constant thickness of predentine (Weinstock and Leblond, 1973).

#### **1.1.1.4 Species Differences in Dentine**

Structural and chemical differences in dentine exist between species. Studies have mainly focussed on human, bovine and rat dentine, however, equine and porcine dentine have also been examined and it is clear from this work that significant inter-species differences exist (Muylle *et al.*, 2000). These differences include the structure, formation and amount of

peritubular matrix in addition to the thickness of root mantle dentine. (Tjäderhane *et al.*, 2009).

There appear to be two definitive groups in dentine structure, based on tissue morphology and protein composition. As rodents have continually erupting teeth, they form a distinct group from bovine, porcine and human dentine, where primary dentinogenesis occurs within a more defined period (Linde and Goldberg, 1993). Rodent teeth lack peritubular dentine, perhaps suggesting rather different secretory mechanisms by the odontoblasts. This also highlights that caution must be exercised when extrapolating data from one species to another.

#### **1.1.1.5 Permeability of Dentine**

Dentine has a permeable structure due to the presence of dentinal tubules, which are approximately 1-3  $\mu\text{m}$  in diameter (Lenzi *et al.*, 2013). This feature allows the diffusion of bacterial metabolic and tissue degradation products during dental caries, which can elicit cellular responses within the pulp. The location of dentinal tubules and the age of the tooth determine the lumen size, and their density varies according to the depth of the dentine and proximity to the pulp. Indeed, near the pulp dentine can contain 65000 tubules per  $\text{mm}^2$  in contrast to the dentine-enamel junction, where 15000 tubules per  $\text{mm}^2$  have been reported (Dourda *et al.*, 1994; Fosse *et al.*, 1992; Garberoglio and Bränström, 1976). Investigations comparing the diameters and numbers of dentine tubules in human and bovine dentines indicated that there were no significant differences between the two species, suggesting that bovine dentine provides a suitable model for humans (Schilke *et al.*, 2000). Tubules are cone-shaped with the largest diameter at the pulp chamber reflecting the time for

peritubular dentine deposition along the tubule (Hargreaves and Goodis, 2002). The permeability of dentine at any depth is considerably lower than would be predicted from the tubular density and diameters (Koutsi *et al.*, 1994), due to the presence of intratubular material, such as collagen fibrils (Pashley *et al.*, 1996).

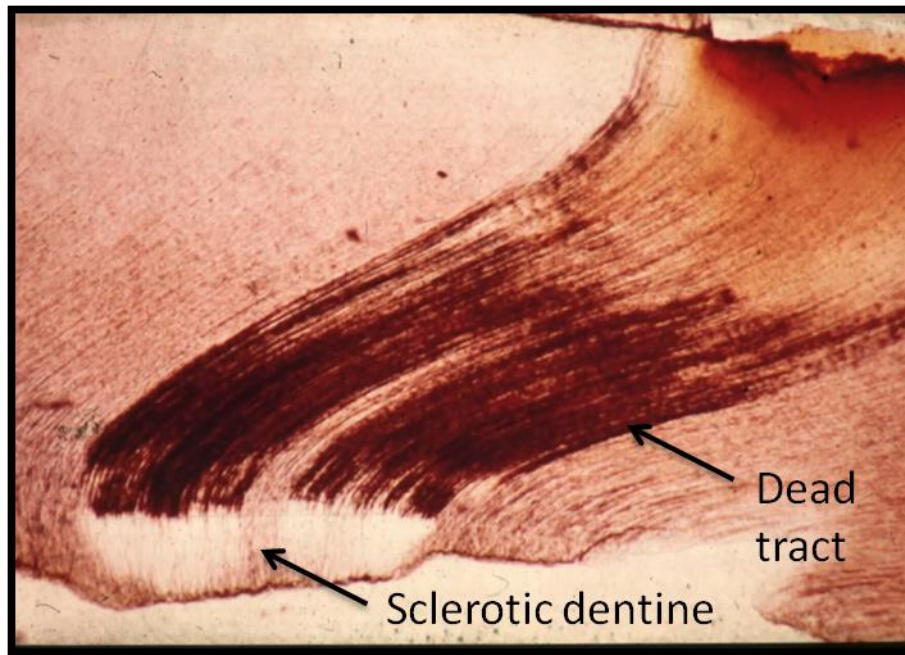
Dentinal tubules follow a sigmoidal course in the tooth crown, known as the primary curvature, which represent the path taken during the inward migration of odontoblasts (Avery, 2002). In the root, the primary curvatures are not evident and the tubules appear straighter in their orientation. The appearance of the tubules, however, is dependent upon the plane in which the tissue has been sectioned and in transverse sections, tubules appear circular. Dentinal tubules show small changes in direction of a few microns, which are known as secondary curvatures and potentially reflect the course of the odontoblasts during secretion. At the junction of primary and secondary dentine, the secondary curvatures often coincide in adjacent tubules and the odontoblasts simultaneously appear to be changing direction (Weiner *et al.*, 1999).

A reduction in the permeability of dentine is observed in the case of sclerosis, where the tubules become filled with calcified deposits (Tagami *et al.*, 1992). Sclerotic dentine may be deposited beneath carious lesions as a defence response to the injury (see Figure 1.4), or as an effect of aging due to the continuous deposition of peritubular dentine throughout life, and is observed as a transparent or translucent zone (Tjäderhane *et al.*, 2009). In the case of unrestored lesions, it is proposed that cariogenic bacterial acids degrade the dentine matrix, releasing latent signalling molecules, which subsequently stimulate odontoblast secretory activity (Dung *et al.*, 1995; Cooper *et al.*, 2010). In restored lesions, it is also

proposed that the dental materials used in the restorative procedures may locally interact with the dentine in a similar manner releasing bioactive signalling molecules, which also stimulate odontoblast secretory activity (Graham *et al.*, 2006; Tomson *et al.*, 2007). The formation of sclerotic dentine may arise from an acceleration in peritubular dentine formation, resulting in tubular occlusion. The consequential reduction in tubular fluid flow will result in the decreased diffusion of noxious substances or bacterial products towards the pulp (Love and Jenkinson, 2002). Sclerosis may occur at all ages, but becomes more prevalent with increasing age; it is also observed more frequently in males rather than females (Stanley *et al.*, 1983).

#### **1.1.1.5.1 Dentine Extracellular Matrix Components**

The dentine extracellular matrix is formed as a result of odontoblast secretory activity and contains a vast array of molecules with multifaceted properties. In addition to their role as structural components, these molecules can act as promoters or inhibitors of crystal nucleation or growth during mineralisation processes (Qin *et al.*, 2007). In addition, if released they can have the capacity to elicit downstream effects on cell phenotype, cell function and gene expression. Dentine extracellular matrix proteins may also act as signalling molecules involved in the recruitment, proliferation and differentiation of odontoblasts-like cells, implicating their activity in repair processes (see Section 1.1.1.5.1.4) (Smith *et al.*, 2012b).



**Figure 1.4 Micrograph of a carious lesion in cross-sectioned dentine.**

Sclerotic dentine is observed, extending into approximately 10 % of the tubule length (*Image sourced from Berkovitz et al., 2002*).

#### **1.1.1.5.1.1 Dentine Extracellular Matrix Molecules**

Although predominantly collagenous, dentine also contains many non-collagenous proteins (NCPs). A key group of NCPs are termed the Small Integrin-Binding Ligand N-linked Glycoproteins (SIBLINGs), which share several biochemical and genetic characteristics (Fisher *et al.*, 2001). The genes for these proteins are located on human chromosome 4q21-23 and the proteins contain an analogous region termed the RGD motif, due to the presence of an Arg-Gly-Asp tripeptide, which interacts with cell-surface integrins mediating cell adhesion and signalling (Qin *et al.*, 2004). This family of proteins is known to regulate hydroxyapatite crystal formation and act as nucleating factors for mineralisation (He *et al.*, 2003; Fisher *et*



*al.*, 2001; Goldberg *et al.*, 1996; Hunter and Goldberg, 1993). This is further evidenced by the marked phenotypic abnormalities in the mineralisation process in dentine that arise as a result of genetic mutations within this protein family (Xu *et al.*, 1998; Xiao *et al.*, 2001).

Of the SIBLING proteins, BSP, DMP1, DSPP and OPN, are all secreted, phosphorylated and sulphated sialoproteins. These proteins are also relatively rich in acidic amino acids, such as glutamic acid (BSP), aspartic acid (DSPP and OPN) or both (DMP1) (Fisher *et al.*, 2001); this unusually high proportion of acidic amino acid residues in DMP1 is thought to be important in its role in regulating mineralisation (Qin *et al.*, 2007). DMP1 is expressed in mature and differentiating odontoblasts (Toyosawa *et al.*, 2004) and plays a key role in dentinogenesis as it is fundamental to the maturation of predentine to dentine (Feng *et al.*, 2003; Ye *et al.*, 2004). Immunolabeling studies have also demonstrated the localisation of DMP1 to dentine tubules and peritubular dentine (Orsini *et al.*, 2008). DSPP is expressed predominantly in odontoblasts, but not exclusively as it is also expressed in bone at considerably lower levels. Once the DSPP protein has been secreted into dentine, it is immediately cleaved into dentine sialoprotein (DSP), dentine phosphoprotein (DPP) and dentine glycoprotein (DGP), by MMP2 and MMP20 (Yamakoshi *et al.*, 2006). DSP and DPP originate from the N-terminal and C-terminal parts of DSPP, respectively. DGP has been identified in pig dentine extracts, but its existence in other species is unknown (Yamakoshi *et al.*, 2005). The cleaved products, DPP and DSP, are mainly expressed in dentine (Ritchie *et al.*, 1995). BSP and OPN differ in the diversity of their tissue distribution, with BSP being specific to mineralised tissues whereas OPN is also expressed in the kidney, nervous tissue and the uterus. Both proteins are postulated to be involved in the initiation of mineralisation in dentine (Hunter *et al.*, 1993). Evidence indicates that BSP is involved in the nucleation of hydroxyapatite at the

mineralisation front, but it may also act as an inhibitor of the formation of hydroxyapatite crystals after the initial production of the crystals (Hunter *et al.*, 1993; Qin *et al.*, 2004; Boskey *et al.*, 2008).

A group of non-phosphorylated proteins are also found in the dentine matrix, known as the small leucine-rich proteoglycans (SLRPs). The proteins are characterised by a central domain containing leucine-rich repeats, flanked by cysteine residues and include proteins such as biglycan, decorin, osteoadherin and lumican. Many of these SLRPs have been identified in a range of tissues, but osteoadherin is found exclusively in mineralised tissues. It is thought that the presence of these proteins in predentine relates to their role in mineralisation processes, facilitated by their calcium binding activity (Embery *et al.*, 2001; Goldberg *et al.*, 2003).

#### **1.1.1.5.1.2 Growth Factors and Cytokines in Dentine**

Growth factors and cytokines are important groups of molecules involved in a broad range of endogenous cellular processes from tissue regeneration to the defence response. These molecules interact with cell surface receptors through which they initiate a cascade of intracellular events, culminating in signalling within the cell nucleus where they regulate gene expression therefore altering cellular behaviours, such as proliferation and differentiation. Within the dentine extracellular matrix, an array of growth factors exist, which can be released in response to tissue damage and injury (Smith, 2003). Arguably the most widely researched growth factors found in dentine include transforming growth factor- $\beta$ 1 (TGF- $\beta$ 1), insulin-like growth factor-I (IGF-I), platelet-derived growth factor (PDGF), fibroblast growth factor-2 (FGF-2), epidermal growth factor (EGF) and adrenomedullin

(ADM) (Finkelman *et al.*, 1990; Cassidy *et al.* 1997; Roberts-Clark and Smith, 2000; Zhao *et al.*, 2000; Silva *et al.* 2004; Musson *et al.*, 2010). The presence of these growth factors in the dentine extracellular matrix is due to their secretion from odontoblasts (Smith *et al.* 1998; Sloan *et al.*, 2000; Sloan *et al.*, 2002). It is evident that although a rich cocktail of growth factors and cytokines are already reported in dentine, it is conceivable that many more remain to be identified.

Much of the research on growth factors in dentine has focussed on TGF- $\beta$ 1, which is now known to regulate an array of processes within the dentine-pulp complex. TGF- $\beta$ 1 is known to be fossilised within the dentine extracellular matrix, which is fundamental to its protection from degradation as unbound, the half-life of this protein can be only minutes (Wakefield *et al.*, 1990). The ability of TGF- $\beta$ 1 to induce the production of primary, reactionary or reparative dentine *in vitro* and *in vivo*, in addition to its involvement in the immune responses of the dental pulp, has been investigated (Bègue-Kirn *et al.*, 1992; Smith *et al.*, 1995; D'Souza *et al.*, 1990; Tziafas *et al.*, 1998; Sloan and Smith; 1999). TGF- $\beta$ 1 has also been shown to stimulate processes pertinent to mineralisation, including alkaline phosphatase activity, type I collagen production and proliferation of human dental pulp cells (Nakashima, 1992; Shirakawa *et al.*, 1994; Shiba *et al.*, 1998). TGF- $\beta$ 1, TGF- $\beta$ 2 and TGF- $\beta$ 3 isoforms have been detected in rabbit dentine, however, the latter two isoforms have not been identified in human dentine indicating species differences (Cassidy *et al.*, 1997). A tooth slice model approach (Magloire *et al.*, 1996) has been used to deliver TGF- $\beta$ 1 to pulp tissue to observe its ability to stimulate three of the main processes involved in pulp repair: cell proliferation, migration and collagen I synthesis (Melin *et al.*, 2000; Sloan and Smith, 1999). The results of this study indicated that TGF- $\beta$ 1 was directly involved in the regulation

of all of these processes. More recently, the effects of TGF- $\beta$ 1 and osteogenic protein-1 were assessed after their application to cavities in dogs' teeth, indicating that these recombinant growth factors were able to induce tertiary dentine formation and intratubular mineralisation (Kalyva *et al.*, 2010).

In addition to growth factors, the presence of inflammatory cytokines has been reported in dentine. These pro- and anti-inflammatory cytokines, including interleukins (e.g. IL-8, IL-1b, IL-10), TNF- $\alpha$  and GM-CSF, were found to be sequestered within the dentine matrix and released by various dental materials and bacterial acids (Graham *et al.*, 2006). The immune responses enable the removal of invading bacteria during caries and are thought to precede any regenerative processes which may occur (Smith *et al.*, 2012b).

It is clear that both growth factors and cytokines are potent bioactive molecules that are able to function at very low (i.e. picogram) levels to stimulate reparative processes. For example, the pro-inflammatory cytokine TNF- $\alpha$  is able to stimulate the differentiation of dental pulp stem cells into an odontoblast-like phenotype and promote the secretion of mineral (Paula-Silva *et al.*, 2009). Therefore, the tendency to classify these molecules into specific functional groups does not convey their multifaceted nature (Smith *et al.*, 2012b).

The innervation of dentine by the *plexus of Raschkow* (see Section 1.1.3) combined with the fact that odontoblasts are derived from the neural crest, alludes to the presence of neuropeptides and neurotrophic factors within dentine (Byers *et al.*, 1990; Nosrat *et al.*, 1998). The roles of these molecules within the dentine-pulp complex are varied as they have been implicated in the innate immune response, dental pain transduction and the stimulation of dentinogenic responses (Haug *et al.*, 2006; Fristad *et al.*, 2007; Smith *et al.*,

2012b). For example, nerve growth factor (NGF), primarily known for its regulation of the growth, maintenance and survival of neurons, has recently been shown to stimulate odontoblast differentiation and promote mineralisation (Arany *et al.*, 2009).

Relatively little is known about the role of serum and plasma proteins found within the dentine. Most research conducted on these proteins has focussed on the most abundant of the plasma proteins, albumin, however, its role in the dentine matrix remains unclear. There is also reportedly a large presence of immunoglobulins in dentine, and these are thought to facilitate the immune response during caries (Mazzoni *et al.*, 2009). AHSG ( $\alpha$ -2-Heremans Schmid-glycoprotein) is produced in the liver and is the most abundant of all serum proteins. AHSG has an affinity for hydroxyapatite (Smith *et al.*, 1985) and immunohistochemical techniques have demonstrated its localisation in dentine (Takagi *et al.*, 1990). Interestingly, negative staining was observed in intertubular dentine, whereas intense staining was reported for peritubular dentine. These data have also suggested a possible role for AHSG in peritubular dentine formation (Takagi *et al.*, 1990; Mazzoni *et al.*, 2009).

#### **1.1.1.5.1.3 Mobilisation and Release of DMCs**

Frequently used restorative dental materials, such as calcium hydroxide [Ca(OH)<sub>2</sub>] and mineral trioxide aggregate [MTA], have a demonstrable ability to release dentine matrix components (DMCs) (Graham *et al.*, 2006; Tomson *et al.*, 2007). These studies have biochemically characterised the DMCs and identified the presence of NCPs, glycosaminoglycans (GAGs) and bioactive molecules, such as TGF- $\beta$ 1 and adrenomedullin. It is postulated that these molecules may stimulate the regeneration of dentine *in vivo* by exerting their effects on either existing odontoblasts or signalling the recruitment and

differentiation of stem/progenitor cells to secrete tertiary dentine (Smith *et al.*, 2012b). A range of reagents with different chemical properties (i.e. acidic, basic and chelating agents) are capable of solubilising DMCs (Smith and Leaver, 1979; Dung *et al.*, 1995; Ferracane *et al.*, 2010). Various acids are widely reported to have demineralising effects on dentine, particularly bacterial acids generated during caries; many of the early studies reporting on the composition of dentine therefore used physiologically relevant acids, such as lactic acid for the dissolution of DMCs (Dung *et al.*, 1995). The chelating agent, EDTA, is generally regarded as the gold standard for isolating DMCs and is thought to solubilise dentine by chelating calcium ions in the hydroxyapatite crystals (Graham *et al.*, 2006). However, it remains to be established whether EDTA is simply releasing mineral bound non-collagenous extracellular matrix components or whether a more intricate mechanism is involved (Graham *et al.*, 2006). Although alkaline reagents, such as MTA and  $\text{Ca(OH)}_2$ , have been shown to release DMCs, it is notable that sodium hydroxide which is of the same pH as  $\text{Ca(OH)}_2$  releases negligible amounts of TGF- $\beta$ 1 (Smith *et al.*, 1995). It is thought that the clinical success of many of these dental restorative agents may in part be due to their ability to stimulate dental repair through their release of bioactive molecules from the dentine matrix (Tomson *et al.*, 2007). Notably, however, the physiochemical properties, antibacterial activity and biocompatibility of these materials also likely contribute to their success in therapeutic application (Siqueira and Lopes, 1999; Mohammadi and Dummer, 2011). By obtaining a more in-depth knowledge of the precise mechanisms by which dental materials interact with dentine, new opportunities for research into regenerative processes and the development of novel treatment approaches may be developed (Smith *et al.*, 2012b).

#### **1.1.1.5.1.4 Role of Bioactive DMCs in Tissue Repair and Regeneration**

The ongoing challenges of dental caries and trauma may cause the degradation of dentine and consequently, the release of dentine matrix components (DMCs) (Smith *et al.*, 2012b). When the tissue becomes injured, the potential of these bioactive components in dentine is observed. Studies have shown that the effects of released dentine components are dose-dependent; at low concentrations they are able to stimulate cell proliferation in pulp, odontoblast-like and endothelial cells, whereas more deleterious effects are exerted upon cells at higher concentrations, whereby an impact on cell metabolism or survival has been demonstrated (Smith *et al.*, 2005; Musson *et al.*, 2010; Zhang *et al.*, 2011). These observations are also confirmed in a clinical setting in which slow progression of caries leads to the formation of tertiary dentine, whereas dentine is unable to recover from more aggressive, acute lesions (Bjørndal *et al.*, 1998, 1999, 2001).

The varying degrees of insult that a tooth may be subjected to throughout its life are reflected in the fate of the odontoblasts. Based on this, tertiary dentinogenesis may be subdivided into *reparative* and *reactionary dentinogenesis*, whereby the respective definitions refer to the nature of the injury and the regenerative process stimulated (see Figure 1.5). It is hypothesized that there are similarities in the initiation molecules for both reparative and reactionary dentinogenesis, although, the fundamental events involved in these processes significantly differ (Smith *et al.*, 1995). In order to stimulate matrix secretion in reactionary dentinogenesis, interaction occurs between the stimuli and the odontoblast. However, a more complex cascade of biological events comprising cell division, chemotaxis, cell adhesion and cytodifferentiation must all occur in order for dentine matrix secretion to occur during reparative dentinogenesis (Smith *et al.*, 1995). In view of the

varying sequences of events, it is important to consider both types of tertiary dentinogenesis separately, although one must acknowledge that reparative dentinogenesis may often follow reactionary dentinogenesis (Smith *et al.*, 2012b).

#### **1.1.1.5.1.4.1 Reactionary Dentinogenesis**

Using histological examination alone, it is difficult to determine the sequence of events that ensue post-injury, however, the observed tubular continuity between secondary dentine matrix and pre-existing odontoblasts is considered to be characteristic of reactionary dentine (Murray *et al.*, 2003). Mild stimuli such as early caries can influence odontoblast secretory activity, which is subsequently focally up-regulated upon injury from its relatively quiescent state during physiological or secondary dentinogenesis (Tziafas *et al.*, 2000). It is postulated that the up-regulation in odontoblast secretory activity is mediated by bioactive DMCs, released by bacterial acids from the dentine (Smith *et al.*, 1995). The response is determined by the extent and duration of the stimulus, but is localised to the dentinal tubules that are in direct communication with the stimulus (Smith *et al.*, 2001).

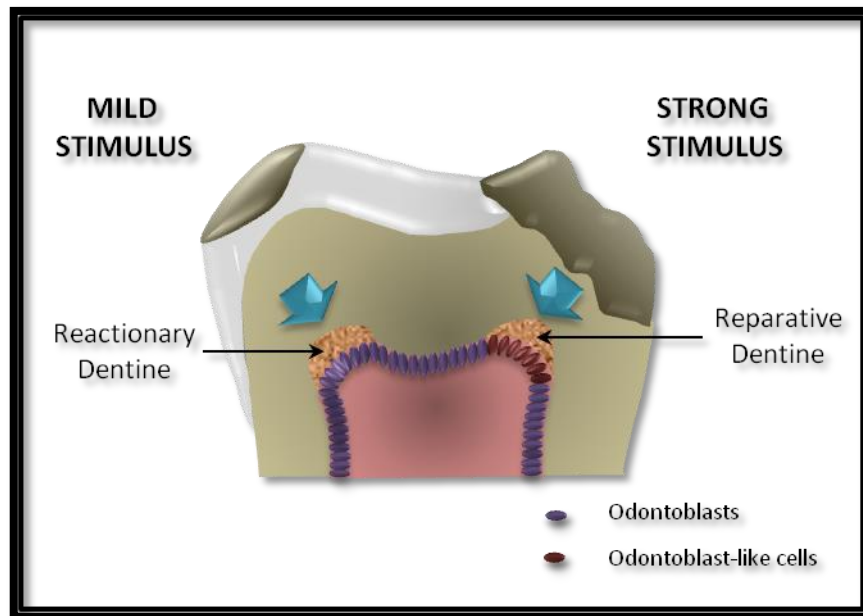
As previously mentioned (see Section 1.1.1.5.1.2), there has been extensive research surrounding the involvement of growth factors in stimulating odontoblast secretory activity, showing potent bioactivity at picogram levels (Tziafas *et al.*, 2000). Whilst the literature has focused on the existence of TGF- $\beta$  isoforms in the dentine matrix, the presence of other growth factors (e.g. IGF-I, IGF-II and angiogenic growth factors) has been detected and their release from the matrix after injury may be critical to the overall reparative responses of the dentine-pulp complex (Roberts-Clark and Smith, 2000). It is therefore evident that the



dentine matrix is not an inert tissue, but contains a mélange of bioactive molecules which may be released following exposure to an appropriate stimulus.

#### **1.1.1.5.1.4.2 Reparative Dentinogenesis**

If the injury is sufficiently intense, reparative dentinogenesis may occur and the sequence of events involved in this process follows a more complex course occurring at the site beneath the lesion. Stimuli, such as severe caries, may induce odontoblast death followed by the recruitment of progenitor cells to the site of injury, requiring a chemotactic response which has been demonstrated using dentine matrix components (Smith *et al.*, 2012c). Although specific constituents are yet to be identified, TGF- $\beta$ 1 is believed to provide a significant migratory stimulus for progenitor cells (Melin *et al.*, 2000; Smith, 2002; Smith *et al.*, 2012c). Subsequent to the recruitment of progenitor cells, signalling of odontoblast-like cell differentiation must occur in order to form reparative dentine (Smith *et al.*, 1995). Odontoblast differentiation during development requires epigenetic signalling from the epithelium (see Section 1.1.2.1.1), however, mature teeth lack this structure and the signal must be derived from alternative sources during reparative dentinogenesis (Smith 2002). Reports of the auto-inductive capability of the dentine matrix on odontoblast-like cell differentiation have been proposed (Smith *et al.*, 1990; Tziafas and Kolokuris, 1990), and this correlates well with the presence of bioactive molecules in dentine as discussed above.



**Figure 1.5 Schematic diagram of the formation of reactionary and reparative dentine.**

Mild stimuli may include mild caries or mild erosion/abrasion resulting in the formation of reactionary dentine, whereas strong stimuli may include severe caries, resulting in the formation in reparative dentine. The dark red ovals represent a new generation of odontoblast-like cells, replacing the original odontoblasts that died during injury (reparative dentinogenesis). Reactionary dentinogenesis involves secretion from surviving odontoblasts (purple ovals). *Image recreated from Smith et al., 1995.*

### **1.1.2 The Dental Pulp**

The pulp is a soft connective tissue sheathed by mineralised dentine and its composition can be divided into four distinct regions. A tightly packed layer of odontoblasts constitutes the outermost section, lining the pulp chamber. A network of capillaries and nerves are also present within this layer, in addition to molecules such as proteoglycans, fibronectin and collagen (Takagi *et al.*, 1990). Subjacent to this layer, is the *zone of Weil* or *cell-free zone* in which there are few cells evident and it is largely comprised of unmyelinated nerves, in

addition to capillaries and fibroblast cell processes (Hargreaves and Goodis, 2002). The subsequent layer in the pulpward direction is the *cell-rich zone*, which contains an abundance of fibroblasts, immunocompetent cells, undifferentiated mesenchymal cells, capillaries and nerves. The innermost area of the pulp is known as the pulpal core, and contains a similar complement of cells as those present in the cell-rich zone (Hargreaves and Goodis, 2002).

### **1.1.2.1 Cells of the Dental Pulp**

#### **1.1.2.1.1 Odontoblasts**

Dentine is formed by odontoblasts, which line the predentine for the duration of the tooth's life in health. Odontoblasts are highly differentiated cells; their morphology is a reflection of their position within the odontoblast lifecycle and therefore, their functional activity. Young, actively secreting odontoblasts exhibit a columnar appearance with a high nucleus/cytoplasmic ratio whereas at later functional stages, cells adopt a more quiescent morphology with a reduced height and lower density of organelles (Couve, 1986).

The *odontoblast process* is located within the dentinal tubule and extends from the cell body into the dentine. Although there is much debate surrounding the extent of the odontoblast process, several investigators are of the opinion that the process is limited to the pulpal half of dentine (Garant, 1972; Holland, 1975; Thomas, 1984), whereas other researchers believe this may be due to its retraction during tissue processing (LaFleche *et al.*, 1985). In support of a more protrusive odontoblast process, is evidence of tubulin, vimentin and actin-containing structures, which extend to the dentino-enamel junction (Sigal *et al.*, 1984 a, b). Although lacking in major organelles required for protein synthesis, the odontoblast process

has many longitudinal filaments and microtubules (Sasaki and Garant, 1996). Branching of the odontoblast process is extensive and enables connections and communications between the odontoblasts and the dentine matrix, in addition to cell-cell communication (Linde and Goldberg, 1993; Lu *et al.*, 2007).

Developmentally, odontoblasts differentiate from the ecto-mesenchyme of the dental papilla and are of neural crest origin (Berkovitz *et al.*, 2002). A detailed understanding of this differentiation process is fundamental to elucidation of normal development, in addition to understanding the involvement of odontoblasts in dentine repair. The terminal differentiation of odontoblasts involves a sequence of cytological and functional changes (Ruch *et al.*, 1995) and this process is under the control of the inner dental epithelium (IDE) and requires temporo-spatially regulated epigenetic signalling (Lisi *et al.*, 2003). In order for odontoblast differentiation to arise, there are several interdependent stages which must occur (described below).

The terminal differentiation of odontoblasts commences with the withdrawal of pre-odontoblasts from the cell cycle, which takes place at the late bell stage of tooth development. During the last division, the mitotic spindle lies perpendicular to the basement membrane. The daughter cell, influenced by the dental epithelial cell, elongates and polarises and finally differentiates into an odontoblast (Nanci, 2003). Although other cells of the dental papilla have odontoblastic differentiation potential, it is only those that are in contact with the basement membrane which differentiate at this point due to their proximity to the epithelial signal (Smith and Lesot, 2001). Consequently, functional odontoblasts are able to secrete predentine, followed by dentine components such as

collagen type I, type I trimer, types V and VI, proteoglycans and non-collagenous proteins (Ruch *et al.*, 1995).

A network of matrix molecules function to control odontoblast differentiation and there has been considerable focus on the growth factors (e.g. TGF- $\beta$ 1, TGF- $\beta$ 3, BMP-2, IGF-1) involved in signalling cytodifferentiation of odontoblasts and odontoblast-like cells (Bègue-Kirn *et al.*, 1992, 1994). The differential gene expression observed at different stages of odontoblast differentiation, in addition to the modifications in transcriptional control, emphasises the need to further characterise the fundamental regulatory pathways. Such knowledge would aid the understanding of the cell phenotype as well as how tertiary dentinogenesis can be exploited in a therapeutic context (Simon *et al.*, 2009).

#### **1.1.2.1.2 Fibroblasts**

The most abundant cells within the dental pulp are fibroblasts and they are located in relatively high numbers in the cell-rich zone. These cells appear to resemble one another morphologically, but a body of evidence suggests they are a heterogeneous population (Moule *et al.*, 1995). Although the primary function of fibroblasts is the synthesis of collagen types I and III, they are also implicated in the remodelling of the pulpal tissue. Fibroblasts degrade extracellular matrix components, such as collagen and proteoglycans, by means of matrix metalloproteinases (MMPs) and lysosomal enzymes (Wisithphrom *et al.*, 2006). An increase in MMP production has been shown when cultured fibroblasts have been exposed to bacterial byproducts or inflammatory cytokines, indicating that these molecules are key in modulating the inflammatory response (Wisithphrom *et al.*, 2006).

#### **1.1.2.1.3 Immunocompetent Cells**

As the dental pulp is a connective tissue, it could be assumed that its cells are comparable to the connective tissue in other parts of the body. However, a network of immunocompetent cells exist, which are capable of eliciting a defence response to an infection whereby the integrity of the tooth is breached (Jontell *et al.*, 1998). These immunocompetent cells include largely dendritic cells and macrophages, in addition to a relatively small number of mast cells and lymphocytes. The cells have a somewhat transient presence in the pulp, and are recruited from the bloodstream and increase in numbers during disease (Jontell *et al.*, 1998).

#### **1.1.2.1.4 Dental Pulp Stem Cells**

Several populations of stem cells have been reported within the dental pulp and their presence is crucial for tissue regeneration and wound healing. A population of putative post-natal stem cells present within the dental pulp has been isolated and termed dental pulp stem cells (DPSCs) (Gronthos *et al.*, 2002). These cells were able to regenerate a dentine-pulp-like complex when implanted into immunocompromised mice. This was composed of a mineralised matrix, tubules lined with odontoblasts and fibrous tissue containing blood vessels, resembling the arrangement in the dentine-pulp complex observed in human teeth (Gronthos *et al.*, 2000). It was also demonstrated that these cells were capable of differentiating into neural-like cells and adipocytes (Gronthos *et al.*, 2002).

The pulp of deciduous teeth also contains a multi-potent population of stem cells termed “stem cells from human exfoliated deciduous teeth” or SHED cells (Miura *et al.*, 2003). These cells are of particular interest, because they are relatively straightforward to collect,

as deciduous teeth are inevitably lost prior to their replacement with permanent teeth. Their potential in regenerating dentine-pulp tissue has been demonstrated *in vivo* and these cells also have the potential to give rise to endothelial cells, thereby facilitating angiogenesis during tissue regeneration (Cordeiro et al., 2008). More recently, SCAP (stem cells from the apical papilla) cells have also been identified (Sonoyama *et al.*, 2008) and are capable of undergoing odontogenic differentiation (Huang *et al.*, 2009b).

#### **1.1.2.2 The Pulp Extracellular Matrix**

The pulp extracellular matrix differs considerably from the hard tissue matrix of dentine and other connective tissues. Type I collagen is the primary constituent of dentine, whereas in the pulp types I and III collagen constitute 54.4 % and 41 %, respectively. However, types V and VI collagen are also present but in considerably lower quantities. The tissue distribution of non-collagenous constituents in the pulp also differs from dentine, particularly in the relative proportions present. Amongst these components are GAGs, which are present as proteoglycans in the pulp present in different proportions to dentine, and are implicated in regulating dentinogenic events (Goldberg and Smith, 2004). Indeed, an *in vitro* study by Tziafas *et al.*, (1988) indicated that GAGs also had a role in maintaining the polarised state of odontoblasts. The characteristic gelatinous consistency of the pulp is due to the presence of hydrophilic proteoglycans (Hargreaves and Goodis, 2002). The lipid content also differs substantially between the dentine and pulp (Goldberg and Septier, 2002).

The lack of mineralisation in the pulp is thought to be due to the absence of various inhibitory components in the dentine, and the presence of mineralisation inhibitors in the pulp, such as proteoglycans, which are indeed abundant in the pulp (Goldberg and Smith,

2004). Therefore, the different compositions of both the dentine and the pulp may also be explained by regulatory mechanisms, whereby the inhibition of mineralisation is equally important as its initiation (Goldberg and Smith, 2004).

### **1.1.3 Vascularisation and Innervation in the Dentine-pulp Complex**

The microcirculatory system in the dentine-pulp complex is integral to many processes. These include the maintenance of tissue homeostasis, the initiation of an immune response to injury or inflammation and angiogenesis (Hargreaves and Goodis, 2002). Blood vessels are not present in dentine, however, arteries infiltrate the apex of the tooth and migrate coronally into the pulp core. The arteries divide and lead to a network of capillaries located beneath the odontoblast layer where they have fenestrations, which allow the rapid passage of nutrients towards the baso-lateral plasma membrane of the odontoblasts (Linde and Goldberg, 1993). A decrease in fenestration and a withdrawal of blood vessels from the odontoblast layer is observed as primary dentine formation nears completion; subsequently, in the mature tooth, the capillary network is confined to the sub-odontoblastic region (Yoshida and Oshima, 1996; Roberts-Clark and Smith, 2000).

In the pulp periphery, a dense network of nerve fibres, known as the *plexus of Raschkow*, is located in the subodontoblast layer. Fibres often penetrate 50-100 µm into the inner part of dentinal tubules as free nerve endings (Fristad, 1997). A small number of unmyelinated axons may pass between the odontoblasts and it is thought that odontoblast activity may be additionally regulated by sympathetic nerve fibre signalling (Linde and Goldberg, 1993).

The sensory innervation of teeth is comprised of different subgroups, which are distinct in their size, function and conduction velocity (Pashley, 1996). The majority of myelinated



nerves are either A-beta (A- $\beta$ ) or A-delta (A- $\delta$ ), which are fast-conducting and relatively large fibres. They are responsible for the sensitivity of dentine (see Section 1.2) as they are most sensitive to hydrodynamic stimuli, which may be thermal, chemical or tactile in nature (Närhi *et al.*, 1990).

## **1.2 Dentine Hypersensitivity**

Dentine hypersensitivity, or cervical dentinal hypersensitivity, is clinically defined as ‘an exaggerated response to non-noxious stimuli’ and is a relatively common, painful dental problem (Curro *et al.*, 1990; Dababneh *et al.*, 1999). It is characterised by a short, sharp pain arising in response to stimuli that are typically thermal, evaporative, osmotic or chemical in their nature (Orchardson and Collins, 1987; Holland *et al.*, 1997). There appear to be substantial discrepancies between reports regarding the incidence of dentine hypersensitivity, perhaps reflecting that much of the data are based on self-reporting by patients. Prevalence data range from 4 - 74 % in the UK, which is potentially attributable to the differing methods of data collection used in the respective studies (Bartold, 2006). Questionnaire studies have yielded subjective indications of pain from patients, which consequently has implications in evaluating the effectiveness of treatment. It is also thought that a proportion of the population do not report dentinal hypersensitivity as they do not consider it to be a severe oral health problem and this therefore may result in its under-reporting (Orchardson and Gillam, 2006).

Interestingly, the prevalence of dentinal hypersensitivity reportedly ranges from 72.5 to 98% in periodontal patients (Chabanski *et al.*, 1997). This may be due to a combination of exposure of root dentine with the presence of periodontal bacteria, as these microorganisms

are thought to penetrate dentinal tubules (Kina *et al.*, 2008). Women also exhibit a marginally higher incidence of dentine hypersensitivity, however, the difference between males and females is not statistically significant (Bartold, 2006).

The correlation between dentinal hypersensitivity and ageing remains unclear. It has been postulated that hypersensitivity will rise with the increasing life expectancy of the population as this corresponds with widespread gingival recession, in addition to loss of enamel and cementum, amongst older individuals (Bartold, 2006). However, confounding evidence in the literature reports most sufferers range in age from 20 to 40 years old (Dababneh *et al.*, 1999). It has been proposed that this may be a consequence of a reduction in the permeability of dentine and neural sensitivity with age (Bartold, 2006). The intra-oral distribution of dentinal hypersensitivity is predominantly found in the canines and first premolars (Rees and Addy, 2002). This is followed by the second premolars and incisors, and molars are generally the least affected. Anatomically, dentinal hypersensitivity is commonly confined to the buccal cervical zones of permanent teeth (Martinez-Ricarte *et al.*, 2008).

### **1.2.1 Aetiology of Dentine Hypersensitivity**

For dentine hypersensitivity to manifest, two processes must occur; these are known as *lesion localisation* and *lesion initiation* and are outlined below (Dababneh *et al.*, 1999).

#### **1.2.1.1 Lesion Localisation**

Dentine may become exposed due to gingival recession, the wearing away, or removal of enamel which occurs often by a combination of the three mechanisms of abrasion, attrition and erosion. Abrasion is caused by the interaction of external objects with teeth, such as

toothpaste and toothbrushes (Addy and Shellis, 2006). However, it is the combined presence of these entities which contributes to abrasion, as their effects alone are deemed clinically insignificant. Attrition is described as wear due to tooth-to-tooth contact. Indeed, bruxism, a parafunctional habit encompassed within attrition, is thought to precede occlusal dentine hypersensitivity (Tokiwa *et al.*, 2008).

A predominant contributing factor to tooth wear is erosion and is defined as 'the dissolution of teeth by acids that are not of a bacterial origin' (Dababneh *et al.*, 1999). The exposure of teeth to acids may occur extrinsically or intrinsically. Extrinsic erosion can be either dietary or environmental, whereas gastric juice is responsible for intrinsic erosion (Addy, 2002). Raw food, citric acid-containing drinks and carbonated drinks have been implicated in erosion (Shaw *et al.*, 2000; Porto *et al.*, 2009). Occupational exposure can also be responsible for tooth erosion, whereby employees are exposed to acids or acidic vapour. For example, wine tasters, workers in battery manufacture and swimmers in poorly maintained pools are particularly vulnerable to erosion of the teeth (Peteron and Gormsen, 1991; Gray *et al.*, 1998; Centerwall *et al.*, 1986). Patients that suffer from chronic alcoholism, hiatus hernia or eating disorders, such as bulimia, are intrinsically exposed to gastric hydrochloric acid, which erodes the teeth (Myllärniemi and Saari, 1985; Hurst *et al.*, 1977).

#### **1.2.1.2 Lesion Initiation**

Once exposure of dentine has occurred, sensitivity is often initiated upon the opening of tubules at the dentine surface. Dentine may be covered by a smear layer or the tubules may be 'plugged' by calcium phosphate deposits arising from the saliva. If the smear layer or

tubular plugs are removed, the outer orifices of the tubules are opened (Pashley, 1992). The removal of the smear layer is thought to be caused by chemical or physical agents that are then responsible for opening the dentinal tubules (Addy, 2002); these agents may either have an abrasive or erosive effect on dentine (Dunitz, 2000). Amongst the most high profile abrasive agents reported in the literature are toothbrushes and toothpastes, however, toothbrushes alone are thought to be clinically insignificant with regard to their effects on the smear layer (Absi *et al.*, 1992; Addy, 2002). It has been found that it takes hours of continuous brushing, (equating to years of normal toothbrushing) during *in vitro* studies, to remove the smear layer in the absence of an abrasive agent (Absi *et al.*, 1992). The use of the toothbrush in conjunction with toothpaste can, however, potentially remove the smear layer by abrasion or detergent action (Hooper *et al.*, 2003).

The effects of erosive agents appear to rapidly lead to a loss in the smear layer of dentine and subsequently, the opening of dentinal tubules. A few minutes are usually sufficient for most soft drinks, some alcoholic beverages and yoghurt to remove the dentine smear layer (Addy, 1991, 2002). It has also been observed that some acidic mouthwashes also dissolve the smear layer relatively easily (Addy *et al.*, 1991). Erosion alone is thought to be the predominant factor in lesion initiation during dentinal hypersensitivity and in combination with abrasion, dentine wear and tubule opening are likely to ensue (Addy, 2002; Dunitz, 2000).

### **1.2.2 Mechanisms of Dentine Hypersensitivity**

Several hypotheses are discussed below, postulating the mechanisms for dentine hypersensitivity which have been proposed over more than a century.

#### **1.2.2.1 Odontoblastic Transduction Theory of Dentine Hypersensitivity**

Stimuli were originally understood to excite the odontoblast processes, which supposedly transmitted their excitation to nerve endings in the pulp or dentinal tubules, closely associated with odontoblast membranes (Bernick, 1948; Frank, 1968; Garg, 2002). This theory was disregarded in 1984 when it was observed that odontoblast processes were predominantly localised in the inner third of dentinal tubules (Garg, 2002; Thomas 1984). It was noted that no synaptic specialisations existed between odontoblasts and nerve terminals, which implied that there were no means for chemical transmission. Odontoblasts were also deemed as non-excitabile cells and therefore, unable to potentiate an electrical response (Avery, 2002).

#### **1.2.2.2 Neural Theory of Dentine Hypersensitivity**

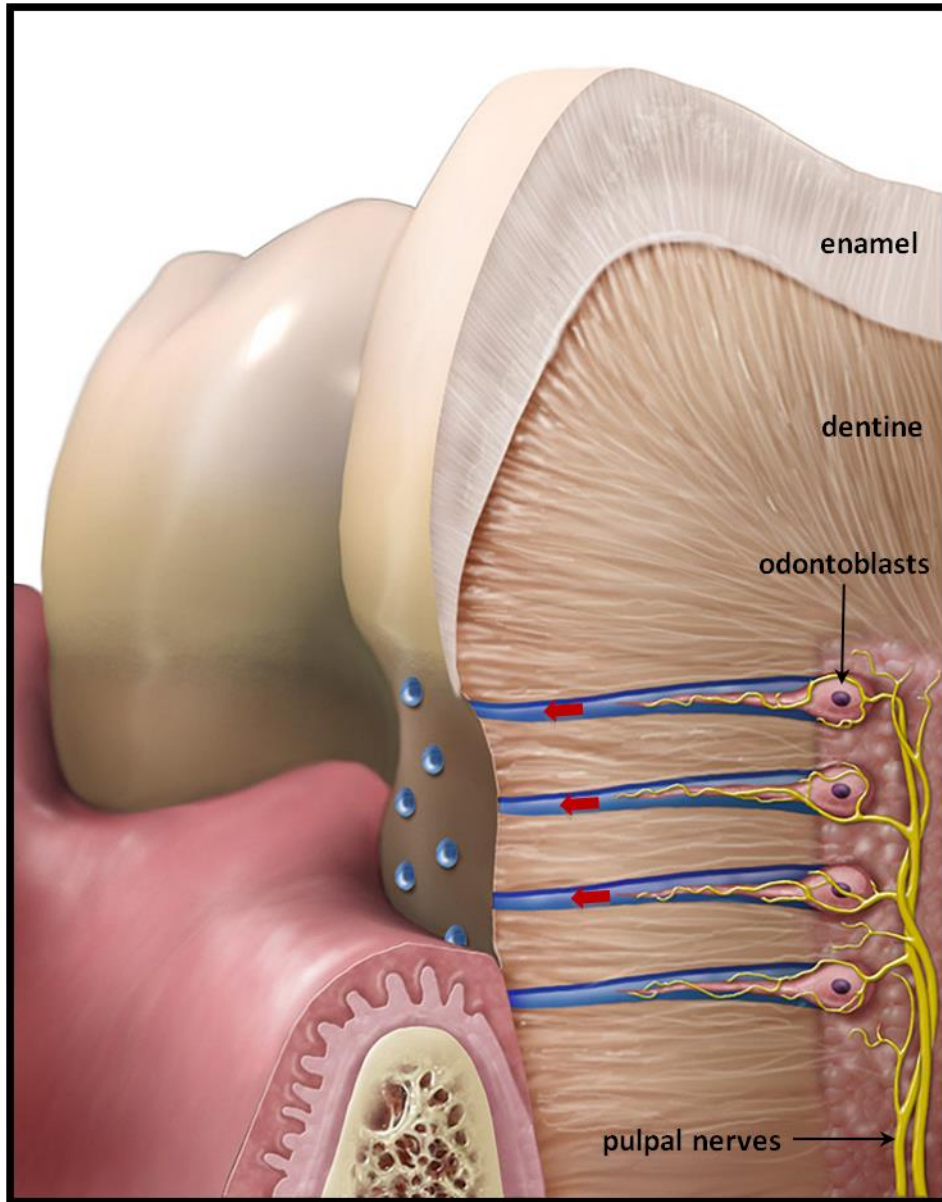
The neural theory involved the supposition that dentine hypersensitivity was initiated at nerve endings within dentinal tubules. It was considered that nervous transmission subsequently led along the parent afferent nerve fibres in the pulp, into dental nerve fibres and ultimately, to the brain (Bartold, 2006). Researchers suggested that free nerve endings were present throughout the entire length of dentinal tubules (Byers, 1984). However, more recent studies proved this to be unlikely when it was discovered that nerve endings penetrated merely 100-200  $\mu\text{m}$  into peripheral dentine (Garg, 2002).

#### **1.2.2.3 Hydrodynamic Theory of Dentine Hypersensitivity**

The theory with the most widespread support is the hydrodynamic theory proposed by Brännström and colleagues in 1963, which was a refinement of observations by Gysi (1900). It was hypothesised that most pain-provoking stimuli increase the centrifugal fluid flow

within dentinal tubules. As a result, a pressure change is evoked throughout the entire dentine activating A- $\delta$  intradental nerves at the pulp-dentine boundary or within the dentinal tubules, thus creating a pain sensation. The mechanism is thought to be reminiscent of the touch response when gentle pressure is applied to skin hair and in a dental context, is considered to occur through a mechanoreceptor response distorting nerves in the pulp (Addy, 2002). It is interesting to note that the most widely reported cases of dentine hypersensitivity are in response to cold or evaporative stimuli rather than heat. It has been postulated that heat evokes a slower movement of fluid within the dentinal tubules, which presumably is less intense and does not cause a pain sensation as a consequence (Orchardson and Gillam, 2006).

The hydrodynamic theory of dentinal hypersensitivity holds much credibility and provides explanation for most reported clinical scenarios. For example, when air passes over exposed dentine, dentinal fluid moves outwards towards the dehydrated surface consequently triggering nerve fibres and therefore pain (Bartold, 2006) (see Figure 1.6). Thermal changes may also cause dentinal tubules to expand or contract, resulting in an altered dentinal fluid flow which excites nerve fibres, once again causing pain (Bartold, 2006). The theory is also applicable to osmotic stimuli, such as sugar, acid and salt, where fluid flow in the dentinal tubules is similarly detected by nerve fibres. However, it remains difficult to rationalise this theory with regard to physical stimuli, although it is thought that mechanical abrasion may be sufficient to initiate unwanted fluid flow (Bartold, 2006).



**Figure 1.6 Illustration of the hydrodynamic theory of dentine hypersensitivity.**

Dentinal tubules may become exposed due to gingival recession, the wearing away, or removal of enamel. A tactile, hot or cold stimulus causes outward dentinal fluid flow (indicated by the red arrows), activating the nerve fibres and therefore eliciting a pain sensation. *Image source: [www.cdeworld.com](http://www.cdeworld.com)*

### **1.2.3 Treatment of Dentine Hypersensitivity**

The diversity and number of current treatments available for dentinal hypersensitivity are vast. It has been stated that few human diseases, with the exception of haemorrhoids, appear to be treatable with such a wide variety of compounds (Addy, 2002). Conventional therapies for dentinal hypersensitivity are aimed at blocking sensitivity and involve the desensitisation of the dentinal nerve or are applied topically with the intent of tubular occlusion, with a secondary aim of remineralising the dentine (Cunha-Cruz *et al.*, 2010).

The ideal desensitising agent 'must not be an irritant, jeopardise the integrity of the pulp, be as painless as possible upon application and shortly afterward, easily applicable, rapidly acting and permanent'. However, the vast array of current treatments suggests that no single treatment satisfies all these criteria (Cuhna-Cruz *et al.*, 2010). Treatments administered in-office by dental professionals are more complex and aimed at specific problem areas, whereas at-home treatments are relatively inexpensive and are less specific in their target, allowing more teeth to be treated. The most widely accessible treatments are desensitising toothpastes containing either potassium salts (typically potassium nitrate) to reduce nerve excitability, or compounds such as strontium acetate which have occlusive action (West *et al.*, 1997). Although these therapies have been found to provide some relief to patients, their physiochemical-based approaches remain somewhat temporary and a need exists for an innovative, biologically-based, more permanent treatment of dentine hypersensitivity. Thus, researchers continue to seek more effective, faster-acting and longer-lasting treatments (Panagakos *et al.*, 2009). A recent development in toothpaste has involved the introduction of a bioactive glass, which aims to treat sensitivity by providing a



more long-lasting treatment approach to dentine hypersensitivity by forming a relatively resilient layer on the tooth surface (see Sections 1.3.4-1.3.5).

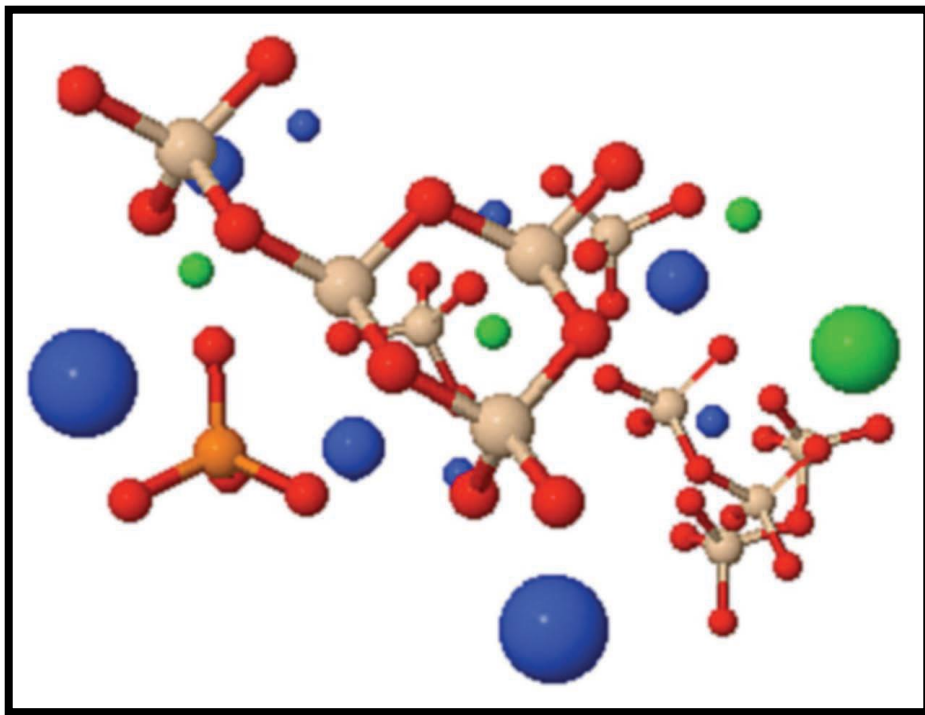
### **1.3 Bioactive Glasses**

The first bioactive glass was invented by Professor Larry Hench at the University of Florida in 1969 (Hench *et al.*, 1971), launching the field of bioactive ceramics. Prior to the invention of bioactive glass, biomaterials were selected on the basis that they were relatively inert. However, it was not uncommon for these materials to fail upon implantation, due to the formation of fibrous tissue. The pioneering work by Professor Hench radically changed the field of biomaterials and instead of deducing ways to minimise the interactions between implanted materials and the body, researchers could foresee the possibility of engineering materials to enhance their interaction with tissues, resulting in more beneficial responses (Greenspan, 2010).

*In vivo* applications have demonstrated the osteoinductive effects of bioactive glass by its capacity to bond to bone, via the formation of a carbonated hydroxyapatite (HCA) layer when in contact with biological fluids (Hench and Paschall, 1973). More recently, *in vitro* experiments have demonstrated the stimulation of osteoprogenitor cells at a transcriptional level in response to the ionic dissolution products of bioactive glass (Xynos *et al.*, 2000b). Bioactive glasses have also been shown to elicit antibacterial properties, in addition to stimulation of angiogenic and inflammatory responses (Allan *et al.*, 2001; Day, 2005). These latter reported effects were somewhat unexpected, but facilitated the understanding of the positive clinical results observed (Greenspan, 2010).

### 1.3.1 Structure and Composition of 45S5 Bioactive Glass

The initial proposed composition of 45S5 bioactive glass comprised of calcium, sodium, phosphorous and silicon and was chosen not only because the elements occur naturally in the body but also, as the Ca/P molar ratio resembled that of hydroxyapatite in bone mineral (Hench, 1971; Layer, 2011). The standard formulation of 45S5 bioactive glass contains 45 wt %  $\text{SiO}_2$ , 24.5 wt %  $\text{Na}_2\text{O}$  and  $\text{CaO}$ , and 6 wt %  $\text{P}_2\text{O}_5$  (Hench *et al.*, 1971), denoted by the chemical formula of  $\text{CaO-Na}_2\text{-P}_2\text{O}_5\text{-SiO}_2$ , structurally represented in Figure 1.7.



**Figure 1.7** Schematic diagram of 45S5 bioactive glass.

Blue represents calcium, sodium (green), oxygen (red), phosphorous (orange) and silicon (beige). *Image sourced from Parkinson and Willson, 2011.*

### **1.3.2 Formation of the HCA Layer**

The bond between the mineral and bioactive glass was discovered to be significant in that it could not be broken without breaking the bone (Hench *et al.*, 1971). Subsequently, researchers began to elucidate a series of reactions at the material surface, which were taking place immediately once the material had been subjected to the local aqueous environment. Surface compositional profiles indicated that  $\text{Na}^+$  was rapidly released from the material surface and exchanged with  $\text{H}^+$  ions in the solution (Clark *et al.*, 1976). This led to an increase in pH, whilst a silica-rich and a cation-deficient surface remained. As a consequence of the high pH, the presence of  $\text{OH}^-$  ions in solution initiated the breakage of Si-O-Si bonds causing the loss of silica in the form of  $\text{Si}(\text{OH})_4$  into solution and the deposition of silanols (Si-OH) at the glass-solution interface (Hench, 1991). The reaction proceeded to take place by the condensation of Si-OH groups near the glass surface, resulting in the formation of a silica-rich layer through which  $\text{Ca}^{2+}$  and  $\text{PO}_4^{3-}$  groups would migrate. A rich amorphous  $\text{CaO-P}_2\text{O}_5$  film would then form on top of the silica-rich layer, which would subsequently crystallise into HCA by the integration of hydroxyls and carbonates (Hench, 1991).

### **1.3.3 Ionic Dissolution Products of Bioactive Glass**

The effect of the above reaction steps on the bioactive glass surface resulted in the bonding of material to living bone tissue. However, a further six reaction steps were postulated to take place, involving various cellular interactions (Hench, 1998). It is thought the surface reactions caused the adsorption of proteins to the HCA layer, which led to a cascade of cellular events involving the attachment, proliferation and differentiation of osteoblasts and eventually, the secretion of bone matrix (Hench, 1998). However, the exact mechanism by

which these processes are triggered remains elusive, as *in vitro* and *in vivo* experiments do not currently provide information in this regard.

#### **1.3.3.1 Ionic Dissolution Products of Bioactive Glass and Osteogenesis**

Although it was demonstrated that bioactive glass could stimulate osteogenesis (Xynos *et al.*, 2000a), it was unclear whether the effects were as a result of direct cellular contact with bioactive glass or the soluble ions released from the material during its resorption. Early flow cytometric analysis demonstrated that the use of bioactive glass as a substrate for the culture of osteoblasts induced proliferation by stimulating the cells to enter the S phase of the cell cycle (Xynos *et al.*, 2000a). However, subsequent experiments indicated that the ionic dissolution products alone could increase cell numbers suggesting that the presence of the bioactive glass substrate itself was not necessary to induce proliferation (Xynos *et al.*, 2000b). High-throughput transcriptional profiling was employed to elucidate the molecular mechanisms underlying the stimulation of cells by the ionic dissolution products of bioactive glass. Table 1.1 outlines the ontological groups that were found to be up-regulated by more than two-fold in response to the ionic dissolution products of bioactive glass after 48 hours exposure (Xynos *et al.*, 2000b). Notably, the up-regulation of an established inducer of osteoblast proliferation, IGF-II (Langdahl *et al.*, 1998; Sandy *et al.*, 1998), was identified, suggesting a possible autocrine mechanism for the increased cell numbers observed in response to bioactive glass dissolution products. Other genes that were up-regulated were cell cycle regulators (e.g. cyclin D1), apoptosis regulators (e.g. calpain), a growth promoting gene (RCL), in addition to cell surface receptors (e.g. CD44) and extracellular matrix regulators, such as metalloproteinase-2 (Xynos *et al.*, 2000b). The results therefore confirmed previous findings where bioactive glass had been shown to stimulate osteoblast

proliferation, as well as identifying the induction of genes that are well-established in osteoblast metabolism and bone formation (Xynos *et al.*, 2000a, 2000b).

Gene Family	Fold Induction
Transcription Factors and Cell Cycle Regulators	Two- to five-fold
Signal Transduction Molecules	Two- to six-fold
Proteins in DNA Synthesis, Repair, Recombination	Two- to three-fold
Growth Factors and Cytokines	Two- to 3.2-fold
Cell Surface Antigens and Receptors	Two- to seven-fold
Extracellular Matrix Components	Two- to 3.7-fold
Apoptosis Regulators	Two- to 4.5-fold

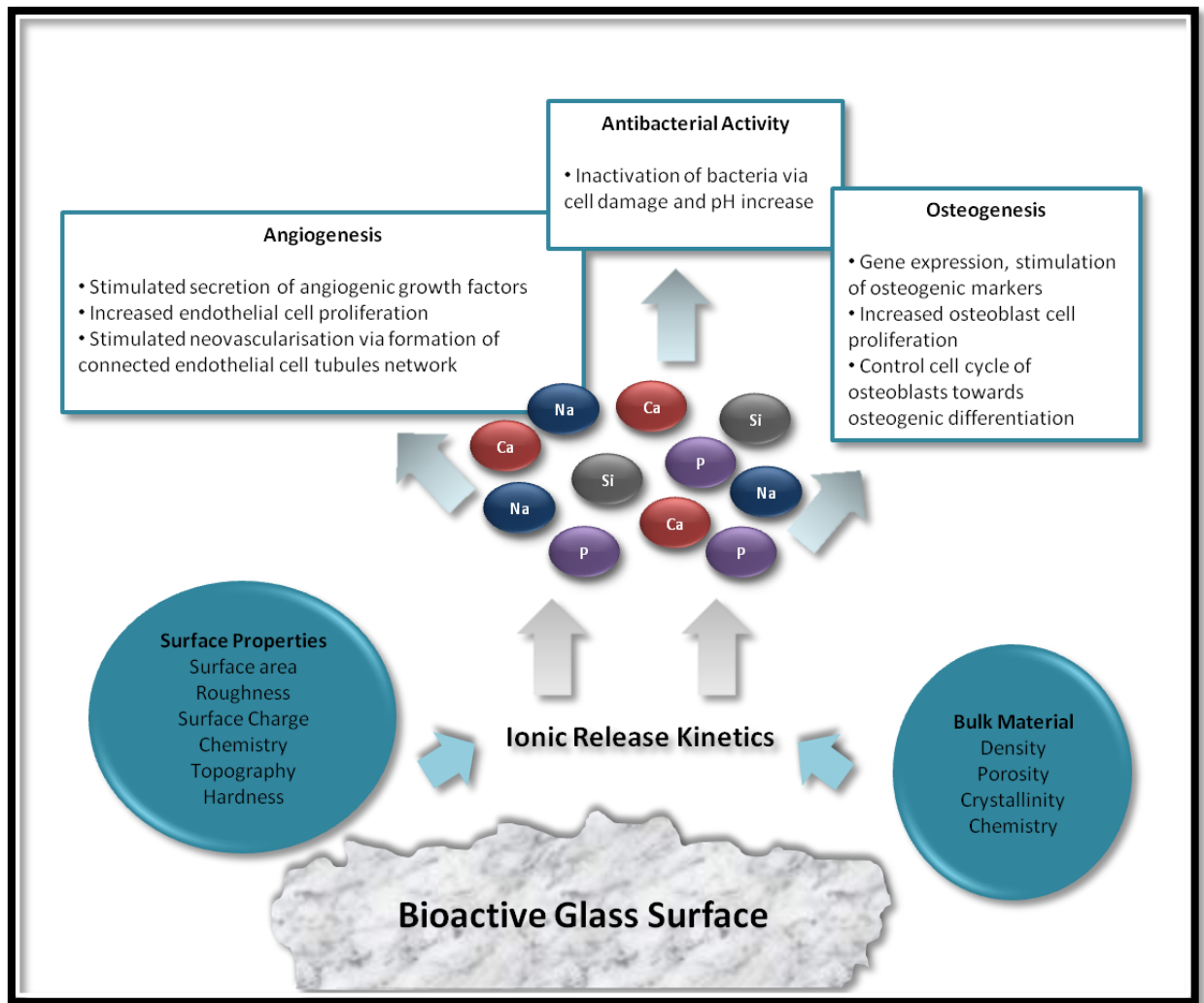
**Table 1.1 Gene families up-regulated by the ionic dissolution products of bioactive glass.**

Human osteoblast cells were exposed to the ionic dissolution products of 45S5 bioactive glass for 48 hours (Xynos *et al.*, 2000b). Table indicates the gene families that were up-regulated two-fold or more in treated cultures in comparison with untreated control cultures.

The concentration of the ions released from bioactive glass is also critical in modulating cellular effects, as relatively high concentrations may be cytotoxic. Data demonstrated that osteostimulation only appeared to occur when the ions were present at optimum concentrations, i.e. 15-30 ppm Si and 60-90 ppm Ca (Xynos *et al.*, 2000a). Elucidating the effects of individual ions or cocktails of ions is imperative to the design of new bioactive materials for the improvement of existing bioactive glasses. The roles of individual inorganic

ions on bone metabolism, angiogenesis, the growth and mineralisation of bone tissue have been extensively reviewed by Hoppe *et al.*, (2011) (see Figure 1.8). Exogenous calcium ions have been shown to induce osteoblast proliferation (Maeno *et al.*, 2005), whereas silica (released in the form of  $\text{Si(OH)}_4$ ) stimulates collagen I production and osteoblast differentiation (Reffitt *et al.*, 2003).

Primary human osteoblasts have been shown to form mineralised nodules when cultured on a bioactive glass scaffold in the absence of mineralising agents (i.e. dexamethasone and beta-glycerophosphate) (Gough *et al.*, 2004). It was hypothesised that silicon ion concentrations played a critical role in the mineralisation process, as there was minimal change in calcium and phosphorous ion levels when the material was diluted. These data are consistent with previous observations in which particular concentrations of silicon ions have been key in inducing mineralised nodule formation (Anderson, 2001).



**Figure 1.8** An overview of the biological impact of the ionic dissolution products of bioactive glass.

Image summarises the capacity of the ions released during bioactive glass dissolution, to exert antibacterial properties and influence osteogenesis and angiogenesis. *Image recreated from Hoppe et al., 2011.*

### 1.3.3.2 Antibacterial Activity of Bioactive Glass

Bioactive glasses exert antibacterial properties when they are immersed in an aqueous solution as a result of the dissolution cascade outlined in Section 1.3.2. The effects have been largely attributed to the high aqueous pH that arises in a closed system, which provides hostile conditions for microbes (Allan *et al.*, 2001). Experiments demonstrated that 45S5 bioactive glass was able to exert antibacterial effects upon a range of oral bacteria associated with caries and periodontal disease, such as *Streptococcus mutans*, and *Aggregatibacter actinomycetemcomitans*, respectively (Allan *et al.*, 2001). It has also been hypothesised that silica release is indirectly associated with the antibacterial properties of bioactive glasses, via the promotion of calcium phosphate precipitation, causing an interference with bacterial cell viability (Zehnder *et al.*, 2006). Although bioglasses in general show potential as disinfectants in dentistry,  $\text{Ca(OH)}_2$  remains superior in its antibacterial activity (Zehnder *et al.*, 2006).

Attempts to substitute the sodium component of bioglasses with silver or zinc have been attempted to enhance its antibacterial efficacy (Bellantone *et al.*, 2002; Oki *et al.*, 2004). However, the clinical applicability of these compositions has been questioned, particularly with zinc, which has also been shown to be cytotoxic to osteoblasts (Aina *et al.*, 2007). A subsequent study used a different approach and instead of altering the formulation of bioactive glass, the researchers simply decreased the particle size (Waltimo *et al.*, 2007). The use of nanoparticles sought to increase the surface area of glass in contact with the surrounding liquid, thus aiming for an enhanced microbial efficacy. Indeed, the pH was raised by three units and a ten-fold silica release was observed with the nanoparticles,



rendering this a relatively successful approach for increasing the antibacterial efficacy of bioactive glass (Waltimo *et al.*, 2007).

#### **1.3.4 Development of Bioactive Glass for an Oral Care Product**

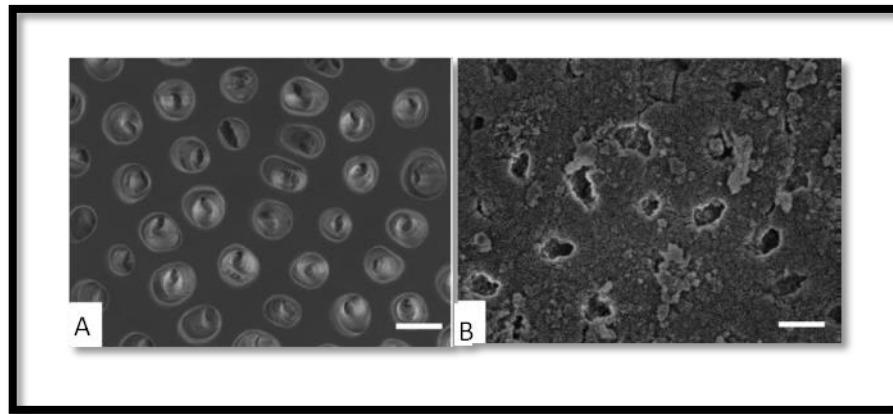
Research using several *in vitro* models has shown that bioactive glass has a strong affinity for collagen and this increases progressively during the precipitation of the HCA layer (Oréface *et al.*, 2009). It is thought that the negative charge on the glass surface permits side groups on Type I collagen fibres to form a bond (Zhong *et al.*, 1994). It was therefore reasonable to assume that as dentine is a primarily collagenous tissue, studies to establish the level of interaction between dentine and bioactive glasses would be appropriate. A strong bond between the glass surface and dentine was observed, whilst chemical analysis revealed that ions from the glass were penetrating into the dentine (Efflandt *et al.*, 2002). It was subsequently hypothesized that bioactive glass would form a protective HCA layer on the dentine surface, providing relief for dentine hypersensitivity. The earliest studies investigating this concept observed significant tubular occlusion with the application of bioactive glass to dentine (Litkowski *et al.*, 1997). These initial results have led to an increase in investigations and the commercial development of the product to be used in oral care.

NovaMin® Technology Inc. was established in 2003 and during the subsequent 10 years, a range of products have been developed, including toothpastes and prophylaxis pastes. In 2010, the company was acquired by GlaxoSmithKline Consumer Healthcare (GSK, Weybridge, UK), when the product was developed into a daily-use toothpaste for the treatment of dentine hypersensitivity, i.e. Sensodyne® Repair and Protect. This product was formulated to contain 5 % w/w NovaMin®, with a water-free base in order to protect the

bioactive glass particles from prematurely reacting. The toothpaste was also designed to deliver 1450 ppm fluoride ions in the form of sodium monofluorophosphate (West *et al.*, 2011).

### **1.3.5 NovaMin®: Evidence of Efficacy in Dentine Hypersensitivity**

To assess the efficacy of dentine hypersensitivity treatments, a number of *in vitro* models exist, of which the most common is the dentine disc model. Teeth are routinely cut into 1 mm-thick sections below the crown and above the root canal, allowing a flat surface for analysis and hydraulic conductance studies (Mordan *et al.*, 1997). Variations on the dentine disc model have been used to test the mode of action and efficacy of NovaMin®. Studies have sought to establish the ability of NovaMin® to rapidly occlude tubules, to form a protective HCA layer on the dentine surface and for this to remain steadfast in the face of acidic insult. The results have shown the success of NovaMin®, demonstrating a strong affinity for dentine after merely one application, which continues to occlude tubules over time in spite of acidic challenges (Burwell *et al.*, 2010). Scanning electron microscopy (SEM) is one of the most widely-used techniques in assessing tubular occlusion. Dentine discs are prepared by acid-etching to remove the smear layer and reveal patent tubules. The SEM micrograph (Figure 1.9) shows the comparison between an untreated dentine disc and the effects of NovaMin® and artificial saliva, 5 days after its application (Earl *et al.*, 2011a). The treated disc shows the HCA layer almost completely covering the dentine surface, and therefore the occlusion of tubules. However, top-down imaging does not measure the depth of tubular occlusion and the authors proceeded to obtain FIB-SEM cross-sections for this purpose, revealing occlusion to at least the level of the milling depth (approximately 3 µm) (Earl *et al.*, 2011a, 2011b).



**Figure 1.9 Scanning electron micrographs of dentine.**

**A)** acid-etched dentine showing patent tubules, **B)** effects of NovaMin® after 5 days showing tubular occlusion. Scale bar represents 5 μm. *Image source: Earl et al., 2011a.*

Clinical evidence has shown an improvement in pain relief when comparing the use of toothpaste containing NovaMin® with a conventional potassium nitrate desensitising toothpaste. The use of both cold water and air were used to measure sensitivity and improvements were observed at 2 and 6 weeks of brushing (Tai *et al.*, 2006). A randomised, double-blind study assessed the reduction in sensitivity in 66 patients treated with 2.5 % and 7.5 % Novamin®-containing and placebo toothpastes at 3 time points during 8 weeks of brushing. The results showed that there was a significant decrease in sensitivity in patients using the 7.5 % toothpaste, relative to the placebo group at all time points (Litkowski and Greenspan, 2010). These results supported the evidence reported by numerous other clinical studies, where toothpastes containing 45S5 bioactive glass were successful at reducing dentine hypersensitivity (Gillam *et al.*, 2002; Salian *et al.*, 2010; Sharma *et al.*, 2010).

Although NovaMin® has demonstrated clinical efficacy in reducing dentine hypersensitivity, a critical void in the research remains. There has been limited research to establish the effects of 45S5 bioactive glass on the dentine-pulp complex and a more in-depth understanding of these effects may assist the optimisation of its action.

#### **1.4 Project Aims**

When a biomaterial is introduced into a tissue, a biological response will inevitably occur (Anderson, 2001) and this is particularly pertinent to dentine in view of its highly permeable structure. The dissolution cascade of bioactive glass when exposed to an aqueous environment is well-established and it is conceivable that the dentinal tubules will provide a route for the ionic dissolution products to interact with pulpal cells. It is also postulated that when bioactive glass is placed in an environment containing tissue fluid, the resultant dissolution products may interact with the dentine to solubilise matrix components which in turn may influence cell behaviour.

This project aims:

- to characterise the influence of dentine on bioactive glass dissolution by measuring the ionic dissolution products of bioactive glass, dentine and saline within a closed system
- to determine whether these ionic dissolution products are able to interact with the dentine to solubilise dentine matrix components (DMCs), which have been previously demonstrated to stimulate dental repair processes
- to determine whether the effects of bioactive glass in saline-released DMCs can trigger dental reparative-associated processes, such as proliferation in pulpal cells

- to characterise released DMCs using high throughput proteomic techniques in order to acquire a better understanding of the effects observed on pulpal cells, in addition to identifying proteins previously not reported in dentine
- to determine whether the ionic dissolution products of bioactive glass have a direct effect on pulpal cells
- to characterise the antibacterial properties of DMCs and the ionic dissolution products of bioactive glass
- to characterise and develop an *in vitro* 3-D culture model that would be suitable to study peritubular dentine formation.

## **2.0 MATERIALS AND METHODS**

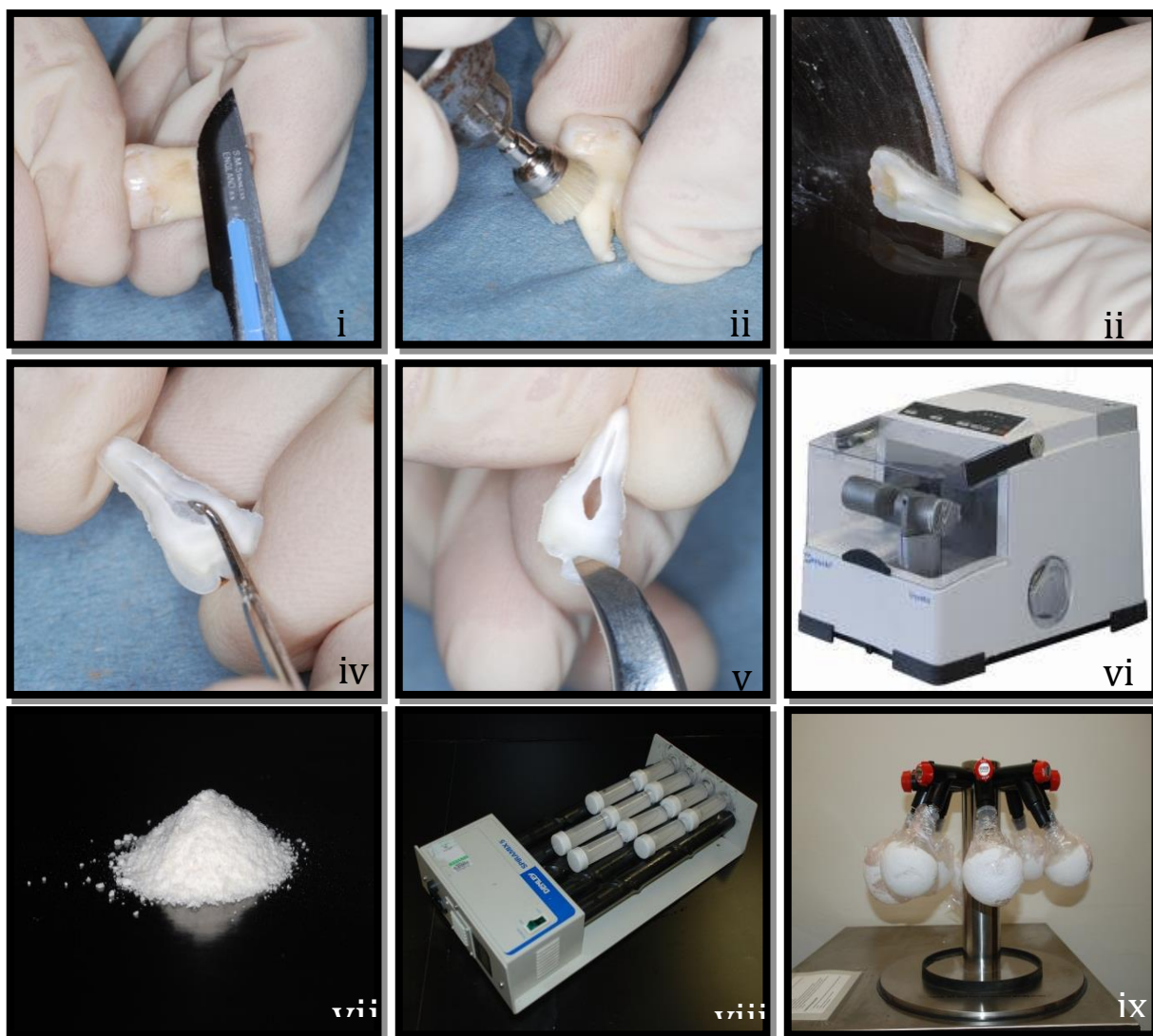
### **2.1 Preparation of Dentine Matrix Components**

#### **2.1.1 Dental Tissue Isolation**

Non-carious human molars were extracted for orthodontic purposes in the Oral Surgery Department, Birmingham Dental Hospital following informed patient consent under ethical approval from the UK National Research Ethics Committee (REC reference: 09/H0405/33). The teeth were collected in 15 mM sodium azide solution (Sigma-Aldrich, UK) for bacteriostatic purposes and subsequently washed copiously with water before storage in the Birmingham Dental School Tooth Bank at -20 °C until used.

#### **2.1.2 Dentine Preparation and Processing**

The soft periodontal connective tissues were removed from teeth using a type 11 scalpel blade (Swann-Morton, UK) and a dental bur (Kaltenbach and Voigt, Germany) was used to remove the cementum. The teeth were sectioned longitudinally, into 1 mm-thick slices using a rotary diamond disc saw (made in-house) cooled with distilled water. The enamel was removed using bone clippers and the pulp tissue was carefully extirpated from the pulp chamber using a dental excavator (Dentsply, UK). The dentine was thoroughly scraped clean to remove any remaining soft tissues and was subsequently powdered using a Retsch CryoMill (Retsch, Germany) cooled with liquid nitrogen, to prevent protein denaturation. The resultant fine powder was graded through a 60 mesh sieve. Figure 2.1 provides representative images of the dentine processing approach described above.



**Figure 2.1** Photographic images of the preparation process used for the extraction of Dentine Matrix Components.

**i-ii)** removal of soft periodontal tissue and cementum using a scalpel and dental bur, **iii)** sectioning of teeth into 1 mm segments using a rotary disk saw, **iv)** removal of pulp tissue using a dental excavator, **v)** removal of enamel using bone clippers, **vi)** cryomill used for the pulverisation of dentine, **vii)** powdered dentine following pulverisation, **viii)** constant agitation of extraction solutions at 4 °C, **ix)** freeze drying of dialysed-extraction supernatants.

*Images courtesy of P. Tomson (personal communication) and Retsch, Germany (vi).*

### **2.1.3 Materials for Extraction**

#### **2.1.3.1 Bioactive Glass**

45S5 bioactive glass powder was provided by GlaxoSmithKline Consumer Healthcare (Weybridge, UK). The composition in weight percentage was 45% SiO<sub>2</sub>, 24.5% CaO, 24.5% Na<sub>2</sub>O and 6% P<sub>2</sub>O<sub>5</sub> (Hench, 1972). The average particle size of the bioactive glass, determined by the manufacturer, used was 16 µm.

#### **2.1.3.2 Saline Solution with Protease Inhibitors**

Saline solution (0.154 M) was prepared by dissolving NaCl (Sigma-Aldrich, UK) in distilled water (pH 4.83). To prevent protein denaturation during the extraction, the saline was supplemented with protease inhibitors, 10 mM *n*-ethylmaleimide (Sigma-Aldrich, UK) and 5 mM phenyl-methyl-sulphonyl fluoride (Sigma-Aldrich, UK).

### **2.1.4 Extraction of Dentine Matrix Components**

Extraction solutions containing 1-10 mg/mL of 45S5 bioactive glass in saline solution, or control solutions of saline only (as described above) were subjected to constant rotation on a Denley Spiramix 5 (Severn Sales, UK), with powdered dentine (1 g/10 mL) at 4 °C, for 7 days (Figure 2.1, Image viii). The extraction solutions were centrifuged (Jouan B4, DJB LabCare Ltd, UK) daily at 3000 rpm for 10 minutes and the supernatant was decanted, pooled and stored at -20 °C.

#### **2.1.5 pH Profile of Extraction Supernatants**

During the 7-day extraction period, the pH of solutions containing bioactive glass, dentine and saline, or saline and dentine only were measured daily using a bench-top pH meter (Beckman Coulter, UK). The measurements were taken from freshly collected extraction



supernatants, prior to their freezing. To observe the effects that dentine exerted on the pH of extraction solutions, bioactive glass and saline only extractions were conducted in parallel, without the presence of dentine powder, as a control.

#### **2.1.6 Extraction Absorbance Profile**

Prior to freezing, the extraction supernatants were also analysed spectrophotometrically using a Jenway 6300 Spectrophotometer (Jenway, UK). The absorbance of the supernatants was measured at 280 nm, to monitor the protein dissolution, daily. A wavelength of 280 nm was selected as this is the maximum absorption wavelength at which the aromatic amino acid residues, tryptophan and tyrosine, are detected within a protein and therefore, provides a surrogate marker for the amount of protein released (Mach *et al.*, 1992).

#### **2.1.7 Dialysis of Extraction Solutions**

Following the 7-day extraction period, the pooled, frozen extraction solutions were thawed and transferred to 19 mm diameter dialysis tubing (Scientific Laboratory Supplies, UK). The solutions were exhaustively dialysed for 7 days at 4 °C, with daily changes of distilled water, to remove salts and impurities.

#### **2.1.8 Lyophilisation**

Following dialysis, the dialysates were transferred to round-bottomed flasks and shell-frozen with liquid nitrogen. To increase the stability of the proteins extracted, the samples were lyophilised (see Figure 2.1, image ix) for 48 hours using a freeze-dryer (Modulyo, Edwards, UK) after which the extracts were stored at -20 °C.

### **2.1.9 Efficiency of Extraction**

The efficiency of the extraction process was calculated using the weight of lyophilised extract recovered and comparing this with the starting weight of powdered dentine used in the original extraction solution. The results were expressed as a percentage yield.

## **2.2 Characterisation of Extracted Dentine Matrix Components**

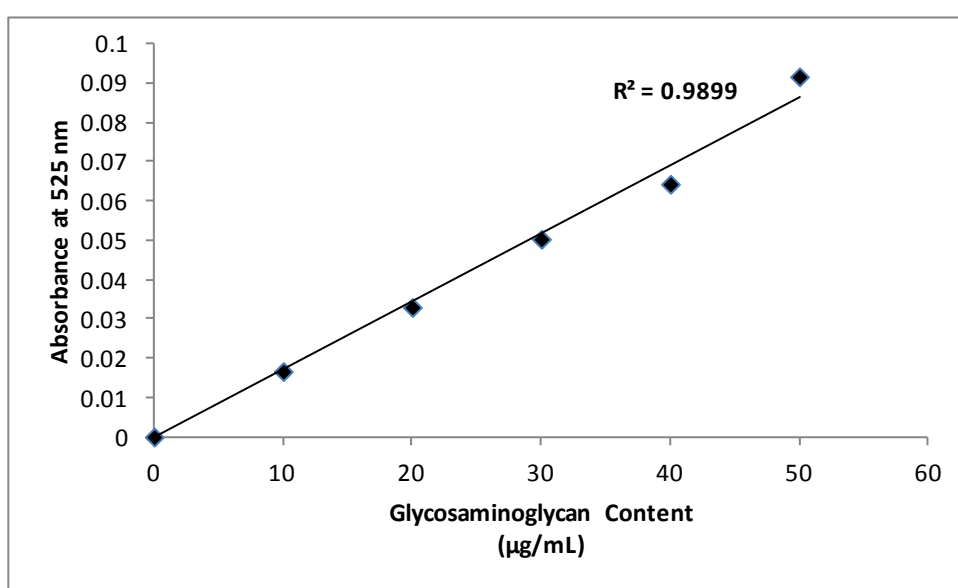
### **2.2.1 Quantification of Glycosaminoglycans**

Glycosaminoglycan (GAG) content of extracted dentine matrix components (DMCs) was determined using a dimethylmethylene blue (DMMB) dye binding assay developed by Farndale *et al.*, (1986). Chondroitin-4-sulphate (Fluka, UK) was solubilised in 0.5 M acetic acid (BDH, UK) from which standard solutions were prepared in a range from 10-50 µg/mL. Farndale Reagent was prepared from 46 µM DMMB (Sigma-Aldrich, UK), 40 mM glycine (BDH, UK), 40 mM sodium chloride (Sigma-Aldrich, UK). The lyophilised DMCs were solubilised in deionised water (1 mg/100 µL) and to each 100 µL of sample or standard 1 mL of Farndale Reagent was added and the absorbance was immediately read at 525 nm using a spectrophotometer (UV/VIS Spectrophotometer, Philips, UK). GAG content was determined by comparison with the chondroitin-4-sulphate calibration curve (see Figure 2.2).

### **2.2.2 Quantification of Total Non-collagenous Protein**

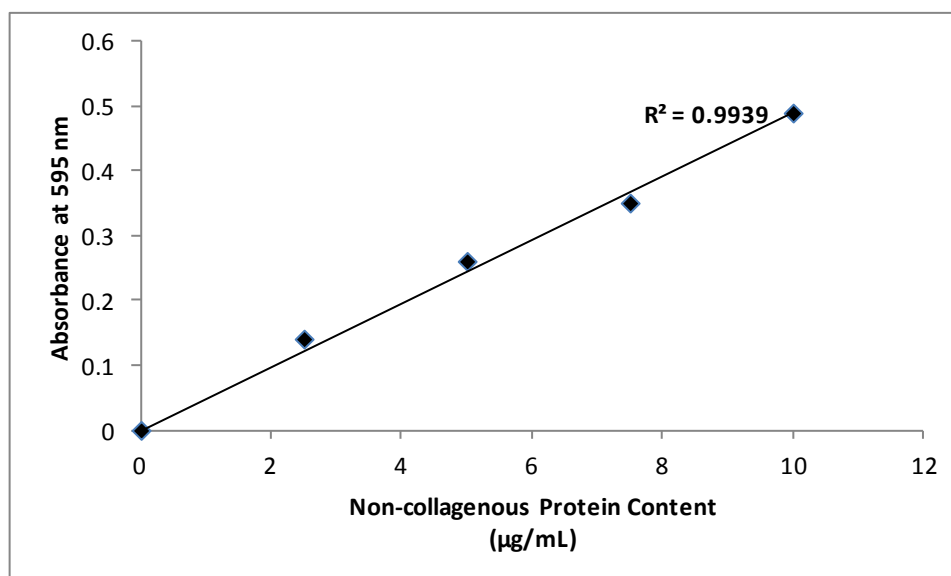
The DMCs were assayed for non-collagenous protein (NCP) content using the quantitative, dye-binding, Bradford Assay (Bradford, 1976). The dye reagent was prepared by the addition of 20 mg Coomassie brilliant blue G-250 (Sigma-Aldrich, UK) to 20 mL of 95% (v/v) methanol (VWR, UK) and 20 mL 85% (v/v) phosphoric acid (Merck, UK), to which 170 mL of dH<sub>2</sub>O was added, according to Bradford (1976). Samples were dissolved in deionised water

(1 mg/100  $\mu$ L). A standard curve (see Figure 2.3) in the range of 0-10  $\mu$ g protein was prepared using a stock solution of Bovine Serum Albumin (Sigma-Aldrich, UK) (10  $\mu$ g protein/100  $\mu$ L deionised water) and used for determination of the NCP content of test samples. Each sample or standard (100  $\mu$ L) was added to 1 mL of Bradford Reagent and the absorbance at 595 nm (UV/VIS Spectrophotometer, Philips, UK) was determined after a 5 minute incubation period at room temperature.



**Figure 2.2 Representative calibration curve generated using Chondroitin-4-sulphate as a standard.**

Absorbance was measured at 525 nm. The coefficient of determination is denoted by the  $R^2$  value on the graph, which demonstrates a significant linear relationship between glycosaminoglycan content within the standards and absorbance.



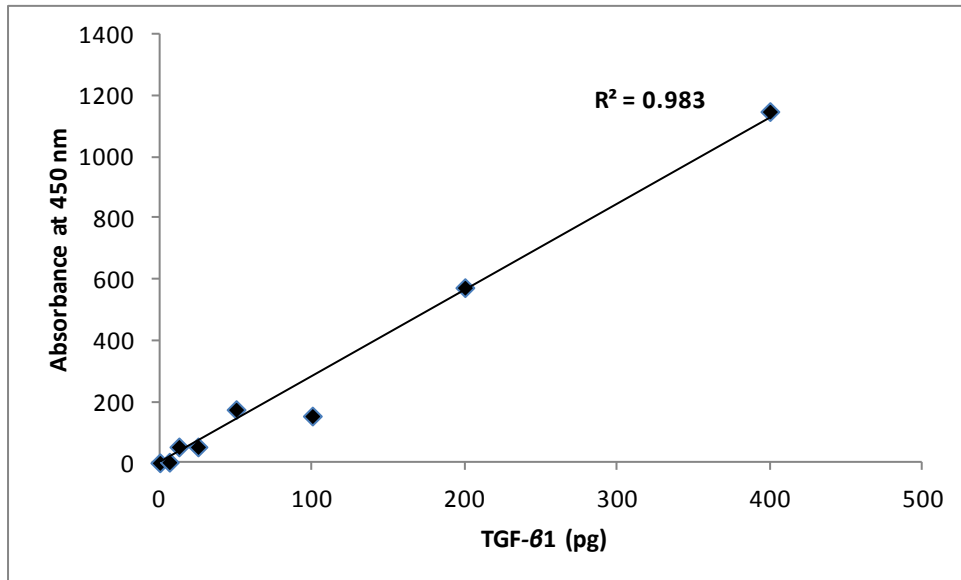
**Figure 2.3** Representative calibration curve using a range of concentrations of non-collagenous protein.

Absorbance was measured at 595 nm. The coefficient of determination is denoted by the  $R^2$  value on the graph which demonstrated a strong linear relationship between non-collagenous protein content within the standards and absorbance.

### 2.2.3 TGF- $\beta$ 1 ELISA

The presence of TGF- $\beta$ 1 is well-established in EDTA-extracted DMCs (Cassidy *et al.*, 1997), and it maintains a pivotal role in pulpal repair and regeneration (Smith, 2003). To quantify the presence of TGF- $\beta$ 1 in bioactive glass-extracted DMCs, the Quantikine Human TGF- $\beta$ 1 ELISA kit (R&D Systems, UK) was used. The assay employs a quantitative sandwich enzyme immunoassay technique, whereby a microplate has been coated previously by the manufacturer with a specific monoclonal antibody for TGF- $\beta$ 1. The samples were solubilised in deionised water (1 mg/100 µL), activated with 1 N HCl, and incubated at room temperature for 10 minutes, in a microcentrifuge tube (Eppendorf, UK); the solutions were

then neutralised with 20  $\mu$ L of 1.2 N sodium hydroxide (Sigma-Aldrich, UK) and 0.5 M HEPES (Sigma-Aldrich, UK). The resultant solutions (50  $\mu$ L) and standards (0-2000 pg/mL) were added in triplicate to 50  $\mu$ L of assay diluents, into wells of the pre-coated 96-well microplate. The samples were incubated at room temperature for 2 hours to allow for any TGF- $\beta$ 1 present to bind to the immobilised antibody. Following this incubation, the contents of the wells were carefully aspirated, and the wells washed 4 times, with a wash buffer, to thoroughly remove any unbound substances. A 100  $\mu$ L solution containing the enzyme-linked polyclonal antibody specific for TGF- $\beta$ 1 (kit reagent) was added to each of the wells and incubated for a further 2 hours, in order to sandwich the TGF- $\beta$ 1 immobilised during the first incubation. The wells were subsequently washed 4 times to remove any unbound antibody-enzyme reagent. A substrate solution (kit reagent) (100  $\mu$ L) was added to the wells and the resultant colour that developed was proportional to the amount of TGF- $\beta$ 1 bound in the initial step. A stop solution (kit reagent) was added after 30 minutes to halt the reaction, so that the intensity of colour could be measured spectrophotometrically. The absorbance values were measured at 450 nm using an ELX800 Universal Microplate Reader (Bio-Tek Instruments, UK). Concentrations were determined by comparison with a standard curve, prepared from standards provided (0-2000 pg/mL).



**Figure 2.4 Representative calibration curve using TGF-β1 recombinant kit standards.**

Absorbance was measured at 450 nm. The coefficient of determination is denoted by the  $R^2$  value on the graph; thus demonstrating a strong linear relationship between TGF-β1 content within the standards and absorbance.

#### **2.2.4 One-dimensional Sodium Dodecyl Sulphate Polyacrylamide Gel Electrophoresis**

##### **(1D-SDS PAGE) Analysis**

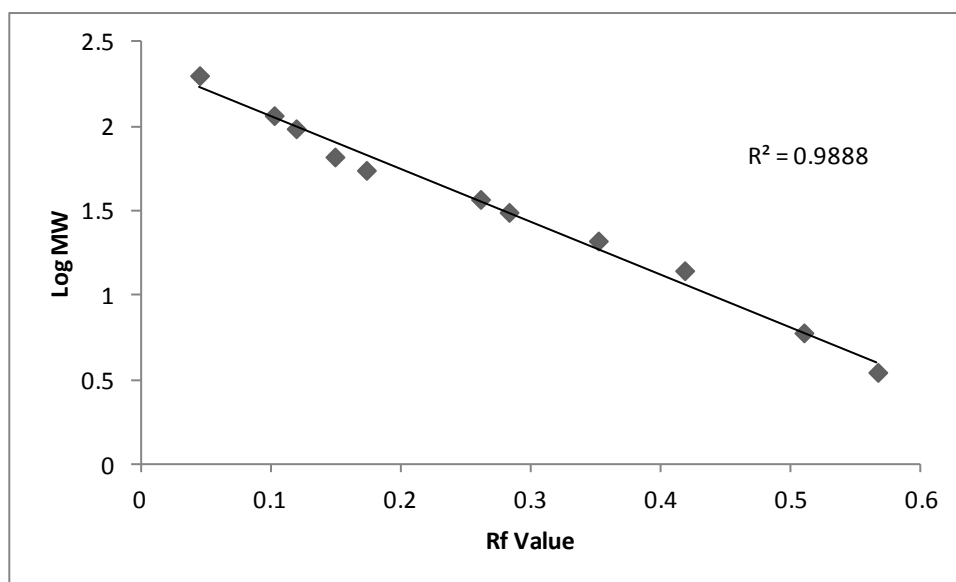
The samples selected for 1D-SDS-PAGE were DMCs extracted by 10 mg/mL bioactive glass-saline solution, saline solution and EDTA, the latter of which was prepared as described in Smith and Leaver, (1979) by Gay Smith (University of Birmingham, UK). The lyophilised DMCs (0.5 mg) were solubilised in 10 µL lithium dodecyl sulphate (LDS) buffer (Invitrogen, UK), 4 µL of reducing agent (Invitrogen, UK) and 26 µL distilled water. The samples were denatured at 105 °C for 2 minutes in a block heater (Grant Instruments, UK). NuPAGE reducing agent (Invitrogen, UK) was subsequently added (4 µL) and the samples were heated

for a further 10 minutes. The molecular weight marker was prepared using 10  $\mu$ L Mark12 MW standard (Invitrogen, UK) containing 12 polypeptides in the range of 2.5-200 kDa, 5  $\mu$ L LDS buffer (Invitrogen, UK) and 5  $\mu$ L ultrapure water. A NuPAGE 10% Bis-Tris pre-cast polyacrylamide gel (Invitrogen, UK) was inserted into a running tray (SureLock mini-cell, Invitrogen, UK) and submerged in NuPAGE 2-(N-morpholino) ethanesulphonic acid (MES) sodium dodecyl sulphate (SDS) 20X Running Buffer (Invitrogen, UK), supplemented with 500  $\mu$ L NuPAGE Antioxidant (Invitrogen, UK).

The wells of the gel were loaded with 2  $\mu$ L of EDTA, saline and bioactive glass-extracted DMCs, and the molecular weight marker. The gel was electrophoresed at 185 V for 40 minutes, after which the gel was removed from the running tray for protein profile visualisation using the silver staining technique. The SilverXpress Staining Kit (Invitrogen, UK) was used for visualisation of proteins within the gel according to the manufacturer's protocol. The gel was fixed with 7% acetic acid (BDH, UK) for 10 minutes, followed by washes in 50 % methanol (VWR, UK) and deionised water. The gel was subsequently stained with staining solution (kit reagent) containing silver nitrate and washed with deionised water. Developing solution (200 mL deionised water, 1 mL 1 % citric acid, 100  $\mu$ L 37 % formaldehyde, prepared by Invitrogen, UK) was used to visualise protein bands on the gel. The developing reaction was stopped using the stop solution provided (Invitrogen, UK) and gel was photographed using a Nikon Coolpix 990 digital camera (Nikon, Japan), under illumination from a light box (Hancocks, UK).

The digital images were loaded into the GelAnalyzer 2010 software. Stained protein bands were automatically detected by the image analysis software, generating a lane profile,

whereby the peaks corresponded to the location of the bands. The molecular weights of the unknown proteins were calculated using their distance migrated, and solving of the equation of the standard curve generated by the molecular weight (MW) markers (see Figure 2.5).



**Figure 2.5** Standard curve used to determine the molecular weight (MW) of unknown proteins by SDS-PAGE.

The curve was generated by plotting the log MW (Mark12 MW standard, Invitrogen, UK) against the corresponding Rf values. A strong linear relationship, determined by the  $R^2$  value, demonstrated the reliability of this graph for predicting MW.

### **2.2.5 Proteomics: In-gel Digestion**

Proteins were separated by 1D-SDS PAGE and stained with SilverXpress stain as described in Section 2.2.4. Proteomic analysis was conducted in order to identify the precise proteins present in the DMCs. The gel was transferred to a clean glass dish and a type 11 sterile scalpel (Swann-Morton, UK) was used to remove any excess gel and molecular weight



marker lanes. The remaining three lanes of interest contained separated DMCs extracted by solutions of 10 mg/mL bioactive glass in saline solution, saline only and EDTA. Each lane was excised and cut into six pieces of approximately the same size. The gel sections were dissected into  $\sim 2 \text{ mm}^3$  cubes and transferred into 1.5 mL microcentrifuge tubes (Eppendorf, UK), for processing, for the mass spectrometric identification of the proteins in each sample (Section 2.2.6).

The remainder of the analytical procedure was undertaken by the Advanced Mass Spectrometry Facility (School of Biosciences, University of Birmingham, UK). The gel pieces were de-stained by immersion in 50 % acetonitrile (Sigma-Aldrich, UK) solution followed by immersion in 100 mM ammonium bicarbonate (Sigma-Aldrich, UK). The purposes of these steps were to reduce the hydrophobic interaction between the protein and the stain, in addition to decreasing the ionic interaction between the negatively charged dye and positively charged proteins. Having removed the stain, it was necessary to reduce and alkylate the protein residues, in order to reduce the protein into its primary structure. The samples were dried by vacuum centrifugation for 5 minutes, rehydrated in 10 mM dithiothreitol (Sigma-Aldrich, UK) and 100 mM ammonium bicarbonate, and were subsequently reduced at 60 °C for 15 minutes. The ammonium bicarbonate was replaced with 50 mM iodoacetamide (Sigma-Aldrich, UK) and 100 mM ammonium bicarbonate. After 45-minute incubation in the dark, the gel sections were washed with 100 mM ammonium bicarbonate and dried by vacuum centrifugation (Concentrator Plus, Eppendorf, UK). The gel pieces were agitated at room temperature for 30 minutes with 20  $\mu\text{g}$  trypsin gold (Promega, USA) and diluted with 100 mM ammonium bicarbonate. Trypsin was used to ensure the cleavage of the peptide bond at the carboxyl terminal of the basic amino acids, arginine and

lysine. The hydrolysis of samples was undertaken overnight at 37 °C. Peptides were extracted initially with a solution of 2 % acetonitrile and 0.1 % formic acid (Sigma-Aldrich, UK), under gentle agitation for 30 minutes at room temperature. The supernatant was transferred to a clean 96-well plate (Corning, UK), and a second extraction was undertaken using 40 % acetonitrile and 0.1 % formic acid, also under agitation for 30 minutes. The supernatant was removed and pooled with the previously extracted peptides. The samples were dried in a dessicator and re-suspended in 0.1 % formic acid.

#### **2.2.6 Proteomics: LC-MS/MS Experiment**

The peptide mixtures, processed as described above, were analysed by liquid chromatography tandem mass spectrometry (LC-MS/MS), at the University of Birmingham Advanced Mass Spectrometry Facility. The peptides were eluted via a Triversa Nanomate nanospray source (Advion Biosciences, USA) into a LTQ Orbitrap Velos instrument (ThermoFisher Scientific, Germany). The peptide mixtures were separated using 15 cm (75 µm inner diameter) Nano Series Standard Columns, packed with C18 beads (Dionex, USA). The gradient used was from 3.2 % to 44 % acetonitrile in 0.1 % formic acid for 30 minutes. The effluent from the HPLC column was electrosprayed directly into the mass spectrometer, which was controlled by Xcalibur 2.1 SP1 software (Thermo Electron Corporation, USA). The mass spectrometer automatically switched between a full FT-MS scan and collision-induced dissociation (CID) MS/MS scans of the 7 most abundant ions. The survey scans were acquired at a resolution of 60 000 and the automatic gain control was set to 100 000. Collision activation was executed in the linear trap using helium gas, with a normalised collision energy of 35 % and a Q value of 0.25. The precursor isolation window width was 2 m/z and only multiply-charged precursor ions were chosen for MS/MS.

The MS/MS scans were searched against the NCBI nr database with the Mascot algorithm (Matrix Sciences, USA). Variable modifications included the deamidation of asparagine and glutamine, oxidation of methionine, and phosphorylation of serine, threonine and tyrosine. Two missed cleavage sites for trypsin were permitted and were accepted as a real hit protein, with at least two high confidence peptides.

A list of the proteins identified in each sample was generated, with their corresponding gene names, gene symbols and accession numbers. The data were uploaded onto the Analysis Wizard tool on the website (<http://david.abcc.ncifcrf.gov>) by DAVID Bioinformatics Resources 6.7 (USA), using the official gene symbol for each protein. This approach enabled an in-depth ontological analysis of the proteins present in bioactive glass, saline and EDTA-extracted DMCs.

#### **2.2.7 Multiplex Sandwich ELISA Array**

A multiplex sandwich ELISA service was employed to establish the concentrations of various proteins present in DMCs released by EDTA and 10 mg/mL bioactive glass in saline solution. The service was conducted by RayBiotech (Norcross, GA, USA), using the Quantibody® system. The Bradford assay (see Section 2.2.2) was used to determine a concentration of 190 µg/mL total protein of lyophilised DMCs in PBS solution. Similar to a conventional sandwich-based ELISA (see Section 2.2.3), antibodies that were specific to the proteins of interest were used (see Table 2.1). The sample diluent was added to each well (100 µL) and incubated for 30 minutes at room temperature, to block the glass slide containing spots of the antibodies. The diluent was subsequently decanted and replaced with either samples or standards and incubated for a further 2 hours at room temperature. Wells were washed

thoroughly with wash buffers and a detection antibody (80  $\mu$ L) was added to each well. Following a 2 hour incubation at room temperature, wells were once again washed with wash buffer and a streptavidin-conjugated fluor was added to wells (80  $\mu$ L). The slide was incubated for 1 hour in the dark to allow for the dye to bind to any cytokine-antibody-biotin complexes. Having washed the wells, the fluorescence was measured at 525 nm at a resolution of 2  $\mu$ m using a fluorescence array scanner (Agilent G2505B, UK). The concentrations of proteins of interest were calculated by comparing the signals to a standard curve, prepared from known standards.

Protein Name	Protein Symbol
Hepatocyte growth factor	HGF
Transforming growth factor beta-1	TGF-B1
Granulocyte colony stimulating factor	G-CSF
Granulocyte macrophage colony stimulating factor	GM-CSF
Macrophage colony stimulating factor	M-CSF
Beta-nerve growth factor	BNGF
Stem cell factor	SCF
Glial cell-derived neurotrophic factor	GDNF
Neurotrophin-3	NT-3
Neurotrophin-4	NT-4
Insulin-like growth factor-1	IGF1
Insulin-like growth factor-binding protein 1	IGF1-BP1
Insulin-like growth factor-surface receptor	IGF1-SR
Insulin-like growth factor-2	IGF2
Platelet-derived growth factor-AA	PDGF-AA
Vascular endothelial growth factor	VEGF
Basic fibroblast growth factor	bFGF
Bone morphogenetic protein-4	BMP4
Bone morphogenetic protein-7	BMP7
Epidermal growth factor	EGF

**Table 2.1 Proteins analysed by Quantibody® human multiplex sandwich ELISA array.**

The concentrations of the listed proteins in DMCs released by EDTA and 10 mg/mL bioactive glass in saline were quantified.

## **2.3 Cell Culture**

### **2.3.1 Cell Culture Medium and Conditions**

Dulbecco's Modified Eagle Medium (DMEM) (Biosera, UK), containing high glucose and sodium pyruvate were used for cell cultures. The medium was supplemented with 2 mM GlutaMAX™ (Invitrogen, UK), 100 units/mL of penicillin and 0.1 mg/mL of streptomycin (Sigma-Aldrich, UK). The addition of 10 % foetal calf serum (FCS) (Biosera, UK) was used, unless stated otherwise. Cells were incubated (Galaxy 41 S+, RS Biotech Ltd, UK) at 37 °C with a humidified atmosphere of 95 % air and 5 % CO<sub>2</sub>.

### **2.3.2 Sterile Phosphate-buffered Saline**

Phosphate-buffered saline (PBS) was prepared by dissolving 7.8 g NaCl (Sigma-Aldrich, UK), 0.2 g KH<sub>2</sub>PO<sub>4</sub> (Sigma-Aldrich, UK), 1.5 g K<sub>2</sub>HPO<sub>4</sub> (Sigma-Aldrich, UK) in 1 litre of distilled water. The pH of the solution was adjusted to pH 7.5, and was subsequently autoclaved at 121 °C for sterility, prior to its use for cell culture or microbiology techniques.

### **2.3.3 Cell Counting**

Cells were detached from flasks or microplates using a trypsin/EDTA solution (Invitrogen, UK). This solution consisted of 2.5 g/L of Trypsin in 0.38 g/L of EDTA, and an appropriate volume (to ensure complete coverage of the area) was added to cultures for 2 minutes, after which an equal volume of DMEM supplemented with FCS was added. Cell suspensions were mixed thoroughly and a 100 µL sample was transferred to a microcentrifuge tube (Eppendorf, UK) in addition to 100 µL trypan blue stain (Sigma-Aldrich, UK). Unstained, viable cells were counted microscopically, using a Neubauer haemocytometer (Hawksley, UK). A minimum of six counts per sample were obtained and averaged, to calculate a

representative cell number in the total volume of cell suspension. Cell suspensions were diluted and seeded at the required densities.

## **2.4 Cell Preparation and Isolation**

### **2.4.1 Recovery of OD-21 Cells from Cryopreservation**

OD-21 cells (immortalised mouse dental papilla cell line) (Hanks *et al*, 1998), donated by Professor Jacques Nör (University of Michigan, USA) were recovered from liquid nitrogen storage and thawed at 37 °C for 2-3 minutes. The cells were added to 1 mL of pre-warmed medium and were subsequently pelleted at 800 rpm for 2 minutes in a centrifuge (Jouan B4, DJB LabCare Ltd, UK) at room temperature, and the supernatant was decanted. The cell pellet was re-suspended in 5 mL fresh medium, prior to seeding into a 25 cm<sup>2</sup> flask (Nunc, UK).

### **2.4.2 Maintenance of Cell Cultures**

Cells were cultured with DMEM (Biosera, UK) supplemented with 10 % FCS (Biosera, UK) as described above. Upon reaching ~80-90 % confluence, in a 25 cm<sup>2</sup> flask, they were trypsinised, pelleted and re-suspended in DMEM (see Section 2.3.3). Cell suspensions were transferred to 15 ml BD Falcon™ conical tubes (BD Biosciences, UK) and centrifuged at 800 rpm for 2 minutes to produce a pellet of cells. Supernatants were discarded, and cells were re-suspended in 1 mL of DMEM, prior to cell counting or subculture.

### **2.4.3 Cryopreservation of OD-21 Cells**

Cells were trypsinised (see Section 2.3.3) and the resultant cell suspension was centrifuged for 2 minutes at 800 rpm and the supernatant was removed. The cell pellet was re-suspended in 1 mL of FCS and 100 µL of DMSO (Sigma-Aldrich, UK), and transferred to a

cryovial (Sarstedt, Germany). The cells were placed in a  $-80^{\circ}\text{C}$  freezer overnight and subsequently transferred to a liquid nitrogen dewar for storage.

#### **2.4.4 Human Dental Pulp Isolation**

Dental pulps were obtained from sound human third molar teeth extracted due to pericoronitis from patients (aged 20-26) that had provided informed consent. A freshly extracted tooth was briefly submerged in 70 % ethanol for disinfection, followed by sterile PBS. The tooth was then wrapped in sterile gauze and crushed using a hammer. The gauze was unfolded and the tooth was visually inspected to ensure the pulp chamber was exposed. The pulp was then carefully removed using forceps and the tissue was subsequently placed onto a glass slide overlaid with DMEM to prevent desiccation.

#### **2.4.5 Explant-derived Dental Pulp Cells**

The isolated pulp tissue (Section 2.4.4) was placed onto a sterile glass slide and dissected into approximately  $1\text{ mm}^2$  sections using a type 11 scalpel (Swann-Morton, UK). The tissue fragments were gently transferred to a  $25\text{ cm}^2$  culture flasks, to which 2 mL DMEM, supplemented with 20 % FCS, was added. The fragments were incubated at  $37^{\circ}\text{C}$ , and allowed to adhere to the flask for 48 hours, after which the medium was replenished to 5 mL. Medium was changed every 3 days until the cultures reached ~80-90 % confluence, at which point the cells were subcultured.

## **2.5 Exposure of Cells to Experimental Conditions**

### **2.5.1 Cellular Exposure to Bioactive Glass and its Dissolution Products**

#### **2.5.1.1 Preparation of Bioactive Glass-conditioned Medium**

Powdered 45S5 bioactive glass (GlaxoSmithKline Consumer Healthcare, Weybridge, UK) was added at the appropriate concentration (1-10 mg/mL) to DMEM, supplemented with 10 % FCS. The bioactive glass-DMEM solutions were continuously rotated for 24 hours at 37 °C in a thermal incubator (Stuart Scientific, UK), and were subsequently sterile filtered using a 0.22 µm membrane (Merck Millipore, UK) to remove the particulate bioactive glass (method adapted from Xynos *et al.*, 2000a).

#### **2.5.1.2 Exposure of Cells to Bioactive Glass Dissolution Products**

OD-21 cells or human dental pulp cells were seeded at a density of  $6 \times 10^3$ /0.5 mL, in a standard 48-well multiwell plate (Iwaki, Japan); the bioactive glass-conditioned media (1-10 mg/mL) and controls of DMEM (10 % FCS) (see Section 2.5.1.1) were administered directly to cells after an overnight adherence-incubation. The cells were subsequently assayed after 24, 48 and 72 hours by cell counting (see Section 2.3.3), the 3-(4,5-dimethylthiazol-2-yl)-2,5-diphenyltetrazolium bromide (MTT) (see Section 2.6.1) and lactate dehydrogenase (LDH) (see Section 2.6.2) assays.

### **2.5.2 Cellular Exposure to Dentine Matrix Components**

#### **2.5.2.1 Preparation of Dentine Matrix Component-supplemented Media**

Extracted and lyophilised DMCs (see Section 2.1) were added to pre-warmed DMEM, at concentrations of 0.1, 1 or 10 µg/mL (Smith *et al.*, 2005) immediately prior to use to avoid

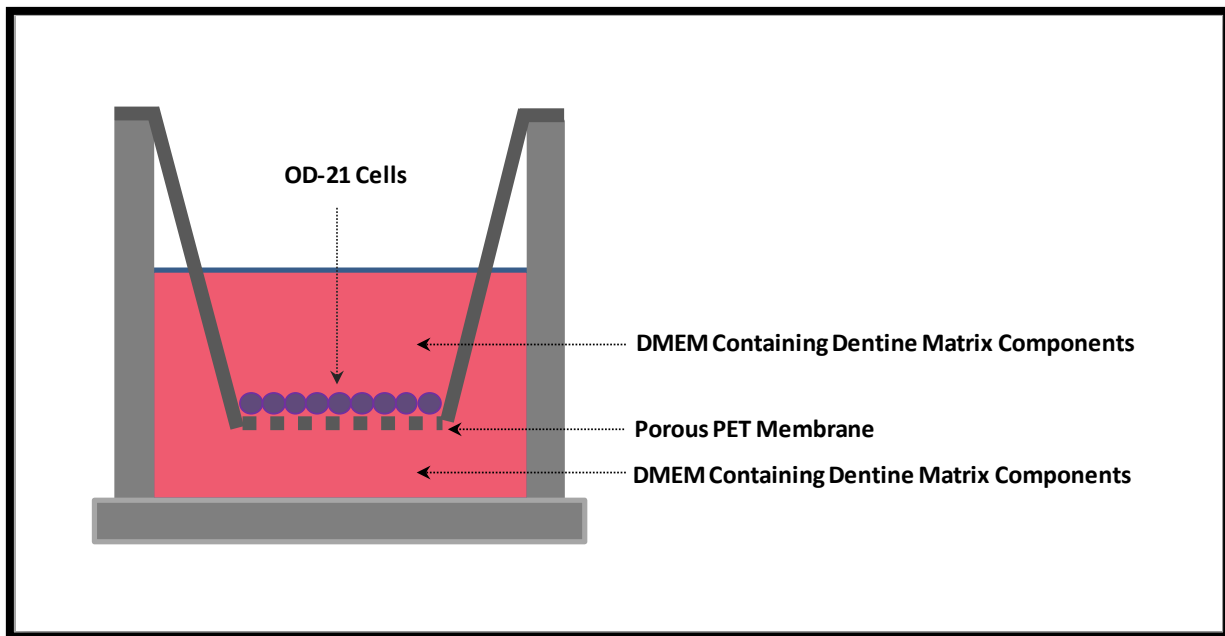


protein degradation. The medium was sterile filtered using a 0.22 µm membrane (Merck Millipore, UK), prior to addition to cell cultures.

#### **2.5.2.2 Exposure of Cells to Dentine Matrix Components**

OD-21 cells were seeded at a density of  $6 \times 10^3$ /0.5 mL, in a 48-well microplate (Iwaki, Japan) and incubated overnight to enable adherence. To ensure the effects of DMCs were not masked by FCS, cells were serum-starved for 24 hours prior to being exposed to the supplemented media (see Section 2.5.2.1). Culture responses were assayed at 24, 48 and 72 hours, following exposure, by cell counting (see Section 2.3.3), the MTT (see Section 2.6.1) and LDH assays (see Section 2.6.2).

In an alternative experimental design, OD-21 cells were seeded onto porous PET Thinserts (Greiner BioOne, UK) at  $3 \times 10^4$  cells/mL, and incubated overnight to adhere. The cells were deprived of FCS for 24 hours after which they were exposed to DMC-supplemented medium, both above and below the membrane (schematically represented in Figure 2.6). Cells cultured without the presence of DMCs served as a control. Cells were either fixed for histological processing (see Section 2.7.1) or scanning electron microscopy (SEM) analysis (see Section 2.8.1), or assayed for metabolic activity with the MTT assay (see Section 2.6.1).



**Figure 2.6 Schematic diagram to illustrate delivery of DMCs to cells cultured on PET Thinserts.**

OD-21 cells cultured on porous PET Thinserts, in the presence of DMC-supplemented medium, present in both the upper and lower chambers.

## **2.6 Functional Response Assays**

### **2.6.1 MTT Assay for Metabolic Activity**

The MTT assay was used to assess the metabolic activity of cells following stimulation. Although the MTT assay is frequently used for cell counting, for this study cell proliferation was assessed as described in Section 2.3.3. The assay principle is based on the cleavage of the yellow-coloured tetrazolium salt by the mitochondrial enzyme succinate-dehydrogenase into the purple-coloured formazan (Mosmann, 1983). It is assumed that this reaction can only take place in living cells with functional mitochondria (Carmichael *et al.*, 1987). Thiazolyl blue tetrazolium bromide (Sigma-Aldrich, UK) was dissolved in sterile PBS (5

mg/mL) and sterile filtered through a 0.22  $\mu$ m membrane (Merck Millipore, UK). The MTT solution (150  $\mu$ L) was added to wells containing cells and culture medium, and incubated for three hours at 37 °C. The medium was subsequently aspirated and 400  $\mu$ L of DMSO (Sigma-Aldrich, UK) was added to dissolve the reduced formazan crystals. To ensure the thorough solubilisation of formazan crystals, the culture plate was placed on an orbital shaker (R100 Luckham, UK) for 15 minutes at room temperature. The optical density of the formazan solution was measured at 570 nm with a microplate reader (Bio-Tex Instruments INC, UK). A blank well with no cells, but containing the same volume of culture medium and MTT solution, was used to allow subtraction of the background absorbance from the experimental values.

### **2.6.2 Lactate Dehydrogenase Assay for Cytotoxicity**

Lactate Dehydrogenase (LDH) is a stable, endogenous enzyme that is rapidly released into the cell culture medium upon damage of the plasma membrane; thus, it is frequently used as a marker of cell death and for analysis of the cytotoxic effects of test reagents (Chao *et al.*, 1992). An increased presence of LDH in the supernatant directly correlates to the amount of formazan formed, which is measured colorimetrically. To assess whether the bioactive glass-conditioned media and DMC-supplemented media elicited cytotoxic effects on the cells, the LDH cytotoxicity kit (Roche Applied Science, UK) was applied. The experimental set-up required a negative control (DMEM only) to measure the LDH activity released from untreated cells, and a positive control lysis buffer (Triton X-100, kit reagent) to measure the maximum releasable activity in the cells. After the cells had been stimulated with the relevant test conditions, the cells used for the positive control were incubated, in a 96-well microplate (Corning, UK) with 5  $\mu$ L of lysis buffer for 30 minutes at 37 °C. The cell

culture medium (100 µL) was subsequently removed from each well and added to 100 µL dye/catalysis solution (kit reagent) and incubated with gentle agitation at room temperature, for 30 minutes. A stop solution (kit reagent) was then added to each well (50 µL) and the absorbance of the samples was measured at 490 nm with an ELX800 universal microplate reader (Bio-Tex Instruments INC). The results were expressed as percentage cytotoxicity by calculating the average absorbance values of triplicate analyses, subtracting the background control and inserting the values into the equation below.

$$\text{Cytotoxicity (\%)} = \frac{\text{experimental value} - \text{background control}}{\text{positive control} - \text{background control}}$$

### **2.6.3 Assessment of Cell Behaviour Cultured on PET Thinserts**

Cells were cultured on PET Thinserts in the presence of DMCs and a control as described in Section 2.5.2.2. After 24 hours of exposure, cells were fixed overnight in 10% (w/v) neutral buffered formalin (Surgipath Europe Limited, UK). Cells were stained with hematoxylin and eosin, outlined in Section 2.7.3. The PET membranes were removed from their casing, using a scalpel and mounted on a glass slide, prior to being photographed (see Section 2.6.4).

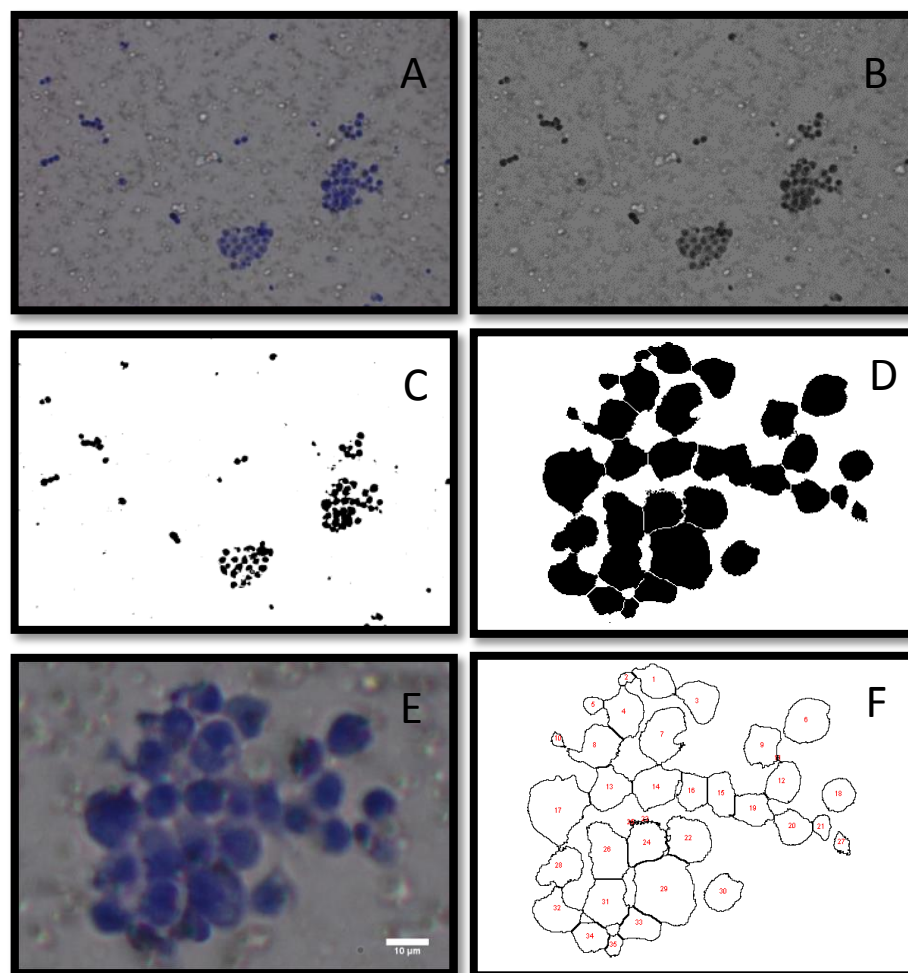
### **2.6.4 Cell Counting Using Image Analysis**

Cells cultured on the 12-well microplates and mounted PET membranes (Section 2.6.3) were observed on a Nikon Eclipse TE300 (Nikon, Japan) microscope and six randomly-selected areas of each well or membrane were captured using a Nikon D40 camera (Nikon, Japan) and the 10X objective lens of the microscope. The colour images were imported into Fiji (ImageJ version 1.45r), in which they were split into red, green and blue channels. For each photograph, the green channel image was selected and the threshold was adjusted to

produce a binary image. The cell boundaries proceeded to be defined using watershed segmentation (Meyer and Beucher, 1990), which enabled the Analyse Particle tool to generate the number of cells in each image. Figure 2.7 summarises the steps involved to count cells using image analysis, as described above.

#### **2.6.4.1 Validation of Counting Cells Using Image Analysis**

Cell counting, using a haemocytometer, is routinely used to assess cell number. The MTT assay, in addition to assessing metabolic activity, has also been frequently used in the literature as a measure of cell proliferation (Roehm, 1991). Both haemocytometer-counting and the MTT assay were validated and compared with cell counts obtained using image analysis (described in Section 2.6.4). OD-21 cells were seeded at 0-7000 cells/mL and incubated at 37 °C to adhere for 4 hours. The cell numbers were subsequently assessed using standard cell counting (Section 2.3.3) image analysis (Section 2.6.4) and mitochondrial activity was measured using the MTT assay (Section 2.6.1). All results were compared using the coefficient of determination ( $R^2$ ).



**Figure 2.7** Images illustrating automated method of cell counting using Fiji (ImageJ version 1.45r).

Original colour images of cultures were captured using a Nikon D40 camera attached to a Nikon Eclipse TE300 microscope. **A)** Original colour image, **B)** selected green channel image, **C)** binary image, **D)** watershed segmentation to define cell boundaries which, for reference, can be compared to colour image, **E)**, **F)** number of particles, i.e. cells, counted and labelled by Fiji, using the Analyse Particle tool. In these representative images cells were cultured on a porous PET membrane.

## **2.7 Histological Techniques**

### **2.7.1 Histological Processing of Cultures on PET Thinserts**

Cells cultured on PET Thinserts for 4 days (see Section 2.5.2.2) were fixed overnight in 10% (w/v) neutral buffered formalin (Surgipath Europe Limited, UK). The PET Thinserts were progressively dehydrated in increasing concentrations of Industrial Denatured Alcohol (IDA) (35% (v/v), 50%, 70%, 95%) for 10 minutes each. The PET membranes were removed from their casing, using a scalpel, and bisected before being placed in cell-safes (CellPath, UK) and histological processing cassettes (Surgipath, UK). The samples were subjected to three changes of 100 % Industrial Denatured Alcohol (IDA) (Genta-medical, UK), followed by two changes of xylene (VWR, UK) for 10 minutes each. The dehydrated samples were imbibed in paraffin wax (Sakura, UK) twice, for 30 minutes each, after which they were embedded.

The samples were embedded at 60-75 °C using a thermal and cryo-console (Sakura Tissue-Tek TEC IV Embedding Console System 4714, Netherlands). The cassettes containing the freshly embedded samples were cooled over the cryo-console at -5 °C for 20 minutes, and were subsequently stored at room temperature.

### **2.7.2 Histological Sectioning of PET Thinserts**

Prior to sectioning, the paraffin-embedded samples were cooled on ice for 10 minutes. A Leica RM 2035 microtome (Leica Instruments GmbH, Germany) was used to cut 5 µm sections using stainless steel disposable microtome blades (R35) (Feather Microtome Blades, Japan). Ribbons of three serial sections were transferred to a water bath (room temperature), followed by a warm water bath (45 °C) to ensure the removal of fine creases. PET sections were prone to tearing and detaching from glass slides during staining. Hence,

to aid their adhesion, a fine layer of silicone sealant (RS692-542, RS, UK) was smeared across a clean glass slide, which was then used to remove the sections from the warm water bath. The samples were dried in an incubator overnight, at 60 °C, before staining.

### **2.7.3 Hematoxylin and Eosin Staining**

Due to the delicate nature of 5 µm histological sections of PET Thinserts, the standard hematoxylin and eosin (H&E) staining protocol (Wissowsky, 1876) was modified. It was found that a long period of clearing in xylene was destructive to the PET membranes, and consequently, the wax was cleared for 2 minutes per section. The sections were dehydrated in 100 % (v/v) IDA, followed by 95 % IDA for 30 seconds each. After washing the sections in tap water, the samples were treated with Gill's III hematoxylin solution (Surgipath Europe Ltd, UK) for 2.5 minutes. The residual stain was washed with tap water and the samples were differentiated with 0.3 % acetic acid (BDH, UK) for 30 seconds. The glass slides were drained and treated with 0.3 % (w/v) hydrochloric acid (Merck Ltd, UK) for 30 seconds and rinsed in tap water. The samples were subsequently treated with Scott's Tap Water Substitute (Surgipath Europe Ltd, UK) for 1 minute and washed thoroughly in tap water. The histological sections were stained for 1 minute with 0.5 % (w/v) eosin solution (Surgipath Europe Ltd, UK), and the residual stain was removed by washing with tap water, followed by 100 % IDA. Finally, the samples were briefly treated with xylene for 1 minute. A droplet of XAM (BDH Laboratory Supplies, UK) was dispensed upon each sample and a coverslip was gently mounted on the glass slides.



#### **2.7.4 Histomorphometric Analysis**

To quantify the cell numbers on each histological section, histomorphometric analysis was conducted.

##### **2.7.4.1 Hunting Curve Analysis**

A Hunting Curve (McLachlan *et al.*, 2003) was plotted to determine the number of sections required to acquire a representative cell number that would not be altered by subsequent cell counts. The cumulative means of cell numbers on each histological section were plotted against the number of sections used for the analysis. When the curve began to plateau, this was deemed an appropriate number of counts of histological sections to use for subsequent experiments in order to gain a representative number of cells per unit area.

The histologically-sectioned PET Thinserts were variable in length in accordance with the region from which they had been sectioned, due to their circular shape. To calculate the length of each section, several photographic images were captured along the length of the sectioned membrane and combined by automated image stitching, to provide a larger image of the entire section. To enable this, images captured using the 10X objective lens on a Nikon Eclipse microscope and Nikon D40 camera, were combined in Fiji (ImageJ version 1.45r) using the Pairwise 2D Stitching plugin (Preibisch *et al.*, 2009). The length of each histological section was subsequently calculated using the Polygon Selection Tool in Fiji.

## **2.8 Scanning Electron Microscopy (SEM)**

### **2.8.1 SEM Analysis of Cells Cultured on Porous PET Thinserts**

Cells cultured on PET Thinserts were fixed in 2.5% (w/v) glutaraldehyde (Agar Scientific, UK) in 0.1 M sodium cacodylate buffer (Fisher Scientific, UK), pH 7.3, for 30 minutes. The cells were progressively dehydrated with increasing concentrations (v/v) of IDA. The concentrations used to dehydrate the samples were as follows: 20 %, 30 %, 40 %, 50 %, 60 %, 70 %, 80 %, 90 %, 95 % and 100 %, and exposure occurred for 10 minutes in each solution. Critical point drying completed the dehydration process, by the evaporation of hexamethyldisilazane (Sigma-Aldrich, UK), for one hour in a fumehood. The PET membrane was subsequently removed from its casing using a scalpel blade and mounted on an aluminium SEM stub (Agar Scientific, UK), with Conductive Acheson Electrodag (Henkel, USA) to aid adhesion. The samples were sputter-coated under vacuum with a fine layer of gold for 2 minutes at 25 milliamps, using an Emitech K550X sputter-coater. Secondary electron photomicrographs were obtained using a Joel JSM-840A scanning electron microscope, at an accelerating voltage of 10 kV.

### **2.8.2 Dentine Disc Preparation for Scanning Electron Microscopy**

Sound human third molars were sectioned above the pulp horns and beneath the enamel, using a diamond-embedded blade (Buehler, UK) cooled with water. The resultant dentine discs were approximately 800 µm in thickness. The grinding marks were removed by hand-grinding on 1200 grit silicon carbide abrasive paper (Struers, UK). The discs were etched with 8 % (w/v) citric acid (Sigma-Aldrich, UK) for 60 seconds, and subsequently ultrasonicated (Bennet Scientific, UK) in distilled water for 5 minutes. The discs were dehydrated in graded alcohol changes (50 %, 75 % and 100 % [v/v] IDA), and finally placed in

an incubator at 37 °C for 2 hours. The samples were sputter-coated under vacuum with a fine layer of gold for 2 minutes at 25 milliamps, using an Emitech K550X sputter-coater. Secondary electron photomicrographs were obtained from Phenom™ G2 desktop scanning electron microscope, at an accelerating voltage of 10 kV.

#### **2.8.2.1 Quantitative Analysis of Dentine Disc and PET Thinsert SEM Images**

SEM images of dentine and PET Thinserts were used for determination of the diameter of the tubules and pores, respectively. Four SEM images of dentine and PET, were imported into Fiji (ImageJ version 1.46i24) and the threshold was adjusted using the Otsu (1979) algorithm. The resultant binary images were used for automated calculations of the feret diameter (the average of the shortest and longest distances across a boundary) of both tubules and pores. To validate and compare this automated approach, 20 manual measurements were collected per image and statistically analysed. The number of pores or tubules, per unit area were calculated using the particle analyser function in Fiji.

#### **2.8.3 Focussed Ion Beam-scanning Electron Microscopy Analysis of Cells Cultured on**

##### **Porous PET Membranes**

Cells cultured on PET Thinserts were prepared (i.e. fixed, dehydrated, mounted on aluminium stubs and sputter coated) as described in Section 2.8.1 for standard SEM. In order to observe the samples in cross-section, focussed ion beam-scanning electron microscopy (FIB-SEM) 'slice and view' was conducted in a Zeiss CrossBeam 1540 (Carl Zeiss AG, Germany) by the Cavendish Laboratories, University of Cambridge, UK. An area of interest was first selected using top-down SEM. The sample was subsequently positioned to allow the ion beam to impact perpendicular to the surface of the PET Thinsert, thus allowing

FIB milling to 'slice' sequential sections from the volume of interest. Sequential images were captured over a 12 hour period, in which a secondary electron image was captured at the freshly exposed sample, to allow the cross-sectional view. The ion beam current was used at a magnitude of 500 pA. A milling depth of 10  $\mu\text{m}$  was selected in a 40  $\mu\text{m}$  by 40  $\mu\text{m}$  area, and a low beam voltage (3.5 kV) was chosen to minimise sample charging and optimise the visualisation of cellular and non-cellular material.

## **2.9 Microbiological Techniques**

### **2.9.1 Bacterial Culture**

*Streptococcus mutans* (ATCC no. 25175) provided by the Forsyth Institute, (Boston, USA) was verified in-house using cellular, molecular and biochemical phenotype tests (Palmer, 2010) as identified in the Bergey's Manual of Determinative Bacteriology (Holt, 1994). The bacteria were cultured on tryptone soya agar plates (Oxoid, UK) containing 5 % (v/v) horse blood (Oxoid, UK) and maintained in a miniMACS anaerobic workstation (Don Whitley Scientific Limited, UK) at 37 °C.

### **2.9.2 Bacterial Turbidity Assay**

Tryptone soya broth (Oxoid, UK) (10 mL) was dispensed in borosilicate glass culture tubes (FB59537 Fisher Scientific) with vented plastic caps (TB51373 Fisher Scientific) and inoculated with an individual colony of cultured bacteria. The bacteria were incubated anaerobically overnight (Section 2.9.1) with gentle agitation (Vibrax VXR basic, IKA). Following bacterial growth, the culture was homogenously suspended by thorough mixing and the optical density of a 1 mL aliquot was measured at 600 nm in a Jenway 6300 spectrophotometer. Non-inoculated tryptone soya broth, was used to obtain a blank

reading. Bacterial cultures were adjusted to contain  $2 \times 10^5$  cells/mL and were aliquoted (100  $\mu$ L) into each well of a 96-well assay plate (Corning, UK) in addition to 20  $\mu$ L DMCs (10  $\mu$ g/mL) in PBS (Smith *et al.*, 2012a) or bioactive glass-conditioned PBS (1-10 mg/mL) and 80  $\mu$ L tryptone soya broth. A negative control of 20  $\mu$ L PBS and a positive control of 20  $\mu$ L penicillin-streptomycin (0.5 units/mL penicillin and 0.5  $\mu$ g/mL streptomycin) were used. The plate was incubated anaerobically for 24 hours, with gentle agitation, at 37 °C. Following incubation, bacterial turbidity was assessed using an ELX800 Universal Microplate reader (Bio-tex Instruments Inc) at 570 nm.

## **2.10 Chemical Analysis of Bioactive Glass Dissolution**

### **2.10.1 Inductively Coupled Plasma Atomic Emission Spectrometry**

Inductively Coupled Plasma Atomic Emission Spectrometry (ICP-AES) is a precise, analytical chemistry technique used to simultaneously detect multiple elements present at minor and trace levels. The elements of interest (Na, Ca, P and Si) were measured from the dissolution products of bioactive glass in various solutions. The instrument was calibrated using standards of known concentration, thus allowing the atoms present to be quantified. However, to ensure that the elements of interest were detected within the calibration range, the concentration of the standards and the absorption wavelengths at which they were measured, varied according to the samples being tested i.e. samples that contained higher background levels of sodium, such as DMEM and saline, were required to have a different calibration range for Na. Absorption wavelengths for the determination of Ca, Na, P and Si are provided in Table 2.2.

Element	Absorption Wavelengths (nm)
Calcium	317.933
Sodium	588.995
Phosphorous	213.618
Silicon	251.611
Indium	230.606

**Table 2.2 Absorption wavelengths used during ICP-AES.**

Absorption wavelengths used for the determination of Ca, Na, P and Si ions within samples analysed by inductively coupled plasma atomic emission spectrometry (ICP-AES). Indium was used as the internal standard.

A 3 % (v/v) nitric acid solution was prepared using trace metal grade concentrated nitric acid (Romil, UK) and ultrapure water ( $\geq 18.2$  Mohm). The acid was used to wash all grade A glassware, in addition to being the dilution solvent for all standards. The presence of an internal standard, Indium (VWR, UK), in all standards and samples was necessary to correct for instrument instability (Vanhaecke *et al.*, 1993). To account for signal drift (e.g. a decrease in signal intensity over time), the addition of a drift standard of known concentration was measured every 6 samples. Having prepared all standards and samples (preparation described in Sections 2.10.1.2-2.10.1.4), the solutions were transferred to 15 mL tubes (Elkay Laboratories, UK) suitable for trace metal analysis. The ICP-AES instrument measured 10 readings per sample.

### 2.10.1.1 ICP-AES Instrument Operational Parameters

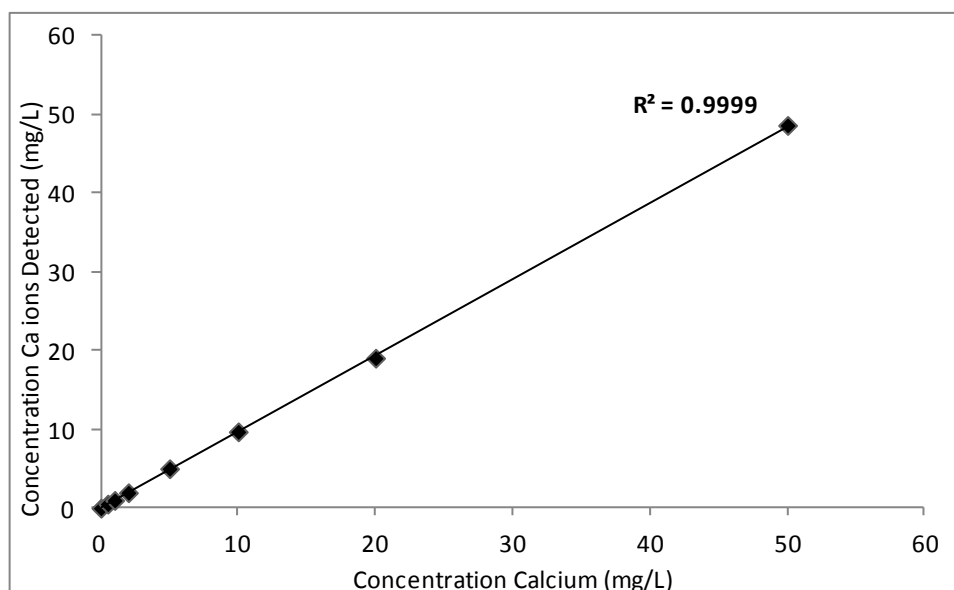
Samples were analysed using a Varian Vista AX ICP. The instrument operating conditions are provided in Table 2.3.

Instrument Condition	Settings
Plasma view	Axial
Power	1.00 kW
Plasma flow	15.0 L/min
Auxiliary flow	1.50 L/min
Nebulizer flow	0.75 L/min
Replicate read time	3.00 s
Instrument stabilisation delay	15 s
Rinse time	30 s
Sample uptake	90 s
Replicates	10
Pump rate	15 rpm

**Table 2.3 Instrument operational parameters used for inductively coupled plasma atomic emission spectrometry.**

### 2.10.1.2 Dissolution of Bioactive Glass in Water

The dissolution of bioactive glass in water was measured to provide a comparison with all other dissolution experiments. The solutions were prepared using the protocol for bioactive glass-conditioned media (see Section 2.5.1.1), however, the addition of DMEM was substituted with distilled water. The solutions were diluted 10-fold, in 3 % (v/v) nitric acid and 10 000 ppm of Indium (VWR) was added. The standards were prepared at 0, 1, 2, 5, 10, 20 and 50 ppm for all four elements analysed (Figure 2.7).



**Figure 2.8 Representative calibration curve used for Inductively Coupled Plasma Analysis.**

Graph displays the concentration of Ca detected in a range of standard solutions prepared in 3 % nitric acid. The coefficient of determination is denoted by the  $R^2$  value on the graph.

#### **2.10.1.3 Dissolution of Bioactive Glass in DMEM**

Bioactive glass-conditioned medium was prepared as described in Section 2.5.1.1. The filtrate was diluted 100-fold in 3 % (v/v) nitric acid, with the addition of 10 000 ppm Indium. The standards were prepared as discussed in Section 2.10.1.2 whereby the Na standards were 10-fold higher than the remaining elements of interest.

#### **2.10.1.4 Bioactive Glass Dissolution in Saline Solution**

Bioactive glass dissolution was assessed in saline solution, with and without the presence of dentine powder. The extraction solutions were prepared as described in Section 2.1.4 and the concentrations of Ca, Na, P and Si were assessed daily in duplicate by ICP-AES. Having centrifuged the samples, they were diluted 20-fold in 3% (v/v) nitric acid and 10 000 ppm



Indium. The standards contained 0, 0.5, 1, 5, 10 and 20 ppm of Ca, P and Si. However, to allow for the increased presence of sodium from the saline solution, the Na standards used were 10-fold more concentrated at 0-200 ppm.

### **2.11 Statistical Analysis**

Data were analysed using Microsoft Excel 2007 (Microsoft Corporation, USA) and SPSS (SPSS Inc, USA). Normal distribution was assessed by the Shapiro-Wilk test, and the paired Student's *t*-test was used to determine statistical significance, whereby  $p \leq 0.05$  (indicated by \*) was considered to be statistically significant. Data are expressed as the mean  $\pm$  standard deviation (SD) and replicates (*n* numbers) are stated in the accompanying text, in forthcoming chapters.

### 3.0 RESULTS CHAPTER ONE

#### 3.1 Biochemical Analysis of Dentine Matrix Components Released by 45S5 Bioactive Glass

The physiochemical reactions of 45S5 bioactive glass are well-established in promoting tubular occlusion for the treatment of dentine hypersensitivity (Greenspan, 2010). However, there is a paucity of data reporting the biological effects of bioactive glass on the dentine-pulp complex. Recent studies have shown that dental materials, such as calcium hydroxide [Ca(OH)<sub>2</sub>] and mineral trioxide aggregate [MTA], are able to interact with human dentine and release proteins and bioactive molecules sequestered within the tissue. It has been proposed that these released molecules may trigger reparative processes by interacting directly with odontoblasts or signalling the recruitment of undifferentiated pulp cells necessary for tissue repair (Graham *et al.*, 2006, Tomson *et al.*, 2007).

This study aimed to investigate the ability of 45S5 bioactive glass, in saline solution, to release dentine matrix components (DMCs) using a well-established *in vitro* extraction technique developed by Smith and Leaver (1979) (as described in Section 2.1.4). The reaction and protein dissolution were monitored daily, throughout the 7-day extraction period, by measuring the pH and absorbance levels of extraction supernatants, respectively. The lyophilised extracts were subsequently biochemically analysed using dye-binding assays and SDS-PAGE gel electrophoresis.

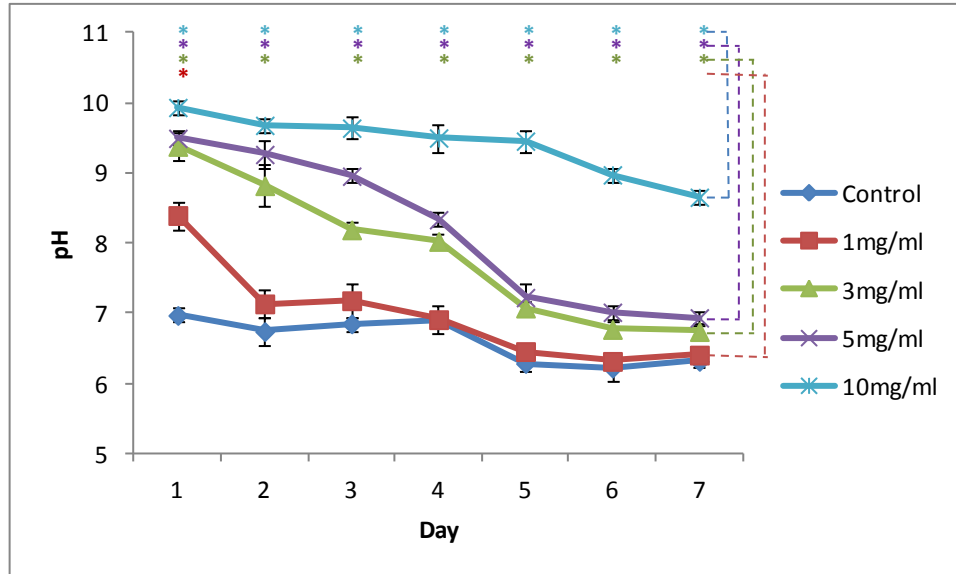
The presence of TGF- $\beta$ 1 is well-characterised in DMCs solubilised by EDTA (Cassidy *et al.*, 1997), Ca(OH)<sub>2</sub> (Graham *et al.*, 2006) and MTA (Tomson *et al.*, 2007). Its function is

fundamental to a wide range of processes from cell proliferation to pulpal repair and regeneration (Smith, 2003). Therefore TGF- $\beta$ 1 levels were determined in the current study as a surrogate marker for bioactive molecule release from the dentine matrix.

### **3.1.1 pH of Extraction Supernatants**

The pH of freshly-collected extraction supernatants was measured daily using a bench-top pH meter (see Figure 3.1). The alkalinity of bioactive glass is well-characterised in the literature and in this study, a dose-dependent increase in pH was observed according to the concentration of bioactive glass in each extraction solution. Despite this trend, the pH was not directly proportional to the concentrations of bioactive glass present in the extraction solutions.

Over the course of the 7-day extraction period, the pH of all extraction solutions exhibited a general decline. At day 1, it was evident that all solutions containing bioactive glass had increased in their pH, as the starting pH of saline containing dentine was approximately 7. A sharp fall in pH of 1.26 units was observed between days 1 and 2 for the 1 mg/mL extraction solution after which its pH profile closely resembled that of the control (saline only) extraction solution and varied minimally. After day 4, extraction solutions (control and 1-5 mg/mL) underwent a minimal rate of pH change for the remaining three days, finally reaching approximately pH 7. In contrast, the 10 mg/mL extraction solution maintained a high pH, with minimal decline over the 7 days. All solutions containing bioactive glass exhibited a significantly higher pH than the relevant controls throughout the course of the extraction period, except the 1 mg/mL solutions, which were only significantly higher ( $p \leq 0.05$ ) than the controls at day 1.



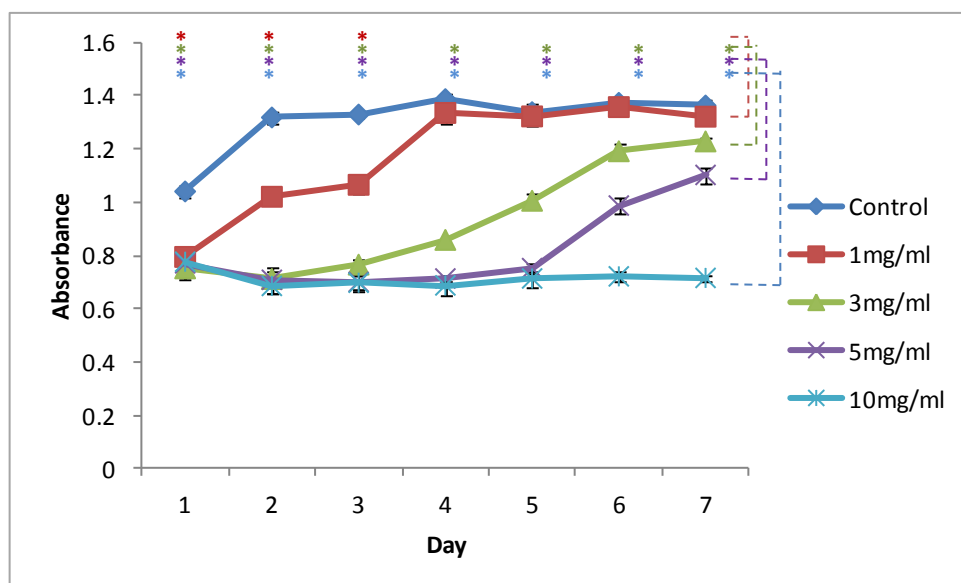
**Figure 3.1 pH profiles of extraction supernatants throughout the 7-day extraction period.**

Extraction solutions contained 1-10 mg/mL bioactive glass powder, 1 g of dentine powder and 10 mL saline solution; control solutions contained saline and dentine only. Solutions were constantly agitated at 4 °C, centrifuged daily and the pH values of the supernatants were measured from days 1-7, prior to solutions being decanted and stored at –20 °C. The centrifuged pellets comprising of bioactive glass and dentine were re-suspended with fresh saline solution daily. Results are a mean of 4 replicates, error bars represent  $\pm$  SD. Statistical significance was assessed using the Student's *t*-test, in which pH values were compared daily to the control solutions (\* =  $p \leq 0.05$ ).

### 3.1.2 Protein Release in Extraction Supernatants

The absorbance of extraction supernatants was measured spectrophotometrically daily at 280 nm, as a surrogate measure of protein release from the powdered dentine (see Figure 3.2). At day 1, all extraction solutions containing bioactive glass had an absorbance value of approximately 0.7, whereas the extraction solutions containing saline only (controls) exhibited a higher absorbance of 1.04. As with the pH, the control and 1 mg/mL bioactive

glass in saline extraction solutions, followed a similar absorbance profile over the 7 day period, whereby the values were significantly higher ( $p \leq 0.05$ ) for the initial 3 days in the control solutions. By day 4, both solutions reached a plateau in absorbance, which mirrored the downward plateau in pH of both solutions after day 4. Extraction solutions containing 3 mg/mL bioactive glass exhibited a steady increase in protein release over the 7-day period, which appeared to stabilise by day 6. In contrast, the absorbance of 5 mg/mL extraction supernatants increased after day 5, which was the point at which they had reached a plateau in pH values for that time period. The absorbance values for the 10 mg/mL extraction solutions were relatively low and exhibited minimal fluctuation over the course of the 7-day extraction period.



**Figure 3.2 Absorbance (280 nm) profiles of extraction supernatants throughout a 7-day extraction period.**

Extraction supernatants were prepared as described in Figure 3.1. The absorbance values of the supernatants at 280 nm, were noted from days 1-7 of the extraction period, to provide a surrogate marker for protein content. Results are a mean of 4 replicates, error bars represent  $\pm$  SD. Statistical significance was assessed using the Student's *t*-test, in which absorbance values were compared daily to the control solutions (\* =  $p \leq 0.05$ ).

### 3.1.3 Percentage Yields of DMCs Recovered

The percentage yield of lyophilised DMCs was calculated from the original weight of dentine powder used in the extraction procedure. The results are tabulated in Table 3.1 and show that a similar yield of lyophilised DMCs was obtained for each of the samples. There were no significant statistical differences detected when compared with the control (saline-released DMCs), potentially reflecting the relatively large standard deviation values.

Concentration of Bioactive Glass in Extraction Solution (mg/mL)	Percentage Yield (%)	± SD
Control (saline)	0.221	0.123
1	0.232	0.082
3	0.261	0.084
5	0.281	0.093
10	0.236	0.050

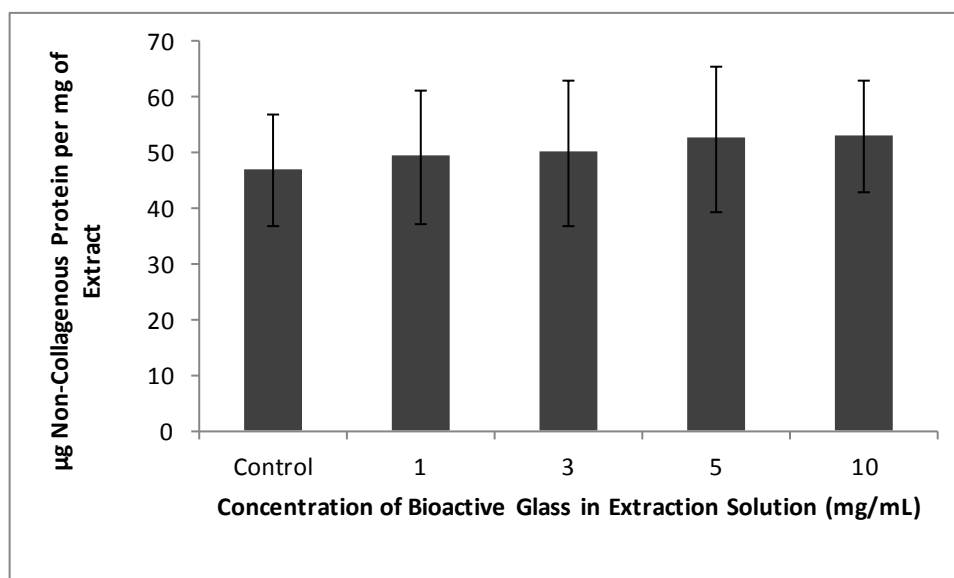
**Table 3.1 Percentage yields of DMCs recovered.**

Values represent the average percentage yield of lyophilised extracts released by bioactive glass in saline solutions (1-10 mg/mL) and control solutions of saline only. Results represent the mean of 5 separate extractions, ± SD. The Student's *t*-test indicated that the yield of DMCs released by 1-10 mg/mL bioactive glass in saline were not statistically different when compared with controls (saline-released DMCs).

### 3.1.4 Characterisation of DMCs

#### 3.1.4.1 Non-collagenous Protein Content of Extracted DMCs

The Bradford dye-binding assay was used to quantify the non-collagenous protein (NCP) content of lyophilised DMCs (see Section 2.2.2). The data (see Figure 3.3) did not show statistical significance when NCP content of bioactive glass-released DMCs was compared with the control (saline-released DMCs). However, the NCP content ranged from 46.92 - 53.56 µg per mg of extract and exhibited a slight trend towards a dose-dependent increase.



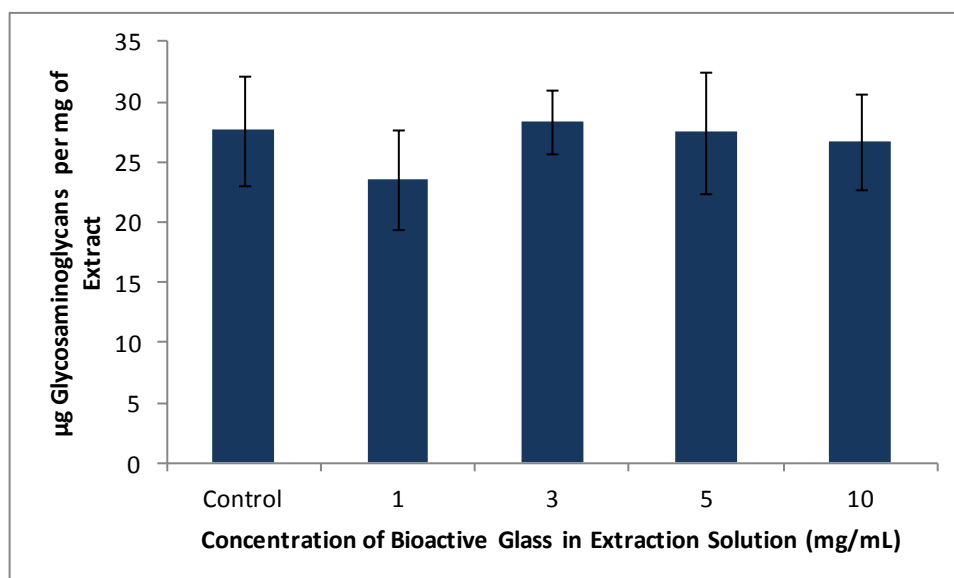
**Figure 3.3 Non-collagenous protein content in extracted DMCs.**

Total weight (per  $\mu\text{g}$  of extract) of non-collagenous proteins extracted by bioactive glass in saline solution (1-10 mg/mL) and control solutions of saline only, determined by the Bradford assay (see Section 2.2.2). Results represent the mean of 5 separate extraction procedures,  $\pm$  SD. Non-collagenous protein content in all DMCs released by 1-10 mg/mL bioactive glass in saline are not statistically different using the Student's *t*-test, when compared against controls (saline-released DMCs).

#### 3.1.4.2 Glycosaminoglycan Content of DMCs

The Farndale assay was used to determine the concentration of glycosaminoglycans (GAGs) present in DMCs released by bioactive glass in saline solutions (1-10 mg/mL) and control solutions (saline only) (see Section 2.2.1). Although statistical significance between controls and test samples was not observed, DMCs released by 1 mg/mL extraction solutions appeared to solubilise the least amount of GAGs (23.53  $\mu\text{g}/\text{mg}$  extract) (see Figure 3.4). However, there was little variation amongst levels of GAGs solubilised by the saline control and the 3-5 mg/mL solutions.





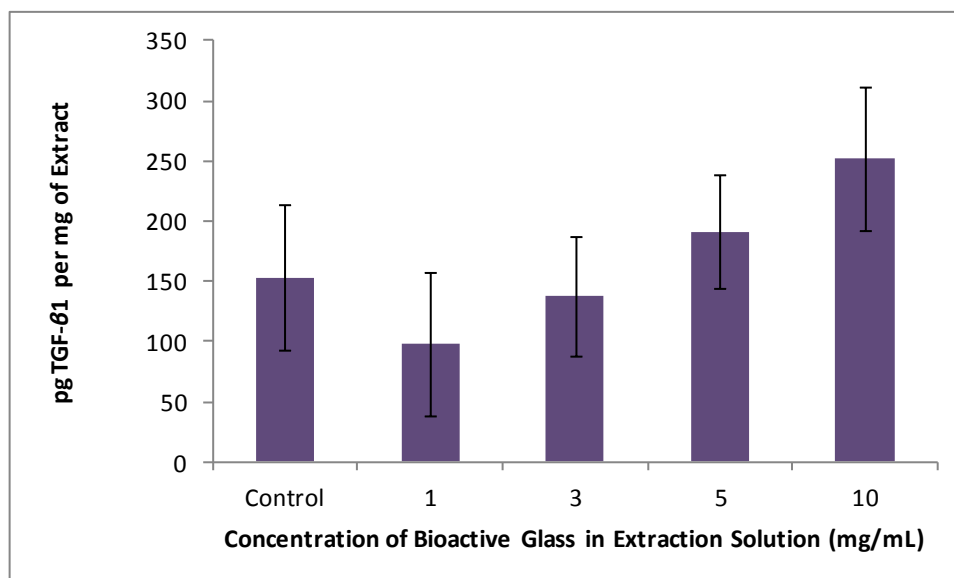
**Figure 3.4 Glycosaminoglycan content in extracted DMCs.**

Total weight (per  $\mu\text{g}$  of extract) of glycosaminoglycans extracted by bioactive glass in saline solution (1-10 mg/mL) and control solutions (saline only), determined by the Farndale assay (see Section 2.2.1). Results represent the mean of 5 separate extraction procedures,  $\pm$  SD. Glycosaminoglycan content in all DMCs released by 1-10 mg/mL bioactive glass in saline are not statistically different when compared against controls (saline-released DMCs), using the Student's *t*-test.

### 3.1.4.3 Quantification of TGF- $\beta$ 1 in Extracted DMCs

The concentrations of TGF- $\beta$ 1 solubilised by bioactive glass and saline solutions (1-10 mg/mL) and controls (saline only) were determined using a solid phase sandwich ELISA (see Section 2.2.3). TGF- $\beta$ 1 was detected in all DMCs (see Figure 3.5) and a clear trend in detected levels was observed. Whilst control and 3 mg/mL extraction solutions released similar amounts of TGF- $\beta$ 1, the 1 mg/mL extraction solution solubilised the least amount. A

trend of a dose-dependent increase in TGF- $\beta$ 1 concentration was observed from DMCs released by 1-10 mg/mL extraction solutions.



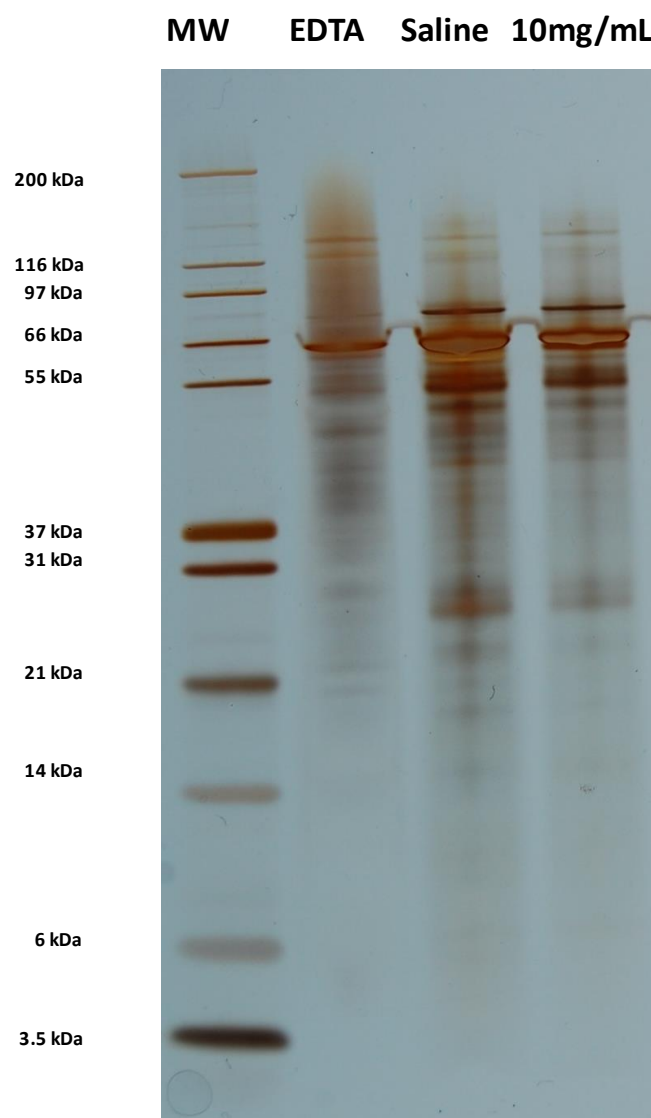
**Figure 3.5 TGF- $\beta$ 1 content in lyophilised extracts.**

Total weight (per pg of extract) of TGF- $\beta$ 1 extracted by 1-10 mg/mL bioactive glass in saline solutions and controls (saline only), determined using a sandwich ELISA (see Section 2.2.3). Results represent the mean of 5 separate extraction procedures,  $\pm$  SD. TGF- $\beta$ 1 content in all DMCs released by 1-10 mg/mL bioactive glass in saline are not statistically different when compared against controls (saline-released DMCs), as determined by the Student's *t*-test.

#### **3.1.4.4 One-dimensional Polyacrylamide Gel Electrophoresis Analysis of DMCs**

Lyophilised DMCs were examined using 1D-SDS PAGE to compare the profiles of proteins solubilised by EDTA, saline and 10 mg/mL bioactive glass in saline (see Section 2.2.4). Figure 3.6 shows a representative silver-stained gel image illustrating proteins separated according to their molecular weight. Upon visual inspection of the gel, the greatest similarities in protein profiles existed between saline- and 10 mg/mL bioactive glass-solubilised DMCs, the

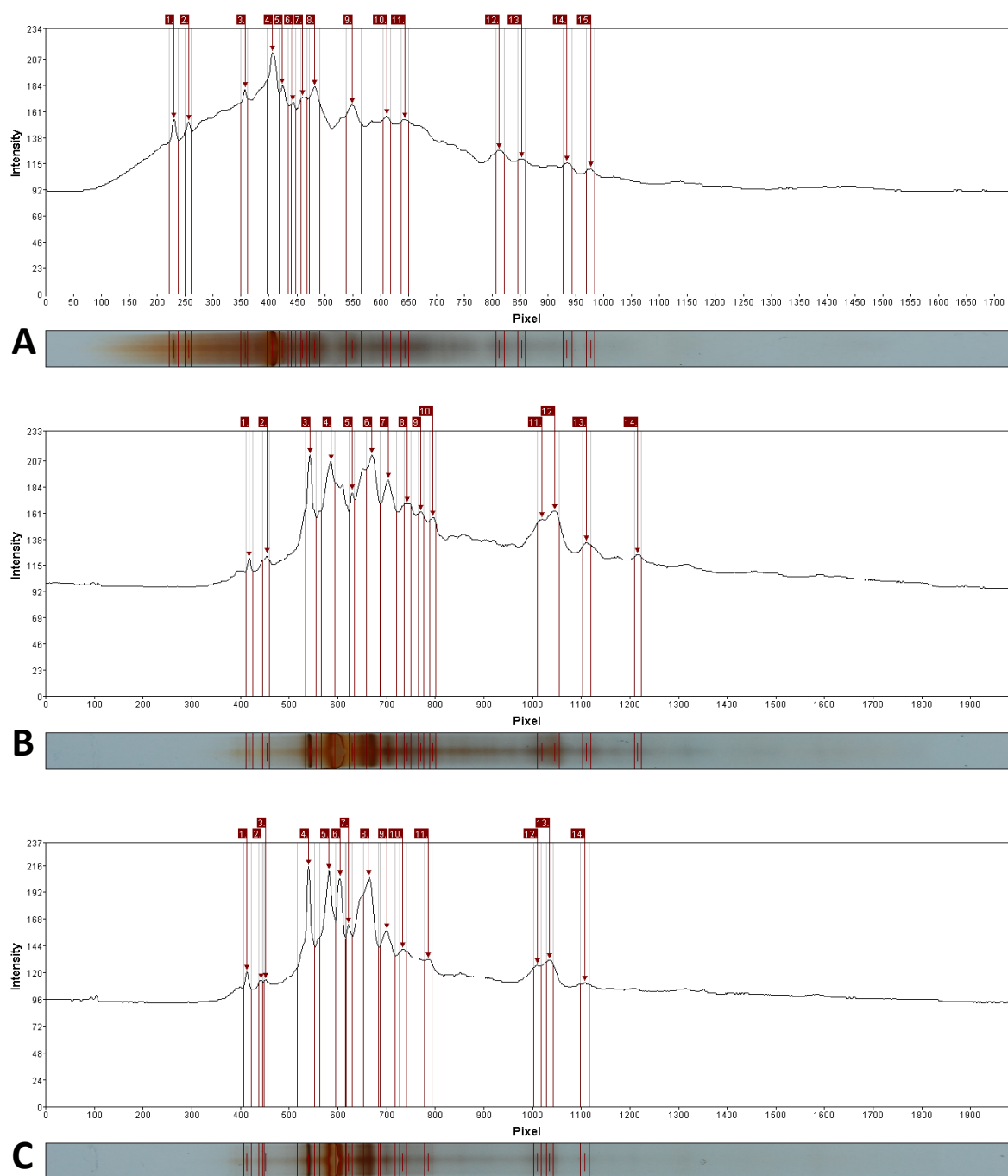
latter of which also contained saline solution as a vehicle. The intensities of the bands appeared greater in the saline-released sample and more bands were also apparent. The profile of EDTA-released DMCs was notably different from the other samples. The intensities of the bands also appeared lower for EDTA-released DMCs, although this may reflect variations in loading of the samples. However, DMCs solubilised by all 3 extraction solutions exhibited many comparable bands, especially in the region of 45-66 kDa, which was also observed in all experimental replicates.



**Figure 3.6 Photographic image of a representative silver-stained SDS-PAGE gel.**

Image shows the different protein profiles of DMCs solubilised by EDTA, saline and 10 mg/mL bioactive glass in saline solution. MW = molecular weight marker, MARK 12 (Invitrogen, UK).

To enable an unbiased and automated examination of the protein bands detected, the gel image was analysed using GelAnalyzer 2010 software (see methods Section 2.2.4). Stained protein bands were automatically detected by the image analysis software generating a lane profile, whereby the peaks corresponded to the location of the bands (Figure 3.7). The molecular weights corresponding to each detected band were calculated using their distance migrated and solving of the equation of the standard curve (see Section 2.2.4) generated by the molecular weight (MW) markers. Table 3.2 summarises the approximate molecular weights of the bands detected by the GelAnalyzer software indicating several similarities in the protein profile of DMCs solubilised by their relative extraction solutions. The data indicate the greatest presence of proteins in the range of 47-126 kDa; within this range, several of the proteins detected were of similar molecular weights across all 3 samples of DMCs. Although fewer bands (12) were detected in the EDTA-solubilised DMCs than bioactive glass and saline-extracted DMCs (14), this may be a reflection of the relative intensities of the different components in the 3 samples or slight differences in the loading of lanes.



**Figure 3.7 Automatic band detection of SDS-PAGE gel by GelAnalyzer software.**

Numbered peaks correspond to position of bands on gel, molecular weights defined in Table 3.2. Lanes represent protein separation of DMCs released by A) EDTA, B) Saline, C) 10 mg/mL bioactive glass in saline solution.

<b>Molecular Weight of Identified Bands (KDa)</b>	<b>EDTA</b>	<b>Saline</b>	<b>10 mg/mL Bioactive Glass in Saline</b>
120-129	125	124	126
110-119	117	114	115, 118
100-109	-	-	-
90-99	90	91	92
80-89	-	82	82
70-79	72, 77	73	74, 77
60-69	65, 69	60, 65	61, 66
50-59	55	51, 56	56
40-49	47	47	49
30-39	-	-	-
20-29	20, 27	21, 25, 27	21, 26, 27
10-19	18	13	-

**Table 3.2 Summary of analysis of SDS-PAGE gel by GelAnalyzer software.**

Separated DMCs were released by EDTA, saline, 10 mg/mL bioactive glass in saline. For the purpose of this table, molecular weights are grouped in increments of 10 kDa. Molecular weights were estimated from a standard curve of MW markers (see Section 2.2.4). Values are to the nearest integer and analysis is of the SDS-PAGE gel in Figure 3.6.

## 4.0 RESULTS CHAPTER TWO

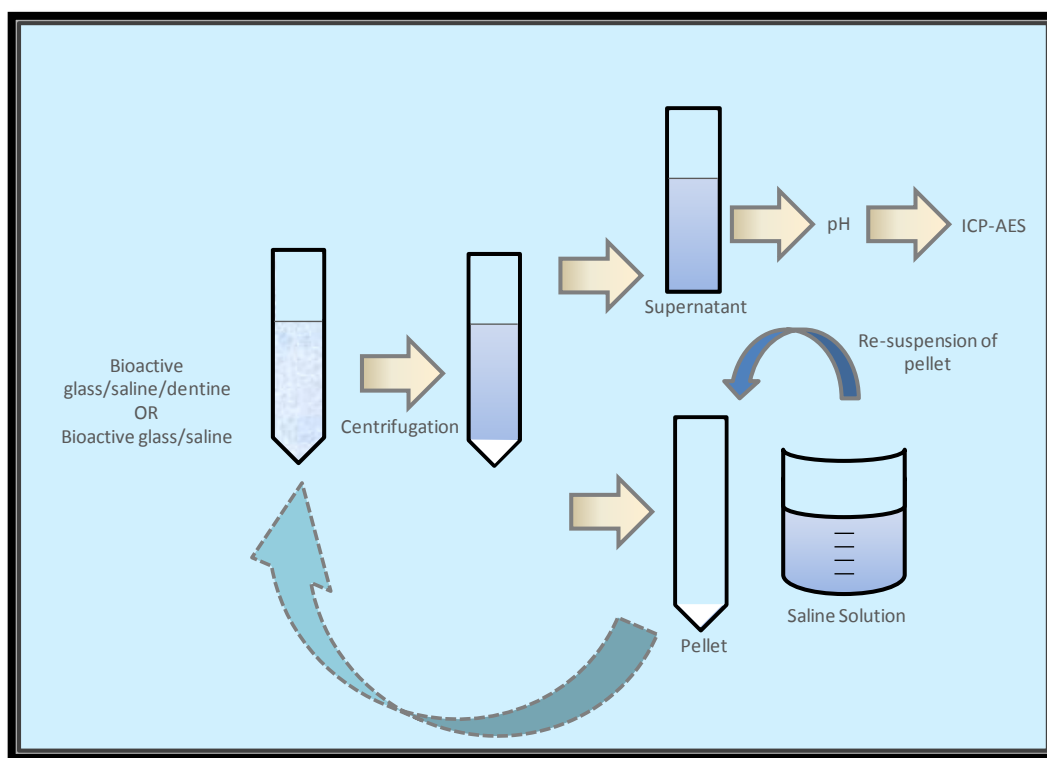
### 4.1 Elemental Analysis of Bioactive Glass Dissolution

When 45S5 bioactive glass is immersed in an aqueous medium, a succession of inorganic chemical processes occur leading to the partial dissolution of the bioactive glass (Hench, 1998). The reported chemical complexity at the glass-liquid interface highlights the requirement for investigating this reaction (Tilocca and Cormack 2011). The previous chapter described the ability of various concentrations (1-10 mg/mL) of bioactive glass in saline solution and control solutions of saline only to release dentine matrix components (DMCs), using a well established *in vitro* extraction technique (Smith and Leaver 1979). The present chapter aims to investigate bioactive glass dissolution during these reactions by assaying the ions released into the daily extraction solutions. This in turn may contribute to our understanding of the mechanism by which DMCs are released from dentine.

To aid the release of DMCs, powdered human dentine in 1-10 mg/mL bioactive glass in saline solution, or control solutions of saline only, were constantly agitated over a 7-day period. The solutions were centrifuged daily, the resultant supernatants were decanted for analysis and fresh saline was added to re-suspend the pellets (see Figure 4.1). As an additional control, an experiment using the same concentrations of bioactive glass in saline solution, was conducted in parallel without the inclusion of dentine (see Section 2.1.4). The supernatants were collected daily and diluted with nitric acid, to stabilise the ionic components of the solutions and prepare them for inductively coupled plasma atomic emission spectroscopy (ICP-AES).



The delivery of bioactive glass dissolution products to cells in previous studies (Xynos *et al.*, 2000a,b) has been via a bioactive glass-conditioned cell culture medium (DMEM), whereby solutions were conditioned with bioactive glass for 24 hours after which the particulate bioactive glass was subsequently removed via filtration. The second part of this chapter aims to use ICP-AES to establish the concentration of the elements of interest that will be delivered to cells (see Results Chapter Three). The elements analysed by ICP-AES were the reported constituents of 45S5 bioactive glass, and therefore ICP-AES was used to determine the concentration of Na, C, P and Si ions.

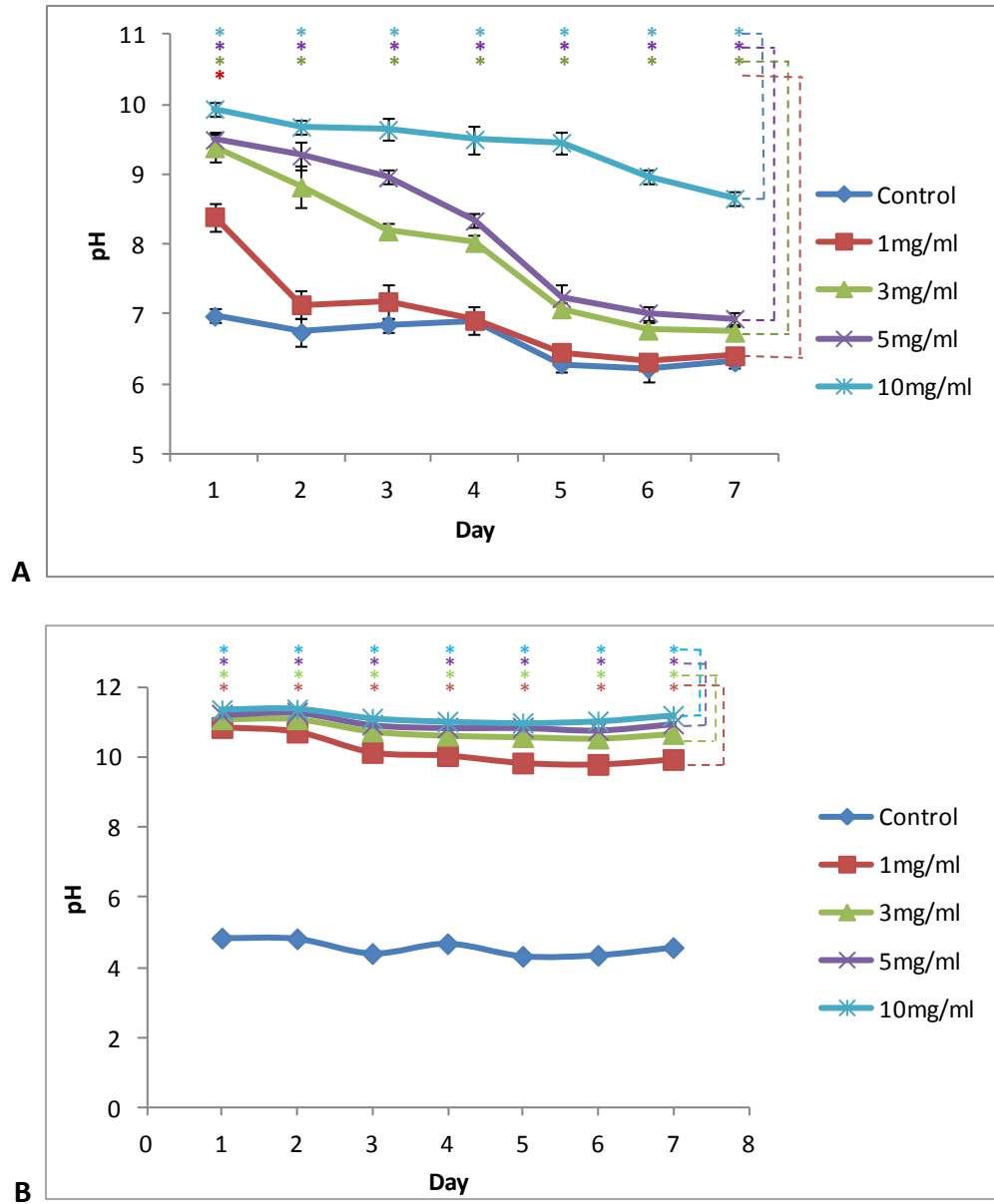


**Figure 4.1 Schematic diagram illustrating the extraction process.**

Solutions of bioactive glass, saline and powdered dentine, or solutions of bioactive glass and saline (without dentine) were constantly agitated for 7 days (see section 2.1.4). Solutions were centrifuged daily, the supernatant was decanted for analyses (pH and ICP-AES) and the pellet was re-suspended in fresh saline solution.

#### **4.1.1 pH of Supernatants Over 7-day Extraction**

The pH values of supernatants were measured daily throughout the 7-day extraction period to monitor the dissolution reactions taking place. Although the pH profile of the dentine extraction supernatants (prepared from dentine, bioactive glass and saline) were discussed in Results Chapter One (see Section 3.0), they have been included below to aid comparison of the pH profile of extraction supernatants prepared from bioactive glass and saline only. The results indicated that the absence of dentine altered the pH profile of solutions considerably. The pH values of the control solutions in the presence of dentine (see Figure 4.2A) were consistently higher than the pH values of the control solutions in the absence of dentine (Figure 4.2B) by approximately 2 units, throughout the 7-day period. Similar to the dentine extraction supernatants, the pH of supernatants prepared from 1-10 mg/mL bioactive glass and saline only, increased in a dose-dependent manner; however, the concentrations of bioactive glass were not directly proportional to the pH values of the supernatants, as also observed with the dentine extraction supernatants. It was also apparent that the pH values, for the corresponding concentrations of bioactive glass, in the supernatants prepared from the bioactive glass and saline only extraction were greater (in the range of 10-12 units) than the dentine extraction supernatants, whereby the pH of all solutions was less than 10 units. The pH profile for the dentine extraction solutions exhibited a general and relatively gradual decline over the 7-day period, whereas the bioactive glass and saline only extraction supernatants maintained relatively consistent pH values over the course of the extraction period. The pH values of solutions containing bioactive glass and saline only differed significantly from control solutions containing saline only ( $p \leq 0.05$ ).



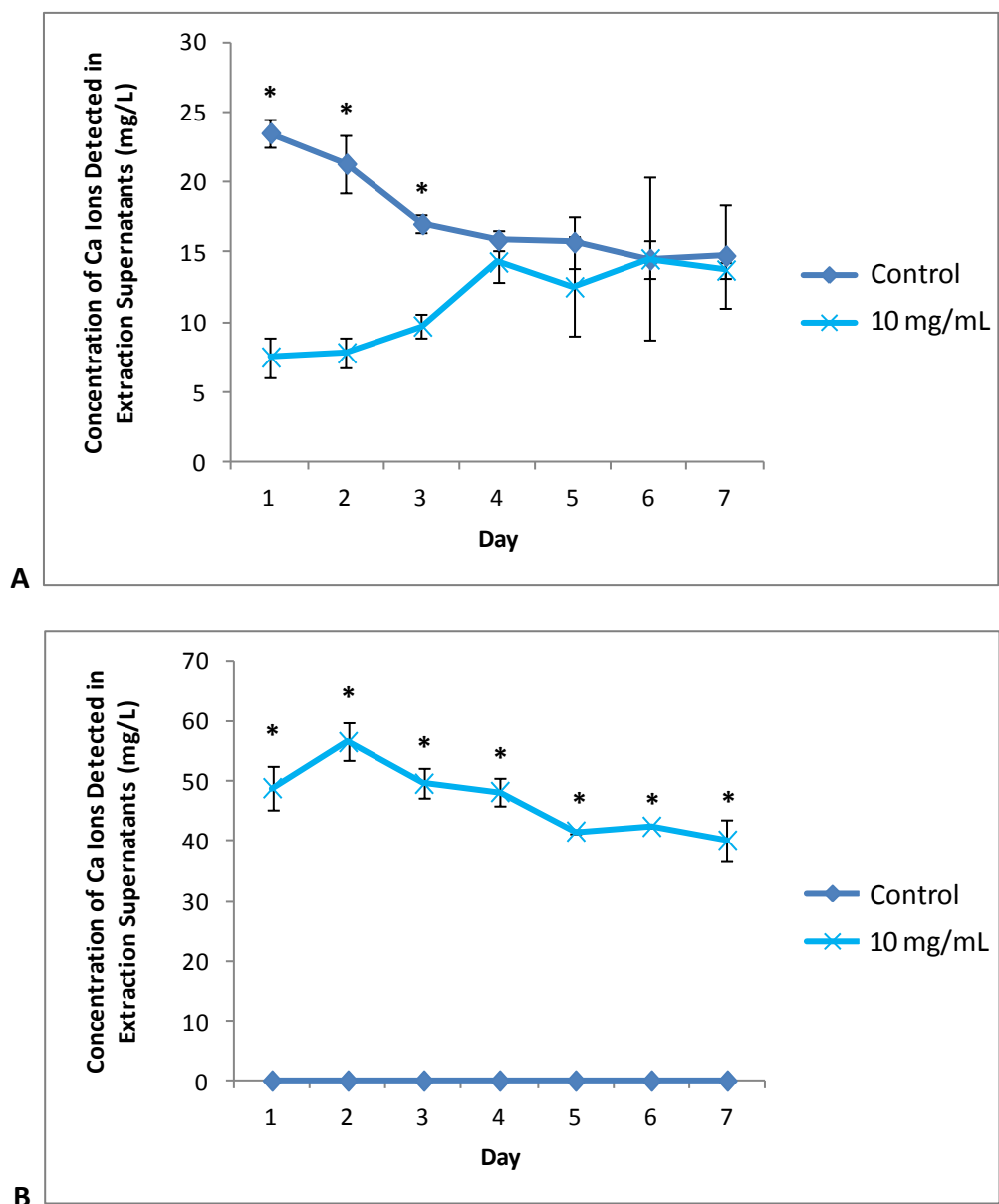
**Figure 4.2 pH profile of extraction supernatants, throughout a 7-day extraction period.**

**Graph A)** pH profile of dentine extraction supernatants. **Graph B)** pH profile of bioactive glass and saline only extraction supernatants. All solutions containing 1-10 mg/mL bioactive glass were constantly agitated at 4 °C, centrifuged daily and the pH values of the supernatants were noted from days 1-7. Results are a mean of 4 replicates, error bars represent  $\pm$  SD. Statistical significance was assessed using the Student's *t*-test, in which pH values were compared daily to the control solutions (\* =  $p \leq 0.05$ ).

## **4.1.2 Bioactive Glass Dissolution in Extraction Supernatants**

### **4.1.2.1 Calcium Ion Concentrations in Extraction Supernatants**

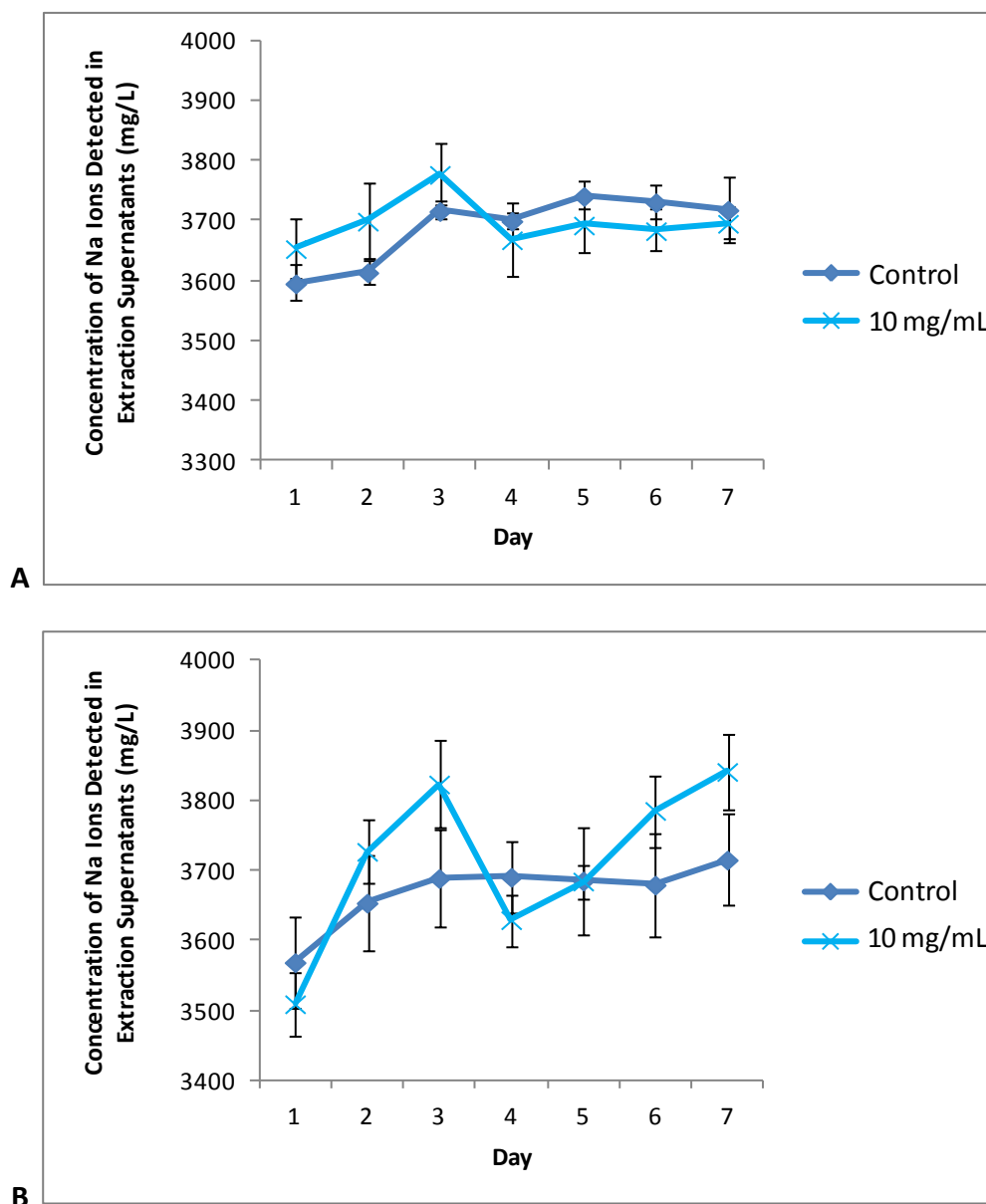
The levels of Ca ions detected in the supernatants from the dentine extraction, and bioactive glass and saline only extraction are graphically represented in Figure 4.3. In the control supernatants (for which extractions did not contain bioactive glass), Ca ions were only detected in those that were prepared with dentine (see Figure 4.3A), and were not detected in solutions prepared in the absence of dentine (i.e. saline only) (see Figure 4.3B). A contrasting effect was observed in the Ca ion levels detected in the dentine extraction supernatants (see Figure 4.3A), whereby during days 1-3 the Ca ion concentrations increased in supernatants prepared with 10 mg/mL bioactive glass, but decreased in control solutions. Statistical analysis indicated that the Ca ion levels in the dentine extraction supernatants prepared with 10 mg/mL bioactive glass were significantly higher than the control solutions during days 1-3; by day 4 the levels had converged and appeared to plateau for the remainder of the extraction period. In the bioactive glass and saline only extraction supernatants (prepared with 10 mg/mL bioactive glass), an increase in Ca ion concentration was observed at day 2, which was followed by a gradual decline for the remainder of the extraction period (see Figure 4.3B). The range of Ca ions detected in the extraction supernatants prepared with 10 mg/mL bioactive glass and saline only, was approximately 5-fold lower in the dentine extraction supernatants prepared with 10 mg/mL bioactive glass.



**Figure 4.3 Concentration of Ca ions detected in daily extraction supernatants by ICP-AES.** Ca ion levels in **A)** dentine extraction supernatants or **B)** bioactive glass and saline only extraction supernatants. Solutions containing dentine and 10 mg/mL bioactive glass in saline, or 10 mg/mL bioactive glass and saline only were constantly agitated for 7 days at 4 °C, and centrifuged daily. Control solutions contained dentine and saline, or saline only. Supernatants were decanted and diluted with nitric acid for ICP-AES, and the pellets were re-suspended with saline solution daily. Results represent a mean of 3 replicates, error bars signify  $\pm$ SD. Statistical significance was assessed by comparing the concentration of Ca ions in solutions prepared with bioactive glass against the control (saline) at each time point using the Student's *t*-test. \* =  $p \leq 0.05$ .

#### **4.1.2.2 Sodium Ion Concentrations in Extraction Supernatants**

The concentration of Na ions detected in all extraction supernatants was relatively high due to the Na present in saline solution. The supernatants prepared from 10 mg/mL bioactive glass in saline solutions in both dentine and saline extractions (Figure 4.4A and B) exhibited similar trends in Na levels during days 1-4, whereby an increase in concentration up to day 3 was observed, followed by a minor decrease at day 4. In the dentine extraction supernatants, the Na levels remained relatively constant after day 4 (see Figure 4.4A), whereas in the saline extraction an increase in Na ion concentration was observed during the remainder of the extraction period (see Figure 4.4B). A similar profile of Na ions was detected in the control solutions for both dentine and saline extraction supernatants. A relative increase in Na ion concentration was detected from days 1-3, but the levels appeared to plateau from days 4-7. The concentration range of Na ions in control solutions was notably similar for both sets of extractions, and no statistical differences were observed between Na levels in extraction supernatants prepared with control and 10 mg/mL bioactive glass.



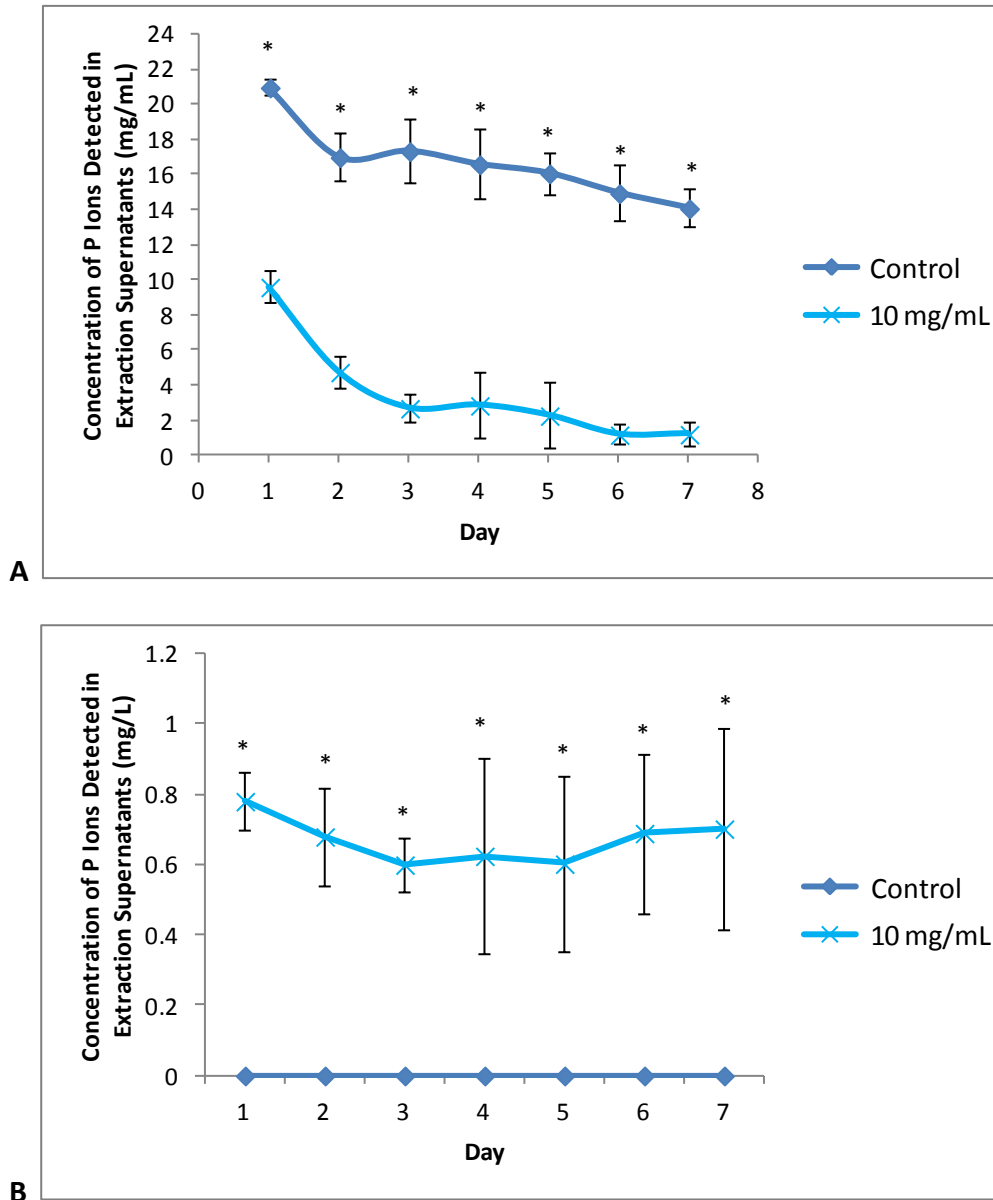
**Figure 4.4 Concentration of Na ions detected in daily extraction supernatants by ICP-AES.**

**Graph A)** Na ion levels in supernatants prepared with 10 mg/mL bioactive glass, saline and dentine or dentine and saline only (controls). **Graph B)** Na ion levels in supernatants prepared with 10 mg/mL bioactive glass and saline only, or saline only (controls). Solutions were prepared as illustrated in Figure 4.1. Data are expressed as a mean of 3 replicates, with error bars representing  $\pm$  SD. Results are not deemed to be statistically significant with the Student's *t*-test ( $p \leq 0.05$ ), when comparing Na ion concentration in 10 mg/mL solutions, against the control at each time point.

#### **4.1.2.3 Phosphorous Ion Concentrations in Extraction Supernatants**

The P ion levels for dentine extraction supernatants prepared with both control solutions and 10 mg/mL bioactive glass in saline declined over the 7-day period (see Figure 4.5A). A significantly higher P ion concentration for all supernatants prepared with control solutions relative to the supernatants prepared with 10 mg/mL bioactive glass at each time point was observed. In the bioactive glass and saline only extraction supernatants, (see Figure 4.5B) notably lower concentrations of P ions were detected, compared with the levels detected in dentine extraction supernatants. P ions were not identified in supernatants prepared with control solutions throughout the extraction period, therefore indicating that dentine was the source of P ions detected in the dentine control extraction solutions. As with the dentine extraction, analysis of the bioactive glass and saline only extraction revealed that the supernatants prepared with 10 mg/mL bioactive glass contained a significantly higher concentration of P ions at all time-points analysed, when compared with the supernatants prepared with control solutions.



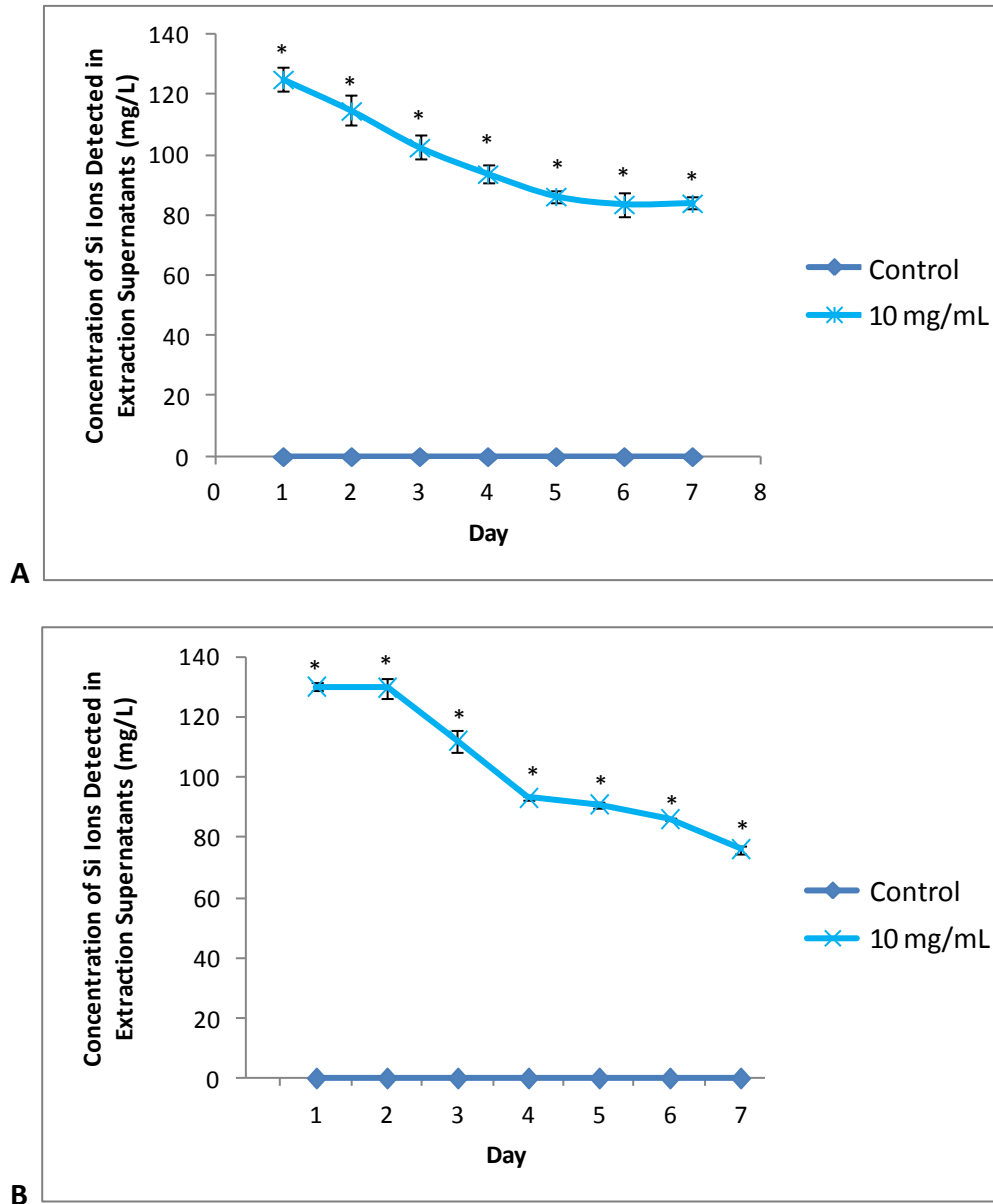


**Figure 4.5 Concentration of P ions detected in daily extraction supernatants by ICP-AES.**

**Graph A)** P ion levels in supernatants prepared with 10 mg/mL bioactive glass, saline and dentine or dentine and saline only (controls). **Graph B)** P ion levels in supernatants prepared with 10 mg/mL bioactive glass and saline only, or saline only (controls). Solutions were prepared as illustrated in Figure 4.1. Results represent a mean of 3 separate extractions, error bars indicate  $\pm$  SD. Statistical significance of P ion concentration at each time point, relative to the control solutions was assessed by the Student's *t*-test. \* =  $p \leq 0.05$ .

#### **4.1.2.4 Silicon Ion Concentrations in Extraction Supernatants**

Comparison of the Si ion concentration detected in supernatants from the dentine extractions and bioactive glass and saline only extractions identified a similar trend (see Figures 4.6A and B, respectively). For both extractions, no Si ions were detected in supernatants prepared with control solutions throughout the entire extraction period, as bioactive glass was not present in the extraction solutions. Over the 7-day period, a decline in Si ions was observed in both dentine and saline extractions prepared with 10 mg/mL bioactive glass, within the range of approximated 80-130 mg/mL. The silicon ion concentration in dentine extractions followed a more sigmoidal-shaped decline as compared with the 10 mg/mL bioactive glass and saline only extraction.



**Figure 4.6 Concentration of Si ions detected in daily extraction supernatants by ICP-AES.**

**Graph A)** Si ion levels in supernatants prepared with 10 mg/mL bioactive glass, saline and dentine or dentine and saline only (controls). **Graph B)** Si ion levels in supernatants prepared with 10 mg/mL bioactive glass and saline only, or saline only (controls). Solutions were prepared as illustrated in Figure 4.1. Results represent a mean of 3 replicates, error bars represent  $\pm$  SD. Statistical significance of Si ion concentration at each time point, relative to the control solutions was assessed by the Student's *t*-test. \* =  $p \leq 0.05$ .

### **4.1.3 Comparison of Bioactive Glass Dissolution in dH<sub>2</sub>O and DMEM**

Three of the elemental constituents of bioactive glass (Ca, P and Na) are reported by the manufacturer to be present in DMEM, which would alter the concentrations of the bioactive glass dissolution products detected by ICP-AES. Therefore to provide a control, distilled water (dH<sub>2</sub>O) was also conditioned with the same concentrations of bioactive glass for 24 hours (see methods Section 2.10.1.2). To observe whether DMEM exerted a buffering effect, the pH values of all solutions were initially measured.

#### **4.1.3.1 pH of Bioactive Glass-conditioned dH<sub>2</sub>O and DMEM**

The pH values of bioactive glass-conditioned dH<sub>2</sub>O and DMEM are listed in Table 4.1. The pH of dH<sub>2</sub>O at the University of Birmingham Dental School is relatively acidic with a pH of 4.9. However, when the dH<sub>2</sub>O was incubated with 1-10 mg/mL bioactive glass, the pH increased to a value of 11, and this did not alter with the different concentrations of bioactive glass added. In contrast, the addition of bioactive glass to DMEM resulted in a dose-dependent increase in pH in the range of 7.9 to 10. This change in pH was not directly proportional to the concentration of bioactive glass added to condition the medium.

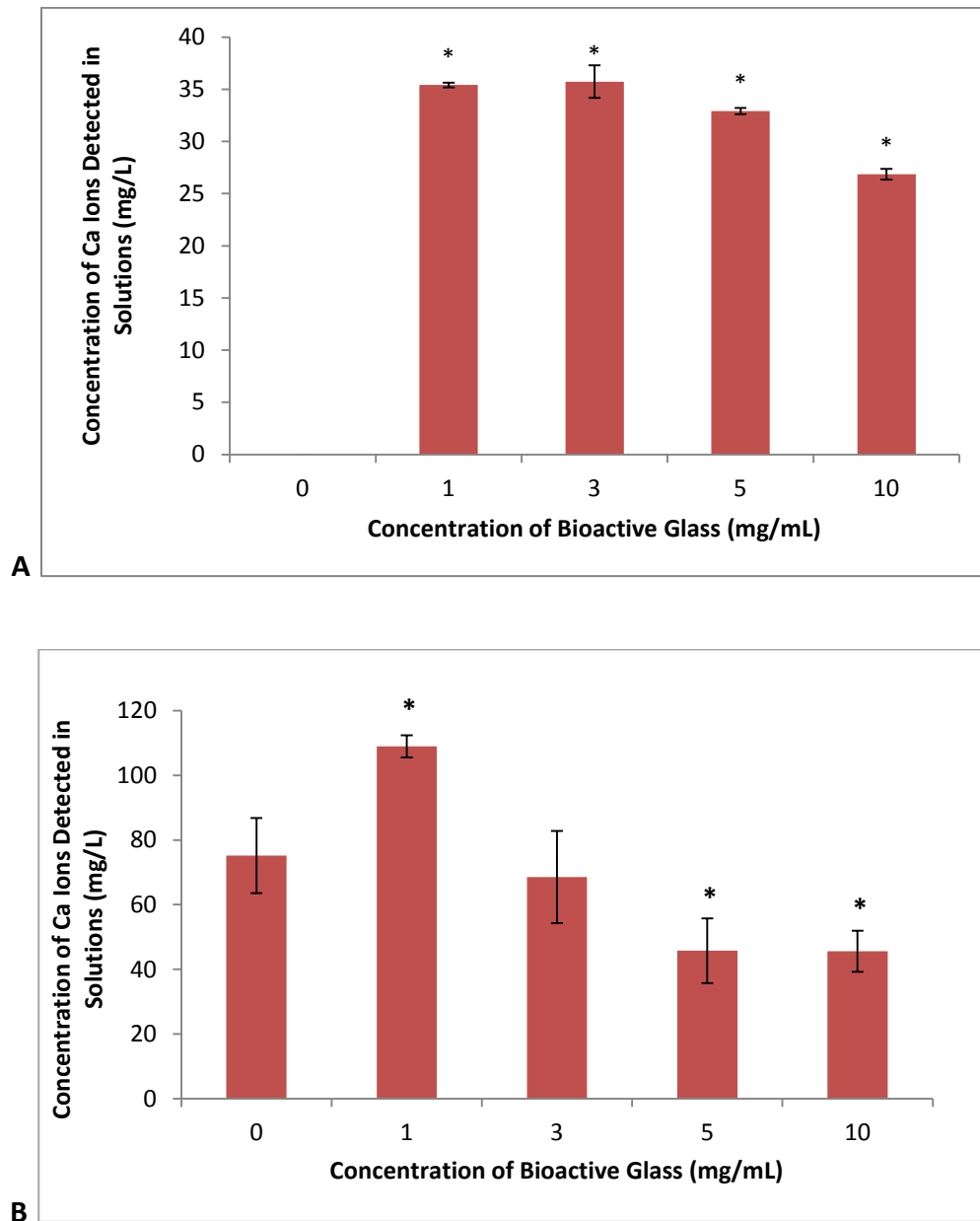
Concentration of Bioactive Glass (mg/mL)	pH in dH <sub>2</sub> O	pH in DMEM
Control (no bioactive glass)	4.9 (0.02)	7.9 (0.01)
1	11 (0)	8.8 (0.02)
3	11 (0)	9.1 (0.01)
5	11 (0)	9.5 (0.01)
10	11 (0)	10 (0.02)

**Table 4.1 pH of bioactive glass-conditioned dH<sub>2</sub>O and DMEM.**

Solutions were prepared with 1-10 mg/mL bioactive glass (see Section 2.5.1.1), and control solutions consisted of either dH<sub>2</sub>O or DMEM only. Results represent n = 4, ± SD are listed in parentheses.

#### **4.1.3.2 Calcium Ion Concentrations in Bioactive Glass-conditioned dH<sub>2</sub>O and DMEM**

The concentrations of Ca ions in bioactive glass-conditioned dH<sub>2</sub>O and DMEM are shown in Figure 4.7. A statistically significant increase in Ca ion concentration, relative to the control, was observed in solutions that had been conditioned with 1-10 mg/mL bioactive glass. Ca ions were not identified in dH<sub>2</sub>O alone, whereas there were approximately 35 mg/L Ca detected in 1 and 3 mg/mL solutions, followed by a dose-dependent decrease for 5 and 10 mg/mL solutions. DMEM alone (control) contained Ca ions and thus, the Ca levels in all bioactive glass-conditioned DMEM solutions were considerably higher than those in the bioactive glass-conditioned dH<sub>2</sub>O. Interestingly, there was an increase in Ca ions seen at 1 mg/mL, whilst higher concentrations of bioactive glass-conditioned DMEM resulted in a decline in the concentration of Ca ions to below controls. A significant difference in concentration, relative to the control, was observed for the 1, 5 and 10 mg/mL solutions, whereas the 3 mg/mL solution contained similar levels of Ca.

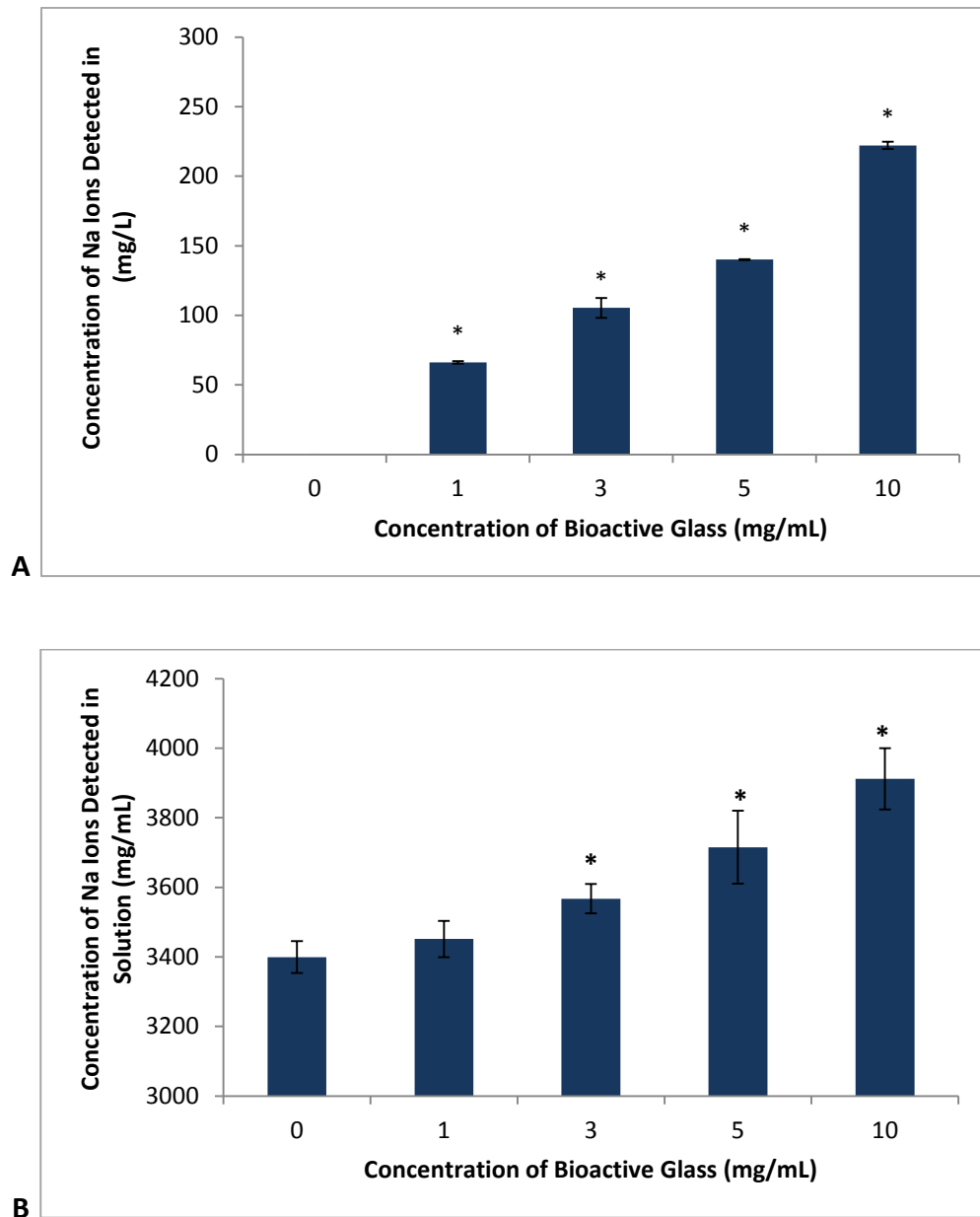


**Figure 4.7 Concentration of calcium ions, detected by ICP-AES.**

Ca ions were measured in **A)** bioactive glass-conditioned dH<sub>2</sub>O or **B)** bioactive glass-conditioned DMEM. 1-10 mg/mL bioactive glass was incubated with either dH<sub>2</sub>O or DMEM (supplemented with 10 % FCS), under constant agitation, for 24 hours at 37 °C. The solutions were filtered through a 0.22 µm membrane, and diluted with 3% (v/v) nitric acid for ICP-AES. Results represent the mean of 4 separate preparations, ± SD. Statistical significance was assessed by the Student's *t*-test, whereby Ca ion levels in 1-10 mg/mL solutions were compared with the controls (DMEM or dH<sub>2</sub>O only). \* =  $p \leq 0.05$ .

#### **4.1.3.3 Sodium Ion Concentrations in Bioactive Glass-conditioned dH<sub>2</sub>O and DMEM**

A comparison of Na ion concentration in bioactive glass-conditioned dH<sub>2</sub>O and DMEM, is provided (Figure 4.8). There were no Na ions detected in dH<sub>2</sub>O control solutions. For the 1-10 mg/mL bioactive glass-conditioned dH<sub>2</sub>O solutions, a dose-dependent increase in Na ions was observed, however, this was not directly proportional to the concentration of bioactive glass. Distinctly higher levels of Na ions were observed in the DMEM solutions, as the medium is supplemented (by the manufacturer) with sodium pyruvate. Na ions were detected in control solutions (DMEM only), and this was at similar levels to the concentration of Na ions observed in the 1 mg/mL solutions. A dose-dependent increase in Na ions was also detected, with increasing concentrations of bioactive glass used to condition the DMEM. DMEM solutions conditioned with 3-10 mg/mL bioactive glass had significantly higher concentrations of Na ions than control solutions.



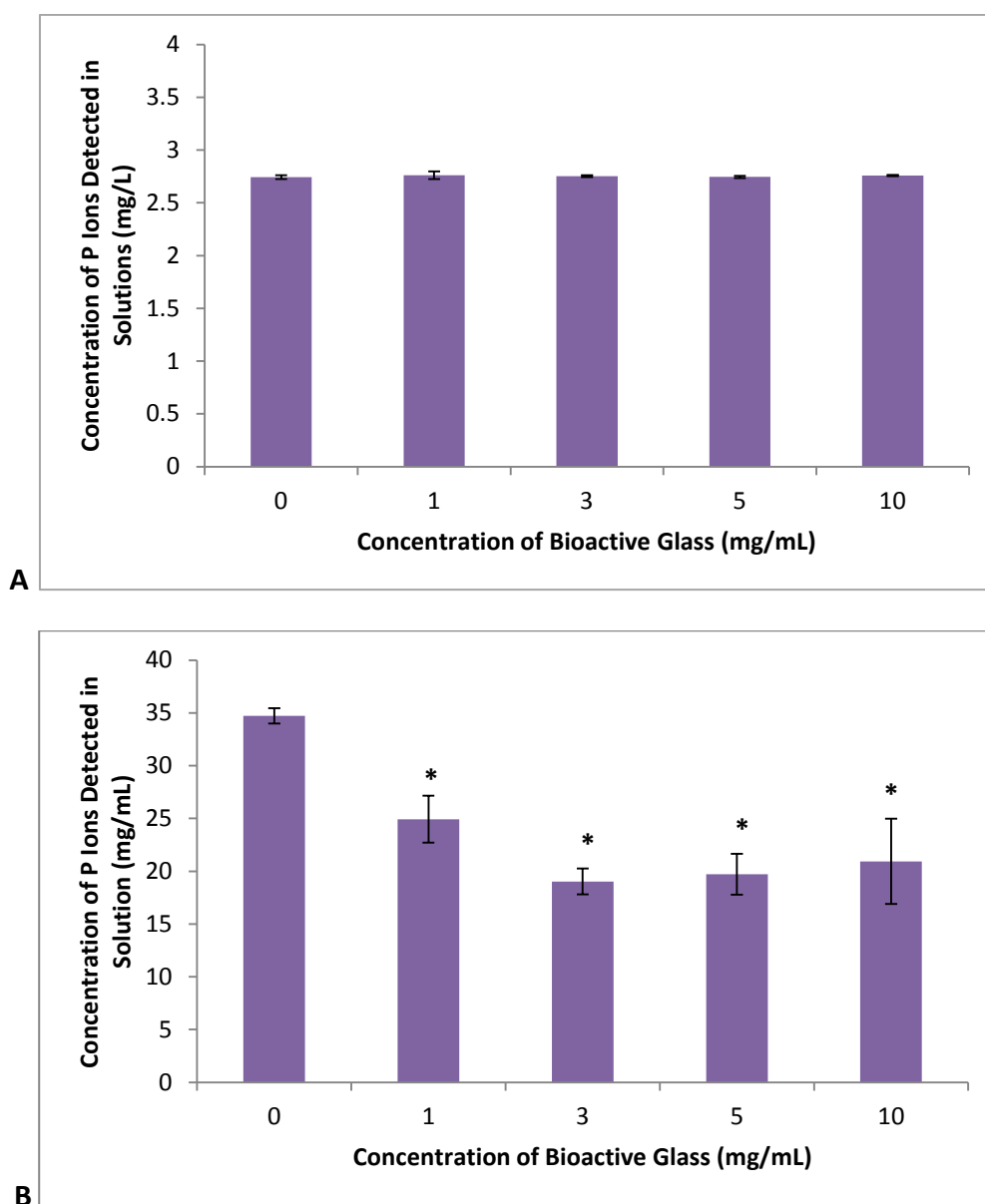
**Figure 4.8 Concentration of sodium ions, detected by ICP-AES.**

Na ions were measured in **A)** bioactive glass-conditioned dH<sub>2</sub>O or **B)** bioactive glass-conditioned DMEM. Solutions were prepared as described in Figure 4.7. Results represent the mean of 4 separate preparations,  $\pm$  SD. Statistical significance was assessed by the Student's *t*-test, in which Na ion levels in 1-10 mg/mL solutions were compared against the control solutions (d H<sub>2</sub>O or DMEM only). \* =  $p \leq 0.05$ .



#### **4.1.3.4 Phosphorous Ion Concentrations in Bioactive Glass-conditioned dH<sub>2</sub>O and DMEM**

The concentration of P ions in solutions conditioned with 1-10 mg/mL bioactive glass are shown graphically in Figure 4.9. The P levels detected in dH<sub>2</sub>O solutions were all relatively low (approximately 2.7 mg/L), regardless of the concentration of bioactive glass. In the DMEM solutions, the control solution (DMEM only) contained the highest level of P ions, and the solutions conditioned with 1-10 mg/mL bioactive glass had significantly lower concentrations of P ions. The decline in P ions appeared to plateau in solutions conditioned with 3-10 mg/mL bioactive glass.

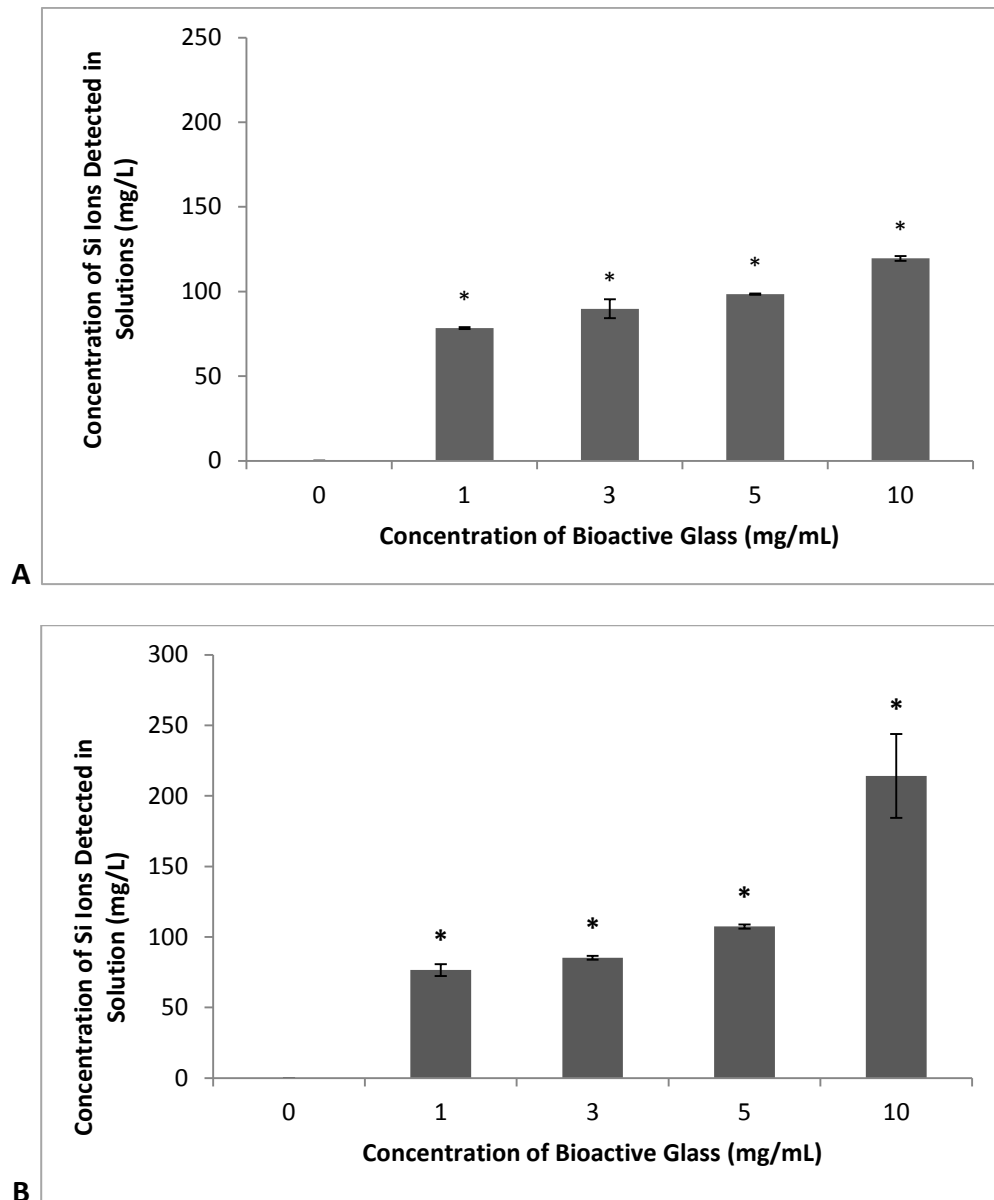


**Figure 4.9 Concentration of phosphorous ions, detected by ICP-AES.**

P ions were measured in **A)** bioactive glass-conditioned dH<sub>2</sub>O or **B)** bioactive glass-conditioned DMEM. Solutions were prepared as described in Figure 4.7. Results represent the mean of 4 separate preparations,  $\pm$  SD. Statistical significance was assessed by the Student's *t*-test, whereby ion levels in 1-10 mg/mL solutions were compared against the control solutions (dH<sub>2</sub>O or DMEM only). \* =  $p \leq 0.05$ .

#### **4.1.3.5 Silicon Ion Concentrations in bioactive glass-conditioned dH<sub>2</sub>O and DMEM**

The concentrations of Si ions detected in bioactive glass-conditioned dH<sub>2</sub>O and DMEM, are displayed in Figure 4.10. There were no Si ions detected in control solutions for dH<sub>2</sub>O and DMEM samples. However, the addition of bioactive glass resulted in a dose-dependent increase in Si ion concentration, in both dH<sub>2</sub>O and bioactive glass-conditioned solutions. Comparing levels of Si ions, dose-by-dose (of bioactive glass) in DMEM and dH<sub>2</sub>O samples, minimal differences were observed between controls, 1, 3 and 5 mg/mL bioactive glass-conditioned solutions. The main difference in Si ion concentration was detected in the solutions conditioned with 10 mg/mL bioactive glass, whereby bioactive glass-conditioned DMEM had much higher levels of Si ions than the bioactive glass-conditioned dH<sub>2</sub>O. A directly proportional increase in Si ion concentration was detected in the bioactive glass-conditioned DMEM for the 5 and 10 mg/mL solutions, whereby the numerical averages were 107.36 and 214.158, respectively.



**Figure 4.10** Concentration of silicon ions, detected by ICP-AES.

Si ions were measured in **A)** bioactive glass-conditioned dH<sub>2</sub>O or **B)** bioactive glass-conditioned DMEM. Solutions were prepared as described in Figure 4.7. Results represent the mean of 4 separate preparations,  $\pm$  SD. Statistical significance was assessed by the Student's *t*-test, whereby Si ion levels in 1-10 mg/mL solutions were compared against the control solutions (dH<sub>2</sub>O or DMEM only). \* =  $p \leq 0.05$ .

## 5.0 RESULTS CHAPTER THREE

### 5.1 Eukaryotic and Prokaryotic Cellular Responses to Bioactive Glass Dissolution

#### Products and Bioactive Glass in Saline-released DMCs

The previous chapter (see Section 4.0) assessed the ionic dissolution products of bioactive glass in DMEM and demonstrated the presence of Ca, Na, P and Si ions released into solution. Studies by Xynos *et al.*, (2000a) have previously shown that the ionic dissolution products of 45S5 bioactive glass in DMEM can promote mineralising cell activity, such as proliferation, in osteoblasts. During the application of dental products, which contain 45S5 bioactive glass, the ionic dissolution products may contact cells of the dentine-pulp complex. The studies described below therefore aimed to analyse the effect of the ionic dissolution products on pulpal cells using assays to assess cell viability and metabolic activity.

In addition, Results Chapter One also demonstrated the ability of various concentrations of bioactive glass in saline solution and control solutions of saline to solubilise dentine matrix components (DMCs); their subsequent biochemical analysis revealed physiologically relevant groups of molecules, such as glycosaminoglycans and non-collagenous proteins. Research has previously shown the cellular effects exerted by released DMCs (Graham *et al.*, 2006) and the studies described below further investigated whether DMCs solubilised by bioactive glass affected cell viability and metabolic activity.

In contrast to the positive effects reported for bioactive glass dissolution products and DMCs on eukaryotic cells, these ions and molecules have also been reported to have inhibitory effects on bacterial growth. Indeed, the high aqueous pH of 45S5 bioactive glass is reported

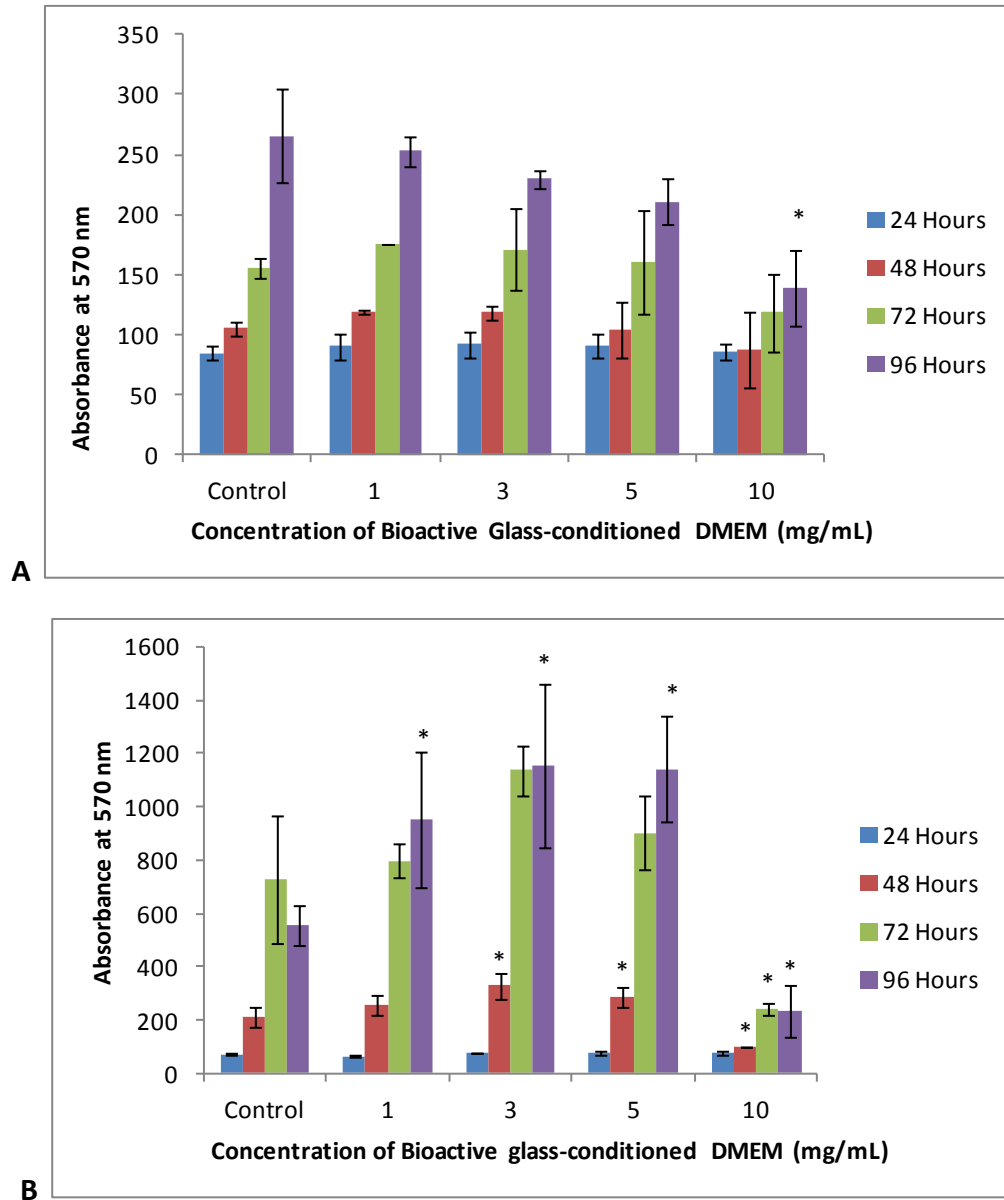
to be responsible for its antibacterial effect (Hu *et al.*, 2009), while recent studies have demonstrated that DMCs released by EDTA possess antibacterial activity against three types of facultative anaerobic bacteria associated with dental disease (Smith *et al.*, 2012a). The present study therefore aimed to determine whether bioactive glass dissolution products and bioactive glass-released DMCs exert similar effects on *S. mutans*, by using bacterial turbidity as a measure of cell growth.

### **5.1.1 Eukaryotic Response to Bioactive Glass Dissolution Products**

#### **5.1.1.1 Preliminary Analyses of Eukaryotic Cell Responses to Bioactive Glass Dissolution Products**

OD-21 cells (murine immortalised pulp cell line) and primary human dental pulp cells were initially exposed to 1-10 mg/mL bioactive glass-conditioned DMEM, and control solutions containing DMEM only, for a 96-hour culture period (see Figure 5.1). Cells were assayed for metabolic activity at 24 hour time-points using the MTT assay. Notably, both cell types responded differently to the bioactive glass-conditioned DMEM. At each time point, human dental pulp cells exposed to bioactive glass-conditioned DMEM, in general did not respond significantly differently to the control solutions, which contained DMEM only. However, at the 96-hour assay time-point, the metabolic activity of cells exposed to 10 mg/mL bioactive glass-conditioned DMEM was significantly lower than the control. Notably, the primary human dental pulp cells exhibited a dose-dependent decline in metabolic activity at 96 hours, which was not observed at the earlier time points (24-72 hours). No significant differences were observed in the metabolic activity of OD-21 cells after 24 hours of exposure to bioactive glass-conditioned DMEM, relative to the control of DMEM only. However at 48,

72 and 96 hours a trend was observed in which cells exhibited a dose-dependent increase in metabolic activity, reaching a peak at the 3 mg/mL exposure concentration. Interestingly, a decline in metabolic activity was observed in cells exposed to 5 and 10 mg/mL bioactive glass-conditioned DMEM compared with cells exposed to 3 mg/mL bioactive glass-conditioned DMEM.

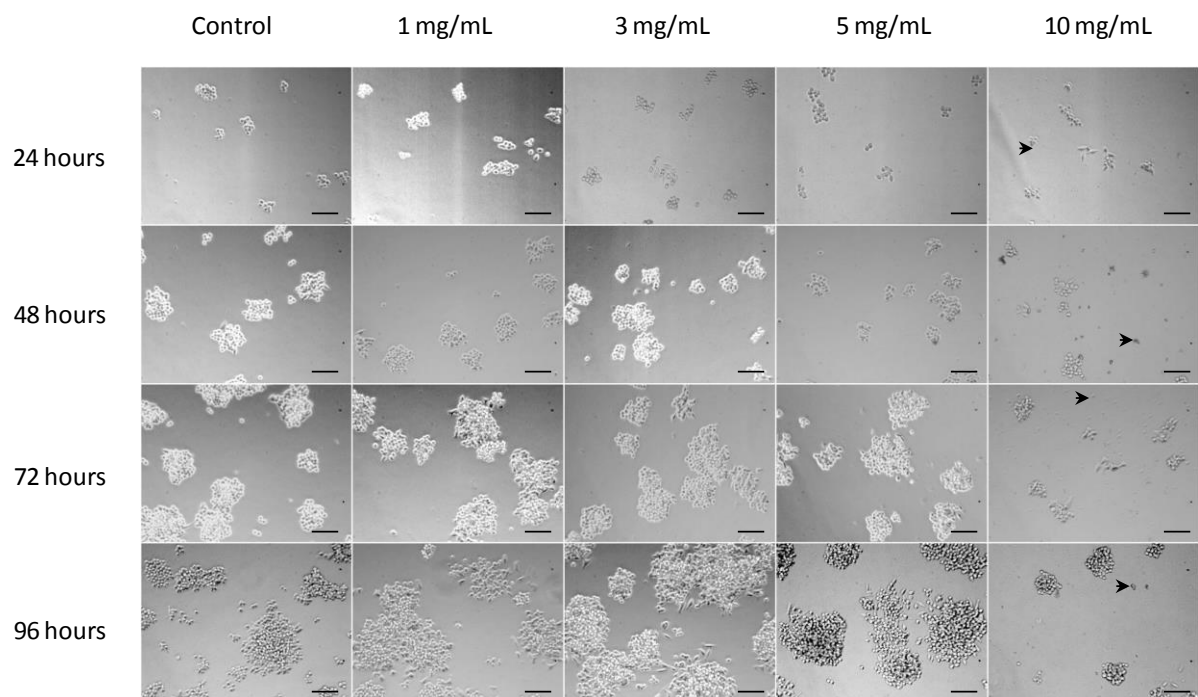


**Figure 5.1 Metabolic activity of cells following exposure to bioactive glass-conditioned DMEM.**

Response of **A)** primary human dental pulp cells and **B)** OD-21 cells. Cells were exposed to 1-10 mg/mL bioactive glass-conditioned DMEM and control solutions (DMEM). Metabolic activity was determined daily (24 – 96 hours) using the MTT assay (see Section 2.6.1). Mean values ( $n = 5$ ) and error bars represent  $\pm$  SD are shown. Statistical significance was determined using the Student's *t*-test, \* =  $p \leq 0.05$ .

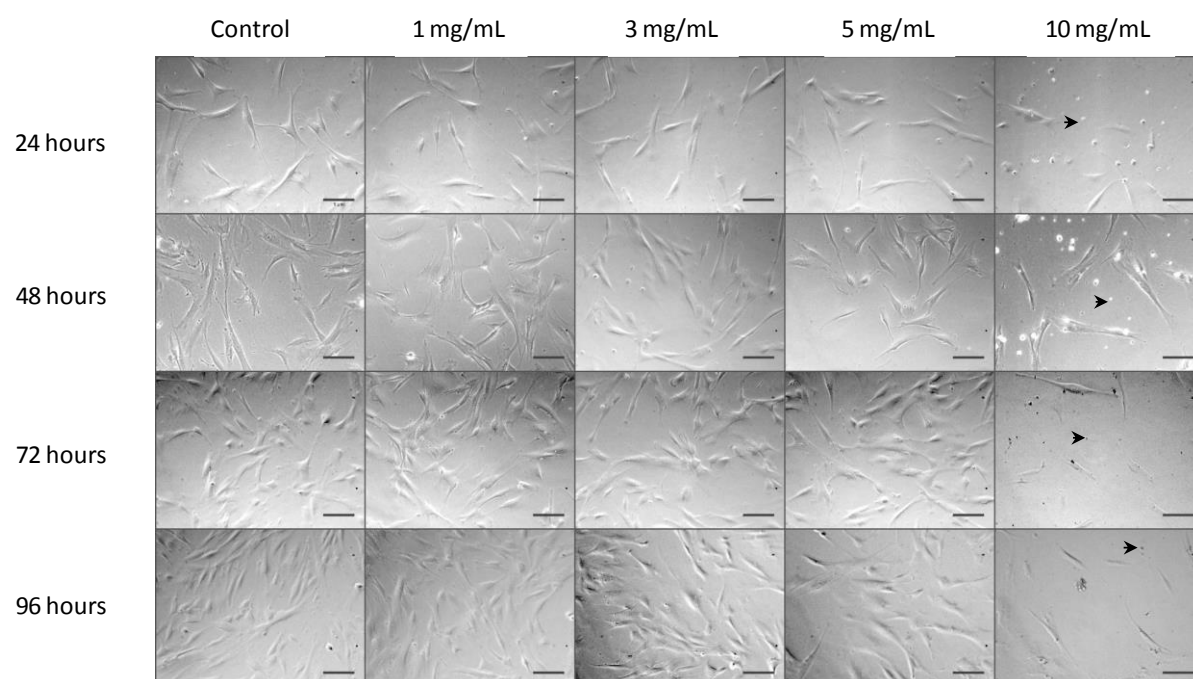


In addition to measuring the metabolic activity, microscopic images of cell cultures were captured at each assay time point (24-96 hours) to qualitatively examine any morphological differences which may result due to exposure to bioactive glass-conditioned DMEM. Figure 5.2 and 5.3 provide representative images for the exposure of OD-21 cells and human dental pulp cells to bioactive glass-conditioned DMEM, respectively. Both cells types exposed to concentrations of 1-5 mg/mL bioactive glass-conditioned DMEM maintained morphologies typical of cells grown under standard culture conditions. Qualitative observations suggested that there was an increasing cell density at each time point in cells exposed to 1-5 mg/mL bioactive glass-conditioned DMEM and control solutions and this may also correlate with the increased metabolic activity previously detected. In cultures exposed to 10 mg/mL bioactive glass-conditioned DMEM, cell density appeared reduced, however, further clarification with cell counts would be needed to confirm this. The qualitative examination of cultures also indicated a larger population of detached cells within the medium in cultures exposed to 10 mg/mL bioactive glass-conditioned DMEM, relative to all other culture conditions. Human dental pulp cells also appeared to lose their fibroblastic morphology at this concentration when observed at 72 and 96 hours.



**Figure 5.2 Representative images of OD-21 cells exposed to bioactive glass-conditioned DMEM.**

Images were captured at 24, 48, 72 and 96 hours during exposure to 1-10 mg/mL bioactive glass-conditioned DMEM and control solutions (DMEM only), using a Nikon D40 camera attached to a Nikon Eclipse TE300 microscope. Scale bars represent 150  $\mu$ m. Images confirm OD-21 cells exposed to concentrations of 1-5 mg/mL bioactive glass-conditioned DMEM maintained morphology typical of cells grown under standard culture conditions. Arrow heads indicate a lower cell density and higher population of detached cells, in cultures exposed to 10 mg/mL bioactive glass-conditioned DMEM.



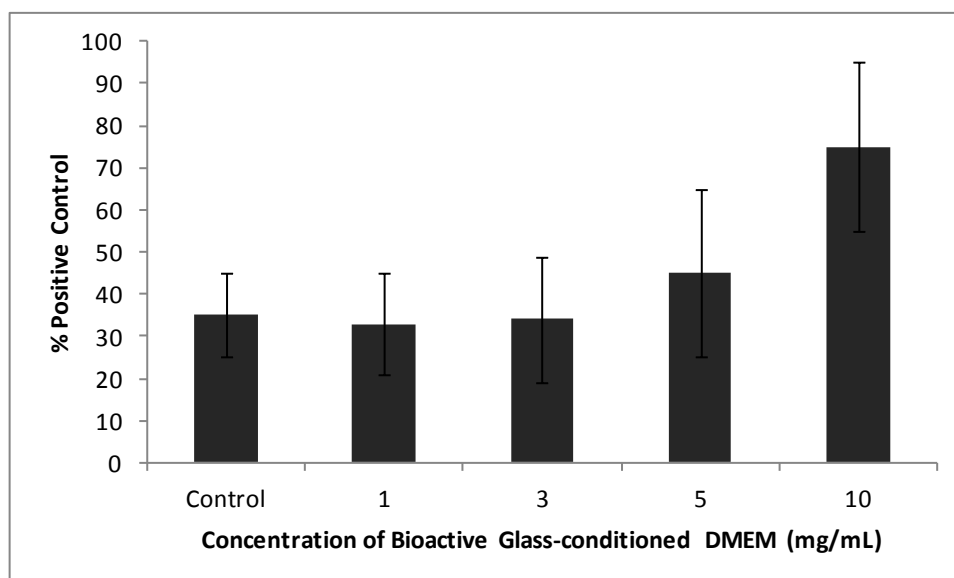
**Figure 5.3 Representative images of primary human dental pulp cells exposed to bioactive glass-conditioned DMEM.**

Images were captured at 24, 48, 72 and 96 hours during exposure to 1-10 mg/mL bioactive glass conditioned DMEM and control solutions (DMEM only). Scale bars represent 150  $\mu$ m. Images confirm human dental pulp cells exposed to concentrations of 1-5 mg/mL bioactive glass-conditioned DMEM maintained a morphology typical of cells grown under standard culture conditions. Arrow heads indicate a lower cell density and higher population of detached cells, in cultures exposed to 10 mg/mL bioactive glass-conditioned DMEM.

The results described above provided preliminary data on the effects of bioactive glass-conditioned DMEM, analysed in cell cultures over a 96-hour period. Based on these data, a 48-hour exposure was selected for the subsequent experiments, as this was the earliest time point at which a significant increase in metabolic activity was detected. Simultaneous experiments were established in which cell number, metabolic activity and LDH release were assayed in cells exposed to 1-10 mg/mL bioactive glass-conditioned DMEM and controls of DMEM only.

#### **5.1.1.2 Lactate Dehydrogenase Release from Cells Exposed to Bioactive Glass-conditioned DMEM**

As preliminary experiments had revealed that cells exposed to relatively high levels of 10 mg/mL bioactive glass-conditioned DMEM resulted in a significant decrease in metabolic activity, the LDH assay was used to determine whether a cytotoxic effect was exerted. LDH release was measured (see Section 2.6.2) 48 hours after the addition of 1-10 mg/mL bioactive glass-conditioned DMEM, or DMEM only for controls (see Figure 5.4). Similar to the controls, minimal LDH was released in cells exposed to 1 and 3 mg/mL bioactive glass-conditioned DMEM; although not significant, a small but statistically insignificant increase in LDH was observed in wells containing 5 mg/mL solutions. A significant increase in LDH release was observed in cells exposed to 10 mg/mL bioactive glass-conditioned DMEM. These cytotoxicity data corroborate the previous studies relating to the reduction in metabolic activity observed at this relatively high concentration of bioactive glass-conditioned DMEM used.

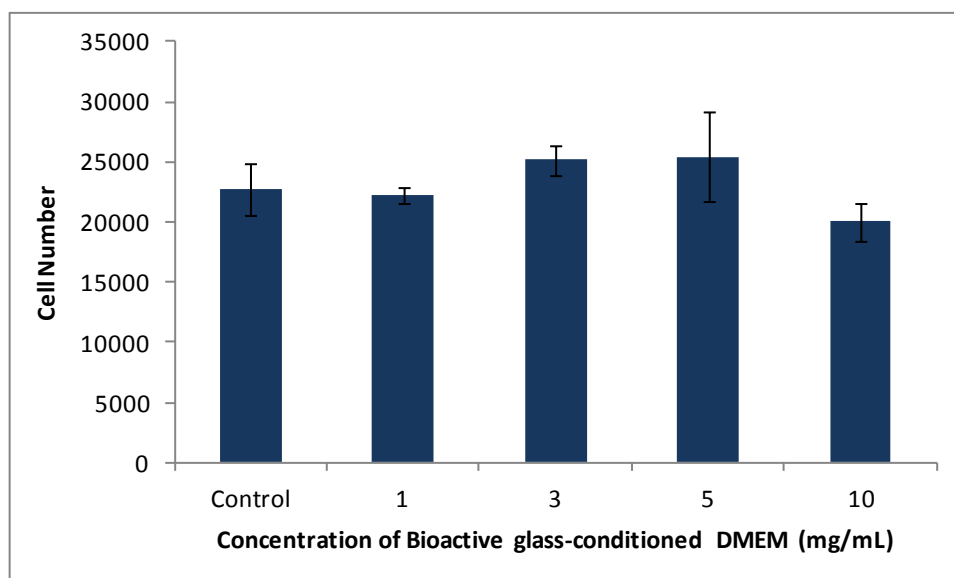


**Figure 5.4 Mean LDH release from OD-21 cultures at 48 hours following exposure to 1-10 mg/mL bioactive glass-conditioned DMEM.**

Results are expressed as percentage of positive control, which included exposure to Triton X-100. Statistical significance was assessed by comparison with control solutions, which contained DMEM only. Statistical significance was determined using the Student's *t*-test. \* =  $p \leq 0.05$ ,  $n = 4$ , error bars represent  $\pm$  SD.

#### **5.1.1.3 Growth of Cells Exposed to Bioactive Glass-conditioned DMEM**

While cell count data at 48 hours culture (Figure 5.5) demonstrated that there were no significant differences between the control and OD-21 cells exposed to 1-10 mg/mL bioactive glass-conditioned DMEM, trends indicated a decrease in cell numbers in cultures exposed to 10 mg/mL bioactive glass-conditioned DMEM. Interestingly, a peak in cell number was observed in wells containing 3 and 5 mg/mL solutions. However, none of these differences were statistically significant.



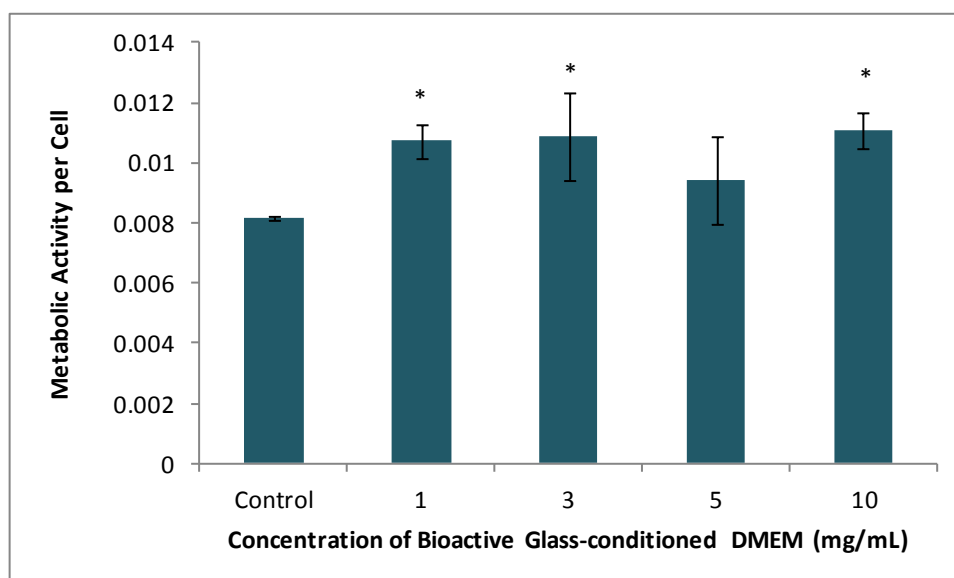
**Figure 5.5 OD-21 cell numbers following exposure to bioactive glass-conditioned DMEM.**

Trypan blue-stained cells were counted using a haemocytometer following a 48 hour exposure to bioactive glass-conditioned DMEM. Results are expressed as a mean of quadruplicate samples; error bars represent  $\pm$  SD. The Student's *t*-test established that there was no statistical significance between cells exposed to the control solutions (DMEM only) and bioactive glass-conditioned DMEM.

#### **5.1.1.4 Metabolic Activity in Cells Exposed to Bioactive Glass-conditioned DMEM**

Metabolic activity was assessed by the MTT assay and concomitant cell counts enabled the determination of metabolic activity per cell. OD-21 cells were assayed at 48 hours following exposure to 1-10 mg/mL bioactive glass-conditioned DMEM and control conditions (DMEM only). The MTT assay corroborated the data presented in Section 5.1.1.1 in which a dose-dependent increase in metabolic activity was observed in cultures exposed to 1 and 3 mg/mL bioactive glass-conditioned DMEM, followed by a reduction in activity for those dosed with 5 and 10 mg/mL solutions. Cultures exposed to 1, 3 and 5 mg/mL bioactive glass-conditioned DMEM had a significantly higher metabolic activity when compared with the

control conditions (data not shown). These data were subsequently normalised with cell count data to establish the metabolic activity per cell (see Figure 5.6). Cells exposed to 1, 3 and 10 mg/mL bioactive glass-conditioned DMEM had a significant increase in metabolic activity per cell compared with controls, and all cells exposed to these concentrations exhibited similar levels of metabolic activity per cell. Cells exposed to 5 mg/mL bioactive glass-conditioned DMEM had a lower metabolic activity per cell than cells exposed to 1, 3 and 10 mg/mL bioactive glass-conditioned DMEM, and did not differ significantly from cells exposed to DMEM alone.



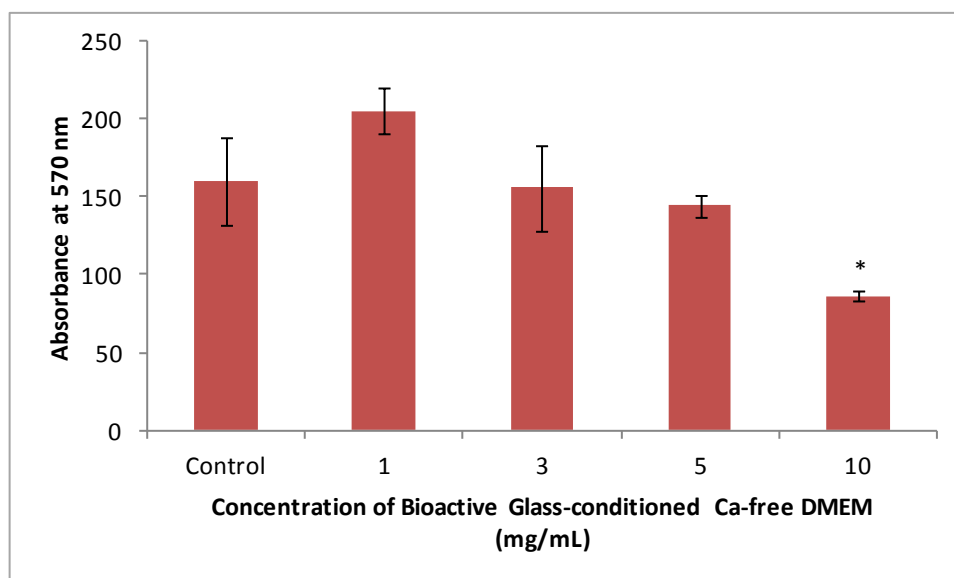
**Figure 5.6 Metabolic activity per cell for OD-21 cells, following a 48 hour exposure to increasing concentrations of bioactive glass-conditioned DMEM.**

Metabolic activity was assessed by the MTT assay and correlated with cell count data to determine metabolic activity per cell. Results are expressed as a mean for quadruplicate samples; error bars represent  $\pm$  SD. The Student's *t*-test was used to determine statistical significance against the control (DMEM only), \* =  $p \leq 0.05$ .

#### **5.1.1.5 Effects of Bioactive Glass Dissolution Products in Calcium-free DMEM**

The results presented in Chapter Two (see Section 4.0) demonstrated that DMEM contained high background levels of calcium and that the addition of bioactive glass to DMEM at concentrations of 3-10 mg/mL lowered the concentration of Ca ions detected in the solutions (see Figure 4.7). The positive proliferative effects of exogenous calcium are well established in pulpal cells (Takita *et al.*, 2006); therefore, to observe cellular effects without the interference of background levels of calcium in the DMEM, bioactive glass-conditioned calcium-free medium was utilised (see Section 2.5.1.1). The effects of the bioactive glass-conditioned calcium-free medium on OD-21 cells were analysed by the MTT assay (see Figure 5.7) and a different trend in metabolic activity was observed in comparison with the standard preparation of bioactive glass-conditioned DMEM previously used. When compared with the control, an increase in metabolic activity was detected in cells exposed to 1 mg/mL bioactive glass-conditioned calcium-free DMEM and a dose-dependent decline in metabolic activity was observed for cells dosed with 3-10 mg/mL bioactive glass-conditioned calcium-free DMEM. Although none of these differences were statistically significant. Solutions of 10 mg/mL bioactive glass-conditioned calcium-free DMEM elicited a significant reduction in metabolic activity (relative to the control of calcium-free DMEM alone), which appeared to be greater than observed in the standard 10 mg/mL bioactive glass-conditioned DMEM previously used (see Section 5.1.1.4).





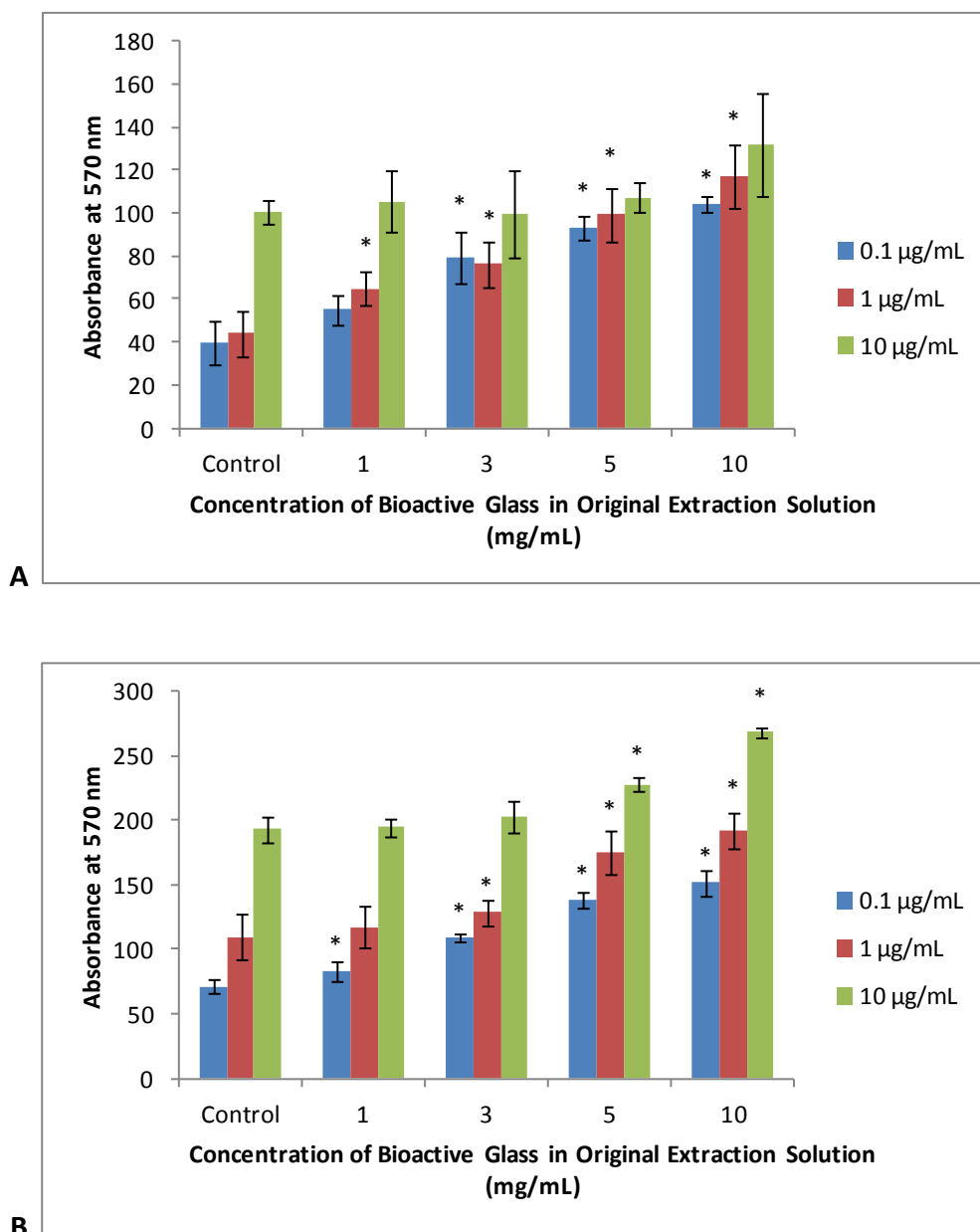
**Figure 5.7 OD-21 cell response to bioactive glass-conditioned calcium-free DMEM.**

1-10 mg/mL bioactive glass was incubated for 24 hours at 37 °C, with calcium-free DMEM under constant agitation. Solutions were filtered to remove particulate bioactive glass and exposed to OD-21 cells for 48 hours. Control solutions consisted of untreated calcium-free DMEM. Cell cultures were assayed for metabolic activity using the MTT assay. Results are expressed as a mean of quadruplicate samples; error bars represent  $\pm$  SD. The Student's *t*-test was used to determine whether absorbance values differed significantly from the control (calcium-free DMEM only), \* =  $p \leq 0.05$ .

## **5.1.2 Eukaryotic Cell Responses to DMCs**

### **5.1.2.1 Preliminary Analyses of Eukaryotic Cellular Response to DMCs**

The MTT assay was used to identify experimental conditions for subsequent experiments. Prior to stimulation with DMCs, OD-21 cells were serum-starved to ensure any observed effects were not masked by FCS. Cells were exposed to 0.1, 1 and 10  $\mu\text{g/mL}$  of DMCs (released by 1-10 mg/mL bioactive glass in saline, and control solutions of saline only), and assayed for metabolic activity at 24 and 48 hours. Results are provided in Figure 5.8, and DMCs are described according to the concentration of bioactive glass used in the original dentine extraction solutions. At both 24 and 48 hours, an increase in metabolic activity relating to the concentration of DMCs suspended in DMEM was observed, whereby cells exposed to 10  $\mu\text{g/mL}$  DMCs exhibited the greatest metabolic activity. Data also indicated DMCs were stimulating the metabolic activity of cells increasingly, according to the concentration of bioactive glass used in the original extraction solutions. The observed effects on metabolic activity were DMC dose-dependent at both 24 and 48 hours, with the exception of cells exposed to 10  $\mu\text{g/mL}$  DMCs at 24 hours in which the metabolic activity did not differ significantly from the control (saline only-released DMCs). Statistical analysis indicated that all DMCs suspended in DMEM at a concentration of 1  $\mu\text{g/mL}$  exerted a significant increase in metabolic activity relative to the control (saline-released DMCs), at 24 hours. For this reason, the concentration of 1  $\mu\text{g/mL}$  DMCs was selected for all subsequent experiments in which OD-21s were exposed to bioactive glass-released DMCs.

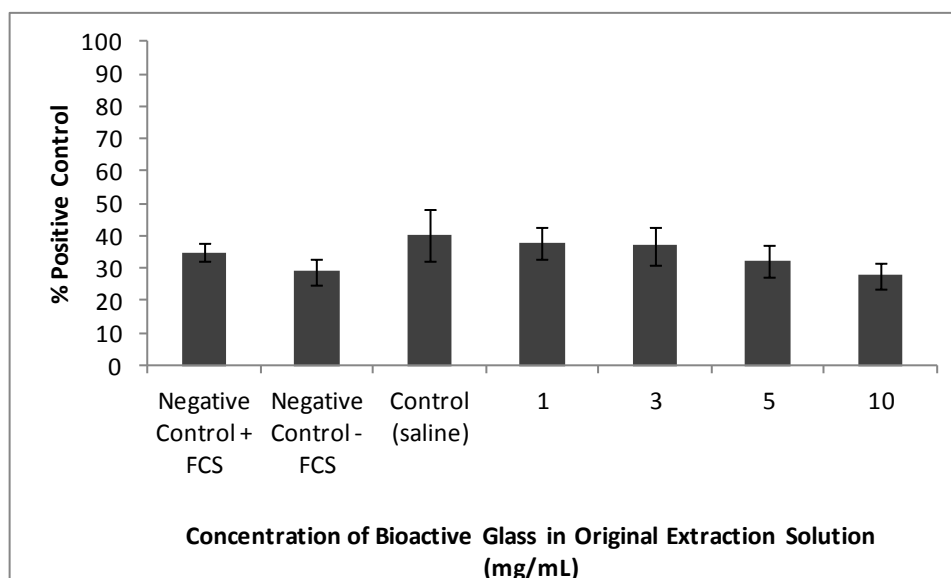


**Figure 5.8 Metabolic activity of OD-21 cells exposed to 0.1-10 µg/mL of DMCs.**

DMCs are expressed as the concentration of bioactive glass used in the original dentine extractions (see Section 2.1.4) in which control extraction solutions contained saline and dentine only. Cells were exposed to DMCs for culture periods of 24 (**Graph A**) and 48 hours (**Graph B**). Statistically significant differences were determined using the Student's *t*-test to compare values to the control (cells exposed to saline-released DMCs) for each concentration of DMCs used (0.1-10 µg/mL). \* =  $p \leq 0.05$ ,  $n = 4$ , error bars represent  $\pm$  SD.

#### **5.1.2.2 Lactate Dehydrogenase Release from Cells Exposed to DMCs**

High concentrations of EDTA-released DMCs have previously been reported to be cytotoxic to OD-21 cells (Musson *et al.*, 2010) therefore, the LDH assay was used to determine whether the bioactive glass-released DMCs elicited similar detrimental effects. OD-21 cells were subsequently exposed to DMC-supplemented DMEM at a concentration of 1 µg/mL for a 24-hour period and LDH release was assayed (see Figure 5.9). Cells exposed to serum-free DMEM, in addition to cells supplemented with FCS served as negative controls, whereas Triton X-100 served as the positive control as a known inducer of cell death and LDH release. Cells that were deprived of serum did not differ significantly in their release of LDH in comparison with those that had been supplemented with FCS. Statistical analyses demonstrated that LDH release did not differ significantly for cells exposed to DMCs in comparison with both serum-deprived and DMC-supplemented cultures. In addition, there appeared to be no significant differences observed for LDH release from cells exposed to 1-10 mg/mL DMC-supplemented DMEM solutions when compared with cells dosed with DMCs released by the saline control dentine extraction solutions. These findings demonstrate that the culture conditions and the addition of DMCs exerted no cytotoxic effect on OD-21 cells.

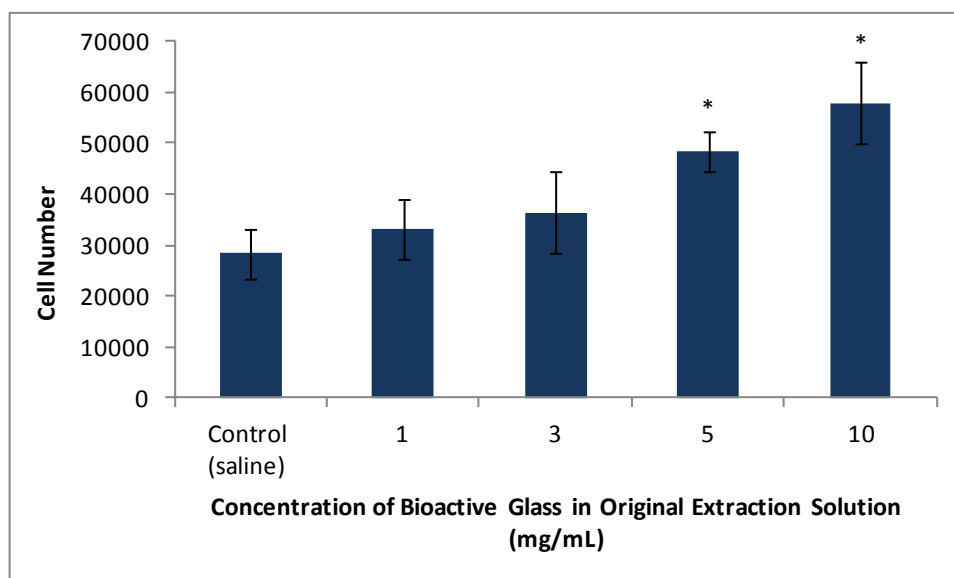


**Figure 5.9 LDH release from OD-21 cells following exposure to DMCs.**

Cells were exposed to 1-10 mg/mL bioactive glass-released DMCs and saline-released DMCs (control) and subsequently assayed for LDH release (see Section 2.6.2). Results are expressed as % positive control where cells were exposed to Triton X-100. Cells exposed to DMCs were serum-deprived for 24 hours, therefore negative controls of cells with and without (+/-) the presence of FCS were also assayed. No statistical significance was observed between cells exposed to DMCs and negative controls determined by the Student's *t*-test. *n* = 4, error bars represent  $\pm$  SD.

#### 5.1.2.3 Growth of Cells Exposed to DMCs

Cell numbers (see Figure 5.10) were analysed in cultures exposed to DMCs for 24 hours. The response in terms of cell number resulted in a comparable trend with that observed for the metabolic activity analysis in which a dose-dependent increase in cell number was observed, according to the concentration of bioactive glass used to release DMCs (see Figure 5.7). However, statistical significance was only observed in cells exposed to DMCs liberated by 5 and 10 mg/mL dentine extraction solutions.



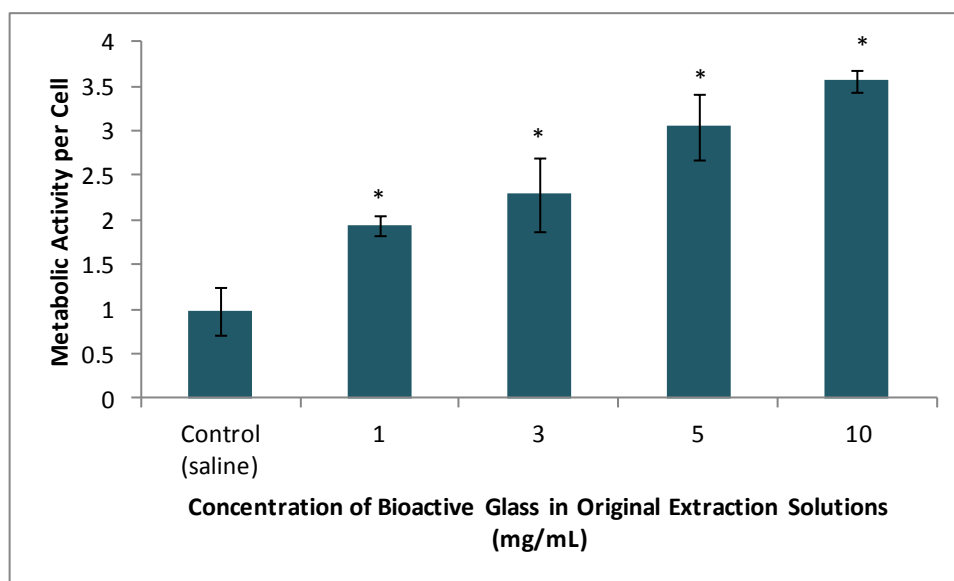
**Figure 5.10 OD-21 cell numbers following exposure to bioactive glass-released DMCs.**

Viable trypan blue-stained cells were counted using a haemocytometer following 24 hours exposure to DMCs. Results are expressed as a mean of quadruplicate samples; error bars represent  $\pm$  SD. The Student's *t*-test was used to determine statistical significance of cells exposed to bioactive glass-released DMCs and the control (saline-released DMCs) \* =  $p \leq 0.05$ .

#### 5.1.2.4 Metabolic Activity in Cells Exposed to DMCs

The metabolic activity of cells exposed to DMC-supplemented DMEM was assessed by the MTT assay. Results were consistent with previous findings reported in Section 5.1.2.1 in which a progressive increase in metabolic activity occurred, correlating with increasing concentrations of bioactive glass used in extraction solutions to release the DMCs. DMCs extracted with 1-10 mg/mL bioactive glass and saline solutions gave rise to a significant increase in metabolic activity of OD-21 cells relative to the control (saline-released DMCs). These data were subsequently normalised with cell numbers to determine the metabolic

activity per cell (see Figure 5.11). When OD-21 cells were exposed to DMCs, a dose-dependent increase in metabolic activity per cell was observed, correlating with the original concentration of bioactive glass present in dentine extractions. All values were significantly higher than cells exposed to DMCs released by the saline control extraction solutions.



**Figure 5.11 Metabolic activity per cell of OD-21 cells exposed to DMCs.**

DMCs were released by 1-10 mg/mL bioactive glass in saline solution and saline control solutions, and were applied to cells at a concentration of 1  $\mu$ g/mL. Metabolic activity was assessed using the MTT assay after 24 hours of exposure to DMC-supplemented DMEM. Results are expressed as a mean of quadruplicate samples; error bars represent  $\pm$  SD. Statistical significance was determined by the Student's *t*-test, in which metabolic activities of cells exposed to DMCs released by 1-10 mg/mL dentine extraction solutions were compared with DMCs released by saline control solutions. \* =  $p \leq 0.05$ .

### 5.1.3 Prokaryotic Cell Responses to Bioactive Glass Dissolution Products

The antibacterial properties of bioactive glass have previously been attributed to its relatively high aqueous alkaline pH (Hu *et al.*, 2009) therefore, the pH of bioactive glass-

conditioned PBS (1-10 mg/mL), solutions were determined prior to their addition to *S. mutans* cultures. The pH values are listed in Table 5.1 and indicate that the addition of bioactive glass to PBS results in alkaline pH changes the generation of which was in a dose-dependent manner. Notably, the addition of 3-10 mg/mL bioactive glass concentrations did not alter the pH greatly compared with each other.

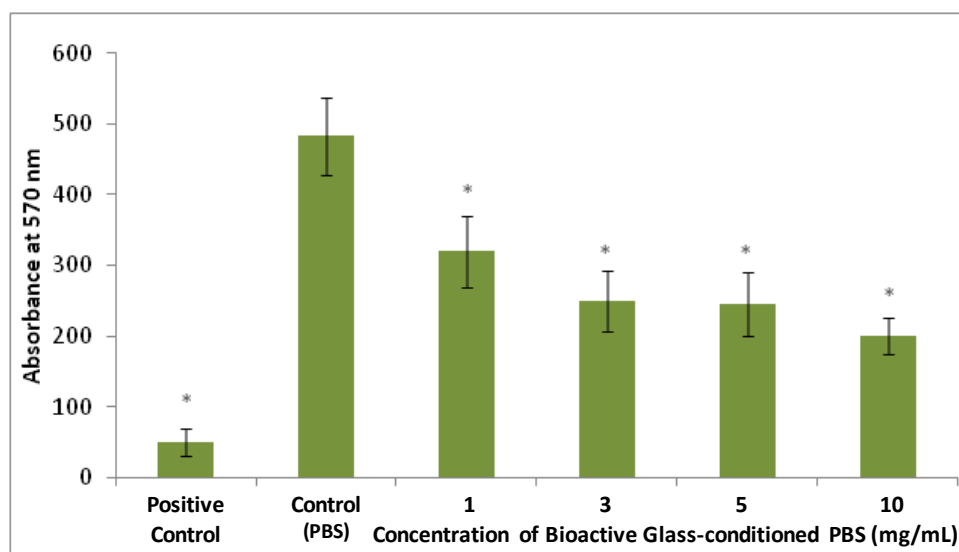
Concentration of bioactive glass (mg/mL)	pH of Bioactive Glass-conditioned PBS	± SD
Control (PBS)	7.5	0.02
1	10.28	0.03
3	11.16	0.03
5	11.59	0.02
10	11.71	0.03

**Table 5.1 pH values of bioactive glass-conditioned PBS.**

Solutions of 1-10 mg/mL bioactive glass and PBS were constantly agitated for 24 hours at 37 °C. The pH of solutions was measured after particulate bioactive glass had been removed by filtration. Control solutions contained PBS only. Results represent an average of triplicates, standard deviation is reported as ± SD.

*S. mutans* cultures were subsequently exposed to bioactive glass-conditioned PBS and bacterial growth was assessed after 24 hours on the basis of the turbidity of cultures. A reduction in absorbance indicated a decrease in growth. Results indicated that with increasing concentrations of bioactive glass-conditioned PBS, a concomitant reduction in growth of *S. mutans* was detected (see Figure 5.12). All absorbance values differed significantly from the negative control of PBS, although the positive control of penicillin/streptomycin resulted in the greatest reduction in bacterial growth.





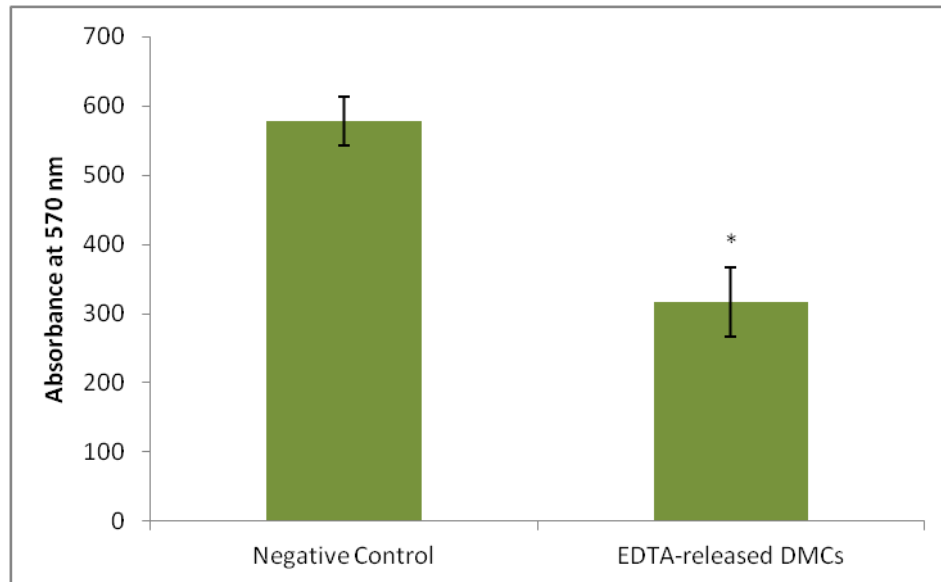
**Figure 5.12 Effects of bioactive glass-conditioned PBS on *S. mutans* growth.**

*S. mutans* cultures were exposed to bioactive glass-conditioned PBS for 24 hours. The addition of 0.5 µg/ml Penicillin/streptomycin to bacterial cultures served as the positive control. Bacterial turbidity was measured at a wavelength of 570 nm. Statistical significance was determined by the Student's *t*-test and data were compared against the negative control (PBS). \* =  $p \leq 0.05$ ,  $n = 4$ , error bars represent  $\pm$  SD.

#### 5.1.4 Prokaryotic Cell Responses to DMCs

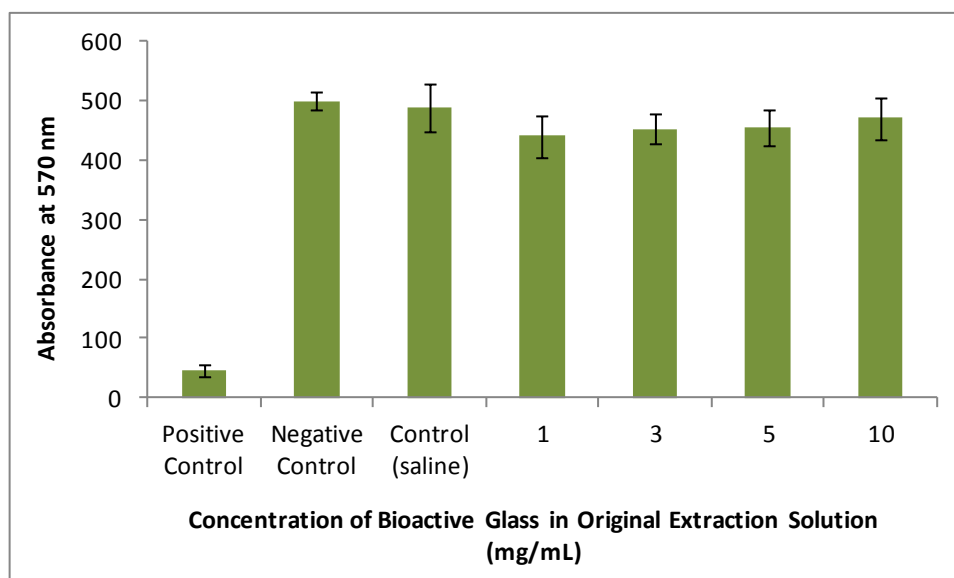
The antibacterial activity of EDTA-solubilised DMCs was recently reported (Smith *et al.*, 2012a) and these findings were corroborated here for *S. mutans* (Figure 5.13). A significant decrease in turbidity, after 24 hours was observed with the addition of DMCs released by EDTA at a concentration of 10 µg/mL relative to the negative control. The antimicrobial activity of bioactive glass-released DMCs against *S. mutans* was subsequently assessed using the same assay (see Figure 5.14). PBS was supplemented with 10 µg/mL of DMCs and added to bacterial cultures for 24 hours. The negative control consisted of PBS alone, whereas the antibiotic cocktail of Penicillin/streptomycin served as a positive control. Following

exposure, there were no statistical differences identified between cultures that had been dosed with DMCs and the negative control.



**Figure 5.13 Effects of EDTA-released DMCs on *S. mutans* growth.**

*S. mutans* cultures were exposed to EDTA-released DMCs for 24 hours. Bacterial turbidity was established at a wavelength of 570 nm. Statistical significance was determined by the Student's *t*-test in which results were compared against the negative control (PBS alone). \* =  $p \leq 0.05$ ,  $n = 4$ , error bars represent  $\pm$  SD.



**Figure 5.14 Effects of bioactive glass and saline-released DMCs on *S. mutans*.**

*S. mutans* cultures were exposed to DMCs for 24 hours. The addition of 0.5 µg/mL penicillin/streptomycin to bacterial cultures served as the positive control and the negative control consisted of PBS alone. Bacterial turbidity was measured at a wavelength of 570 nm. Statistical significance was determined by the Student's *t*-test in which results were compared against the negative control (PBS). \* =  $p \leq 0.05$ ,  $n = 4$ , error bars represent  $\pm$  SD.

## 6.0 RESULTS CHAPTER FOUR

### 6.1 Development of a Cell Culture Model to Study Peritubular Dentinogenesis

A reduction in dentine permeability is the principal objective in the treatment of dentine hypersensitivity and currently, this is largely achieved by the topical application of various crystalline materials, to provide tubular occlusion (Cunha-Cruz *et al.*, 2010). These physical-based approaches provide only a temporary treatment, however, and a need exists for an innovative, biologically-based, more permanent approach to treat dentine hypersensitivity. Ideally, the rapid production of peritubular dentine may entirely reduce dentine permeability, but the biological regulation and control of its formation remains elusive (Pashley, 1996). Therefore, to assist future investigations, the studies presented here aimed to identify a suitable tissue culture model to study peritubular dentinogenesis and develop various assays that are compatible with the model to aid research in this area.

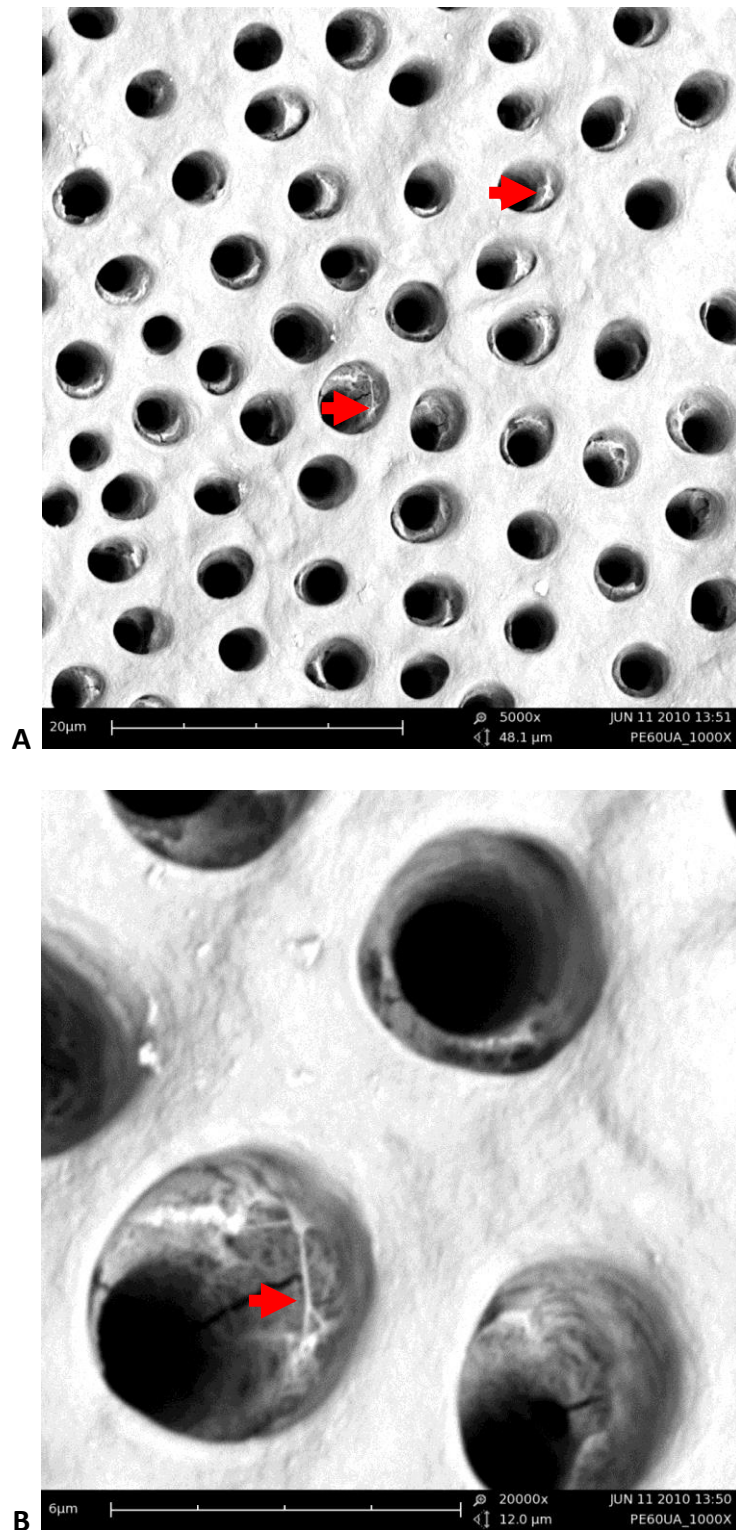
Dentine discs, which are isolated from below the dentino-enamel junction and above the pulp horn, are used routinely as a model to study the efficacy of dentine hypersensitivity treatments (Mordan *et al.*, 1997). Although relatively reproducible, this model presents various challenges in the context of studying peritubular dentinogenesis. For instance, as dentine is a bioactive and mineralised tissue it would not be possible to detect the formation of new peritubular dentine in this model. Due to the opacity of dentine, it is also not compatible with the colorimetric assays used in the previous chapter, to assess metabolic activity or cytotoxicity. To overcome these issues, a transparent, readily-available, and biologically-inert substrate was sought. The porosity of dentine was also considered, in order to create a representative topographical environment for cell culture.

To the best of the author's knowledge this is the first application in which PET Thinserts have been used to provide a representative structure of dentine. It is, therefore, the premise of this chapter to establish whether the model itself and associated cell-based assays are robust, for their use in future studies on peritubular dentinogenesis.

### **6.1.1 Physical Characterisation of PET Thinserts**

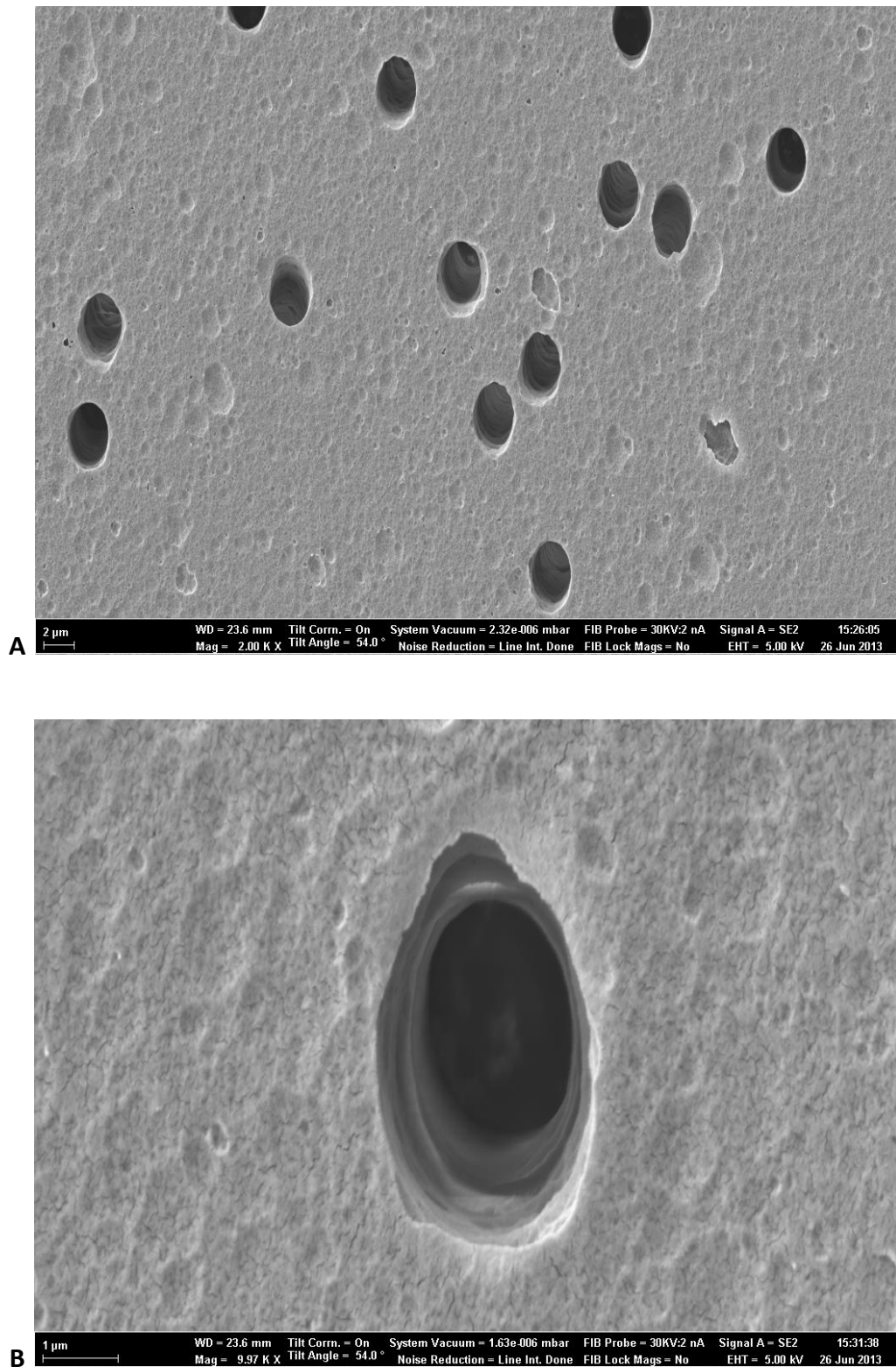
The tubular structure of dentine is a prominent feature, with the average tubule diameter being 3  $\mu\text{m}$  near the pulp in health (Garberoglio and Brännström, 1976). On this basis, PET Thinserts with a uniform pore size of 3  $\mu\text{m}$  were selected for this study. To compare the surface morphology of the PET Thinsert with acid-etched dentine discs (see Section 2.8.2), top-down SEM images were obtained. Figure 6.1 provides representative images of an etched dentine disc, prepared from dentine directly above the pulp horns (see Section 2.8.2). It was a common observation that the appearance of tubules varied according to their location on the dentine disc; towards the centre of the disc tubules appeared more circular, whereas towards the periphery of the discs closer to the enamel, tubules appeared to be more oval. The presence of fibrillar structures were also evident within many of the tubules.

The SEM images of PET Thinserts revealed the presence of pores that had been produced by the manufacturer using a precise track-etching process (see Figure 6.2). However, the pores in the PET Thinserts appeared not as evenly distributed, nor as dense across the sample, compared with the tubules observed on the dentine discs. The surface of the PET Thinserts appeared to be textured, possibly due to the surface treatment applied by the manufacturing process to facilitate cell adhesion.



**Figure 6.1 Representative SEM image of etched dentine surface.**

Images captured at **A)** 5000 X and **B)** 20000 X magnification. Image shows the presence of patent tubules, revealed by citric acid etching. Arrow heads indicate the presence of fibrillar structures within dentinal tubules.

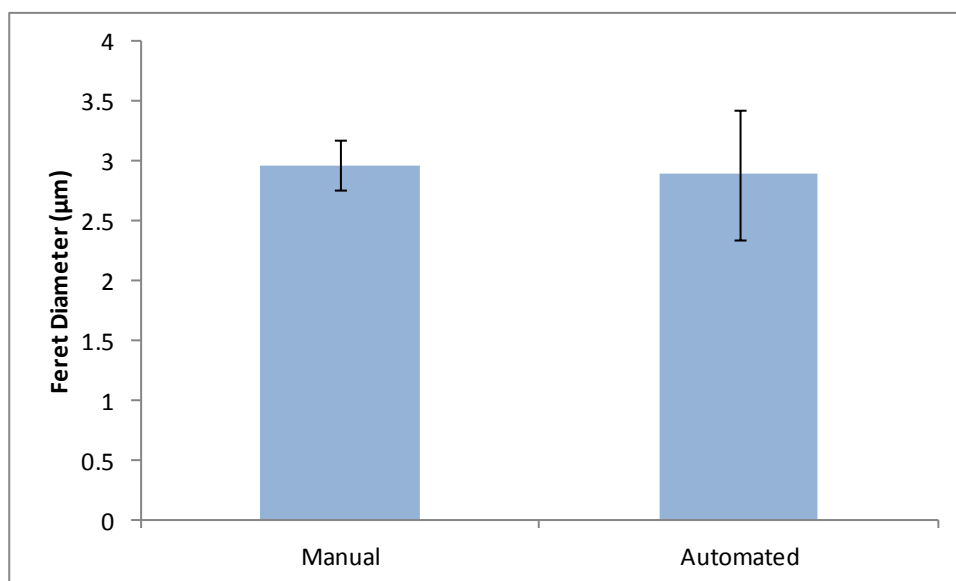


**Figure 6.2 Representative SEM image of PET Thinserts.**

Images were captured at **A)** 2000 X and **B)** 9970 X magnification, revealing the presence of pores in the PET Thinsert.

To determine further whether the dentinal tubules and PET Thinsert pores were comparable in size and density, the SEM images of both substrates were analysed using ImageJ processing. The software allowed a semi-automated approach to detect the tubules or pores, and subsequently calculate the feret diameter (the average of the shortest and longest distances across a boundary) and their number per unit area (see Section 2.8.2.1). To ensure that ImageJ analysis was accurately detecting and measuring the tubules or pores, manual measurements of dentinal tubules were compared with ImageJ-produced values. Figure 6.3 compares the feret diameter of dentinal tubules determined by ImageJ analysis with manual measurements. There was no statistical difference between the manual and automated calculations of the feret diameter of dentinal tubules; therefore, as the automated approach was a more efficient and objective approach, this method was selected for subsequent SEM image analysis.



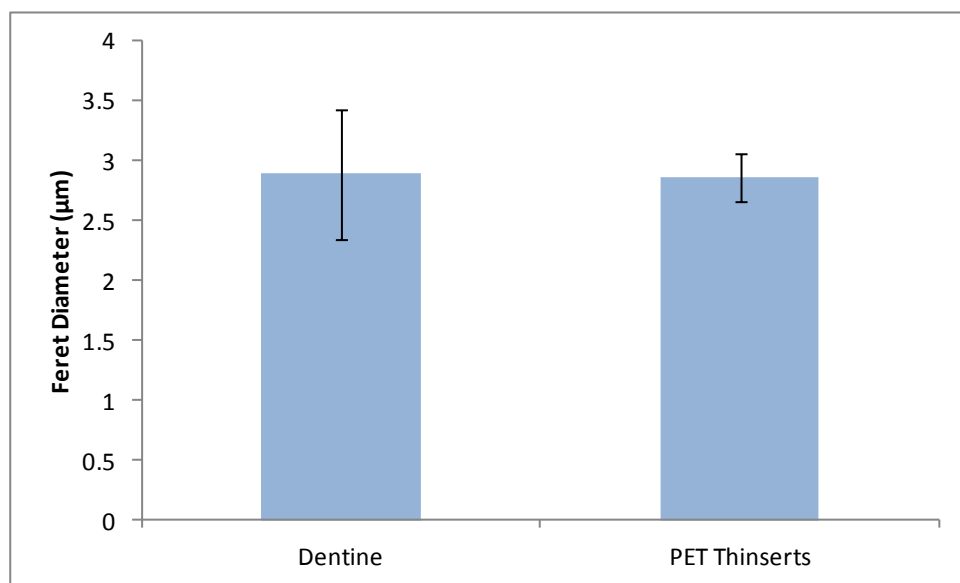


**Figure 6.3 Comparison of the feret diameters of dentine tubules using manual and semi-automated measuring techniques.**

The feret diameter is defined as the average of the shortest and longest distances across a boundary. Twenty random measurements were acquired manually or using ImageJ, from the same SEM images of 4 dentine discs (see Section 2.8.2.1), error bars represent  $\pm$  SD. Statistical significance between manual and semi-automated measurements was not observed using the Student's *t*-test.

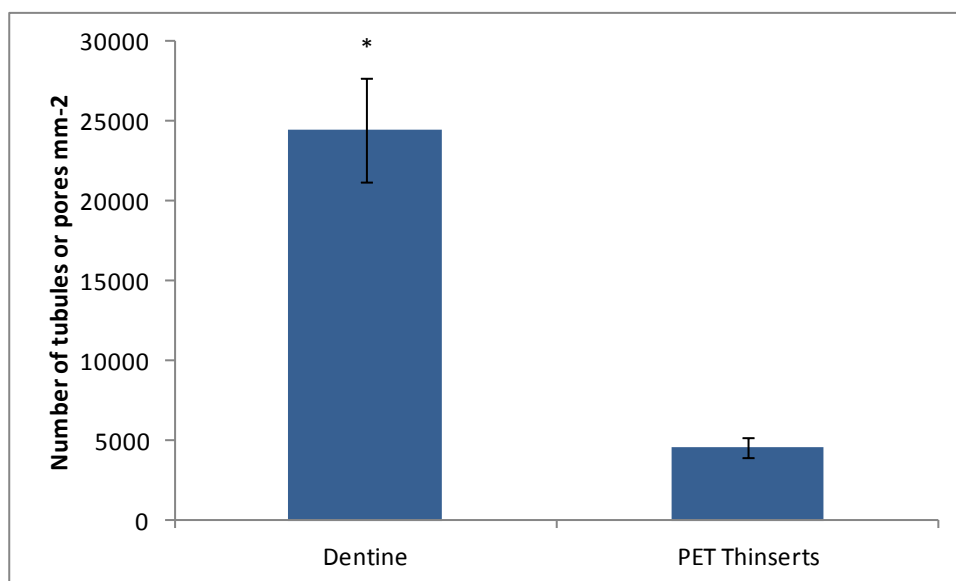
To assess the suitability of the PET Thinsert pores to represent dentinal tubules, SEM images of the surfaces of the PET Thinsert were also analysed using the ImageJ software. Figure 6.4 presents a comparison of the feret diameters of both tubules and pores, determined by the semi-automated approach assessed in the previous section. The average feret diameters for both were 2.9  $\mu\text{m}$ , and were not significantly different to one another. However, there appeared to be more variation in dentine samples, (indicated by a larger standard deviation, i.e.  $\pm$  0.53  $\mu\text{m}$  for dentine and  $\pm$  0.21  $\mu\text{m}$  for PET Thinserts), as might be expected when

comparing biological specimens with manufactured samples. The densities of pores and tubules confirmed the qualitative observations from the SEM images, indicating that the density of tubules per unit area ( $24457 \text{ tubules/mm}^2$ ) was significantly greater than the number of pores per unit area ( $5300 \text{ pores/mm}^2$ ) (see Figure 6.5). Results, therefore, indicated that the PET Thinsert pores provided a reproducible representation of the size of tubules, at the dentine-pulp interface.



**Figure 6.4 Comparison of the average feret diameters of dentine tubules and PET Thinsert pores.**

Feret diameters were calculated automatically, using ImageJ software analysis (see Section 2.8.2.1), from SEM images of dentine discs and PET Thinserts. Statistical significance was not observed using the Student's *t*-test when comparing the feret diameters of PET Thinsert pores with dentinal tubules. The results represent an average of  $n = 4$ , error bars represent  $\pm$  SD.



**Figure 6.5 Comparison of the numbers of tubules or pores per unit area of dentine tubules and PET Thinserts, respectively.**

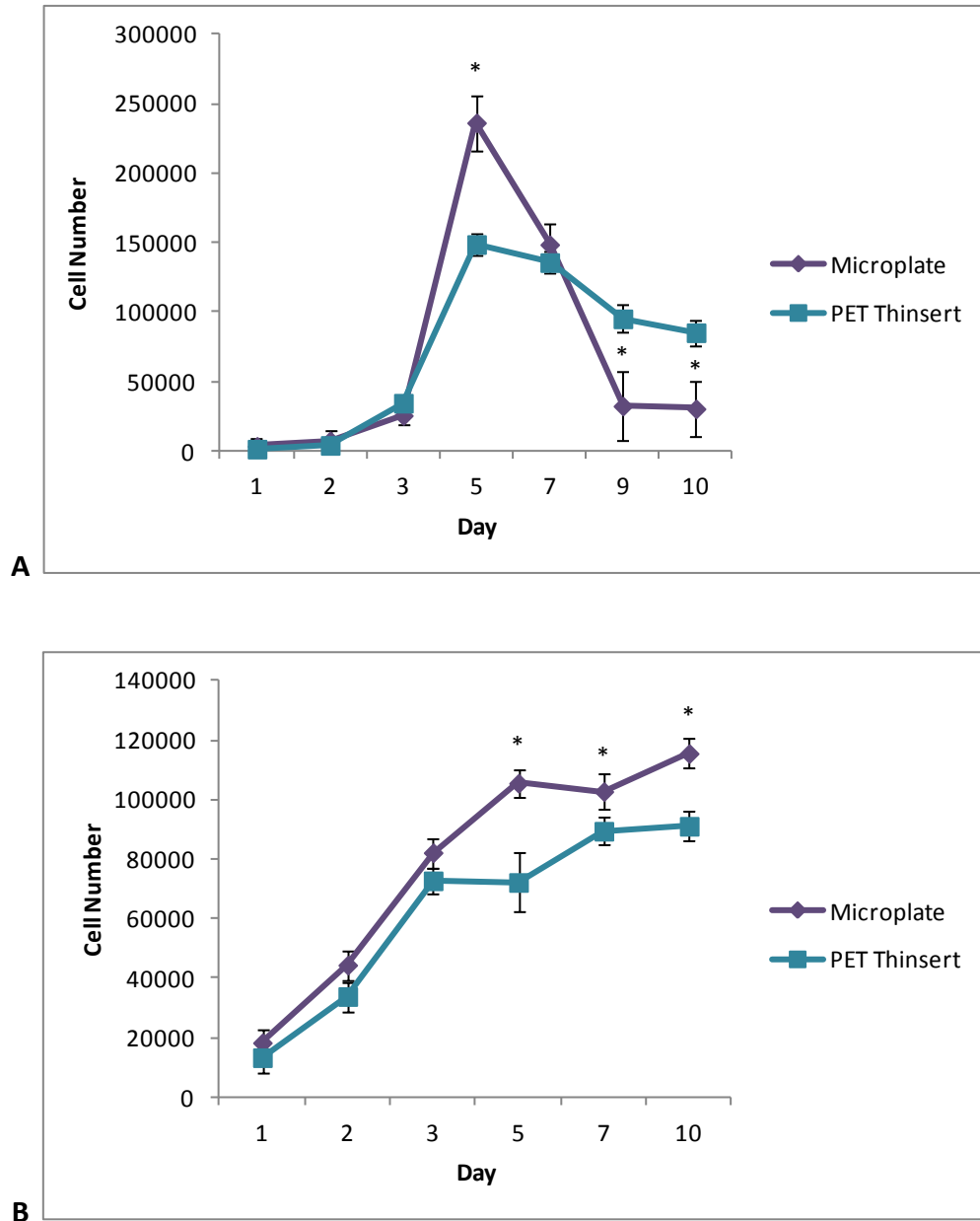
The numbers of tubules or pores per unit area were calculated automatically, using ImageJ software analysis (see methods Section 2.8.2.1), from SEM images of dentine discs and PET Thinserts. The numbers of tubules per unit area were significantly greater than the numbers of pores per unit area as determined by the Student's *t*-test. The results are an average of  $n = 4$ , error bars represent  $\pm$  SD.

### 6.1.2 Growth Profile of Cells Cultured on PET Thinserts

For the PET Thinsert to be used as a successful model to study peritubular dentinogenesis, the substrate must be able to support cell growth for both short and long-term assays. Therefore, the growth profiles of an immortalised murine pulp cell line (OD-21s) and primary human dental pulp cells cultured on standard 12-well tissue culture plastic microplates were compared with cells cultured on PET Thinserts over a 10 day period (see Figure 6.6). OD-21 cells cultured on PET Thinserts and standard 12-well microplates followed similar growth profiles from days 1-3 of culture, in which cell numbers were comparable and exhibited a

steady, day-by-day, cell number increase. At day 5, cell numbers appeared to reach a peak value, when cells cultured on the microplate were significantly greater in number compared with those cultured on PET Thinerts. This difference was likely to be due to the higher surface area available for cell growth. Qualitative observational data indicated cell confluence was reached at day 5 and that metabolic activity was relatively high as indicated by the colour change of culture medium from red to yellow; subsequently, medium was changed daily at this point. Consistent with a decline in cell number from days 5-10, microscopic observations also revealed the widespread detachment of cells from both the PET Thinert and plastic culture substrates during this period. Notably, the decline in cell numbers was greater in cells cultured on standard culture plasticware in comparison with those cultured on PET Thinerts (data not shown).

Human primary dental pulp cells exhibited a different growth profile in comparison with that observed for OD-21 cells. A relatively steady increase in cell numbers was observed throughout the culture period for cells cultured on both PET Thinerts and in 12-well plastic microplates. Cell numbers were consistently higher for cells cultured on the microplates in comparison with those cultured on the PET membrane, which was likely to be due to the difference in the surface area of the two substrates. Cell numbers were significantly higher for cells cultured on the microplates on days 5, 7 and 10, as determined by the Student's *t*-test, when comparing cell numbers with those cultured on PET.

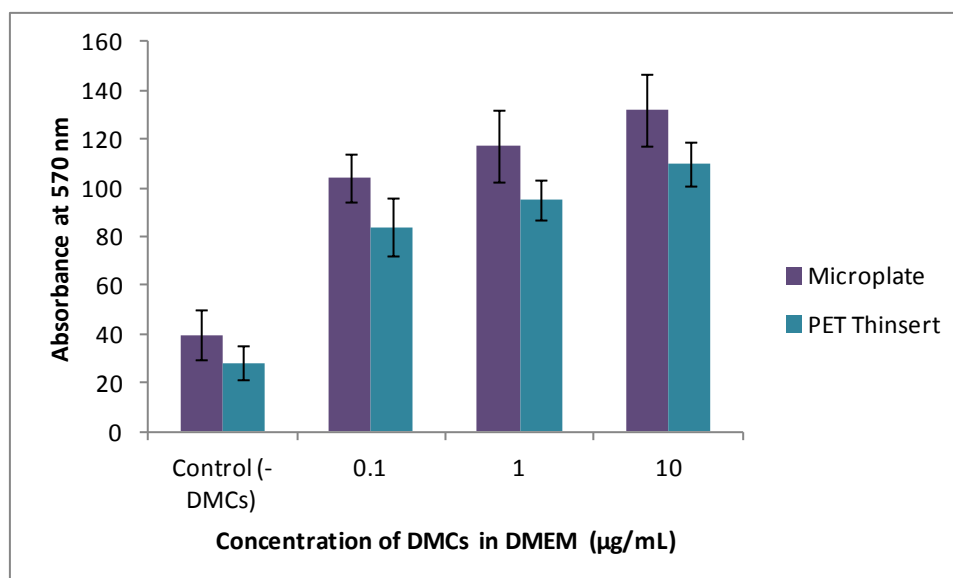


**Figure 6.6 Growth profiles of cells cultured on PET Thinserts and 12-well microplates.**

**Graph A)** growth profile of OD-21 cells. **Graph B)** growth profile of primary human dental pulp cells. Cells were initially seeded at 500 cells/cm<sup>2</sup> and cultured under standard conditions for 10 days. Cells were trypsinised and counted as described in Section 2.3.3. Error bars represent  $\pm$  SD, n = 3. Statistical significance was assessed using the Student's *t*-test, \* =  $p \leq 0.05$ .

### **6.1.3 Substrate Comparison of OD-21 Cell Response to DMCs**

As the growth profiles of OD-21 cells differed according to the substrate on which they were cultured in standard culture conditions (see Section 6.1.2), it was necessary to determine whether their responses differed when experimental conditions were applied (i.e. the addition of DMCs). Results Chapter Three established that the greatest metabolic activity was observed when OD-21 cells were exposed to DMCs released by 10 mg/mL bioactive glass in saline solution (see Section 5.1.2.4) therefore, DMCs (released by 10 mg/mL bioactive glass in saline solution) were applied to cultures at a concentration of 0.1-10 µg/mL. Cellular responses after 24 hours culture are graphically presented in Figure 6.7. The results are similar to those observed in Section 5.1.2.4, in which DMCs exerted a dose-dependent increase in metabolic activity according to their concentration. Although the metabolic activity was lower for cells cultured on PET Thinserts, no significant differences were detected when these values were compared with cells cultured on 12-well microplates for each concentration of DMCs.



**Figure 6.7 Comparison of the metabolic activities of OD-21 cells cultured on standard 12-well microplates and PET Thinserts surfaces in response to bioactive glass-released DMCs.**

DMCs (released by 10 mg/mL bioactive glass in saline solution) were applied to cells at concentrations of 0.1-10 µg/mL for 24 hours. Control conditions contained DMEM only. Cells were assayed using the MTT assay and absorbance was measured spectrophotometrically at 570 nm. No statistical significances (as determined by the Student's *t*-test) were observed when the metabolic activities of cells cultured on PET Thinserts were compared with the responses of cells cultured on microplates for each concentration of DMCs. Error bars represent  $\pm$  SD, *n* = 4.

#### 6.1.4 Validation of Methods to Assess Cell Number

Several methods exist to quantify cell number, each have their limitations as well as advantages for certain applications. The most conventional method of counting cells is using a haemocytometer in combination with a cell viability dye such as trypan blue. This is a straightforward, inexpensive method and is often considered to be a gold-standard. However, it is also subject to operational errors, it can be time consuming and is therefore

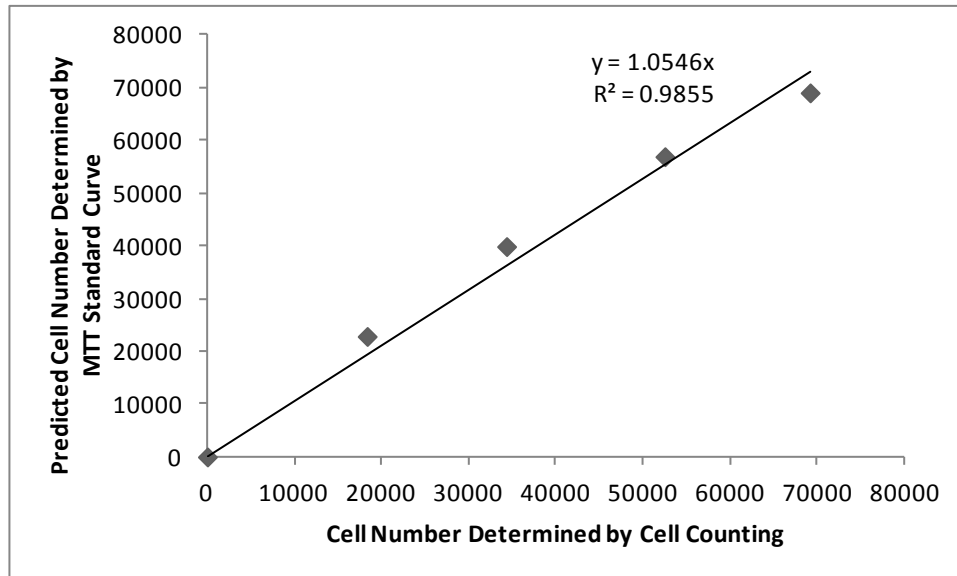
inadequate for high-throughput experiments. A range of colorimetric assays, originally developed with the intention of measuring cytotoxicity towards reagents are often also used to measure cell proliferation. These include the MTT, MTS and WST-1 assay, and measure the reduction of yellow tetrazolium salts to purple formazan by mitochondrial succinate dehydrogenase. As the reaction can only take place in metabolically active cells, this provides a measure of cell viability. However, these assays do not directly measure cell number and are end-point assays, therefore cells must be sacrificed. Obtaining cell counts and using the MTT assay do not allow the acquisition of cell numbers *in situ*, therefore a method was developed to count cells cultured on PET Thinserts using image analysis. The techniques of assessing cell number (i.e. manual cell counting, the MTT assay and the use of image analysis) were subsequently compared to assess their reliability in this model.

MTT absorbance was plotted against cell number (determined manually using a haemocytometer) to generate a standard curve and the equation of the line of best fit was solved to predict cell numbers for subsequent experiments. To validate this technique for accurately predicting cell numbers, cells were seeded at a range of densities (0-50000 cells/well), and the MTT assay was used to determine the absorbance value for each density. From these data, the absorbance values were converted to cell numbers by solving for the equation of the initial standard curve. The predicted cell numbers (calculated from the MTT standard curve) were then plotted against actual cell number, determined from concomitant manual cell counts (see Figure 6.8). The line of best fit shows good correlation with an  $R^2$  value of 0.99 indicating that using a standard curve with the MTT assay is a good predictor of cell number within the cell density range studied.



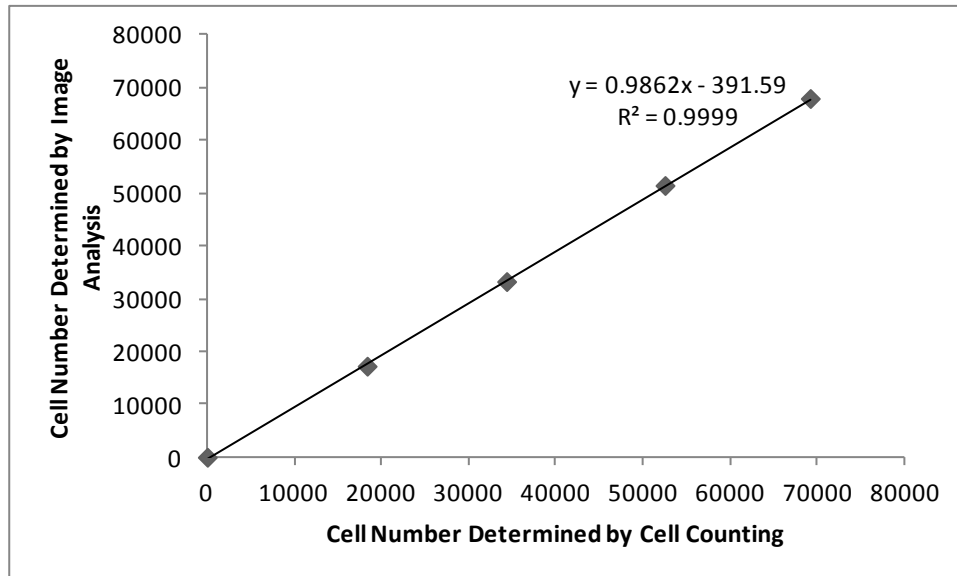
An additional experiment was established in which cells were counted using image analysis (see Section 2.6.4), allowing the comparison of these values to manual cell counting and data from the MTT assay. Briefly, cells were seeded at 0-50000 cells/well and fixed after 24 hours; cells were stained with hemotxylin and eosin, after which microscopic images were captured and processed using ImageJ software. The values generated from the ImageJ particle analyser tool were graphically compared with the manual cell counts (see Figure 6.9). The graph showed excellent correlation between actual cell numbers and those determined by image analysis, with an  $R^2$  of 0.99. This indicated that the image analysis approach provided a reliable method of counting cells cultured on PET Thinserts *in situ*. Finally, this method was compared with the MTT assay for determining cell number (see Figure 6.10) and the results indicated that there was a good correlation ( $R^2 = 0.98$ ) between cell numbers generated by image analysis and those determined from an MTT standard curve.

The validation of all three techniques for assessing cell number deduced that they were reliable and provided comparable cell numbers. Manual cell counting was evidently a reliable technique, but was not ideal for large experiments. The MTT assay was relatively more high-throughput, but indeed caution must be exercised when extrapolating absorbance values to cell numbers. The MTT assay may be useful in mineralisation experiments, which are notoriously challenging for being able to count cells due to the visual obstruction that mineral formation presents. Cell counts obtained using ImageJ were a valuable resource of semi-automated counting, but would only be suitable for short-term assays when cells remain in a mono-layer. Therefore in future experiments, the duration and size of the experiment must be considered when choosing an appropriate assay.



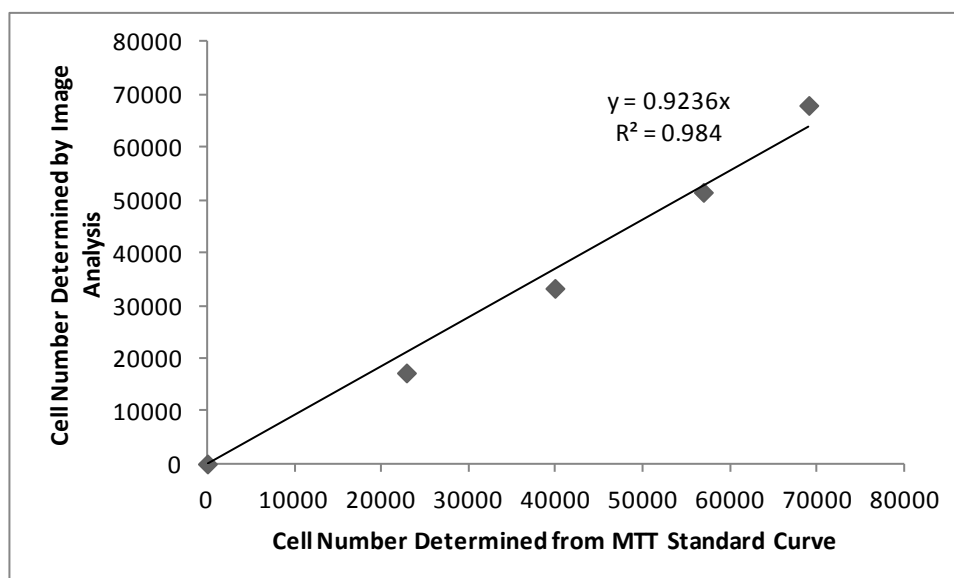
**Figure 6.8 Validation of the MTT assay to assess cell numbers.**

Cells were seeded at 0-50000 cells/well, and counted after 24 hours. Actual cell numbers (x-axis) were determined by manual cell counts (see Section 2.3.3) and absorbance-predicted cell numbers (y-axis) were obtained from the linear regression equation of an MTT standard curve. The linear regression equation and  $R^2$  coefficient ( $> 0.9$ ) are displayed above the trend line.



**Figure 6.9 Validation of the use of ImageJ to assess cell numbers.**

Cells were seeded at 0-50000 cells/well, and counted after 24 hours. Actual cell numbers (x-axis) were determined by the manual cell counting approach and ImageJ-generated cell numbers (y-axis) were obtained from the photographic images of H&E stained cells (see Section 2.6.4.1). The linear regression equation and  $R^2$  coefficient ( $> 0.9$ ) are displayed above the trend line.

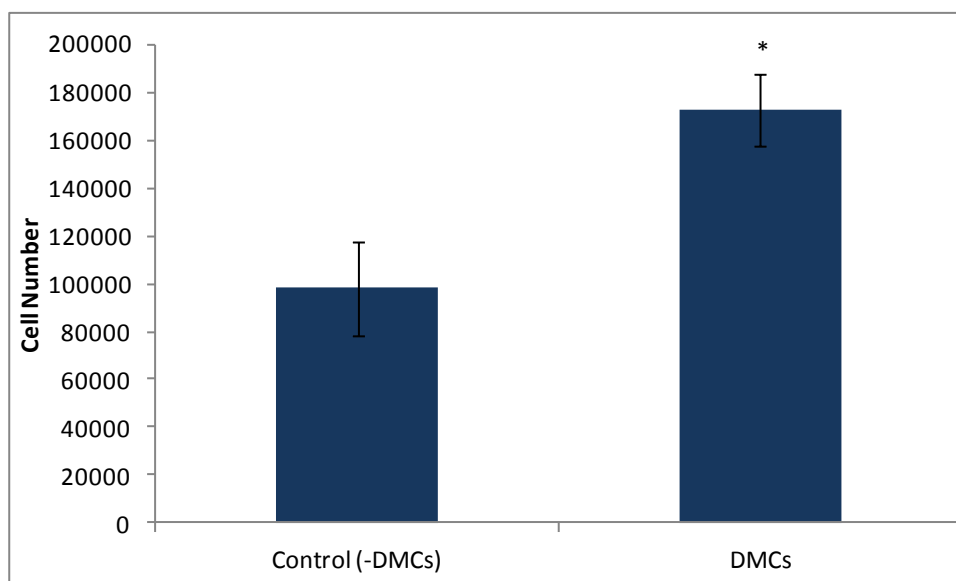


**Figure 6.10 Comparison of cell numbers generated from an MTT assay standard curve with cell numbers determined by image analysis.**

Cells were seeded at 0-50000 cells/well, and counted after 24 hours. Cell numbers (x-axis) were predicted from an MTT standard curve and ImageJ-generated cell numbers (y-axis) were obtained from the photographic images of H&E stained cells (see methods Section 2.6.4.1). The linear regression equation and  $R^2$  coefficient ( $> 0.9$ ) are displayed above the trend line.

#### **6.1.5 Counts for OD-21 Cells Cultured on PET Thinerts Using Image Analysis**

Having established the reliability of image analysis in assessment of cell numbers, this method was used to count cells *in situ* cultured on PET Thinerts with and without the presence of DMCs. Cells were exposed to DMCs released by 10 mg/mL bioactive glass in saline solution by the addition of DMC-supplemented DMEM (see Figure 6.11). A significant increase in cell numbers was observed in cells exposed to DMCs relative to cells cultured in DMEM. This concurred with previous findings in which cells were exposed to DMCs in a 2-D environment using standard culture plasticware.



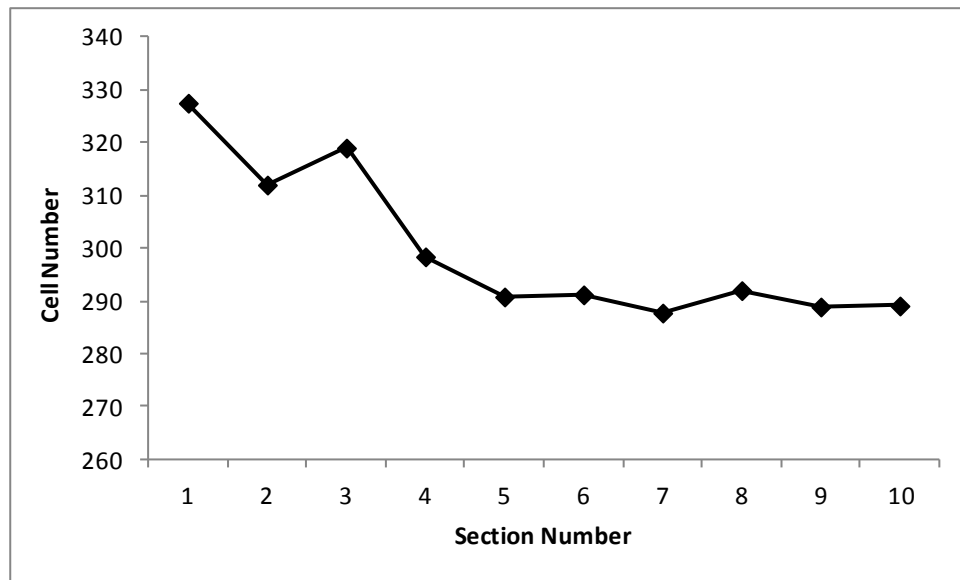
**Figure 6.11 Cell numbers, determined by image analysis, of OD-21s cultured in the presence and absence (control) of DMCs.**

DMCs were solubilised using 10 mg/mL bioactive glass in saline solution, and were used at a concentration of 1 µg/mL. Results are an average of three experimental replicates, error bars represent  $\pm$  SD. Statistical significance was assessed by the Student's *t*-test in which cell numbers of those exposed to DMCs were compared against the control. \* =  $p \leq 0.05$ .

#### **6.1.6 Histomorphometric Analysis of Cells Cultured on PET Thinserts**

Although counting cells *in situ* using image analysis proved to be effective, this technique is only appropriate during short time point assays when there is a monolayer of cells. For longer term experiments, as cells continue to proliferate, cells may not remain in a monolayer and may grow in more complex 3-D arrangements. To overcome this issue, having cultured cells on PET Thinserts, they were histologically processed and observed in cross-section. To enable the determination of cell numbers per unit area, a Hunting Curve (see Section 2.7.4.1) was plotted to determine the number of sections required to provide a representative cell number that would not be altered by subsequent cell counts. The

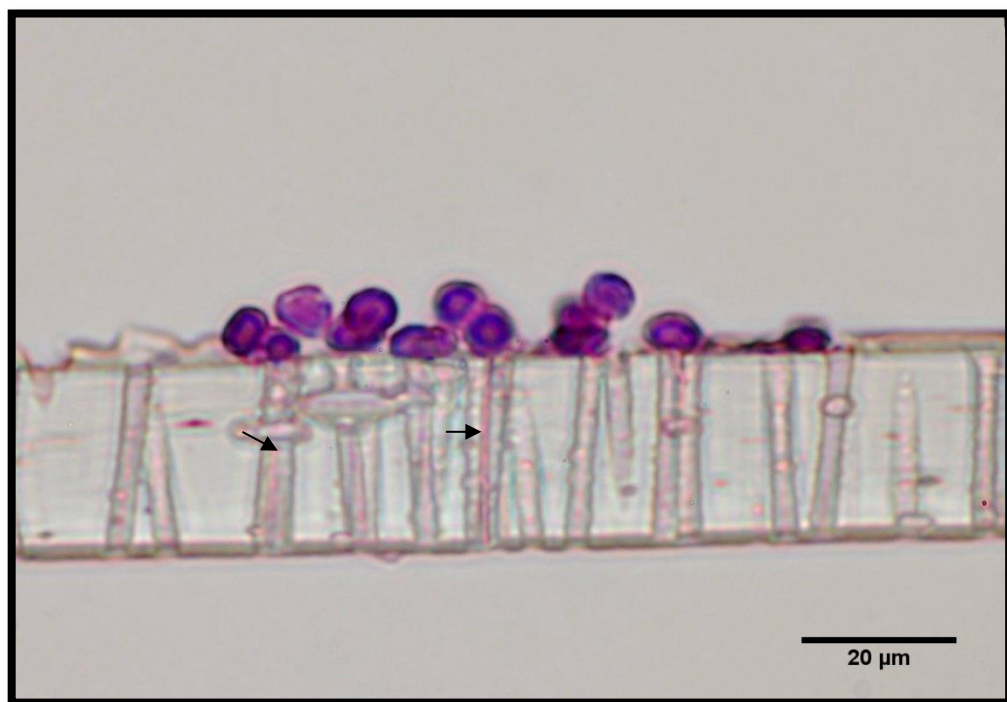
cumulative means of cell numbers on each histological section were plotted against the number of sections used for the analysis (see Figure 6.12). The curve began to plateau after 6 sections; therefore this was deemed an appropriate number of histological sections to use for subsequent experiments, in order to gain a representative number of cells per unit area.



**Figure 6.12 Hunting Curve analysis to determine the number of histological sections required to gain a representative number of cells per unit area.**

OD-21 cells cultured on PET Thinerts were fixed and the samples were histologically sectioned (see methods Section 2.7.4.1). The cumulative means of cell numbers per unit area were plotted against the number of sections used to obtain a particular cumulative mean.

Figure 6.13 provides a representative histological section of cells cultured on a PET Thinsert. From the cross-sectional images, it was possible to distinguish the pores penetrating the PET membrane, however, these were not always perpendicular within the section and several obliquely-cut pores were also evident. Cells were stained using hematoxylin and eosin, rendering the cell nuclei and cytoplasm visible. Stained cellular extensions were also observed, protruding from cells into the pores.



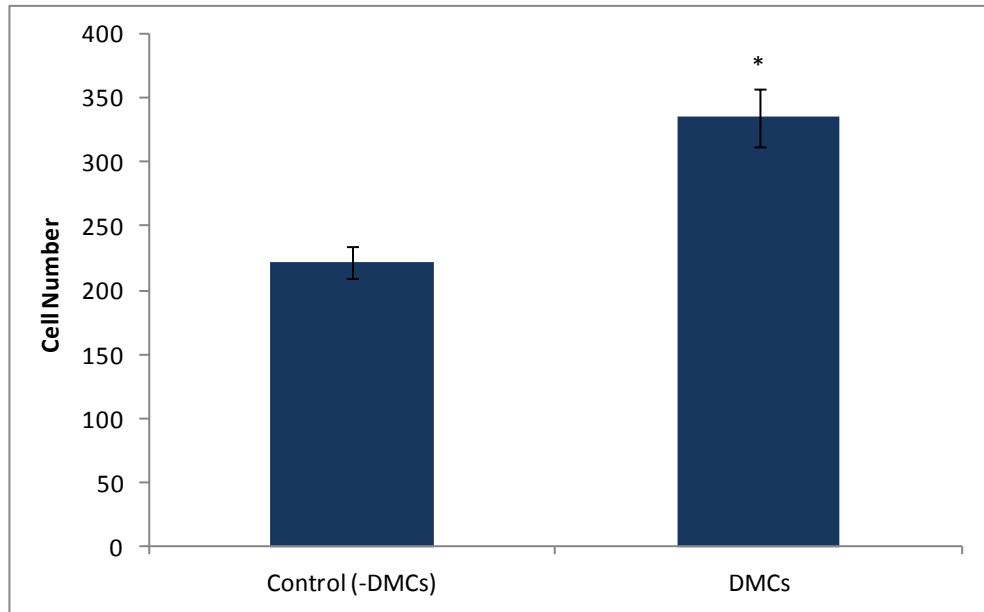
**Figure 6.13** Representative histological cross-section of OD-21 cells cultured on PET Thinserts.

Cells were stained with hematoxylin and eosin (see Section 2.7.3). Arrow heads indicate the presence of stained cellular extensions protruding into 3 μm pores. There are no intensely stained structures visible in pores that do not have cells above.

### **6.1.7 Cellular Responses to DMCs**

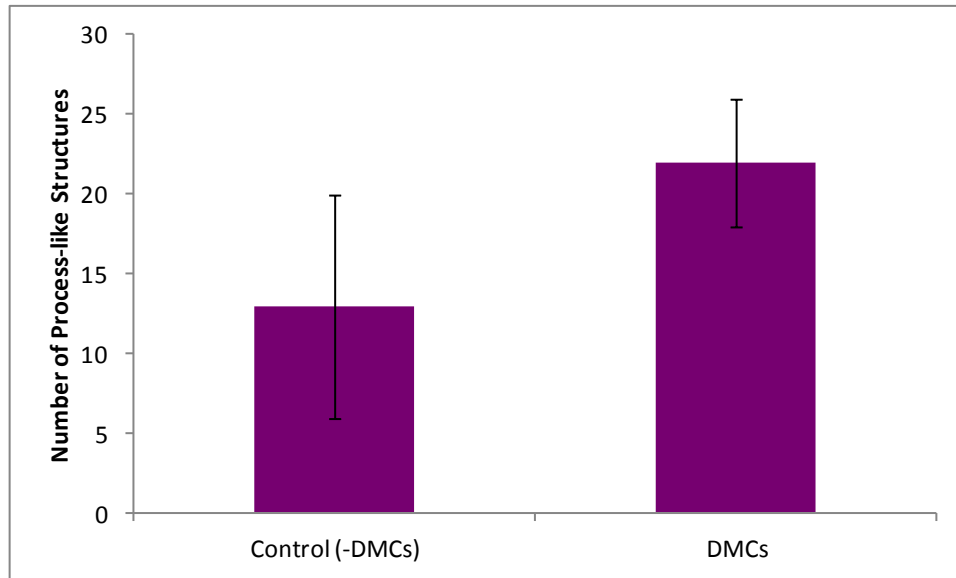
Histological sections of PET Thinserts were obtained from OD-21 cells cultured in the presence and absence (control) of DMCs. The numbers of cells per unit area were determined (see Figure 6.14) and significantly higher cell numbers were observed when cells were exposed to DMCs, relative to the controls which were not exposed to DMCs. These findings confirmed those determined by cell counts obtained using image analysis, indicating the reliability of both the results and techniques for counting cells. The frequency of cellular extensions protruding into the pores was also established (see Figure 6.15). Although statistical significance was not achieved, the number of cellular extensions was greater for cells cultured in the presence of DMCs.





**Figure 6.14 Cell numbers per unit area of OD-21 cells cultured on PET Thinerts in response to DMCs.**

DMCs were used at a concentration of 1  $\mu\text{g/mL}$  and were released by 10 mg/mL bioactive glass in saline solution. Cell numbers were manually counted from H&E-stained histological sections. Values represent the average of 4 experimental replicates in which 6 histological sections were randomly selected from 3 different samples within an experiment. Statistical significance was assessed by the Student's *t*-test in which cell numbers of OD-21s exposed to DMCs were compared with cell numbers cultured in DMEM only. Error bars represent  $\pm\text{SD}$ , \* =  $p \leq 0.05$ .

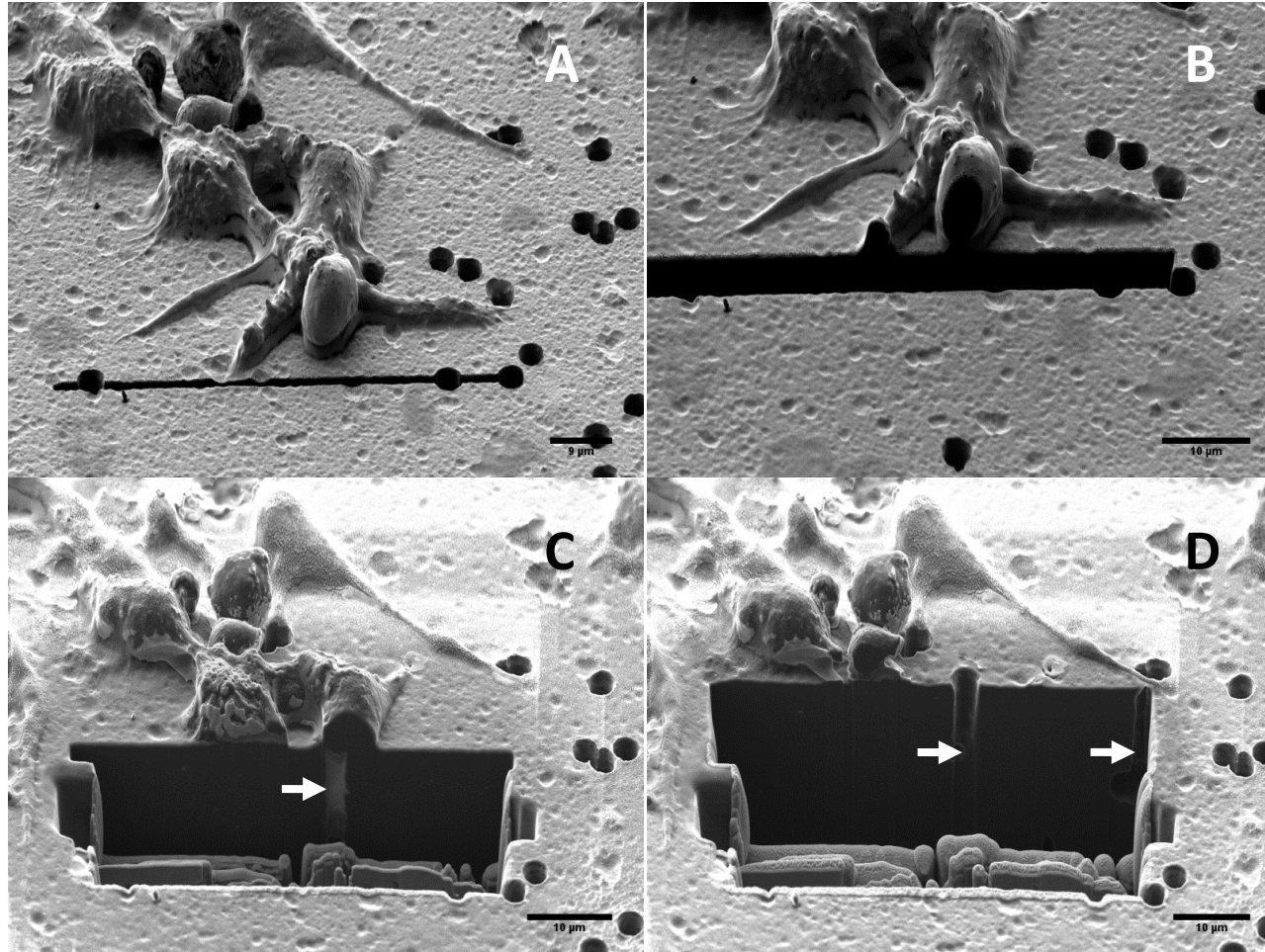


**Figure 6.15** Numbers of cellular extensions per unit area of cells cultured on PET Thininserts in the presence and absence (control) of DMCs.

DMCs were applied at a concentration of 1  $\mu\text{g}/\text{mL}$  and were released from dentine by 10  $\text{mg}/\text{mL}$  bioactive glass in saline solution. Results are an average of four separate experiments in which 6 histological sections were obtained from 3 technical replicates. Error bars represent  $\pm$  SD; no statistical significance was observed with the Student's *t*-test when cell numbers of those exposed to DMCs were compared against the control.

#### **6.1.8 FIB-SEM Slice-and-view**

To confirm the presence of cellular extensions projecting into the PET Thinsert pores, dual beam FIB-SEM preliminary analysis was used to prepare sequential sections through the PET to allow a cross-sectional view. The technique employed the 'slice-and-view' approach, in which a cross-sectional secondary electron image was captured at the freshly exposed sample (see methods Section 2.8.3). Figure 6.16 provides selected sequential images of the milling process, obtained over a 12 hour period. From the cross-sectional Image C (Figure 6.16), there is sufficient contrast to facilitate the observation of a cellular extension within a pore. A direct comparison with the occupied pore is provided in Image D (Figure 6.16) in which there are distinctly two empty pores (see image annotations). This corroborates the histomorphometric observations whereby the presence of cellular extensions projecting into PET Thinsert pores was first observed (see Section 6.1.6).



**Figure 6.16 Sequential FIB-SEM process used to observe OD-21 cells cultured on PET Thinserts in cross-section.**

Sequential images were captured over a 12 hour period, using the 'slice-and-view' method, in which a secondary electron image was captured at the freshly exposed sample, to allow a cross-sectional view. **A)** and **B)** Early secondary electron images of the FIB milling process. **C)** Arrow head indicating a cellular extension penetrating a PET Thinsert pore. **D)** Arrow heads indicating unoccupied pores. Scale bars are shown.

## 7.0 RESULTS CHAPTER FIVE

### 7.1 Proteomic Analysis of Dentine Matrix Components

The previous chapters have reported on the ability of various concentrations of bioactive glass in saline solution to release components from human dentine. Although these dentine matrix components (DMCs) were characterised biochemically using more preliminary techniques in Results Chapter One (see Section 3.0), there is scope for application of more sophisticated techniques to characterise the constituents. This chapter describes studies using high throughput techniques to characterise the DMC protein profile. The samples selected for this study were DMCs released by 10 mg/mL bioactive glass in saline solution, DMCs released by the control solution of saline only and DMCs released by the gold-standard solution, EDTA. Knowledge of the constituents of solubilised DMCs may provide a clearer understanding of how they exert their cellular effects as described in the previous chapters, whilst their comparison to the routinely used EDTA-released DMCs should provide context within the literature. In addition, this work may assist the understanding of the different mechanisms of action of the various extractants.

Results Chapter One demonstrated the protein profile of DMCs on a 1D-SDS PAGE gel; subsequently, for the analysis presented here, protein bands were excised and analysed by LC-MS/MS (see Section 2.2.6). The resultant lists of identified proteins were uploaded into the publicly available DAVID (Database for Annotation, Visualization and Integrated Discovery) Bioinformatics tool, which is able to extract ontological information from such large protein datasets. The second part of this study involved the use of a multiplex sandwich ELISA to quantify the levels of 20 proteins pertinent to repair processes, in EDTA-

and 10 mg/mL bioactive glass in saline solution-released DMCs. Abbreviations of proteins discussed during this chapter are provided on the subsequent pages.

## LIST OF PROTEIN ABBREVIATIONS

<b>ACTB</b>	Actin, cytoplasmic 1
<b>ACTBL2</b>	Beta-actin-like protein 2
<b>ACTG1</b>	Actin, cytoplasmic 2
<b>ACTG2</b>	Actin, gamma-enteric smooth muscle
<b>AFP</b>	Alpha-fetoprotein
<b>AHSG</b>	Alpha-2-HS-glycoprotein
<b>ALB</b>	Lipid-binding protein albumin
<b>AMBN</b>	Ameloblastin
<b>APLP2</b>	Amyloid-like protein 2
<b>APOD</b>	Apolipoprotein D
<b>ARF3</b>	ADP-ribosylation factor 3
<b>ARG1</b>	Arginase-1
<b>ARPC5</b>	Actin-related protein 2/3 complex subunit 5
<b>ATP5D</b>	ATP synthase subunit delta, mitochondrial
<b>BGN</b>	Biglycan
<b>BMP</b>	Bone morphogenetic protein
<b>C8B</b>	Complement component C8 beta chain
<b>CA3</b>	Carbonic anhydrase 3
<b>CALM1</b>	Calmodulin
<b>CAPG</b>	Macrophage-capping protein
<b>CAPN2</b>	Calpain-2 catalytic subunit
<b>CASP12</b>	Inactive caspase-12
<b>CFHR2</b>	Complement factor H-related protein 2
<b>CFI</b>	Complement factor I
<b>CFL1</b>	Cofilin-1
<b>CFL2</b>	Cofilin-2
<b>CLU</b>	Clusterin
<b>COL11A1</b>	Collagen alpha-1(XI) chain
<b>COL14A1</b>	Collagen alpha-1(XIV) chain
<b>COL18A1</b>	Collagen alpha-1(XVIII) chain
<b>COL1A1</b>	Collagen alpha-1(I) chain
<b>COL1A2</b>	Collagen alpha-1(II) chain
<b>CRP</b>	C-reactive protein
<b>CST1</b>	Cystatin-SN
<b>CST4</b>	Cystatin-S
<b>CST7</b>	Cystatin-F
<b>CSTA</b>	Cystatin-A
<b>CTHRC1</b>	Collagen triple helix repeat-containing protein 1

<b>DCD</b>	Dermcidin
<b>DEFA1</b>	Neutrophil defensin 1
<b>DMCs</b>	Dentine matrix components
<b>DMD</b>	Dystrophin
<b>DSP</b>	Desmoplakin
<b>EGF</b>	Epidermal growth factor
<b>EIF4A1</b>	Eukaryotic initiation factor 4A-I
<b>F12</b>	Coagulation factor XII
<b>F2</b>	Prothrombin
<b>FABP3</b>	Fatty acid-binding protein, heart
<b>FGF</b>	Fibroblast growth factor
<b>FLG</b>	Filaggrin
<b>FN1</b>	Fibronectin
<b>FRZB</b>	Secreted frizzled-related protein 3
<b>GAS6</b>	Growth arrest-specific protein 6
<b>GDI2</b>	Rab GDP dissociation inhibitor beta
<b>GDNF</b>	Glial cell-derived neurotrophic factor
<b>GGCT</b>	Gamma-glutamylcyclotransferase
<b>GLO1</b>	Lactoylglutathione lyase
<b>GM-CSF</b>	Granulocyte-macrophage colony-stimulating factor
<b>GMFB</b>	Glia maturation factor beta
<b>GPI</b>	Glucose-6-phosphate isomerase
<b>GSS</b>	Glutathione synthetase
<b>H1FO</b>	Histone H1.0
<b>HBB</b>	Hemoglobin subunit beta
<b>HGF</b>	Hepatocyte growth factor
<b>HIST1H2AH</b>	Histone H2A type 1-H
<b>HIST1H2BK</b>	Histone H2B type 1-K
<b>HNRNPA2B1</b>	Heterogeneous nuclear ribonucleoproteins A2/B1
<b>HNRNPH3</b>	Heterogeneous nuclear ribonucleoprotein H3
<b>HNRNPK</b>	Heterogeneous nuclear ribonucleoprotein K
<b>HSP90AB1</b>	Heat shock protein HSP 90-beta
<b>HSPA7</b>	Putative heat shock 70 kDa protein 7
<b>IGF1</b>	Insulin-like growth factor I
<b>IGF1-BP1</b>	Insulin-like growth factor-binding protein 1
<b>IGF1-SR</b>	Insulin-like growth factor-surface receptor
<b>IGF2</b>	Insulin-like growth factor 2
<b>IGFALS</b>	Insulin-like growth factor-binding protein complex acid labile chain
<b>IGHG1</b>	Immunoglobulin gamma-1 chain C region



<b>IGJ</b>	Immunoglobulin J chain
<b>IGKC</b>	Immunoglobulin kappa chain C region
<b>IGLC1</b>	Immunoglobulin lambda-1 chain C regions
<b>IGLC2</b>	Immunoglobulin lambda-2 chain C regions
<b>ITIH1</b>	Inter-alpha-trypsin inhibitor heavy chain H1
<b>ITM2B</b>	Integral membrane protein 2B
<b>KCNN4</b>	Intermediate conductance ca-activated potassium channel protein 4
<b>LAMP2</b>	Lysosome-associated membrane glycoprotein 2
<b>LC-MS/MS</b>	Liquid chromatography-tandem mass spectrometry
<b>LUM</b>	Lumican
<b>LXN</b>	Latexin
<b>MANF</b>	Mesencephalic astrocyte-derived neurotrophic factor
<b>M-CSF</b>	Macrophage colony stimulating factor
<b>MDH1</b>	Malate dehydrogenase, cytoplasmic
<b>MDH2</b>	Malate dehydrogenase, mitochondrial
<b>MIF</b>	Macrophage migration inhibitory factor
<b>MMP20</b>	Matrix metalloproteinase-20
<b>MUC5AC</b>	Mucin-5AC (Fragments)
<b>MUCL1</b>	Mucin-like protein 1
<b>MYO5B</b>	Myosin-Vb
<b>NGF</b>	Nerve growth factor
<b>NUCB1</b>	Nucleobindin-1
<b>PBXIP1</b>	Pre-B-cell leukemia transcription factor-interacting protein 1
<b>PCOLCE</b>	Procollagen C-endopeptidase enhancer 1
<b>PDGFF-AA</b>	Platelet-derived growth factor-AA
<b>PDLIM1</b>	PDZ and LIM domain protein 1
<b>PEPD</b>	Xaa-Pro dipeptidase
<b>PFN1</b>	Profilin-1
<b>PGLYRP2</b>	N-acetylmuramoyl-L-alanine amidase
<b>PIP</b>	Prolactin-inducible protein
<b>POSTN</b>	Periostin
<b>PRDX3</b>	Thioredoxin-dependent peroxide reductase, mitochondrial
<b>PRDX5</b>	Peroxiredoxin-5, mitochondrial
<b>PREPL</b>	Prolyl endopeptidase-like
<b>PRKCSH</b>	Glucosidase 2 subunit beta
<b>PRSS3</b>	Trypsin-3
<b>PSMB1</b>	Proteasome subunit beta type-1
<b>PSMB6</b>	Proteasome subunit beta type-6
<b>PSME1</b>	Proteasome activator complex subunit 1

<b>PTN</b>	Pleiotrophin
<b>PYGM</b>	Glycogen phosphorylase, muscle form
<b>RAB10</b>	Ras-related protein Rab-10
<b>RAB11A</b>	Ras-related protein Rab-11A
<b>RAB1C</b>	Putative Ras-related protein Rab-1C
<b>RAB2A</b>	Ras-related protein Rab-2A
<b>RAB7A</b>	Ras-related protein Rab-7a
<b>RBP4</b>	Retinol-binding protein 4
<b>RCN3</b>	Reticulocalbin-3
<b>RPLP0</b>	60S acidic ribosomal protein P0
<b>RPS3</b>	40S ribosomal protein S3
<b>SCGB1D2</b>	Secretoglobin family 1D member 2
<b>SEMA3E</b>	Semaphorin-3E
<b>SEMG2</b>	Semenogelin-2
<b>SERPINA1</b>	Alpha-1-antitrypsin
<b>SERPINA4</b>	Kallistatin
<b>SERPINA5</b>	Plasma serine protease inhibitor
<b>SERPINA7</b>	Thyroxine-binding globulin
<b>SERPINB12</b>	Serpin B12
<b>SERPINC1</b>	Antithrombin-III
<b>SERPIND1</b>	Heparin cofactor 2
<b>SERPINF1</b>	Pigment epithelium-derived factor
<b>SET</b>	Protein SET
<b>SFRS1</b>	Splicing factor, arginine/serine-rich 1
<b>SOD2</b>	Superoxide dismutase [Mn], mitochondrial
<b>SPRY2</b>	Protein sprouty homolog 2
<b>SPTAN1</b>	Spectrin alpha chain, brain
<b>SRI</b>	Sorcin
<b>TALDO1</b>	Transaldolase
<b>TF</b>	Serotransferrin
<b>TGF</b>	Transforming growth factor
<b>THBS1</b>	Thrombospondin-1
<b>TIMP2</b>	Metalloproteinase inhibitor 2
<b>TIMP3</b>	Metalloproteinase inhibitor 3
<b>TKT</b>	Transketolase
<b>TNC</b>	Tenascin
<b>TPT1</b>	Triosephosphate isomerase
<b>TUBB4</b>	Tubulin beta-4 chain
<b>UBC</b>	Polyubiquitin-C

<b>VEG-F</b>	Vascular endothelial growth factor
<b>VIM</b>	Vimentin
<b>VIT</b>	Vitrin

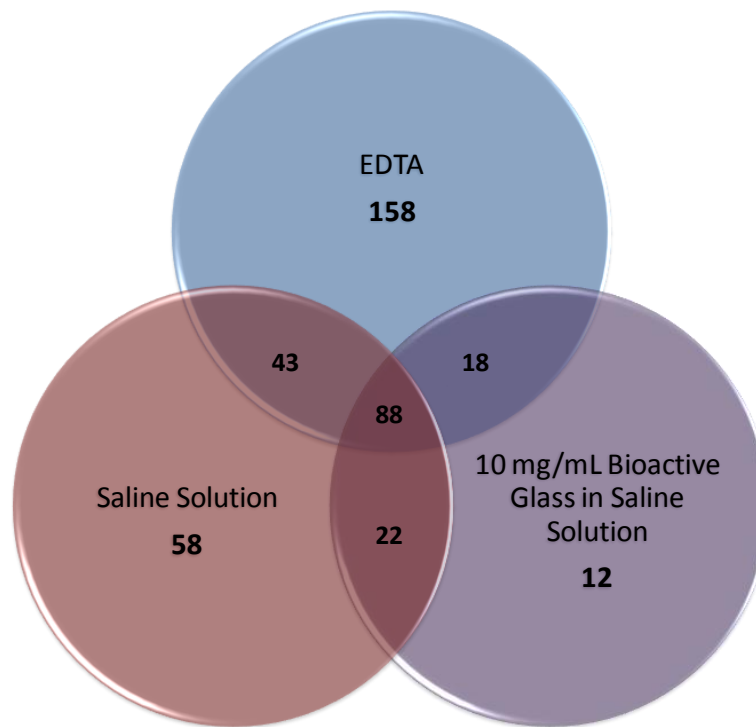
### 7.1.1 Proteins Identified in Dentine Matrix Components

A common issue arising during proteomic studies is the contamination of samples with dermal proteins, such as keratins from skin, and proteins in dust arising during sample preparation (Jagr *et al.*, 2012). Subsequently it is extremely difficult to determine whether these contaminants are present in the sample itself or have arisen due to cross-contamination (Petrak *et al.*, 2008; Jagr *et al.*, 2012). In previous proteomic studies of human dentine, it has been customary to subtract keratins as background (Jagr *et al.*, 2012; Park *et al.*, 2009); therefore, for the present study keratins have also been removed prior to further analyses.

The number of proteins detected in DMCs released by EDTA, saline solution and 10 mg/mL bioactive glass in saline are presented in the form of a Venn diagram (see Figure 7.1). The greatest numbers of proteins were detected in DMCs released by EDTA (307), followed by saline (211), whilst 140 proteins were identified in DMCs solubilised by 10 mg/mL bioactive glass in saline solution. Eighty-eight proteins were in common with all 3 samples, 83 in 2 samples, and 228 proteins were unique to their relative extractant (i.e. 158 proteins identified in EDTA-released DMCs only, followed by 58 in saline-released DMCs and 12 proteins uniquely identified in DMCs released by 10 mg/mL bioactive glass in saline).

Upon inspection of the datasets of the proteins detected in all DMCs, it was evident that a number of well-characterised dentine matrix proteins were present. These included collagenous proteins (e.g. COL1A1, COL1A2), non-collagenous proteins (e.g. LUM, BGN) and bioactive molecules (e.g. POSTN, TNC). Proteins involved in odontogenesis, mineralisation and extracellular matrix formation processes were also identified in all DMCs (e.g. FN1, THBS1, F2, ACTB, MMP20, PTN, CLU). These data provided validation to the approaches

used to both solubilise and identify proteins released from the dentine matrix. However, a comparison with previously published proteomic studies of human dentine would provide further validation of the study whilst contextualising the results and may identify proteins that had not previously been reported within dentine.



**Figure 7.1 Venn diagram showing number of proteins detected in DMCs released by EDTA, saline solution and 10 mg/mL bioactive glass in saline solution.**

Currently, there have been three published relatively comprehensive studies of the dentine proteome and these data have identified the presence of a complex mix of proteins with a diverse range of functions, in addition to many proteins with, thus far, unknown function (Park *et al.*, 2009; Chun *et al.*, 2011; Jagr *et al.*, 2012). The proteins detected in EDTA-released DMCs were compared with those listed by Jagr *et al.*, (2012), Park *et al.*, (2009) and Chun *et al.*, (2011), which also used EDTA in their extraction techniques. In the current

study a total of 307 proteins were detected in the EDTA-released DMCs, whereas previous publications identified 233, 147 and 296 proteins (Park *et al.*, 2009; Chun *et al.*, 2012 and Jagr *et al.*, 2012, respectively). Of the 307 proteins detected in the present study, 103 were unique to the work presented here and had not previously been reported in the published dentine proteomic studies, whereas the remaining 204 proteins were in common with the other studies. There were 58 proteins in common with the present and previously published studies.

#### **7.1.1.1 Relatively Abundant Proteins Detected in DMCs**

Tables 7.1 A-C list the 10 most abundant proteins detected in all samples of DMCs, ordered according to their MASCOT Score. This is not a fully quantitative measure as the MASCOT score is the probability that a match (of a peptide mass or MS/MS fragment ion mass) is a random event (Jagr *et al.*, 2012). Proteins that are measured with a higher confidence have a larger score and are generally the most abundant. The most abundant protein detected in all 3 samples was the lipid-binding protein albumin (ALB). All 3 samples of DMCs also contained the serine protease inhibitor, SERPINA1, the iron binding protein, TF, and the intermediate filament protein, VIM, in their 10 most abundant proteins, although they were ranked differently in abundance in each sample. Saline and 10 mg/mL bioactive glass in saline solution-released DMCs had a further 5 identical proteins present in their 10 most abundant proteins (DCD, LUM, IGKC, IGHG1 and COL1A2). However DSP and HBB were uniquely in the 10 most abundant proteins in DMCs released by saline and 10 mg/mL bioactive glass in saline solution, respectively. Six of the most abundant proteins in the EDTA-released DMCs (i.e. F2, AHSG, SERPINF1, PCOLCE, BGN and SERPINC1), were not found in the 10 most abundant proteins of the other 2 samples.

<b>Ten Most Abundant Proteins</b>	<b>MASCOT Score</b>	<b>No. Unique Peptide Hits</b>
Serum albumin (ALB)	10128.64	52
Serotransferrin (TF)	3159.50	33
Alpha-1-antitrypsin (SERPINA1)	1468.02	18
Ig gamma-1 chain C region (IGHG1)	1197.88	1
Desmoplakin (DSP)	1020.06	27
Vimentin (VIM)	945.34	15
Lumican (LUM)	898.39	9
Dermcidin (DCD)	853.31	4
Ig kappa chain C region (IGKC)	745.69	6
Collagen alpha-2(I) chain (COL1A2)	745.35	3

**A**

<b>Ten Most Abundant Proteins</b>	<b>MASCOT Score</b>	<b>No. Unique Peptide Hits</b>
Serum albumin (ALB)	6681.53	47
Serotransferrin (TF)	2210.41	27
Alpha-1-antitrypsin (SERPINA1)	1161.96	19
Vimentin (VIM)	984.37	14
Ig gamma-1 chain C region (IGHG1)	913.85	4
Dermcidin (DCD)	791.72	4
Collagen alpha-2(I) chain (COL1A2)	594.43	3
Ig kappa chain C region (IGKC)	569.49	6
Lumican (LUM)	550.95	8
Hemoglobin subunit beta (HBB)	550.87	7

**B**

<b>Ten Most Abundant Proteins</b>	<b>MASCOT Score</b>	<b>No. Unique Peptide Hits</b>
Serum albumin (ALB)	8357.30	45
Prothrombin (F2)	5990.78	28
Alpha-2-HS-glycoprotein (AHSG)	3781.28	13
Vimentin (VIM)	3437.43	27
Pigment epithelium-derived factor (SERPINF1)	3068.51	14
Serotransferrin (TF)	2673.46	25
Procollagen C-endopeptidase enhancer 1 (PCOLCE)	2090.30	12
Biglycan (BGN)	2081.94	12
Alpha-1-antitrypsin (SERPINA1)	1985.60	13
Antithrombin-III (SERPINC1)	1819.47	14

**C**

**Table 7.1 Ten most abundant proteins detected in DMCs.**






DMCs released by **A)** saline solution, **B)** 10 mg/mL bioactive glass in saline solution and **C)** EDTA. Proteins are arranged according to the MASCOT score and number of unique peptide hits, with the most abundant listed first.

#### **7.1.1.2 Ontological Analysis**

While EDTA solubilised 103 proteins that are thus far unreported in dentine proteomic studies, saline and 10 mg/mL bioactive glass in saline solutions released 80 and 36 novel proteins, respectively. To aid interpretation of these data, the publicly-available DAVID Bioinformatics tool was used to extract ontological information (Huang *et al.*, 2009a). The software generated information on biological processes, molecular functions and cellular components associated with proteins detected in DMCs. The modified Fisher Exact p-value was used as a measure of enrichment, i.e. the probability of proteins being specifically associated to a particular ontological term rather than random chance. A p-value of less than 0.05 was deemed statistically significant.




The significant cellular components of proteins previously not detected in dentine proteomic studies are listed in Tables 7.2-7.4. In corroboration with the nature of the sample, the majority of proteins detected in all DMCs had extracellular association. However, some proteins in saline-released DMCs also associated with cytoplasmic membrane-bound vesicles. There were also numerous cytosolic and cytoskeletal proteins identified in EDTA-released DMCs.



Cellular Components	% of Total Proteins	p Value	Protein Symbols
extracellular space	 16%	7.87E-05	COL18A1, RBP4, F12, CRP, SEMG2, MIF, GPI, SERPINA7, APOD, SCGB1D2, PRSS3, DEFA1, CFI
extracellular region	 29%	8.19E-05	COL18A1, DCD, RBP4, F12, CRP, SEMG2, IGJ, CST1, MANF, MIF, GPI, AMBN, APOD, SERPINA7, CST7, SCGB1D2, PGLYRP2, PRSS3, PIP, DEFA1, CFI, IGLC2, IGLC1, CALM1
extracellular region part	 18%	4.94E-04	COL18A1, RBP4, F12, CRP, SEMG2, MIF, GPI, AMBN, SERPINA7, APOD, SCGB1D2, PRSS3, DEFA1, CFI
heterogeneous nuclear ribonucleoprotein complex	 4%	0.003	HNRNPH3, HNRNPK, HNRNPA2B1
cytoplasmic membrane-bounded vesicle	 9%	0.047	RAB2A, RAB7A, LAMP2, FLG, SEMG2, CAPG, RAB11A








**Table 7.2 Cellular components associated with proteins detected in saline-released DMCs.**

Significant ( $p < 0.05$ ) cellular localisation of proteins were selected from a list generated by the DAVID Bioinformatics tool. Numerical values represent the percentage of total number of proteins that have previously not been reported in dentine proteomic studies, originating in the corresponding cellular compartment.

Cellular Components	% of Total Proteins	p Value	Protein Symbols
extracellular region	 42%	7.99E-06	DCD, SEMG2, CST1, MUCL1, GPI, AMBN, SERPINA7, APOD, ITIH1, CST7, SCGB1D2, PRSS3, PIP, DEFA1, IGLC2
extracellular space	 19%	0.002	GPI, APOD, SERPINA7, SCGB1D2, SEMG2, PRSS3, DEFA1
extracellular region part	 22%	0.002	GPI, AMBN, APOD, SERPINA7, SCGB1D2, SEMG2, PRSS3, DEFA1

**Table 7.3 Cellular components associated with proteins detected in 10 mg/mL bioactive glass in saline solution-released DMCs.**

Significant ( $p < 0.05$ ) cellular localisation of proteins were selected from a list generated by the DAVID Bioinformatics tool. Numerical values represent the percentage of total number of proteins that have previously not been reported in dentine proteomic studies, originating in the corresponding cellular compartment.

Cellular Components	% of Total Proteins	p Value	Protein Symbols
extracellular region	 36%	2.63E-09	DCD, RBP4, CTHRC1, CRP, TIMP2, VIT, TIMP3, MIF, TGFB2, CFHR2, ITIH1, SERPINA5, PGLYRP2, SERPINA4, SEMA3E, PRSS3, TPT1, PIP, COL11A1, IGFALS, IGF1, IGF2, FRZB, GAS6, NUCB1, AFP, GPI, C8B, AMBN, COL14A1, CST7, SCGB1D2, CST4, DEFA1, MUC5AC, SERPIND1, CALM1
extracellular region part	 23%	3.22E-08	RBP4, CTHRC1, CRP, IGF1, IGFALS, IGF2, VIT, TIMP2, TIMP3, MIF, TGFB2, NUCB1, C8B, AFP, GPI, AMBN, COL14A1, SCGB1D2, PRSS3, SEMA3E, TPT1, DEFA1, MUC5AC, COL11A1
extracellular space	 16%	3.47E-05	RBP4, CRP, IGF1, IGFALS, IGF2, MIF, TGFB2, NUCB1, C8B, AFP, GPI, SCGB1D2, SEMA3E, PRSS3, TPT1, DEFA1
extracellular matrix	 9%	0.002	CTHRC1, AMBN, COL14A1, MUC5AC, VIT, TIMP2, COL11A1, TIMP3, TGFB2
proteinaceous extracellular matrix	 8%	0.005	CTHRC1, AMBN, COL14A1, MUC5AC, VIT, TIMP2, COL11A1, TIMP3
extracellular matrix part	 5%	0.007	COL14A1, MUC5AC, TIMP2, COL11A1, TIMP3
actin cytoskeleton	 7%	0.008	ACTG1, PFN1, ACTG2, CFL1, ARPC5, MYO5B, SPTAN1








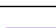










**Table 7.4a Cellular components associated with proteins detected in EDTA-released DMCs.**

Significant ( $p < 0.05$ ) cellular localisation of proteins were selected from a list generated by the DAVID Bioinformatics tool. Numerical values represent the percentage of total number of proteins that have previously not been reported in dentine proteomic studies, originating in the corresponding cellular compartment. (*Table continued on next page*).

Cellular Components	% of Total Proteins	p Value	Protein Symbols
cytosol	 17%	0.012	GGCT, TKT, PRDX3, RPS3, ACTG1, SET, PSMB6, PBXIP1, PSME1, PSMB1, RPLP0, EIF4A1, UBC, CALM1, TUBB4, SPTAN1, MDH1
insulin-like growth factor binding protein complex	 2%	0.026	IGFALS, IGF1
cytoskeleton	 16%	0.034	ACTBL2, H1FO, ARPC5, ACTG1, ACTG2, PFN1, PBXIP1, DMD, CFL2, CFL1, TPT1, CSTA, MYO5B, CALM1, TUBB4, SPTAN1
Z disc	 3%	0.037	SRI, DMD, SPTAN1
contractile fiber part	 4%	0.038	SRI, ACTG2, DMD, SPTAN1
cortical cytoskeleton	 3%	0.041	ACTG1, CFL1, SPTAN1
contractile fiber	 4%	0.045	SRI, ACTG2, DMD, SPTAN1









**Table 7.4b (Continued from 7.4a) Cellular components associated with proteins detected in EDTA-released DMCs.**

The significant biological processes associated with proteins that had not been previously identified during dentine proteomic studies were wide-ranging in all extracted DMC samples (see Tables 7.5-7.7). The majority of proteins detected in DMCs released by 10 mg/mL bioactive glass in saline were associated with the immune response or metabolic processes. These biological processes were also associated with proteins detected in saline-only released DMCs, in addition to a large proportion of proteins linked to the regulation of apoptosis. Saline-released DMCs also contained proteins associated with epithelial development and the response to inorganic substances. There were also several proteins identified in EDTA-released DMCs associated with the immune response, metabolic processes and the regulation of cell death. Proteins relevant to skeletal system development, regulation of growth, GTPase signal transduction and regulation of protein modification were also detected in EDTA-released DMCs that had not been reported in other dentine proteomic studies.

Biological Processes	% of Total Proteins	p Value	Protein Symbols
response to organic substance	 10%	0.049	RBP4, F12, SERPINA7, CFL1, CASP12, FABP3, PRDX3, MANF
epithelium development	 6%	0.021	COL18A1, PFN1, FLG, CFL1, CSTA
monosaccharide metabolic process	 6%	0.020	GPI, RBP4, TALDO1, MDH2, MDH1
regulation of cell death	 13%	0.013	COL18A1, CFL1, CASP12, UBC, PRDX5, GLO1, PRDX3, SART1, SOD2, MIF
regulation of programmed cell death	 13%	0.012	COL18A1, CFL1, CASP12, UBC, PRDX5, GLO1, PRDX3, SART1, SOD2, MIF
hexose metabolic process	 6%	0.012	GPI, RBP4, TALDO1, MDH2, MDH1
regulation of apoptosis	 13%	0.012	COL18A1, CFL1, CASP12, UBC, PRDX5, GLO1, PRDX3, SART1, SOD2, MIF
defense response	 11%	0.007	DCD, KCNN4, F12, PGLYRP2, CRP, PRDX5, DEFA1, CFI, MIF
response to oxidative stress	 6%	0.007	GSS, PRDX5, PDLIM1, PRDX3, SOD2
negative regulation of cell death	 9%	0.006	CFL1, UBC, PRDX5, GLO1, PRDX3, SOD2, MIF
negative regulation of programmed cell death	 9%	0.006	CFL1, UBC, PRDX5, GLO1, PRDX3, SOD2, MIF
negative regulation of apoptosis	 9%	0.006	CFL1, UBC, PRDX5, GLO1, PRDX3, SOD2, MIF
glucose metabolic process	 6%	0.006	GPI, RBP4, TALDO1, MDH2, MDH1
immune response	 13%	0.004	GPI, F12, CST7, PGLYRP2, CRP, IGJ, DEFA1, CFI, IGLC2, IGLC1, MIF
response to inorganic substance	 8%	0.003	ATP5D, GSS, PRDX5, PRDX3, CALM1, SOD2
cofactor metabolic process	 8%	0.002	GSS, TALDO1, GLO1, MDH2, SOD2, MDH1
carbohydrate catabolic process	 6%	0.002	GPI, TALDO1, PGLYRP2, MDH2, MDH1
coenzyme metabolic process	 8%	7.19E-04	GSS, TALDO1, GLO1, MDH2, SOD2, MDH1












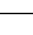
**Table 7.5 Biological processes associated with proteins detected in saline-released DMCs.**

Significant ( $p < 0.05$ ) molecular functions of proteins were selected from a list generated by the DAVID Bioinformatics tool. Numerical values represent the percentage of the total number of proteins that have previously not been reported in dentine proteomic studies, associated with the corresponding biological processes.

Biological Processes	% of Total Proteins	p Value	Protein Symbols
defense response to fungus	 6%	0.0209	DCD, DEFA1
killing of cells of another organism	 6%	0.0225	DCD, DEFA1
cell killing	 6%	0.0383	DCD, DEFA1
response to fungus	 6%	0.0383	DCD, DEFA1
glutathione metabolic process	 6%	0.0446	GSS, GLO1
negative regulation of catalytic activity	 8%	0.0438	SPRY2, UBC, CSTA
peptide metabolic process	 6%	0.0428	GSS, GLO1
immune response	 11%	0.0491	GPI, CST7, DEFA1, IGLC2


**Table 7.6 Biological processes associated with proteins detected in 10 mg/mL bioactive glass in saline solution-released DMCs.**

Significant ( $p < 0.05$ ) molecular functions of proteins were selected from a list generated by the DAVID Bioinformatics tool. Numerical values represent the percentage of the total number of proteins that have previously not been reported in dentine proteomic studies, associated with the corresponding biological processes.

Biological Processes	% of Total Proteins	p Value	Protein Symbols
skeletal system development	 6%	0.040	RBP4, AMBN, IGF1, IGF2, FRZB, COL11A1
cellular macromolecular complex assembly	 6%	0.040	H1FO, SET, HIST1H2BK, HIST1H2AH, SFRS1, TUBB4
response to wounding	 8%	0.037	C8B, CRP, IGF1, IGF2, SERPIND1, TIMP3, MIF, TGFB2
small GTPase mediated signal transduction	 6%	0.034	GDI2, ARF3, CFL1, RAB1C, IGF1, RAB10
anti-apoptosis	 5%	0.034	CFL1, UBC, TPT1, IGF1, GLO1
chemical homeostasis	 8%	0.032	SRI, RBP4, PYGM, TPT1, IGF1, IGF2, PRDX3, APLP2
response to bacterium	 5%	0.027	DCD, HIST1H2BK, PGLYRP2, DEFA1, PRDX3
wound healing	 5%	0.027	IGF1, IGF2, SERPIND1, TIMP3, TGFB2
response to organic substance	 10%	0.026	HSP90AB1, AFP, RBP4, PYGM, CFL1, HSPA7, IGF2, PRDX3, TIMP3, TGFB2
positive regulation of molecular function	 9%	0.022	PSMB6, PSMB1, PSME1, UBC, IGF2, PRDX3, CALM1, RPS3, TGFB2
cell motion	 8%	0.022	ACTG1, CTHRC1, PRSS3, CFL1, UBC, IGF1, ARPC5, TGFB2
extracellular structure organization	 5%	0.016	COL14A1, MUC5AC, COL11A1, APLP2, TGFB2







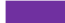






**Table 7.7a Biological processes associated with proteins detected in EDTA-released DMCs.**

Significant ( $p < 0.05$ ) molecular functions of proteins were selected from a list generated by the DAVID Bioinformatics tool. Numerical values represent the percentage of the total number of proteins that have previously not been reported in dentine proteomic studies, associated with the corresponding biological processes (*Table continued on next page*).

Biological Processes	% of Total Proteins	p Value	Protein Symbols
regulation of growth	 7%	0.015	RBP4, UBC, IGF1, IGF2, TKT, GAS6, TGFB2
positive regulation of protein metabolic process	 6%	0.014	PSMB6, PSMB1, PSME1, UBC, IGF1, IGF2
positive regulation of cellular protein metabolic process	 6%	0.012	PSMB6, PSMB1, PSME1, UBC, IGF1, IGF2
negative regulation of macromolecule metabolic process	 11%	0.011	HSP90AB1, SET, PSMB6, PBXIP1, PSMB1, PSME1, SERPINA5, UBC, IGF2, TIMP3, RPS3
monosaccharide metabolic process	 6%	0.010	GPI, RBP4, PYGM, IGF2, MDH2, MDH1
regulation of organelle organization	 6%	0.009	SET, CFL1, IGF1, IGF2, ARPC5, SPTAN1
muscle organ development	 5%	0.008	SRI, RBP4, DMD, IGF1, COL11A1, TGFB2
regulation of protein modification process	 5%	0.008	SET, PSMB6, PSMB1, PSME1, UBC, IGF1, IGF2
hexose metabolic process	 10%	0.006	GPI, RBP4, PYGM, IGF2, MDH2, MDH1
negative regulation of protein modification process	 9%	0.005	SET, PSMB6, PSMB1, PSME1, UBC
negative regulation of cell death	 8%	0.005	CFL1, UBC, TPT1, IGF1, IGF2, GLO1, PRDX3, MIF
negative regulation of programmed cell death	 5%	0.005	CFL1, UBC, TPT1, IGF1, IGF2, GLO1, PRDX3, MIF









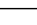

**Table 7.7b (Continued from 7.7a) Biological processes associated with proteins detected in EDTA-released DMCs.** (*Table continued on next page*).



Biological Processes	% of Total Proteins	p Value	Protein Symbols
positive regulation of protein modification process	 6%	0.005	PSMB6, PSMB1, PSME1, UBC, IGF1, IGF2
negative regulation of apoptosis	 8%	0.005	CFL1, UBC, TPT1, IGF1, IGF2, GLO1, PRDX3, MIF
carbohydrate catabolic process	 5%	0.004	GPI, PYGM, PGLYRP2, MDH2, MDH1
extracellular matrix organization	 5%	0.003	COL14A1, MUC5AC, COL11A1, APLP2, TGFB2
regulation of cell death	 13%	0.003	IGF1, IGF2, PRDX3, ITM2B, TIMP3, TGFB2, MIF, RPS3, CFL1, TPT1, UBC, GLO1, MUC5AC
regulation of programmed cell death	 13%	0.003	IGF1, IGF2, PRDX3, ITM2B, TIMP3, TGFB2, MIF, RPS3, CFL1, TPT1, UBC, GLO1, MUC5AC
regulation of apoptosis	 13%	0.003	IGF1, IGF2, PRDX3, ITM2B, TIMP3, TGFB2, MIF, RPS3, CFL1, TPT1, UBC, GLO1, MUC5AC
glucose metabolic process	 6%	0.002	GPI, RBP4, PYGM, IGF2, MDH2, MDH1
regulation of cellular protein metabolic process	 10%	0.002	HSP90AB1, SET, PSMB6, PSMB1, PSME1, SERPINA5, UBC, IGF1, IGF2, TIMP3
negative regulation of catalytic activity	 8%	0.001	PSMB6, PSMB1, PSME1, UBC, IGF2, CSTA, PRDX3, TGFB2
negative regulation of molecular function	 10%	1.52E-04	PSMB6, PSMB1, PSME1, UBC, IGF2, CSTA, PRDX3, CALM1, RPS3, TGFB2
negative regulation of protein metabolic process	 9%	1.42E-05	HSP90AB1, SET, PSMB6, PSMB1, PSME1, SERPINA5, UBC, IGF2, TIMP3
negative regulation of cellular protein metabolic process	 9%	1.08E-05	HSP90AB1, SET, PSMB6, PSMB1, PSME1, SERPINA5, UBC, IGF2, TIMP3






**Table 7.7c (Continued from 7.7b) Biological processes associated with proteins detected in EDTA-released DMCs.**

The significant molecular functions of proteins previously not detected in dentine proteomic studies are listed in Tables 7.8-7.10. The majority of proteins detected in all DMCs were associated with enzyme inhibitor activity. There were also proteins that were relevant to structural molecule activity present in DMCs released by 10 mg/mL bioactive glass in saline, whereas saline-released DMCs contained proteins implicated in metabolic enzyme and antioxidant activities. The molecular functions associated with proteins identified in EDTA-released DMCs supported the detection of cytoskeletal and actin cellular components (see Table 7.4), i.e. several cytoskeletal and actin binding proteins were detected. There were also proteins associated with growth factor activity, calcium binding and nickel ion binding detected in the EDTA-released DMCs that were not reported in the studies by Jagr *et al.*, (2012), Park *et al.*, (2009) and Chun *et al.*, (2011).

Molecular Function	% of Total Proteins	p Value	Protein Symbols
endopeptidase inhibitor activity	 10%	6.84E-06	SERPINA7, CST7, LXN, PRDX5, CST1, SERPINB12, CSTA, PRDX3
peptidase inhibitor activity	 10%	9.74E-06	SERPINA7, CST7, LXN, PRDX5, CST1, SERPINB12, CSTA, PRDX3
cysteine-type endopeptidase inhibitor activity	 6%	3.14E-05	CST7, PRDX5, CST1, CSTA, PRDX3
enzyme inhibitor activity	 10%	3.51E-04	SERPINA7, CST7, LXN, PRDX5, CST1, SERPINB12, CSTA, PRDX3
L-malate dehydrogenase activity	 3%	0.010	MDH2, MDH1
antioxidant activity	 4%	0.022	PRDX5, PRDX3, SOD2
peroxiredoxin activity	 3%	0.039	PRDX5, PRDX3
malate dehydrogenase activity	 3%	0.039	MDH2, MDH1
serine-type endopeptidase activity	 5%	0.040	F12, PRSS3, PREPL, CFI
manganese ion binding	 5%	0.040	DCD, ARG1, PEPD, SOD2















**Table 7.8 Molecular functions associated with proteins detected in saline-released DMCs.**

Significant ( $p < 0.05$ ) biological processes of proteins were selected from a list generated by the DAVID Bioinformatics tool. Numerical values represent the percentage of the total number of proteins that have previously not been reported in dentine proteomic studies, associated with the corresponding molecular functions.

Molecular Function	% of Total Proteins	p Value	Protein Symbols
endopeptidase inhibitor activity	 14%	9.34E-05	SERPINA7, CST7, ITIH1, CST1, CSTA
peptidase inhibitor activity	 14%	1.15E-04	SERPINA7, CST7, ITIH1, CST1, CSTA
enzyme inhibitor activity	 14%	9.96E-04	SERPINA7, CST7, ITIH1, CST1, CSTA
cysteine-type endopeptidase inhibitor activity	 8%	1.76E-03	CST7, CST1, CSTA
structural molecule activity	 11%	4.96E-02	AMBN, SEMG2, UBC, CSTA

**Table 7.9 Molecular functions associated with proteins detected in 10 mg/mL bioactive glass in saline solution-released DMCs.**

Significant ( $p < 0.05$ ) biological processes of proteins were selected from a list generated by the DAVID Bioinformatics tool. Numerical values represent the percentage of the total number of proteins that have previously not been reported in dentine proteomic studies, associated with the corresponding molecular functions.

Molecular Function	% of Total Proteins	p Value	Protein Symbols
endopeptidase inhibitor activity	 11%	3.39E-08	CST7, ITIH1, CST4, SERPINA5, SERPINA4, SERPIND1, CSTA, PRDX3, TIMP2, TIMP3, APLP2
peptidase inhibitor activity	 11%	5.65E-08	CST7, ITIH1, CST4, SERPINA5, SERPINA4, SERPIND1, CSTA, PRDX3, TIMP2, TIMP3, APLP2
enzyme inhibitor activity	 13%	1.75E-07	PRDX3, TIMP2, TIMP3, APLP2, GMFB, SET, ITIH1, CST7, SERPINA5, CST4, SERPINA4, CSTA, SERPIND1
structural molecule activity	 13%	8.28E-04	ARPC5, RPS3, ACTG1, AMBN, COL14A1, RPLP0, DMD, UBC, CSTA, MUC5AC, COL11A1, TUBB4, SPTAN1
actin binding	 9%	1.30E-03	GMFB, PFN1, CFL2, DMD, CFL1, PIP, ARPC5, MYO5B, SPTAN1
cytoskeletal protein binding	 11%	1.63E-03	GMFB, PFN1, CFL2, DMD, CFL1, PIP, ARPC5, CAPN2, MYO5B, CALM1, SPTAN1
cysteine-type endopeptidase inhibitor activity	 4%	1.79E-03	CST7, CST4, CSTA, PRDX3
serine-type endopeptidase inhibitor activity	 5%	3.09E-03	ITIH1, SERPINA5, SERPINA4, SERPIND1, APLP2
growth factor activity	 6%	4.07E-03	GMFB, GPI, AMBN, IGF1, IGF2, TGFB2
calcium ion binding	 14%	6.53E-03	SRI, CRP, TKT, CAPN2, PRKCSH, GAS6, NUCB1, ITIH1, DMD, PRSS3, TPT1, RCN3, CALM1, SPTAN1
structural constituent of cytoskeleton	 4%	1.26E-02	ACTG1, DMD, ARPC5, SPTAN1
L-malate dehydrogenase activity	 2%	1.31E-02	MDH2, MDH1
extracellular matrix structural constituent	 4%	1.88E-02	AMBN, COL14A1, MUC5AC, COL11A1
nickel ion binding	 2%	0.032	AFP, CA3

**Table 7.10 Molecular functions associated with proteins detected in EDTA-released DMCs.**

Significant ( $p < 0.05$ ) biological processes of proteins were selected from a list generated by the DAVID Bioinformatics tool. Numerical values represent the percentage of the total number of proteins that have previously not been reported in dentine proteomic studies, associated with the corresponding molecular functions.

Having analysed ontological information associated with the proteins uniquely identified in this study, the lists of all proteins detected in DMCs were analysed. The greatest proportion (62 %) of proteins exclusively associated with extracellular localisations were detected in DMCs released by 10 mg/mL bioactive glass in saline solution, whereas DMCs released by saline only and EDTA both contained 47 % proteins associated with this region. Twenty-eight percent of proteins detected in DMCs released by saline solution only were associated with enzyme inhibitor activity, while 22 % of proteins in DMCs released by 10 mg/mL bioactive glass in saline and 15 % EDTA-released DMCs were associated with this activity. The greatest percentage (25 %) of proteins linked to inflammatory processes were detected in the saline-released DMCs, followed by those identified in 10 mg /mL bioactive glass in saline released DMCs (14 %) and EDTA-released DMCs (8%). The greatest proportion of proteins related to angiogenesis (4 %) and metabolic processes (6 %) were detected in 10 mg /mL bioactive glass in saline-released DMCs (4 %), whereas only 1 % of proteins detected in EDTA-released DMCs were associated with angiogenesis and 4 % with metabolic processes. Approximately 14 % of proteins detected in all 3 samples of DMCs were associated with the regulation of apoptosis, and 9 % were linked to calcium ion binding. EDTA-released DMCs had the largest proportion (11 %) of proteins associated with skeletal system development, whereas DMCs released by the other two solutions both had 6 % of their proteins associated with this ontological term.

#### **7.1.1.3 Multiplex Sandwich ELISA Analysis**

To provide a comparison with the global proteomics approach described above, a multiplex sandwich ELISA was used to specifically assess the levels of several growth factors in 10 mg/mL bioactive glass in saline solution and EDTA-released DMCs. The levels of twenty

proteins implicated in a variety of processes pertinent to repair were analysed (Table 7.1); these included colony-stimulating factors, angiogenic growth factors, neurotrophic growth factors, and bone morphogenic proteins, in addition to other well-characterised growth factors such as TGF- $\beta$ 1 and EGF. Six of the proteins analysed (G-CSF, SCF, NT-3, NT-4, IGF1-SR, BMP 4) were below the limit of detection in both EDTA and 10 mg/mL bioactive glass in saline-released DMCs. The results indicated that the presence of TGF- $\beta$ 1 in both EDTA and bioactive glass-released DMCs was above the uppermost limit of detection (100000 pg/mL), which was also the case for IGF1-BP1 and HGF in EDTA-released DMCs.

The majority of the remaining proteins analysed were present at higher levels in EDTA-released DMCs than DMCs released by 10 mg/mL bioactive glass in saline; these included HGF, GM-CSF, GDNF, bNGF, IGF-I, IGF-I SR, IGF2, PDGF-AA, VEG-F and bFGF. However, BMP 7, M-CSF and EGF were detected at higher levels in bioactive glass-released DMCs, relative to EDTA-released DMCs.

The proteins detected in the multiplex ELISA were compared with the proteins detected by LC-MS/MS. There was only partial correlation in the information acquired by both techniques (discussed in Section 8.6); TGF- $\beta$ 1 in DMCs released by 10 mg/mL bioactive glass in saline solution was the only protein detected by both techniques, although it was too concentrated to quantify in the multiplex ELISA. Proteins detected in both techniques in the EDTA-released DMCs were IGF I, IGF II and IGF-BP1.

<i>Protein</i>	EDTA-released DMCs <i>Concentration of Proteins Detected (pg/mL)</i>	Bioactive Glass-released DMCs <i>Concentration of Proteins Detected (pg/mL)</i>
Hepatocyte growth factor (HGF)	457.83	54.90
Transforming growth factor beta-1 (TGF-B1)	sample too concentrated	sample too concentrated
Granulocyte colony stimulating factor (G-CSF)	below limit of detection	below limit of detection
Granulocyte macrophage colony stimulating factor (GM-CSF)	14.90	below limit of detection
Macrophage colony stimulating factor (M-CSF)	below limit of detection	4.70
Beta-nerve growth factor (BNGF)	0	23.63
Stem cell factor (SCF)	below limit of detection	below limit of detection
Glial cell-derived neurotrophic factor (GDNF)	53.53	4.10
Neurotrophin-3 (NT-3)	below limit of detection	below limit of detection
Neurotrophin-4 (NT-4)	below limit of detection	below limit of detection
Insulin-like growth factor-1 (IGF1)	19963.00	below limit of detection
Insulin-like growth factor-binding protein 1 (IGF1-BP1)	sample too concentrated	3449.10
Insulin-like growth factor-surface receptor (IGF1-SR)	below limit of detection	below limit of detection
Insulin-like growth factor-2 (IGF2)	2502.90	227.60
Platelet-derived growth factor-AA (PDGF-AA)	4386.47	72.80
Vascular endothelial growth factor (VEGF)	53.93	15.50
Basic fibroblast growth factor (bFGF)	2227.85	below limit of detection
Bone morphogenetic protein-4 (BMP4)	below limit of detection	below limit of detection
Bone morphogenetic protein-7 BMP7	below limit of detection	33584.33
Epidermal growth factor (EGF)	3.00	4.70

**Table 7.11 Multiplex ELISA analysis of proteins detected in bioactive glass and EDTA-released DMCs.**

DMCs were released from human dentine samples using either EDTA or 10 mg/mL bioactive glass in saline solution. Concentration of proteins detected are expressed in pg/mL, n = 1.

## 8.0 DISCUSSION

The principle aims of dentine hypersensitivity treatment are either to promote the surface occlusion of dentinal tubules, or to desensitise pulpal nerves (Pashley, 1986). Occlusal treatments generally involve the deposition of crystalline materials on the dentine surface, whereas potassium ions are usually administered for desensitisation treatment (McCormack and Davies, 1996). However the latter approach leaves the tooth vulnerable to further demineralisation and the potential passage of noxious substances into the pulp via patent tubules (Love and Jenkinson, 2002). Although both these treatment approaches have advanced and been refined, they have been utilised for many years; thus, there is now a requirement for a more innovative and permanent approach to the treatment of dentine hypersensitivity. One potential way in which this may be accomplished is by accelerating tubular occlusion by promoting the physiological process of peritubular dentine secretion as this would likely provide a more enduring treatment for dentine hypersensitivity.

The recent introduction of 45S5 bioactive glass as a constituent of toothpaste for the treatment of dentine hypersensitivity has motivated this present study. The physico-chemical properties of 45S5 bioactive glass are well-established in promoting tubular occlusion (West *et al.*, 2011; Gendreau *et al.*, 2011), however, our understanding of its effects on cellular behaviour in the dentine-pulp complex are, as yet, poorly understood. Therefore, the broad aims of this project were to investigate the physiochemical interaction of 45S5 bioactive glass with dentine and to identify whether this interaction could enable the release of bioactive molecules with the potential to up-regulate odontoblast secretory



activity, which is likely to be necessary for peritubular dentine deposition. Indeed, previous studies have already shown the potential of isolated dentine matrix components (DMCs) to interact with odontoblasts and stimulate their secretory activity (Smith *et al.*, 1994).

## **8.1 Bioactive Glass Dissolution**

The reactions of bioactive glasses are controlled by their dissolution rates in the human body, which is a relatively dynamic environment; thus, their biodegradability, and indeed bioactivity, are essential to the control of interactions between the glass and surrounding tissues (Valério *et al.*, 2007). Previous *in vitro* studies have shown that the local reaction conditions are fundamental in the determination of the bioactivity of bioactive glass (Duychevne *et al.*, 1999; Radin *et al.*, 1997). The rate of bioactive glass dissolution is a function of its porosity, particle size and surface area, while the temperature of the reaction, the agitation rate, pH and the concentration of bioactive glass are also important factors in the dissolution of bioactive glass (Jones *et al.*, 2001). The composition of the bioactive glass and the leaching solution also affect its dissolution behaviour; these are interdependent factors since the glass alteration, which takes place during dissolution, will inevitably modify the properties of the solution (Devreux *et al.*, 2001). The experiments in this present study observed the interaction of 45S5 bioactive glass with a physiologically relevant fluid, saline. Dentine was also introduced to mimic the oral environment and to observe whether the presence of the dentine extracellular matrix would influence the dissolution behaviour of the bioactive glass.

The bioactive glass dissolution reaction was monitored by daily pH measurements; the high pH of solutions containing bioactive glass is attributable to the first stage of the bioactive

glass dissolution process. This reaction involves an ion-exchange mechanism between cations from the glass (i.e.  $\text{Na}^+$ ) and protons (i.e.  $\text{H}^+$ ) from solution, thereby resulting in an alkaline pH (Hench *et al.*, 1991). This reaction has been shown to occur within 30 seconds of bioactive glass exposure to an aqueous solution, although with a notably smaller particle size ( $2\text{ }\mu\text{m}$ ) than those used in the present study ( $16\text{ }\mu\text{m}$ ) (Cerruti *et al.*, 2005a). The dose-dependent increase in pH in response to the concentration of bioactive glass in solutions has been ascribed to the greater quantities of ions available for ion exchange (Jones *et al.*, 2001).

The present study identified pH changes during bioactive glass dissolution, which implied that the presence of dentine was altering the ionic release profile of bioactive glass in saline solution. The pH of saline was relatively acidic prior to the addition of dentine, but was raised to a neutral pH following dentine interactions. In addition, the pH of solutions containing bioactive glass, saline and dentine was lowered compared with the corresponding concentrations of bioactive glass in saline alone. These observations corroborated previous studies that have demonstrated the buffering capacity of dentine in which it has been postulated that hydroxyl ions are buffered by the displacement of phosphorous ions, which are less electro-negative, from hydroxyapatite (Camps and Pashley, 2000; Wang and Hume, 1988). It is also possible that dentine contains counter ions, such as phosphate or carbonate, which may contribute to the lowering of pH; this would also support the consistently elevated pH observed in bioactive glass and saline only reactions, relative to those containing bioactive glass, saline and dentine. The pH of bioactive glass in the cell culture medium, DMEM, resembled that observed in the presence of dentine, which may reflect a buffering effect of constituents of the DMEM or the presence of counter ions. However, after 24 hours there were no changes in pH with increasing concentrations of

bioactive glass in water, as was also observed with bioactive glass and saline which may reflect the fact that these solutions were not buffered.

ICP-AES analysis revealed the release of calcium and phosphorous ions from dentine during treatment with saline over the course of the 7-day extraction period. This was highlighted by the absence of these ions in solutions containing saline, but lacking dentine. The mechanism by which saline was resulting in the release of these ions from dentine is unknown and requires further work, however, it is possible that the sodium and chloride ions were reacting with the hydroxyapatite crystals within dentine, by an ionic substitution mechanism, and releasing both calcium and phosphorous into solution.

The calcium and phosphorous levels were distinctly lower in the bioactive glass/dentine/saline reactions, compared with the dentine/saline reactions. This was possibly due to the re-precipitation of calcium phosphate on the surface of the glass and the dentine decreasing their rate of release into solution. This premise is supported by the decreased solubility of calcium phosphate observed at higher pH levels (Cerruti *et al.*, 2005a). Both calcium and phosphorous ion levels appeared to plateau during the course of the extraction period and it is possible that precipitation of calcium phosphate may create a protective layer, prohibiting further dissolution of the glass (Cerruti *et al.*, 2005b). Alternatively, the aforementioned plateau effect may reflect the limit of solubility of calcium and phosphate ions, as in the presence of dentine these ions are already present in the system.

An increase in calcium ions was observed in the bioactive glass/dentine/saline reaction during the first 3 days of the extraction period and it is possible that this was due to the rate

of calcium ion release from bioactive glass and dentine being faster than the rate of precipitation of calcium phosphate. The phosphorous ion concentrations in the bioactive glass/dentine/saline reaction were relatively low and varied between replicates, indicating they were at the limit of optimal detection. Indeed, it is well-known that phosphorous is relatively challenging to detect by ICP-AES due its high first ionisation potential and nitrogen polyatomic interferences (Richardson *et al.*, 2006). It is also possible that the abundance of sodium ions, contributed by the saline vehicle solution, was interfering with the phosphorous ion determination (Olivares and Houk, 1986). The sodium ion concentrations over the course of the 7-day extraction were also highly variable and are therefore a challenge to interpret. There is evidence that high levels of sodium chloride can lead to blockages within the ICP-AES equipment, however, this was overcome by higher dilutions of the samples, which may have been at the expense of the detection of ions (Hsiung *et al.*, 1997). Future experiments would benefit from separate elemental analyses to avoid signal masking by abundant ions. The gradual decline in silicon and phosphorous ions over the course of the 7-day period was likely to be a reflection of the daily removal of solution, without the replacement of bioactive glass.

Numerous studies have measured the ionic dissolution products of a variety of bioactive glasses in different media, such as simulated body fluid (SBF) and Dulbecco's Modified Eagle's Medium (DMEM) (Jones *et al.*, 2001; Xynos *et al.*, 2000a; Sun *et al.*, 2007). DMEM is rich in inorganic ions as well as organic components, including carbohydrates and amino acids, which add complexity to its reaction with bioactive glass. For example, a delayed onset in apatite formation has been observed when bioactive glass was immersed in DMEM,

which was hypothesised to be due to the adsorption of proteins on the amorphous calcium phosphate layer occupying sites where precipitation would occur (Theodorou *et al.*, 2011).

The dose-dependent increases in sodium and silicon ions in both bioactive glass-conditioned-DMEM and bioactive glass-conditioned dH<sub>2</sub>O were consistent with previous findings investigating the dose-dependency of bioactive glass by ICP analysis (Jones *et al.*, 2001). Although dose-dependency was not assessed in other studies measuring the ionic dissolution products of bioactive glass in DMEM in comparison with controls of DMEM only, results exhibited comparable trends for all ions reported in this study (Sun *et al.*, 2007). The decreases in calcium and phosphorous levels were attributed to the formation of calcium phosphate on the glass surface (Sun *et al.*, 2007). The reason for which an increase in calcium ion concentration was detected (in DMEM prepared with 1 mg/mL bioactive glass) remains elusive, however, this was also previously observed in studies by Xynos *et al.*, (2000a).

## **8.2 Effects of the Ionic Dissolution Products of Bioactive Glass on Dental Pulp**

### **Cells**

There have been numerous investigations into the effects of ionic dissolution products of bioactive glass on osteoblast cells *in vitro* (as discussed in detail in Section 1.3.3.1). Notably, the ICP-AES analysis presented in this study revealed that bioactive glass-conditioned DMEM contained soluble silicon, calcium and phosphorous ions, all of which have been shown to individually stimulate biological responses in mineralising cells. A recent study has also now reported that extracellular calcium ions are able to promote the differentiation and mineralisation of human dental pulp cells (An *et al.*, 2012), while calcium and silicon ions

released from the tricalcium silicate-based cement Biodentine™ have been hypothesised to be involved in odontoblast-like cell differentiation and the initiation of mineralisation (Laurent *et al.*, 2012). In addition, calcium ions are well-established in promoting osteoblast proliferation and metabolic processes; studies have also shown the ability of calcium ions to up-regulate the expression of growth factors such as IGF-I and IGF-II in osteoblasts (Maeno *et al.*, 2005; Valerio *et al.*, 2009; Marie, 2010; Carlisle, 1981). Silicon ions are also known to have a key role in metabolic processes (Carlisle, 1981), while inorganic phosphate can stimulate matrix Gla protein expression in osteoblast cells (Julien *et al.*, 2009). Based on these studies, in combination with the evidence of these ions detected in bioactive glass-conditioned DMEM acquired from the ICP-AES, have led to the hypothesis that the ionic dissolution products of bioactive glass may be exerting an effect on dental pulp cells.

Preliminary observations into the effects of different concentrations of bioactive glass-conditioned DMEM over time indicated that primary human dental pulp cells responded differently from the murine OD-21 immortalised pulp cell line. Results demonstrated that the bioactive glass-conditioned DMEM did not enhance the metabolic activity of human dental pulp cells (an effect observed with the OD-21 cells), but nevertheless the concentrations used were not cytotoxic. The lack of change in metabolic activity with human dental pulp cells was also observed when bioactive glass was applied in the form of a paste, demonstrating no significant changes in MTT absorbance upon its application to cells, in comparison to two other routinely used dental materials (Bakry *et al.* 2011).

In contrast to the responses of primary cells, the metabolic activity of OD-21 cells was stimulated by bioactive glass-conditioned DMEM; furthermore, treated cells continued to be

significantly more metabolically active in comparison to the controls, indicating a more prolonged stimulatory effect. It is possible that the difference in species or the immortalisation and transformation procedure (i.e. primary human cells and mouse-derived OD-21 cells) are attributable to the difference in response to bioactive glass-conditioned DMEM, however, further work is required to build upon these preliminary observations. In addition, metabolic activity data are difficult to interpret due to the uncertainty of cell number contribution to metabolic output; therefore, concomitant cell counts were conducted to enable the determination of metabolic activity per cell. These data indicated that the increase in metabolic activity observed was not merely a reflection of an increase in cell number. There is evidence to suggest that silicon ions are able to enhance metabolic activity in human osteoblast cells (Zou *et al.*, 2009), however, further experiments are required to determine whether the OD-21 cell response was attributable to the bioactive glass-released silicon ions, as it is also plausible that other ionic dissolution products had an effect on the cells.

The highest concentration of bioactive glass-conditioned DMEM (10 mg/mL) appeared to be cytotoxic to OD-21 cells from both microscopic observations and the significant reduction in metabolic activity, and this was confirmed using the LDH cytotoxicity assay. These effects might be ascribed to the generation of a high pH or high ionic concentrations. Indeed, there is a body of evidence indicating that high concentrations of ions found in bioactive glass dissolution products can have detrimental effects on cell viability (Maeno *et al.*, 2005; Saravanpavan *et al.*, 2004).

As the DMEM was supplemented (by the manufacturer) with calcium chloride, there was a considerable amount of background calcium in the medium; therefore, a calcium-free DMEM was conditioned with bioactive glass. Interestingly, the OD-21 cell response was different to that for cells exposed to bioactive glass-conditioned DMEM (prepared from standard DMEM). It is possible that the dissolution of bioactive glass was modified in the different media; standard DMEM may have been saturated in calcium ions whereas the calcium-free DMEM initially would have been relatively calcium deficient, therefore affecting the amount of calcium leached into solution from the bioactive glass. Although ICP-AES was not conducted on calcium-free bioactive glass-conditioned DMEM, it is plausible that the lack of calcium in the solution may have affected the amount of calcium phosphate that had re-precipitated on the glass surface. This may have had an impact on the concentrations of ions leached into solution and may explain why cells showed differential behaviour to those exposed to standard bioactive glass-conditioned DMEM.

### **8.3 Antibacterial Activity of Bioactive Glass Ionic Dissolution Products**

The bactericidal properties of bioactive glass have often been attributed to its alkalinity (Allan *et al.*, 2001). The hydroxyl ions in a high pH environment are likely to induce damage to bacterial proteins, DNA and cytoplasmic membranes, in addition to interfering with key intracellular processes such as metabolism (Mohammadi *et al.*, 2012). Experiments have also observed needle-like debris associated with bioactive glass dissolution, which was hypothesised to break down bacterial cells walls, although its precise mechanism is not known (Hu *et al.*, 2009). It has also been shown that direct contact with particulate bioactive glass is not necessary in order to elicit antibacterial effects. Experiments have observed the ability of a bioactive glass supernatant to kill bacteria, implying that the surface reactions



(see Section 1.3.2) were sufficient to produce this effect (Allan *et al.*, 2001). Indeed, this was supported in the experiments presented here, where a dose-dependent decrease in *S. mutans* growth was observed after 24 hours of exposure to bioactive glass-conditioned PBS. The pH of bioactive glass-conditioned PBS also increased dose-dependently, resulting in increasing alkalinity according to the concentration of bioactive glass used to condition the PBS. As previously mentioned, the dose-dependent increase in pH may be attributable to the increased availability of ions for ion exchange (see Section 8.1). However, from these experiments alone, it is not possible to deduce whether the increase in bactericidal activity in conjunction with the increasing concentrations of bioactive glass-conditioned PBS was solely due to a pH effect. It would not have been appropriate to attempt to neutralise the solutions, as this may have altered the solubility of key ions that may be responsible for exerting an antibacterial effect. Furthermore, it has been postulated that the silicon component of bioactive glass dissolution products may also contribute to the antibacterial effects (Zehnder *et al.*, 2006) and studies on *Escherichia coli* have also reported these effects of silicon in a high pH environment (Weber *et al.*, 2004). Based on the ICP analysis of bioactive glass and saline only extractions and bioactive glass-conditioned DMEM, showing a dose-dependent increase in silicon ions after 24 hours, it is possible to speculate that this trend in silicon ion concentrations would be similar for bioactive glass-conditioned PBS.

#### **8.4 Effects of Bioactive Glass-released DMCs on *Streptococcus mutans***

An alternative mechanism for bioactive glass antibacterial activity was considered in light of its ability to release DMCs from dentine. The antibacterial activity of EDTA-solubilised DMCs was recently reported (Smith *et al.*, 2012a) and these findings were corroborated in the present study for *S. mutans*. These findings were also in agreement with previous studies in

which extracellular matrix molecules derived from the bladder and small intestine also demonstrate antibacterial activity (Sarıkaya *et al.*, 2002). The presence of antimicrobial peptides (AMPs), which physically disrupt bacterial cell membranes via direct electrostatic interactions, may explain the antibacterial properties elicited by EDTA-released DMCs (Brennan *et al.*, 2006; Smith *et al.*, 2012a). However, DMCs released by 1-10 mg/mL bioactive glass in saline and control solutions of saline only, did not exert an antibacterial effect when exposed to *S. mutans*. The possibility of this being a result of the concentration of DMCs applied to cultures was eliminated by further experiments. Concentrations of up to 1000 µg/mL bioactive glass in saline-released DMCs did not succeed in eliciting antimicrobial activity (data not shown), which exceeded the concentrations used by Smith *et al.*, (2012a) with EDTA-released DMCs by 10-fold. The bioactivity of the AMPs in bioactive glass in saline-released DMCs is not known and it is possible that they may not be as potent as those in EDTA-released DMCs possibly due to chemical modifications due to bioactive glass exposure.

Having characterised the DMCs using proteomics techniques, it was interesting to note the presence of proteins associated with antimicrobial activity in DMCs released by EDTA, saline and 10 mg/mL bioactive glass in saline solution. Defensin alpha 1 (DEFA1), demicidin (DCD), lysozyme renal amyloidosis (LYZ) and S100 calcium binding protein A8 (S100A8) were detected in all DMCs. However, histone cluster 1 H2BK (HIST1H2BK) was the only protein unique to EDTA-released DMCs that is associated with antimicrobial activity. This AMP has previously been associated with the formation of an antibacterial barrier in colonic epithelium (Howell *et al.*, 2003) and it has also been associated with the antimicrobial activity of amniotic fluid (Kim *et al.*, 2002). While it is therefore possible to speculate that the absence of HIST1H2BK may explain the lack of antibacterial activity observed with DMCs

released by saline and bioactive glass solutions, it is, however, likely that the associated antimicrobial activity of DMCs is more complex.

Interestingly, the incubation of bioactive glass and dentine powder in the presence of saline has shown enhanced antibacterial activity in comparison with bioactive glass and saline alone (Zehnder *et al.*, 2006). These authors suggested that dentine powder may enhance bioactive glass dissolution, as they detected an increase in silicon ions in the presence of dentine. The ICP-AES results presented in this study are in contrast to this finding as the concentrations of silicon ions released in extraction solutions were comparable in the presence and absence of dentine.

## **8.5 Characterisation of Bioactive Glass in Saline-released DMCs**

The percentage yields of DMCs released by 1-10 mg/mL bioactive glass in saline and control solutions (saline alone) were similar and did not differ significantly from one another. The percentage recovery was low in comparison with the yield typically achieved with 10 % EDTA (pH 7.2) (Graham *et al.*, 2006; Tomson *et al.*, 2007) indicating a greater efficacy of EDTA at releasing DMCs. However, the percentage yield of DMCs reported to be released by calcium hydroxide in previous publications is comparable with those obtained in this study using bioactive glass and saline.

Ten per cent of the dentine extracellular matrix consists of numerous proteins, collectively known as non-collagenous proteins (NCPs). These NCPs are comprised of several key groups of proteins including the Small Integrin-Binding Ligand N-linked Glycoproteins (SIBLINGs), the small leucine-rich proteoglycans (SLRPs) and the secretory calcium-binding phosphoproteins (SCPPs) and these families of proteins are regarded as being critical to the regulation of

dentine regeneration (see Section 1.1.1.5.1.4) (Goldberg *et al.*, 2011). Glycosaminoglycans play a fundamental role in dentinogenesis and their affinity for collagen implicates their function in a fibrinogenesis which precedes mineralisation (Hargreaves and Goodis, 2002). The Bradford and Farndale dye-binding assays were used to quantify the NCPs and GAGs present within DMCs released by 1-10 mg/mL bioactive glass in saline and control solutions of saline alone. The NCP content detected in all DMCs did not differ significantly from the control, however, a slight trend of dose-dependency was observed in the data, in which a greater concentration of bioactive glass in the original extraction solution was associated with greater concentrations of NCPs released. The concentrations of NCPs released by bioactive glass in saline solutions and control solutions were similar to those reported by Tomson *et al.*, (2007) for DMCs released by white mineral trioxide aggregate (WMTA). There were also few differences in the amounts of GAGs detected in DMCs, however, the range of concentrations were comparable with those reported for EDTA and Ca(OH)<sub>2</sub>-released DMCs (Tomson *et al.*, 2007).

There appeared to be significant similarities between the protein profiles of DMCs released by 10 mg/mL bioactive glass in saline solution and saline only, as observed by 1D-SDS PAGE. Estimations of the molecular masses of the unknown bands further supported the conclusion that the protein profiles of these two samples were similar, whereas the protein profile of EDTA-released DMCs was markedly different, based on both visual inspection of the gel and using automated band detection. However, these techniques were relatively preliminary methods of assessing the differences in the samples of DMCs obtained and there was clearly a requirement for further analysis, which was subsequently provided by the proteomic techniques discussed below.

## 8.6 Proteomic Analysis of Dentine Matrix Components

Liquid chromatography-tandem mass spectrometry (LC-MS/MS) is a powerful tool in proteomics allowing the rapid identification of a substantial number of proteins. However, bioinformatics analysis is an extensive task and the translation of such large volume datasets into meaningful biological information is challenging. Manual literature searches are an impractical data-mining approach and lack the use of a common language (McLachlan *et al.*, 2005). Therefore, the support of bioinformatics software packages, such as the publicly available DAVID software (Huang *et al.*, 2009a) (as applied here), is required, enabling the use of a standardised ontological vocabulary.

The present study identified proteins (using LC-MS/MS) present in DMCs released by EDTA, 10 mg/mL bioactive glass in saline and a vehicle control of saline alone. Analysis demonstrated that an extensive number of proteins are sequestered within the dentine matrix, which can be differentially released using different extractants. However, the diverse protein profiles detected may not be simply a function of the different extraction solutions, since previous studies also using EDTA to release proteins from the dentine matrix have observed differing profiles (Park *et al.*, 2009; Chun *et al.*, 2011; Jagr *et al.*, 2012). Indeed, data comparison showed that the present study identified a greater number of proteins compared with the three previously published dentine proteomic analysis studies (Park *et al.*, 2009; Chun *et al.*, 2011; Jagr *et al.*, 2012). These variations may reflect the different protocols applied which used EDTA to release proteins, i.e. the sequential two-step extraction using guanidine followed by EDTA (Jagr *et al.*, 2012), the 16 day-extraction using EDTA alone (Park *et al.*, 2009), and the 4-week extraction also using EDTA alone (Chun *et al.*, 2011), in addition to the protocol used in the present study (Smith and Leaver, 1979).

Interestingly, the only study in which the extraction did not involve the powdering of dentine (Park *et al.*, 2009) resulted in the lowest number of proteins detected implying that the generation of a larger surface area of dentine for the extractant(s) to interact with may be optimal for protein release. It is possible that variations in reaction conditions (e.g. temperature) and the duration of the extraction also had an impact on the proteins detected in each of the studies. Furthermore, the differences may also reflect individual sample variation; for example, studies by Park and colleagues (2009) detected distinct differences in proteins between the individuals from which samples were taken, despite using the same extraction technique.

Keratins, potentially arising from the skin or general laboratory dust, are a common contaminant in proteomic studies and it is customary to exclude these from further analysis (Jagr *et al.*, 2012; Park *et al.*, 2009). However, it is also plausible that the keratins may be an integral part of the dentine matrix; to investigate this hypothesis, future studies would benefit from a control lane in the SDS-PAGE gel, containing sample buffer only. This lane could then be excised and processed identically to those containing DMCs and any proteins detected in these samples could be justifiably removed from subsequent analyses.

Many of the proteins detected in all of the DMC preparations represented previously well-characterised dentine matrix proteins involved in processes such as mineralisation and extracellular matrix regulation. However, it became evident that several key previously reported proteins were not detected by LC-MS/MS, for example members of the BMP family. The LC-MS/MS technique used to detect proteins is not without limitations and a common issue is masking by highly abundant proteins, impacting on the detection of low

abundance proteins (Qian *et al.*, 2008). This limitation may also explain the detection of growth factors in the multiplex ELISA assays that were not identified by LC-MS/MS.

A myriad of growth factors have been confirmed to be present within dentine, which have individually been shown to stimulate regenerative processes within cells in the dentine-pulp complex (Smith *et al.*, 2012b). These include angiogenic growth factors (Roberts-Clark and Smith, 2000), members of the TGF- $\beta$  superfamily (Cassidy *et al.*, 1997), insulin-like growth factors (Finkelman *et al.*, 1990), and BMPs (Bessho *et al.*, 1991). As mentioned above, there were no members of the BMP family detected by LC-MS/MS in the present study, whereas the multiplex ELISA detected high levels of BMP-7 (also known as OP-1). BMP-7 levels were also below the limit of detection in EDTA-released DMCs, but highly concentrated in DMCs released by 10 mg/mL bioactive glass in saline; this was a trend that was not generally observed when comparing growth factors released by both of these extractants in the multiplex ELISA. The detection of BMP-7 was an interesting finding, as there have been a number of studies in which this protein has been shown to indirectly stimulate the formation of reparative dentine (Rutherford *et al.*, 1993; Rutherford *et al.*, 1994; Nakashima, 1990; Gu *et al.*, 1996).

The multiplex ELISA also detected the presence of M-CSF in DMCs released by 10 mg/mL bioactive glass in saline, and this molecule has not previously been reported in human dentine. CSF proteins are glycoprotein family members that are multifunctional, but have been implicated in the stimulation of proliferation and differentiation of bone marrow-derived cells (Wakefield *et al.*, 1990). M-CSF has recently been proposed as a key inducer of proliferation and differentiation of macrophages in the dental pulp (Iwasaki *et al.*, 2011).

Furthermore, TNF- $\alpha$  has been reported to induce the production of M-CSF by dental pulp fibroblasts, contributing to processes which are likely to play roles in pulp defence mechanisms (Sawa *et al.*, 2003). Indeed, an extensive number of proteins involved in the immune response were detected in DMCs by LC-MS/MS. Many of the immunoglobulins detected here are now reported in the dentine proteome for the first time and it is likely that they play a role in the defence against cariogenic plaque bacteria (Jagr *et al.*, 2012).

Angiogenesis is a fundamental component of wound healing and enables the sustained supply of nutrients, growth factors and immunocompetent cells to the site of tissue injury (Gurtner *et al.*, 2008). In the present study, the greatest proportions of proteins related to angiogenesis were detected in DMCs released by 10 mg/mL bioactive glass in saline, some of which have not previously been reported in dentine, e.g. angiotensin (AGT), and ATP synthase, H<sup>+</sup> transporting, mitochondrial F1 complex, beta polypeptide (ATP5B). Studies have previously demonstrated the presence of additional pro-angiogenic factors in the dentine, such as platelet-derived growth factor (PDGF) and vascular endothelial growth factor (VEGF), which were both confirmed to be present by multiplex ELISA in this present study (Roberts-Clark and Smith, 2000). The effects of these angiogenic factors have been studied *in vitro* in depth and they provide a likely signalling source contributing to the regeneration of the dentine-complex (Zhang *et al.*, 2011).

A significant proportion of DMCs released by 10 mg/mL bioactive glass in saline were associated with metabolic processes, which potentially provides insight into the cellular effects observed, whereby a significant increase in metabolic activity was detected in response to DMCs released by bioactive glass and saline, relative to DMCs released by saline



alone. The enzyme transketolase has not been previously reported in dentine prior to this study and was detected in DMCs released by bioactive glass in saline. This enzyme has broad specificity and reversibly links the pentose phosphate pathway and glycolysis allowing cells to shuttle glycolytic intermediates between both pathways (Ikeda *et al.*, 1999). The significant presence of metabolic proteins in dentine suggests that it is a dynamic and active tissue. This is contrary to previous perceptions that dentine is a physiologically inert tissue, whereby it was thought that restorative dental procedures exerted minimal influence on the tissue's response (Smith *et al.*, 2012b). This work potentially highlights a myriad of opportunities to exploit the response of dentine for novel treatment approaches.

Another notable observation in this present study was the detection of a high proportion of apoptotic proteins in DMCs, particularly in those released by saline. Apoptosis is often a protective mechanism for a host organism (Ashida *et al.*, 2011) and it is possible that these proteins may be associated with defence responses to limit the spread of infection and to diminish its opportunity to become more widespread. This may therefore present new opportunities to modulate cell vitality within the dentine-pulp complex, with significant therapeutic potential in the context of infection.

The present study also identified a number of microfilament and microtubule proteins e.g. moesin (MSN) and vinculin (VCL). This detection is pertinent to the presence of odontoblastic processes extending into dentinal tubules (Holland, 1975). Ontological analysis revealed that the cellular localisation associated with most of the proteins detected was extracellular, however, identification of vesicular proteins may have been due to odontoblast secretory activity.

This study has also detected the presence of leucine-rich alpha-2 glycoprotein (LGR1), which was released by both saline and 10 mg/mL bioactive glass in saline solution. The physiological function of this serum glycoprotein protein remains elusive, but there is a possibility, based on its structural similarity, that the function of LGR1 may be similar to other small-leucine rich proteoglycans in dentine. These include biglycan, decorin and mimecan, which were also detected in DMCs, and thus corroborating the suggestion that LGR1 may have a role in dentine mineralisation (Haruyama *et al.*, 2009).

Amongst the best-described growth factors in dentine are members of the TGF- $\beta$  superfamily. The roles of TGF- $\beta$ 1 in tooth development and dental tissue repair have been extensively researched (Bègue-Kirn *et al.*, 1992; Smith *et al.*, 1998; Sloan and Smith, 1999; Dobie *et al.*, 2002; Sloan *et al.*, 2002). In the present study, TGF- $\beta$ 1 was detected in DMCs using a solid phase sandwich ELISA and was too concentrated to allow the determination of a precise concentration in the multiplex ELISA. However, using LC-MS/MS, TGF- $\beta$ 1 was only identified in EDTA-released DMCs, indicating the limitations of this technique and highlighting the requirement for confirmatory and complementary study approaches. TGF- $\beta$ 1 induced protein ig-h3 (TGFBI) was also detected in both EDTA and 10 mg/mL bioactive glass in saline-released DMCs. As its nomenclature indicates, TGFBI is induced by TGF- $\beta$ 1 and is implicated in adhesion, migration, proliferation and differentiation in a variety of cell types (Kim *et al.*, 2009). The presence of TGF- $\beta$ 2 was also identified in EDTA-released DMCs, although this isoform was not detected in human dentine during a previous study by Cassidy *et al.*, (1997) perhaps reflecting differences in sensitivity between the assays used.

Although dentine has been recognised as a rich source of potent signalling molecules for many years, this study has identified many proteins that have not previously been reported as being sequestered within the dentine extracellular matrix. Notably, many of these proteins are multi-functional, whilst the physiological roles of several proteins are not yet known. Our understanding of the synergistic relationships of these proteins in signalling processes is currently limited and this study emphasises the need for further work to understand this complex signalling environment.

## **8.7 Mechanisms for DMC Release**

The root canal irrigant, EDTA, has been used to release DMCs *in vitro* for the last 34 years (Smith and Leaver, 1979; Lesot *et al.*, 1988; Smith *et al.*, 1990; Tziafas *et al.*, 1995; Zhao *et al.*, 2000; Zhang *et al.*, 2011; Smith *et al.*, 2012b). EDTA solubilises dentine via chelation of the calcium ions in the hydroxyapatite crystals in dentine, which is potentially the mechanism by which bioactive molecules sequestered in the dentine matrix are released (Graham *et al.*, 2006). A variety of other chemical agents have also demonstrated the ability to release DMCs, including lactic acid, which may be present *in vivo* during caries, via demineralisation and dissolution of dentine (Zhao *et al.*, 2000; Finkelman *et al.*, 1990). The restorative material  $\text{Ca(OH)}_2$  also solubilises DMCs, however, the mechanism(s) by which it does this is also yet to be determined. Nevertheless, it has recently been postulated that the dissociation of  $\text{Ca(OH)}_2$  in solution may result in ionic exchange with apatite crystals in dentine (Tomson, 2013). Notably, another alkaline agent, NaOH, has shown limited ability to release DMCs (Smith *et al.*, 1995), therefore indicating that the process of releasing DMCs is more complex than simply a pH effect.

This is the first study to date involving the use of bioactive glass to examine the release of DMCs and its mode(s) of action may be important in understanding how and which bioactive molecules are released. During the 7-day extraction period, protein release was measured spectrophotometrically in extraction supernatants. The absorbance increased over the 7-day period and subsequently plateaued. Interestingly, the increase in absorbance appeared to occur progressively later with increasing concentrations of bioactive glass. It is proposed that the precipitation of a calcium phosphate layer on the dentine surface occurs to a greater extent with increasing concentrations of bioactive glass, thereby forming a protective layer and initially preventing the dissolution of dentine. The delayed onset of absorbance increase associated with increasing concentrations of bioactive glass may reflect a better-defined calcium phosphate layer, which may have been gradually disrupted during the course of the 7-day extraction period allowing the release of DMCs. The absorbance profiles of solutions prepared with 10 mg/mL bioactive glass in saline remained consistently low, potentially indicating that there had been minimal breakdown of any proposed protective layer. These data were paralleled by the proteomic data, which revealed considerably fewer proteins detected in DMCs released by 10 mg/mL bioactive glass in saline compared with those released by saline alone. Notably, however, OD-21 cells exposed to DMCs released by 10 mg/mL bioactive glass in saline exhibited significantly higher cell growth and metabolic activity in comparison with cells exposed to saline-released DMCs (discussed below in Section 8.8).

## 8.8 Effects of Bioactive Glass in Saline-released DMCs on Pulpal Cells

The cellular effects of both EDTA and  $\text{Ca(OH)}_2$ -released DMCs are well-established in the promotion of dentine repair and regeneration (Smith *et al.*, 1990; 1995). Experiments have observed the pro-angiogenic effects of DMCs, in addition to the stimulation of cell proliferation at relatively low concentrations (Musson *et al.*, 2010; Graham *et al.*, 2006; Zhang *et al.*, 2011). These studies have also reported that high concentrations (i.e. 1000  $\mu\text{g/mL}$ ) of EDTA-released DMCs are inhibitory to cell proliferation and this has been attributed to induction of apoptosis (Smith *et al.*, 2005). Although it is acknowledged that these apoptotic effects cannot be ascribed to any one protein, experiments have demonstrated Smad-mediated stimulation of apoptosis via  $\text{TGF-}\beta 1$  in pulpal cells (He *et al.*, 2004). However, the proteomic data presented in this study have identified several other candidates in EDTA-released DMCs potentially involved in the regulation of apoptosis, including TIMP metalloproteinase inhibitor 3 (TIMP3), actinin alpha 1 (ACTN1) and plasminogen (PLG).

The bioactive glass in saline-released DMCs also demonstrated a dose and time-dependent increase in cell proliferation and metabolic activity of OD-21 cells. However, perhaps the most interesting finding was that DMCs appeared to be stimulating cells increasingly according to the concentration of bioactive glass used in the original extraction solutions. The lowest metabolic activity and cell numbers were observed in cells exposed to DMCs released by control solutions of saline. Based on the number of proteins released by saline alone (211) relative to the highest concentration of bioactive glass in saline (140), it might be expected that the DMCs released by saline have the potential to contain a broader range of more biologically active proteins. However, it is possible that there are various bioactive

components in the saline-released DMCs that are impeding signalling of proliferative pathways. Alternatively, there may be certain candidate proteins absent in saline-released DMCs that are released by bioactive glass in saline solution.

Interestingly, DMCs released by saline alone contained several additional negative regulators of cell proliferation, including retinol-binding protein 4 (RBP4), dermatopontin (DPT) and ATP synthase subunit alpha, (ATP5A1). These were not detected within DMCs released by bioactive glass in saline suggesting another possible reason for lower cell numbers for OD-21s exposed to saline-released DMCs. With such a vast array of proteins present in DMCs, it is likely that a complex interplay will be involved in eliciting cellular effects; thus, it is difficult to attribute the effects observed in these studies to individual components. Nonetheless, stem/progenitor cell proliferation is a key step preceding differentiation during dental reparative processes (Smith *et al.*, 2012b) and the potential of DMCs to drive these processes is promising, as observed by the cellular response to bioactive glass in saline-released DMCs.

## **8.9 Characterisation of a Cell Culture Model to Study Peritubular Dentinogenesis**

Ethical concerns have led to a growing focus on the use of three-dimensional cell culture models to replace animal experimentation. This has therefore resulted in the requirement for an alternative *in vitro* approach, which could potentially mirror aspects of tissue behaviour and responses. Pioneering work in the 1950s used filters to study morphogenetic interactions between mouse embryonic tissues (Grobstein, 1953), which led to the commercial development of filters for cell culture. Filter well inserts are designed to be secured in place by a culture vessel allowing a compartment above and below the

membrane. Their microporous structure allows the secretion of molecules on both apical and basal surfaces, in addition to allowing the directional polarised metabolic processes that occur *in vivo* (Justice *et al.*, 2009).

Numerous studies have used dentine discs as scaffolds for cell culture to mimic *in vivo* conditions, on the basis of its morphological and compositional features (Schmalz *et al.*, 2001; Huang *et al.*, 2006; Shao *et al.*, 2011). The PET Thinserts selected for the present study were chosen to model the porous (i.e. tubular) structure of dentine. However, in the literature there are discrepancies reported between the number of tubules per unit area of dentine. This may be due to several factors such as small sample numbers, a lack of standardisation of the area/region from which teeth are sectioned and the age and type of teeth (Lenzi *et al.*, 2013). The discs prepared during this study were derived from coronal dentine located directly above the pulp cavity. Image analysis of SEM images was conducted to compare the tubular density with the density of pores in the PET Thinserts and measurements indicated that the density of pores was 5-fold lower than that of the dentinal tubules. Unfortunately, it was not possible to specify this parameter as a requirement to the supplier for manufacturing, however, the diameters of both pores and tubules were comparable.

The PET Thinserts offered numerous advantages over dentine discs for cell culture. The transparency of the membrane in contrast to the opacity of dentine meant that cell viability could be assessed microscopically throughout an experiment, in addition to allowing compatibility in colorimetric assays. The PET Thinserts are also readily available, involving no preparation for cell culture. In contrast, dentine discs rely on a healthy tooth extraction and

involve several subsequent processing steps lasting over a week in order for discs to be able to be used in the sterile cell culture environment (Shao *et al.*, 2011). The purpose of the use of PET Thinserts in this context was for its application in studying peritubular dentinogenesis; the model is therefore advantageous for the detection of new mineral formation, which would be somewhat challenging in the dentine disc model given that dentine is already a mineralised tissue.

There also appeared to be advantages in culturing OD-21 cells on PET Thinserts in preference to standard polystyrene microplates. Notably, OD-21 cells exhibited the capacity to proliferate extremely rapidly and frequently became confluent relatively quickly and subsequently detached from standard polystyrene plasticware. This meant that culture conditions had to be carefully controlled for seeding density and FCS concentration, both of which can impact on cellular phenotypic characteristics and responses to stimuli (Watt, 1988; Pirkmajer and Chibalin; 2011). However, when cells were cultured on PET Thinserts, despite the smaller surface area, a greater retention of cell number during longer term cell culture was evident as compared with the standard polystyrene cultureware. It is postulated that the cellular prolongations may have assisted in the adhesion of cells implying that the porous nature of the membranes was more suited for OD-21 cell culture. This improved cellular adhesion will be particularly advantageous for longer-term assays such as mineralisation-inducing experiments. Preliminary experiments on human dental pulp cells showed potential for induction of enhanced mineralisation when cells were cultured in a bioactive glass-conditioned osteogenic medium (data not shown), which is an avenue that should be pursued in further work.



The experiments presented in this study cultured pulpal cells on the biologically-inert porous PET Thinserts in the presence and absence of DMCs. Interestingly, cross-sectional images acquired from histological sections and FIB-SEM indicated the presence of cellular extensions protruding into the pores. Although a greater density of cellular extensions were observed in cells exposed to DMCs, they were also observed in control conditions (the absence of DMCs). Therefore, the increased density of cellular extensions may have been due to the increase in cell numbers as a result of DMC exposure. Based on these observations, it is possible that the cells were responding to the surface topography as this is reported to act synergistically with biochemical cues in promoting biological response (Hoffman-Kim *et al.*, 2010). Notably, many studies have shown that a porous surface topography can direct the differentiation of mesenchymal stem cells (Wang *et al.*, 2013; Dalby *et al.*, 2007; Popat *et al.*, 2007).

It is also possible that the cell prolongations may represent cellular processes, reflective of a more odontoblast-like cell morphology. Similar findings have been reported in several studies outlined below. Bovine dental pulp cells cultured on dentine discs have been reported to extend cellular processes into dentinal tubules (Schmalz *et al.* 2001) and subsequent studies demonstrated similar findings in addition to the odontoblast-like cell morphology of human dental pulp cells (Huang *et al.*, 2006; Shao *et al.*, 2011). It has also long been recognised that odontoblast-like cells have the capacity to secrete mineralised matrix *in vitro* (About *et al.*, 2000; Nakashima and Akamine *et al.*, 2005). The ability of TGF- $\beta$ 1 to stimulate odontoblast secretion for reactionary dentine formation, in addition to up-regulation of type I collagen expression, has also been reported (Sloan *et al.*, 2000; Magloire *et al.*, 2001). The studies described have demonstrated that a combination of the

environmental cues from dentine in addition to the presence of dentinal tubular structures themselves may be key in the mediation of dentinogenesis (Shao *et al.*, 2011; Huang *et al.*, 2006; Schmalz *et al.* 2001). It was postulated that surface demineralisation of dentine discs may expose collagen binding sites affecting the differentiation of cells (Shao *et al.*, 2011), it was also hypothesised that the solubilisation of various non-collagenous DMCs and growth factors during the chemical treatment of dentine in these studies may have promoted differentiation (Dobie *et al.*, 2002; Huang *et al.*, 2006). Thus, based on the above evidence, it is plausible that the release of DMCs by bioactive glass in saline solution may exert similar effects.

Numerous chemoattractants have been reported to be present in the dentine matrix, including TGF- $\beta$ 1, FGF and EGF (Brenmoehl *et al.*, 2009; Kwon *et al.*, 2010; Howard *et al.*, 2010). To eliminate the possibility of cellular extensions resulting from a chemoattractant effect, DMCs were applied to both the lower and upper compartments of the culture arrangement (see Figure 2.6). Incidentally, periodontal ligament cells cultured on dentine discs did not extend cellular extensions into tubules (Shao *et al.*, 2011), while recent research that involved culturing primary rat keratinocytes and H400 cells on PET Thinserts also did not extend cellular extensions into pores (Khan, 2012). This would suggest that these responses may be unique to dental pulp cells.

## 9.0 CONCLUSIONS

- This study has demonstrated by ICP-AES analysis that the buffering capacity of dentine, in addition to its abundance of calcium and phosphorous, considerably influences the ionic dissolution of bioactive glass. Results demonstrated that the vehicle solution also affected the dissolution behaviour of the glass; in particular, media containing high background levels of calcium and phosphorous influenced the amounts of these ions released from the glass into the solution.
- This study has demonstrated that bioactive glass, in contact with a surrogate physiological fluid (saline), is able to release DMCs, as previously observed with other routinely used dental irrigants/materials, such as EDTA,  $\text{Ca(OH)}_2$  and MTA.
- The DMCs released by bioactive glass in saline and saline only (vehicle control) were characterised and subsequently compared with EDTA as a control using high-throughput proteomic analysis. Results indicated that the solutions released proteins differentially, although there was also an overlap in several of the proteins released by all solutions. There were numerous proteins identified in bioactive glass in saline-released DMCs that have not been previously detected in dentine, including several proteins associated with metabolic, immune and angiogenic processes, and these may have implications for dental repair processes.
- The DMCs released by bioactive glass in saline were shown to exhibit enhanced proliferative and metabolic activity on OD-21 cells compared with cells exposed to

DMCs released by saline only controls. Cell proliferation and metabolic activity were stimulated, which are processes pertinent to repair and regeneration of the dental pulp.

- Preliminary experiments indicated that bioactive glass demonstrated good biocompatibility towards primary human dental pulp cells. Stimulatory effects of the ionic dissolution products of bioactive glass were observed with OD-21 cells, however, higher concentrations were cytotoxic.
- Pores on PET Thinserts were used to model the tubular structure of dentine. Cell culture on the PET Thinserts showed several advantages to culturing cells on standard culture plasticware and dentine discs, including improved cellular adhesion and compatibility with colorimetric assays, respectively.
- The culture of OD-21 cells in a 3-D environment resulted in cells extending prolongations into the pores of the PET Thinserts. It is suggested that the cells may be exhibiting morphological traits of the odontoblast and evidence to support this from previous studies have indicated that only pulpal cells were capable of this behaviour. Alternatively, it is feasible that cells may have been responding to their topographical environment.

## 10.0 FUTURE WORK

The results from this study have demonstrated positive stimulatory effects for DMCs released by bioactive glass in saline. Our current understanding of how these growth factors and bioactive molecules are bound in the dentine extracellular matrix is rather limited and this impacts on our understanding of the mechanisms for their release. Thus, future work would benefit from a multidisciplinary approach, which could consider both the dissolution kinetics of bioactive glass in the presence of dentine and its interaction with the protein content of the tissue. This may enable the development of “smart glasses” in which the properties can be tailored for various medical and dental applications, also known as “third generation biomaterials” (Hench, 2006). Further investigation into the cellular effects of individual ionic constituents of bioactive glass may also help tailor future compositions of the glass to exert optimal biological effects.

The maintenance of odontoblastic phenotype through continued cell-matrix interactions remains poorly understood (Smith *et al.*, 2012b); the identification of a number of proteins, during this present study, that have not previously been reported in dentine provides opportunities to better understand some of these interactions and their influence on cellular behaviour. Further analysis of these molecules, in addition to characterising their synergistic effects with other bioactive molecules, may also provide opportunities to develop novel treatment approaches not only for dentine hypersensitivity but also, for other diseases associated with the dentine-pulp complex.

It is possible that the bioactive molecules identified during this study may have the ability to accelerate tubular occlusion through promoting peritubular dentine matrix secretion, which

would offer the possibility of long-lasting tooth desensitisation. Future work would therefore benefit from exploiting the PET Thininserts, characterised during this study, as a model to study peritubular dentinogenesis, which can subsequently be correlated with fluid flow research to determine the efficacy of reducing permeability. The model may also be used to study the combined biological effect of both the ionic dissolution products of bioactive glass and the DMCs released by the glass. Use of primary human dental pulp cells in order to optimise the relevance of the research would be beneficial, whilst also alleviating the ethical concerns associated with animal research.

## REFERENCES

- ABOUT, I., BOTTERO, M.J., DE DENATO, P., CAMPS, J., FRANQUIN, J.C. and MITSIAIDIS, T.A., 2000. Human dentin production in vitro. *Experimental cell research*, 258(1), pp. 33-41.
- ABSI, E.G., ADDY, M. and ADAMS, D., 1992. Dentine hypersensitivity--the effect of toothbrushing and dietary compounds on dentine in vitro: an SEM study. *Journal of oral rehabilitation*, 19(2), pp. 101-110.
- ADDY M., 2002. Dentine hypersensitivity: new perspectives on an old problem. *International journal of developmental biology*, 52, pp. 367-375.
- ADDY, M., LOYN, T. and ADAMS, D., 1991. Dentine hypersensitivity--effects of some proprietary mouthwashes on the dentine smear layer: a SEM study. *Journal of dentistry*, 19(3), pp. 148-152.
- ADDY, M. and SHELLIS, R.P., 2006. Interaction between attrition, abrasion and erosion in tooth wear. *Monographs in oral science*, 20, pp. 17-31.
- AINA, V., PERARDI, A., BERGANDI, L., MALAVASI, G., MENABUE, L., MORTERRA, C. and GHIGO, D., 2007. Cytotoxicity of zinc-containing bioactive glasses in contact with human osteoblasts. *Chemico-biological interactions*, 167(3), pp. 207-218.
- ALLAN, I., NEWMAN, H. and WILSON, M., 2001. Antibacterial activity of particulate bioglass against supra- and subgingival bacteria. *Biomaterials*, 22(12), pp. 1683-1687.
- AN, S., GAO, Y., LING, J., WEI, X. and XIAO, Y., 2012. Calcium ions promote osteogenic differentiation and mineralization of human dental pulp cells: implications for pulp capping materials. *Journal of materials science: materials in medicine*, 23(3), pp. 789-795.
- ANDERSON, S., 2001. The effect of silicon, silica and silicates on the osteoblast in vitro. *PhD thesis submitted to the University of Nottingham*.
- ARANY, S., KOYOTA, S. and SUGIYAMA, T., 2009. Nerve growth factor promotes differentiation of odontoblast-like cells. *Journal of cellular biochemistry*, 106(4), pp. 539-545.
- ASHIDA, H., MIMURO, H., OGAWA, M., KOBAYASHI, T., SANADA, T., KIM, M. and SASAKAWA, C., 2011. Cell death and infection: a double-edged sword for host and pathogen survival. *The Journal of cell biology*, 195(6), pp. 931-942.
- AVERY, J., and AVERY, N., 2002. *Oral development and histology*. 3rd ed. New York: Thieme.
- BAKRY, A.S., TAMURA, Y., OTSUKI, M., KASUGAI, S., OHYA, K. and TAGAMI, J., 2011. Cytotoxicity of 45S5 bioglass paste used for dentine hypersensitivity treatment. *Journal of dentistry*, 39(9), pp. 599-603.
- BARTOLD, P.M., 2006. Dentinal hypersensitivity: a review. *Australian dental journal*, 51(3), pp. 212-8.
- BÈGUE-KIRN, C., SMITH, A.J., LORIOT, M., KUPFERLE, C., RUCH, J.V. and LESOT, H., 1994. Comparative analysis of TGF betas, BMPs, IGF1, msxs, fibronectin, osteonectin and bone sialoprotein gene expression during normal and in vitro-induced odontoblast differentiation. *The International journal of developmental biology*, 38(3), pp. 405-420.

- BÈGUE-KIRN, C., SMITH, A.J., RUCH, J.V., WOZNEY, J.M., PURCHIO, A., HARTMANN, D. and LESOT, H., 1992. Effects of dentin proteins, transforming growth factor beta 1 (TGF beta 1) and bone morphogenetic protein 2 (BMP2) on the differentiation of odontoblast in vitro. *The International journal of developmental biology*, 36(4), pp. 491-503.
- BELLANTONE, M., WILLIAMS, H.D. and HENCH, L.L., 2002. Broad-spectrum bactericidal activity of Ag(2)O-doped bioactive glass. *Antimicrobial agents and chemotherapy*, 46(6), pp. 1940-1945.
- BERKOVITZ, B., HOLLAND, G., and MOXHAM, B., (2002). *Oral anatomy, histology and embryology*. 3rd ed. Missouri: Mosby.
- BERNICK, S., 1948. Innervation of the human tooth. *The anatomical record*, 101(1), pp. 81-107.
- BESSHO, K., TANAKA, N., MATSUMOTO, J., TAGAWA, T. and MURATA, M., 1991. Human dentin-matrix-derived bone morphogenetic protein. *Journal of dental research*, 70(3), pp. 171-175.
- BJØRNDAL, L. and DARVANN, T., 1999. A light microscopic study of odontoblastic and non-odontoblastic cells involved in tertiary dentinogenesis in well-defined cavitated carious lesions. *Caries research*, 33(1), pp. 50-60.
- BJØRNDAL, L., DARVANN, T. and THYLSTRUP, A., 1998. A quantitative light microscopic study of the odontoblast and subodontoblastic reactions to active and arrested enamel caries without cavitation. *Caries research*, 32(1), pp. 59-69.
- BJØRNDAL, L. and MJØR, I.A., 2001. Pulp-dentin biology in restorative dentistry. Part 4: Dental caries--characteristics of lesions and pulpal reactions. *Quintessence international*, 32(9), pp. 717-736.
- BOSKEY, A.L., DOTY, S.B., KUDRYASHOV, V., MAYER-KUCKUK, P., ROY, R. and BINDERMAN, I., 2008. Modulation of extracellular matrix protein phosphorylation alters mineralization in differentiating chick limb-bud mesenchymal cell micromass cultures. *Bone*, 42(6), pp. 1061-1071.
- BRADFORD, M.M., 1976. A rapid and sensitive method for the quantitation of microgram quantities of protein utilizing the principle of protein-dye binding. *Analytical biochemistry*, 72(1-2), pp. 248-254.
- BRÄNNSTRÖM, M., 1963. Dentin sensitivity and aspiration of odontoblasts. *Journal of the american dental association*, 66, pp. 366-370.
- BRENMOEHL, J., MILLER, S.N., HOFMANN, C., VOGL, D., FALK, W., SCHOLMERICH, J. and ROGGER, G., 2009. Transforming growth factor-beta 1 induces intestinal myofibroblast differentiation and modulates their migration. *World journal of gastroenterology*, 15(12), pp. 1431-1442.
- BRENNAN, E.P., REING, J., CHEW, D., MYERS-IRVIN, J.M., YOUNG, E.J. and BADYLAK, S.F., 2006. Antibacterial activity within degradation products of biological scaffolds composed of extracellular matrix. *Tissue engineering*, 12(10), pp. 2949-2955.
- BURWELL, A., JENNINGS, D., MUSCLE, D. and GREENSPAN, D.C., 2010. NovaMin and dentin hypersensitivity--in vitro evidence of efficacy. *The Journal of clinical dentistry*, 21(3), pp. 66-71.
- BYERS, M.R., 1984. Dental sensory receptors. *International review of neurobiology*, 25, pp. 39-94.
- BYERS, M.R., SCHATTEMAN, G.C. and BOTHWELL, M., 1990. Multiple functions for NGF receptor in developing, aging and injured rat teeth are suggested by epithelial, mesenchymal and neural immunoreactivity. *Development*, 109(2), pp. 461-471.



- CAMPS, J. and PASHLEY, D.H., 2000. Buffering action of human dentin in vitro. *The journal of adhesive dentistry*, 2(1), pp. 39-50.
- CARLISLE, E., 1981. Silicon: A requirement in bone formation independent of vitamin D1. *Calcified tissue international*, 33(1), pp. 27-34.
- CARMICHAEL, J., DEGRAFF, W.G., GAZDAR, A.F., MINNA, J.D. and MITCHELL, J.B., 1987. Evaluation of a tetrazolium-based semiautomated colorimetric assay: assessment of chemosensitivity testing. *Cancer research*, 47(4), pp. 936-942.
- CASSIDY, N., FAHEY, M., PRIME, S.S. and SMITH, A.J., 1997. Comparative analysis of transforming growth factor- $\beta$  isoforms 1-3 in human and rabbit dentine matrices. *Archives of oral biology*, 42(3), pp. 219-223.
- CENTERWALL, B.S., ARMSTRONG, C.W., FUNKHOUSER, L.S. and ELZAY, R.P., 1986. Erosion of dental enamel among competitive swimmers at a gas-chlorinated swimming pool. *American journal of epidemiology*, 123(4), pp. 641-647.
- CERRUTI, M., GREENSPAN, D. and POWERS, K., 2005a. Effect of pH and ionic strength on the reactivity of Bioglass® 45S5. *Biomaterials*, 26(14), pp. 1665-1674.
- CERRUTI, M.G., GREENSPAN, D. and POWERS, K., 2005b. An analytical model for the dissolution of different particle size samples of Bioglass® in TRIS-buffered solution. *Biomaterials*, 26(24), pp. 4903-4911.
- CHABANSKI, M.B., GILLAM, D.G., BULMAN, J.S. and NEWMAN, H.N., 1997. Clinical evaluation of cervical dentine sensitivity in a population of patients referred to a specialist periodontology department: a pilot study. *Journal of oral rehabilitation*, 24(9), pp. 666-672.
- CHAO, C.C., HU, S., MOLITOR, T.W., SHASKAN, E.G., AND PETERSON, P.K., 1992. Activated microglia mediate neuronal cell injury via a nitric oxide mechanism. *Journal of Immunology*, 149:2736-41
- CHUN, S.Y., LEE, H.J., CHOI, Y.A., KIM, K.M., BAEK, S.H., PARK, H.S., KIM, J.Y., AHN, J.M., CHO, J.Y., CHO, D.W., SHIN, H.I. and PARK, E.K., 2011. Analysis of the soluble human tooth proteome and its ability to induce dentin/tooth regeneration. *Tissue engineering. Part A*, 17(1-2), pp. 181-191.
- CLARK, A.E., PANTANO, C.G. and HENCH, L.L., 1976. Auger Spectroscopic Analysis of Bioglass Corrosion Films. *Journal of the american ceramic society*, 59(1-2), pp. 37-39.
- COOPER, P.R., TAKAHASHI, Y., GRAHAM, L.W., SIMON, S., IMAZATO, S. and SMITH, A.J., 2010. Inflammation-regeneration interplay in the dentine-pulp complex. *Journal of dentistry*, 38(9), pp. 687-697.
- CORDEIRO, M.M., DONG, Z., KANEKO, T., ZHANG, Z., MIYAZAWA, M., SHI, S., SMITH, A.J. and NOR, J.E., 2008. Dental pulp tissue engineering with stem cells from exfoliated deciduous teeth. *Journal of endodontics*, 34(8), pp. 962-969.
- COUVE, E., 1986. Ultrastructural changes during the life cycle of human odontoblasts. *Archives of oral biology*, 31(10), pp. 643-651.
- CUNHA-CRUZ, J., WATAHA, J.C., ZHOU, L., MANNING, W., TRANTOW, M., BETTENDORF, M.M., HEATON, L.J. and BERG, J., 2010. Treating dentin hypersensitivity: therapeutic choices made by dentists of the northwest PRECEDENT network. *Journal of the american dental association*, 141(9), pp. 1097-1105.

- CURRO, F.A., 1990. Tooth hypersensitivity in the spectrum of pain. *Dental clinics of north america*, 34(3), pp. 429-437.
- DABABNEH, R.H., KHOURI, A.T. and ADDY, M., 1999. Dentine hypersensitivity - an enigma? A review of terminology, mechanisms, aetiology and management. *British dental journal*, 187(11), pp. 606-11.
- DALBY, M.J., GADEGAARD, N., TARE, R., ANDAR, A., RIEHLE, M.O., HERZYK, P., WILKINSON, C.D. and OREFFO, R.O., 2007. The control of human mesenchymal cell differentiation using nanoscale symmetry and disorder. *Nature materials*, 6(12), pp. 997-1003.
- DAY, R.M., 2005. Bioactive glass stimulates the secretion of angiogenic growth factors and angiogenesis in vitro. *Tissue engineering*, 11(5-6), pp. 768-777.
- DEVREUX, F., BARBOUX, PH., FILOCHE, M. and SAPOVAL, B., 2001. A simplified model for glass dissolution in water. *Journal of materials science*, 36(6), pp. 1331-1341.
- DOBIE, K., SMITH, G., SLOAN, A.J. and SMITH, A.J., 2002. Effects of alginate hydrogels and TGF-beta 1 on human dental pulp repair in vitro. *Connective tissue research*, 43(2-3), pp. 387-390.
- DOURDA, A.O., MOULE, A.J. and YOUNG, W.G., 1994. A morphometric analysis of the cross-sectional area of dentine occupied by dentinal tubules in human third molar teeth. *International endodontic journal*, 27(4), pp. 184-189.
- D'SOUZA, R.N., BACHMAN, T., BAUMGARDNER, K.R., BUTLER, W.T. and LITZ, M., 1995. Characterization of cellular responses involved in reparative dentinogenesis in rat molars. *Journal of dental research*, 74(2), pp. 702-709.
- D'SOUZA, R.N., HAPPONEN, R.P., FLANDERS, K.C. and BUTLER, W.T., 1990. Histochemical localization of transforming growth factor-beta 1 in developing rat molars using antibodies to different epitopes. *Journal de biologie buccale*, 18(4), pp. 299-306.
- DUCHEYNE, P. and QIU, Q., 1999. Bioactive ceramics: the effect of surface reactivity on bone formation and bone cell function. *Biomaterials*, 20(23-24), pp. 2287-2303.
- DUNG, S.Z., GREGORY, R.L., LI, Y. and STOOKEY, G.K., 1995. Effect of lactic acid and proteolytic enzymes on the release of organic matrix components from human root dentin. *Caries research*, 29(6), pp. 483-489.
- DUNITZ, M., (2000). Tooth Wear and Sensitivity: Clinical Advances in Restorative Dentistry. London: *Informa Healthcare*.
- EARL, J.S., TOPPING, N., ELLE, J., LANGFORD, R.M. and GREENSPAN, D.C., 2011a. Physical and chemical characterization of the surface layers formed on dentin following treatment with a fluoridated toothpaste containing NovaMin. *The Journal of clinical dentistry*, 22(3), pp. 68-73.
- EARL, J.S., LEARY, R.K., MULLER, K.H., LANGFORD, R.M. and GREENSPAN, D.C., 2011b. Physical and chemical characterization of dentin surface following treatment with NovaMin technology. *The Journal of clinical dentistry*, 22(3), pp. 62-67.
- EFFLANDT, S.E., MAGNE, P., DOUGLAS, W.H. and FRANCIS, L.F., 2002. Interaction between bioactive glasses and human dentin. *Journal of materials science. Materials in medicine*, 13(6), pp. 557-565.

- EMBERY, G., HALL, R., WADDINGTON, R., SEPTIER, D. and GOLDBERG, M., 2001. Proteoglycans in dentinogenesis. *Critical reviews in oral biology and medicine: an official publication of the american association of oral biologists*, 12(4), pp. 331-349.
- FARNDAL, R.W., BUTTLE, D.J. and BARRETT, A.J., 1986. Improved quantitation and discrimination of sulphated glycosaminoglycans by use of dimethylmethylene blue. *Biochimica et biophysica acta*, 883(2), pp. 173-177.
- FENG, J.Q., HUANG, H., LU, Y., YE, L., XIE, Y., TSUTSUI, T.W., KUNIEDA, T., CASTRANIO, T., SCOTT, G., BONEWALD, L.B. and MISHINA, Y., 2003. The Dentin matrix protein 1 (Dmp1) is specifically expressed in mineralized, but not soft, tissues during development. *Journal of dental research*, 82(10), pp. 776-780.
- FERRACANE, J.L., COOPER, P.R. and SMITH, A.J., 2010. Can interaction of materials with the dentin-pulp complex contribute to dentin regeneration? *Odontology the society of the nippon dental university*, 98(1), pp. 2-14.
- FINKELMAN, R.D., MOHAN, S., JENNINGS, J.C., TAYLOR, A.K., JEPSEN, S. and BAYLINK, D.J., 1990. Quantitation of growth factors IGF-I, SGF/IGF-II, and TGF-beta in human dentin. *Journal of bone and mineral research: the official journal of the american society for bone and mineral research*, 5(7), pp. 717-723.
- FISHER, L.W., TORCHIA, D.A., FOHR, B., YOUNG, M.F. and FEDARKO, N.S., 2001. Flexible Structures of SIBLING Proteins, Bone Sialoprotein, and Osteopontin. *Biochemical and biophysical research communications*, 280(2), pp. 460-465.
- FOSSE, G., SAELE, P.K. and EIDE, R., 1992. Numerical density and distributional pattern of dentin tubules. *Acta odontologica scandinavica*, 50(4), pp. 201-210.
- FRANK, R.M., 1968. Attachment sites between the odontoblast process and the intradentinal nerve fibre. *Archives of Oral Biology*, 13(7), pp. 833-834.
- FRISTAD, I., 1997. Dental innervation: functions and plasticity after peripheral injury. *Acta odontologica scandinavica*, 55(4), pp. 236-254.
- FRISTAD, I., BLETSA, A. and BYERS, M., 2007. Inflammatory nerve responses in the dental pulp. *Endodontic topics*, 17(1), pp. 12-41.
- GARANT, P.R., 1972. The organization of microtubules within rat odontoblast processes revealed by perfusion fixation with glutaraldehyde. *Archives of oral biology*, 17(7), pp. 1047-1077.
- GARBEROGLIO, R. and BRÄNNSTRÖM, M., 1976. Scanning electron microscopic investigation of human dentinal tubules. *Archives of oral biology*, 21(6), pp. 355-362.
- GARG, N., and GARG, A., (2002). *Textbook of endodontics*. New Delhi: Jaypee Brothers Publishers.
- GENDREAU, L., BARLOW, A.P. and MASON, S.C., 2011. Overview of the clinical evidence for the use of NovaMin in providing relief from the pain of dentin hypersensitivity. *The Journal of clinical dentistry*, 22(3), pp. 90-95.
- GILLAM, D.G., ARIS, A., BULMAN, J.S., NEWMAN, H.N. and LEY, F., 2002. Dentine hypersensitivity in subjects recruited for clinical trials: clinical evaluation, prevalence and intra-oral distribution. *Journal of oral rehabilitation*, 29(3), pp. 226-231.
- GOLDBERG, H.A., WARNER, K.J., STILLMAN, M.J. and HUNTER, G.K., 1996. Determination of the hydroxyapatite-nucleating region of bone sialoprotein. *Connective tissue research*, 35(1-4), pp. 385-392.

- GOLDBERG, M., KULKARNI, A.B., YOUNG, M. and BOSKEY, A., 2011. Dentin: structure, composition and mineralization. *Frontiers in bioscience*, 3, pp. 711-735.
- GOLDBERG, M. and LASFARGUES, J., 1995. Pulpo-dentinal complex revisited. *Journal of dentistry*, 23(1), pp. 15-20.
- GOLDBERG, M., RAPOPORT, O., SEPTIER, D., PALMIER, K., HALL, R., EMBERY, G., YOUNG, M. and AMEYE, L., 2003. Proteoglycans in predentin: the last 15 micrometers before mineralization. *Connective tissue research*, 44, pp. 184-188.
- GOLDBERG, M. and SEPTIER, D., 2002. Phospholipids in amelogenesis and dentinogenesis. *Critical reviews in oral biology and medicine: an official publication of the American Association of Oral Biologists*, 13(3), pp. 276-290.
- GOLDBERG, M. and SMITH, A.J., 2004. Cells and Extracellular Matrices of Dentin and Pulp: a Biological Basis for Repair and Tissue Engineering. *Critical reviews in oral biology and medicine : an official publication of the American Association of Oral Biologists*, 15(1), pp. 13-27.
- GOTLIV, B.A. and VEIS, A., 2007. Peritubular dentin, a vertebrate apatitic mineralized tissue without collagen: role of a phospholipid-proteolipid complex. *Calcified tissue international*, 81(3), pp. 191-205.
- GOUGH, J.E., JONES, J.R. and HENCH, L.L., 2004. Nodule formation and mineralisation of human primary osteoblasts cultured on a porous bioactive glass scaffold. *Biomaterials*, 25(11), pp. 2039-2046.
- GRAHAM, L., COOPER, P.R., CASSIDY, N., NOR, J.E., SLOAN, A.J. and SMITH, A.J., 2006. The effect of calcium hydroxide on solubilisation of bio-active dentine matrix components. *Biomaterials*, 27(14), pp. 2865-2873.
- GRAY, A., FERGUSON, M.M. and WALL, J.G., 1998. Wine tasting and dental erosion. Case report. *Australian Dental Journal*, 43(1), pp. 32-34.
- GREENSPAN, D.C., 2010. NovaMin and tooth sensitivity--an overview. *The Journal of clinical dentistry*, 21(3), pp. 61-65.
- GROBSTEIN, C., 1953. Morphogenetic Interaction between Embryonic Mouse Tissues separated by a Membrane Filter. *Nature*, 172(4384), pp. 869-871.
- GRONTHOS, S., BRAHIM, J., LI, W., FISHER, L.W., CHERMAN, N., BOYDE, A., DENBESTEN, P., ROBEY, P.G. and SHI, S., 2002. Stem cell properties of human dental pulp stem cells. *Journal of dental research*, 81(8), pp. 531-535.
- GRONTHOS, S., MANKANI, M., BRAHIM, J., ROBEY, P.G. and SHI, S., 2000. Postnatal human dental pulp stem cells (DPSCs) in vitro and in vivo. *Proceedings of the National Academy of Sciences of the United States of America*, 97(25), pp. 13625-13630.
- GU, K., SMOKE, R.H. and RUTHERFORD, R.B., 1996. Expression of genes for bone morphogenetic proteins and receptors in human dental pulp. *Archives of Oral Biology*, 41(10), pp. 919-923.
- GURTNER, G.C., WERNER, S., BARRANDON, Y. and LONGAKER, M.T., 2008. Wound repair and regeneration. *Nature*, 453 (7193), pp. 314-321.
- GYSI, A., 1900. An attempt to explain the sensitiveness of dentine. *British journal of dental science*, 43, pp. 865.

- HANKS, C.T., FANG, D., SUN, Z., EDWARDS, C.A. and BUTLER, W.T., 1998. Dentin-specific proteins in MDPC-23 cell line. *European journal of oral sciences*, 106, pp. 260-266.
- HARUYAMA, N., SREENATH, T.L., SUZUKI, S., YAO, X., WANG, Z., WANG, Y., HONEYCUTT, C., IOZZO, R.V., YOUNG, M.F. and KULKARNI, A.B., 2009. Genetic evidence for key roles of decorin and biglycan in dentin mineralization. *Matrix biology : journal of the international society for matrix biology*, 28(3), pp. 129-136.
- HARGREAVES, K., and GOODIS, H., 2002. *Seltzer and Bender's dental pulp*. Surrey: Quintessence Publishing Company.
- HAUG, S.R. and HEYERAAS, K.J., 2006. Modulation of dental inflammation by the sympathetic nervous system. *Journal of dental research*, 85(6), pp. 488-495.
- HE, G., DAHL, T., VEIS, A. and GEORGE, A., 2003. Nucleation of apatite crystals in vitro by self-assembled dentin matrix protein 1. *Nature materials*, 2(8), pp. 552-558.
- HE, W.X., NIU, Z.Y., ZHAO, S.L., JIN, W.L., GAO, J. and SMITH, A.J., 2004. TGF-beta activated Smad signalling leads to a Smad3-mediated down-regulation of DSPP in an odontoblast cell line. *Archives of Oral Biology*, 49(11), pp. 911-918.
- HENCH, L.L., 2006. The story of Bioglass. *Journal of materials science. Materials in medicine*, 17(11), pp. 967-978.
- HENCH, L.L., CLARK, A.E. and SCHAAKE, H.F., 1972. Effects of microstructure on the radiation stability of amorphous semiconductors. *Journal of non-crystalline solids*, 8-10(0), pp. 837-843.
- HENCH, L.L. and PASCHALL, H.A., 1973. Direct chemical bond of bioactive glass-ceramic materials to bone and muscle. *Journal of biomedical materials research*, 7(3), pp. 25-42.
- HENCH, L.L., SPLINTER, R.J., ALLEN, W.C. and GREENLEE, T.K., 1971. Bonding mechanisms at the interface of ceramic prosthetic materials. *Journal of biomedical materials research*, 5(6), pp. 117-141.
- HENCH, L.L., SPLINTER, R.J., ALLEN, W.C. and GREENLEE, T.K., 1971. Bonding mechanisms at the interface of ceramic prosthetic materials. *Journal of biomedical materials research*, 5(6), pp. 117-141.
- HENCH, L.L., 1998. Bioceramics. *Journal of the American Ceramic Society*, 81(7), pp. 1705-1728.
- HENCH, L.L., 1991. Bioceramics: From Concept to Clinic. *Journal of the american ceramic society*, 74(7), pp. 1487-1510.
- HOFFMAN-KIM, D., MITCHEL, J.A. and BELLAMKONDA, R.V., 2010. Topography, cell response, and nerve regeneration. *Annual review of biomedical engineering*, 12, pp. 203-231.
- HOLLAND, G.R., 1975. The dentinal tubule and odontoblast process in the cat. *Journal of anatomy*, 120 (Pt 1), pp. 169-177.
- HOLLAND, G.R., NARHI, M.N., ADDY, M., GANGAROSA, L. and ORCHARDSON, R., 1997. Guidelines for the design and conduct of clinical trials on dentine hypersensitivity. *Journal of clinical periodontology*, 24(11), pp. 808-813.
- HOOPER, S., WEST, N.X., PICKLES, M.J., JOINER, A., NEWCOMBE, R.G. and ADDY, M., 2003. Investigation of erosion and abrasion on enamel and dentine: a model in situ using toothpastes of different abrasivity. *Journal of clinical periodontology*, 30(9), pp. 802-808.

- HOPPE, A., GÜLDAL, N.S. and BOCCACCINI, A.R., 2011. A review of the biological response to ionic dissolution products from bioactive glasses and glass-ceramics. *Biomaterials*, 32(11), pp. 2757-2774.
- HOWARD, C., MURRAY, P.E. and NAMEROW, K.N., 2010. Dental Pulp Stem Cell Migration. *Journal of endodontics*, 36(12), pp. 1963-1966.
- HOWELL, S.J., WILK, D., YADAV, S.P. and BEVINS, C.L., 2003. Antimicrobial polypeptides of the human colonic epithelium. *Peptides*, 24(11), pp. 1763-1770.
- HSIUNG, C., ANDRADE, J.D., COSTA, R. and ASH, K.O., 1997. Minimizing interferences in the quantitative multielement analysis of trace elements in biological fluids by inductively coupled plasma mass spectrometry. *Clinical chemistry*, 43(12), pp. 2303-2311.
- HU, S., CHANG, J., LIU, M. and NING, C., 2009. Study on antibacterial effect of 45S5 Bioglass. *Journal of materials science. Materials in medicine*, 20(1), pp. 281-286.
- HUANG DA, W., SHERMAN, B.T. and LEMPICKI, R.A., 2009a. Systematic and integrative analysis of large gene lists using DAVID bioinformatics resources. *Nature protocols*, 4(1), pp. 44-57.
- HUANG, G.T., GRONTHOS, S. and SHI, S., 2009b. Mesenchymal stem cells derived from dental tissues vs. those from other sources: their biology and role in regenerative medicine. *Journal of dental research*, 88(9), pp. 792-806.
- HUANG, G.T., SHAGRAMANOVA, K. and CHAN, S.W., 2006. Formation of odontoblast-like cells from cultured human dental pulp cells on dentin in vitro. *Journal of endodontics*, 32(11), pp. 1066-1073.
- HUNTER, G.K. and GOLDBERG, H.A., 1993. Nucleation of hydroxyapatite by bone sialoprotein. *Proceedings of the national academy of sciences of the united states of america*, 90(18), pp. 8562-8565.
- HURST, P.S., LACEY, L.H. and CRISP, A.H., 1977. Teeth, vomiting and diet: a study of the dental characteristics of seventeen anorexia nervosa patients. *Postgraduate medical journal*, 53(620), pp. 298-305.
- IKEDA, M., OKAMOTO, K. and KATSUMATA, R., 1999. Cloning of the transketolase gene and the effect of its dosage on aromatic amino acid production in *Corynebacterium glutamicum*. *Applied microbiology and biotechnology*, 51(2), pp. 201-206.
- IWASAKI, Y., OTSUKA, H., YANAGISAWA, N., HISAMITSU, H., MANABE, A., NONAKA, N. and NAKAMURA, M., 2011. In situ proliferation and differentiation of macrophages in dental pulp. *Cell and tissue research*, 346(1), pp. 99-109.
- JAGR, M., ECKHARDT, A., PATARIDIS, S. and MIKSIK, I., 2012. Comprehensive proteomic analysis of human dentin. *European journal of oral sciences*, 120(4), pp. 259-268.
- JONES, J.R., SEPULVEDA, P. and HENCH, L.L., 2001. Dose-dependent behavior of bioactive glass dissolution. *Journal of biomedical materials research*, 58(6), pp. 720-726.
- JONTELL, M., OKIJI, T., DAHLGREN, U. and BERGENHOLTZ, G., 1998. Immune defense mechanisms of the dental pulp. *Critical reviews in oral biology and medicine: an official publication of the American Association of Oral Biologists*, 9(2), pp. 179-200.

JULIEN, M., KHOSHNIAT, S., LACREUSETTE, A., GATIUS, M., BOZEC, A., WAGNER, E.F., WITTRANT, Y., MASSON, M., WEISS, P., BECK, L., MAGNE, D. and GUICHEUX, J., 2009. Phosphate-dependent regulation of MGP in osteoblasts: role of ERK1/2 and Fra-1. *Journal of bone and mineral research: the official journal of the american society for bone and mineral research*, 24(11), pp. 1856-1868.

JUSTICE, B.A., BADR, N.A. and FELDER, R.A., 2009. 3D cell culture opens new dimensions in cell-based assays. *Drug discovery today*, 14(1–2), pp. 102-107.

KALYVA, M., PAPADIMITRIOU, S. and TZIAFAS, D., 2010. Transdental stimulation of tertiary dentine formation and intratubular mineralization by growth factors. *International endodontic journal*, 43(5), pp. 382-392.

KHAN, E., 2012. Characterisation of 2D And 3D Oral Keratinocyte Cultures. PhD thesis submitted to the University of Birmingham.

KIM, H.S., CHO, J.H., PARK, H.W., YOON, H., KIM, M.S. and KIM, S.C., 2002. Endotoxin-neutralizing antimicrobial proteins of the human placenta. *Journal of immunology*, 168(5), pp. 2356-2364.

KIM, H., KIM, P., BAE, S.M., SON, H., THOUDAM, D.S., KIM, J., LEE, B., PARK, R. and KIM, I., 2009. Transforming growth factor-induced protein (TGFB $\beta$ 1/ ig-h3) activates platelets and promotes thrombogenesis. *Blood*, 114(25), pp. 5206-5215.

KINA, J.R., KINA, J., KINA, E.F., KINA, M. and SOUBHIA, A.M., 2008. Presence of bacteria in dentinal tubules. *Journal of applied oral science: revista FOB*, 16(3), pp. 205-208.

KOUTSI, V., NOONAN, R.G., HORNER, J.A., SIMPSON, M.D., MATTHEWS, W.G. and PASHLEY, D.H., 1994. The effect of dentin depth on the permeability and ultrastructure of primary molars. *Pediatric dentistry*, 16(1), pp. 29-35.

KWON, S.M., KIM, S.A., YOON, J.H. and AHN, S.G., 2010. Transforming growth factor beta1-induced heat shock protein 27 activation promotes migration of mouse dental papilla-derived MDPC-23 cells. *Journal of endodontics*, 36(8), pp. 1332-1335.

LITKOWSKI, L.J., HACK, G.D., SHEAFFER, H.B., AND GREENSPAN D.C., IN: L. SEDEL AND C. REY, ed, 1997. *Bioceramics*, Occlusion of Dentine Tubules by 45S5 Bioglass®.

LA FLECHE, R.G., FRANK, R.M. and STEUER, P., 1985. The extent of the human odontoblast process as determined by transmission electron microscopy: the hypothesis of a retractable suspensor system. *Journal de Biologie Buccale*, 13(4), pp. 293-305.

LANGDAHL, B.L., KASSEM, M., MOLLER, M.K. and ERIKSEN, E.F., 1998. The effects of IGF-I and IGF-II on proliferation and differentiation of human osteoblasts and interactions with growth hormone. *European journal of clinical investigation*, 28(3), pp. 176-183.

LAURENT, P., CAMPS, J. and ABOUT, I., 2012. Biodentine(TM) induces TGF-beta1 release from human pulp cells and early dental pulp mineralization. *International endodontic journal*, 45(5), pp. 439-448.

LAYER, T.M., 2011. Development of a fluoridated, daily-use toothpaste containing NovaMin technology for the treatment of dentin hypersensitivity. *The Journal of clinical dentistry*, 22(3), pp. 59-61.

LENZI, T.L., GUGLIELMI, C.D., ARANA-CHAVEZ, V.E. and RAGGIO, D.P., 2013. Tubule Density and Diameter in Coronal Dentin from Primary and Permanent Human Teeth. *Microscopy and microanalysis : the official journal of microscopy society of america, microbeam analysis society, microscopical society of canada*, pp. 1-5.

LESOT, H., SMITH, A.J., MATTHEWS, J.B. and RUCH, J.V., 1988. An extracellular matrix protein of dentine, enamel, and bone shares common antigenic determinants with keratins. *Calcified tissue international*, 42(1), pp. 53-57.

LINDE, A., (1984). *Dentin and Dentinogenesis, Volume 1*. Florida: CRC Press.

LINDE, A. and GOLDBERG, M., 1993. Dentinogenesis. *Critical reviews in oral biology and medicine: an official publication of the American Association of Oral Biologists*, 4(5), pp. 679-728.

LINDE, A., 1989. Dentin matrix proteins: Composition and possible functions in calcification. *The Anatomical Record*, 224(2), pp. 154-166.

LISI, S., PETERKOVA, R., PETERKA, M., VONESCH, J.L., RUCH, J.V. and LESOT, H., 2003. Tooth morphogenesis and pattern of odontoblast differentiation. *Connective tissue research*, 44, pp. 167-170.

LITKOWSKI, L.J., HACK, G.D., SHEAFFER, H.B., *et al.*, 1997. Occlusion of Dentin Tubules by 45S5 Bioglass®, in Sedel, L. And Rey, C. (eds), *Bioceramics 10. Proceedings of the 10<sup>th</sup> international symposium on ceramics in medicine*, Elsevier, New York. pp. 411-414

LITKOWSKI, L. and GREENSPAN, D.C., 2010. A clinical study of the effect of calcium sodium phosphosilicate on dentin hypersensitivity--proof of principle. *The Journal of clinical dentistry*, 21(3), pp. 77-81.

LOVE, R.M. and JENKINSON, H.F., 2002. Invasion of Dentinal Tubules by Oral Bacteria. *Critical reviews in oral biology & medicine*, 13(2), pp. 171-183.

LU, Y., XIE, Y., ZHANG, S., DUSEVICH, V., BONEWALD, L.F. and FENG, J.Q., 2007. DMP1-targeted Cre expression in odontoblasts and osteocytes. *Journal of dental research*, 86(4), pp. 320-325.

MACH, H., MIDDAUGH, C.R. and LEWIS, R.V., 1992. Statistical determination of the average values of the extinction coefficients of tryptophan and tyrosine in native proteins. *Analytical biochemistry*, 200(1), pp. 74-80.

MAENO, S., NIKI, Y., MATSUMOTO, H., MORIOKA, H., YATABE, T., FUNAYAMA, A., TOYAMA, Y., TAGUCHI, T. and TANAKA, J., 2005. The effect of calcium ion concentration on osteoblast viability, proliferation and differentiation in monolayer and 3D culture. *Biomaterials*, 26(23), pp. 4847-4855.

MAGLOIRE, H., JOFFRE, A. and BLEICHER, F., 1996. An in vitro model of human dental pulp repair. *Journal of dental research*, 75(12), pp. 1971-1978.

MAGLOIRE, H., ROMEAS, A., MELIN, M., COUBLE, M., BLEICHER, F. and FARGES, J., 2001. Molecular Regulation of Odontoblast Activity under Dentin Injury. *Advances in Dental Research*, 15(1), pp. 46-50.

MAGNE, D., GUICHEUX, J., WEISS, P., PILET, P. and DACULSI, G., 2002. Fourier transform infrared microspectroscopic investigation of the organic and mineral constituents of peritubular dentin: a horse study. *Calcified tissue international*, 71(2), pp. 179-185.

MARIE, P.J., 2010. The calcium-sensing receptor in bone cells: a potential therapeutic target in osteoporosis. *Bone*, 46(3), pp. 571-576.

MARTINEZ-RICARTE, J., FAUS-MATOSES, V., FAUS-LLACER, V.J., FLICHY-FERNANDEZ, A.J. and MATEOS-MORENO, B., 2008. Dentinal sensitivity: concept and methodology for its objective evaluation. *Medicina oral, patologia oral y cirugia bucal*, 13(3), pp. E201-6.



- MAZZONI, A., BRESCHI, L., CARRILHO, M., NASCIMENTO, F.D., ORSINI, G., RUGGERI, A., GOBBI, P., MANZOLI, L., TAY, F.R., PASHLEY, D.H. and TJÄDERHANE, L., 2009. A review of the nature, role, and function of dentin non-collagenous proteins. Part II: enzymes, serum proteins, and growth factors. *Endodontic topics*, 21(1), pp. 19-40.
- MCCORMACK, K. and DAVIES, R., 1996. The enigma of potassium ion in the management of dentine hypersensitivity: is nitric oxide the elusive second messenger? *Pain*, 68(1), pp. 5-11.
- MCLACHLAN, J.L., SMITH, A.J., BUJALSKA, I.J. and COOPER, P.R., 2005. Gene expression profiling of pulpal tissue reveals the molecular complexity of dental caries. *Biochimica et biophysica acta*, 1741(3), pp. 271-281.
- MCLACHLAN, J.L., SMITH, A.J., SLOAN, A.J. and COOPER, P.R., 2003. Gene expression analysis in cells of the dentine-pulp complex in healthy and carious teeth. *Archives of oral biology*, 48(4), pp. 273-283.
- MELIN, M., JOFFRE-ROMEAS, A., FARGES, J.C., COUBLE, M.L., MAGLOIRE, H. and BLEICHER, F., 2000. Effects of TGF beta-1 on dental pulp cells in cultured human tooth slices. *Journal of dental research*, 79(9), pp. 1689-1696.
- MEYER, F. and BEUCHER, S., 1990. Morphological segmentation. *Journal of visual communication and image representation*, 1(1), pp. 21-46.
- MIURA, M., GRONTHOS, S., ZHAO, M., LU, B., FISHER, L.W., ROBEY, P.G. and SHI, S., 2003. SHED: Stem cells from human exfoliated deciduous teeth. *Proceedings of the national academy of sciences*, 100(10), pp. 5807-5812.
- MOHAMMADI, Z. and DUMMER, P.M.H., 2011. Properties and applications of calcium hydroxide in endodontics and dental traumatology. *International endodontic journal*, 44(8), pp. 697-730.
- MOHAMMADI, Z., SHALAVI, S. and YAZDIZADEH, M., 2012. Antimicrobial activity of calcium hydroxide in endodontics: a review. *Chonnam medical journal*, 48(3), pp. 133-140.
- MORDAN, N.J., BARBER, P.M. and GILLAM, D.G., 1997. The dentine disc. A review of its applicability as a model for the in vitro testing of dentine hypersensitivity. *Journal of oral rehabilitation*, 24(2), pp. 148-156.
- MOSMANN, T., 1983. Rapid colorimetric assay for cellular growth and survival: application to proliferation and cytotoxicity assays. *Journal of immunological methods*, 65(1-2), pp. 55-63.
- MOULE, A.J., LI, H. and BARTOLD, P.M., 1995. Donor variability in the proliferation of human dental pulp fibroblasts. *Australian dental journal*, 40(2), pp. 110-114.
- MURRAY, P.E., ABOUT, I., LUMLEY, P.J., FRANQUIN, J.-., WINDSOR, L.J. and SMITH, A.J., 2003. Odontoblast morphology and dental repair. *Journal of dentistry*, 31(1), pp. 75-82.
- MUSSON, D.S., MCLACHLAN, J.L., SLOAN, A.J., SMITH, A.J. and COOPER, P.R., 2010. Adrenomedullin is expressed during rodent dental tissue development and promotes cell growth and mineralization. *Biology of the cell*, 102(3), pp. 145-157.
- MUYLLE, S., SIMOENS, P. and LAUWERS, H., 2000. Tubular contents of equine dentin: a scanning electron microscopic study. *Journal of veterinary medicine*, 47(6), pp. 321-330.
- MYLLARNIEMI, H. and SAARIO, I., 1985. A new type of sliding hiatus hernia. *Annals of Surgery*, 202(2), pp. 159-161.

- NAKASHIMA, M., 1992. The effects of growth factors on DNA synthesis, proteoglycan synthesis and alkaline phosphatase activity in bovine dental pulp cells. *Archives of oral biology*, 37(3), pp. 231-236.
- NAKASHIMA, M., 1990. The induction of reparative dentine in the amputated dental pulp of the dog by bone morphogenetic protein. *Archives of oral biology*, 35(7), pp. 493-497.
- NAKASHIMA, M. and AKAMINE, A., 2005. The application of tissue engineering to regeneration of pulp and dentin in endodontics. *Journal of endodontics*, 31(10), pp. 711-718.
- NANCI, A., 2003. *Ten Cate's oral histology: development, structure and function*. Missouri: Mosby.
- NÄRHI, M., 1990. The neurophysiology of the teeth. *Dental clinics of north america*, 34(3), pp. 439-448.
- NOSRAT, C.A., FRIED, K., EBENDAL, T. and OLSON, L., 1998. NGF, BDNF, NT3, NT4 and GDNF in tooth development. *European journal of oral sciences*, 106 Suppl 1, pp. 94-99.
- OKI, A., PARVEEN, B., HOSSAIN, S., ADENIJI, S. and DONAHUE, H., 2004. Preparation and in vitro bioactivity of zinc containing sol-gel-derived bioglass materials. *Journal of biomedical materials research. Part A*, 69(2), pp. 216-221.
- OLIVARES, J.A. and HOUK, R.S., 1986. Suppression of analyte signal by various concomitant salts in inductively coupled plasma mass spectrometry. *Analytical chemistry*, 58(1), pp. 20-25.
- ORCHARDSON, R. and COLLINS, W.J., 1987. Clinical features of hypersensitive teeth. *British dental journal*, 162(7), pp. 253-256.
- ORCHARDSON, R. and GILLAM, D.G., 2006. Managing dentin hypersensitivity. *Journal of the american dental association*, 137(7), pp. 990-8;
- ORÉFICE, R., HENCH, L. and BRENNAN, A., 2009. Evaluation of the interactions between collagen and the surface of a bioactive glass during in vitro test. *Journal of biomedical materials research part A*, 90A(1), pp. 114-120.
- ORSINI, G., RUGGERI, A., MAZZONI, A., NATO, F., FALCONI, M., PUTIGNANO, A., DI LENARDA, R., NANCI, A. and BRESCHI, L., 2008. Immunohistochemical localization of dentin matrix protein 1 in human dentin. *European journal of histochemistry* : 52(4), pp. 215-220.
- OTSU, N., 1979. A Threshold Selection Method from Gray-Level Histograms. *Systems, Man and Cybernetics, IEEE Transactions*, 9(1), pp. 62-66.
- PAEWINSKY, E., PFEIFFER, H. and BRINKMANN, B., 2005. Quantification of secondary dentine formation from orthopantomograms--a contribution to forensic age estimation methods in adults. *International journal of legal medicine*, 119(1), pp. 27-30.
- PANAGAKOS, F., SCHIFF, T. and GUIGNON, A., 2009. Dentin hypersensitivity: effective treatment with an in-office desensitizing paste containing 8% arginine and calcium carbonate. *American journal of dentistry*, 22 Spec No A, pp. 3A-7A.
- PARK, E.S., CHO, H.S., KWON, T.G., JANG, S.N., LEE, S.H., AN, C.H., SHIN, H.I., KIM, J.Y. and CHO, J.Y., 2009. Proteomics analysis of human dentin reveals distinct protein expression profiles. *Journal of proteome research*, 8(3), pp. 1338-1346.

- PARKINSON, C.R. and WILLSON, R.J., 2011. A comparative in vitro study investigating the occlusion and mineralization properties of commercial toothpastes in a four-day dentin disc model. *The Journal of clinical dentistry*, 22(3), pp. 74-81.
- PASHLEY, D.H., 1996. Dynamics of the pulpo-dentin complex. *Critical reviews in oral biology and medicine : an official publication of the american association of oral biologists*, 7(2), pp. 104-133.
- PASHLEY, D.H., 1992. Smear layer: overview of structure and function. *Proceedings of the Finnish Dental Society.Suomen Hammaslaakariseuran toimituksia*, 88 Suppl 1, pp. 215-224.
- PASHLEY, D.H., 1986. Dentin permeability, dentin sensitivity, and treatment through tubule occlusion. *Journal of endodontics*, 12(10), pp. 465-474.
- PAULA-SILVA, F.W., GHOSH, A., SILVA, L.A. and KAPILA, Y.L., 2009. TNF-alpha promotes an odontoblastic phenotype in dental pulp cells. *Journal of dental research*, 88(4), pp. 339-344.
- PETERSEN, P.E. and GORMSEN, C., 1991. Oral conditions among German battery factory workers. *Community dentistry and oral epidemiology*, 19(2), pp. 104-106.
- PETRAK, J., IVANEK, R., TOMAN, O., CMEJLA, R., CMEJLOVA, J., VYORAL, D., ZIVNY, J. and VULPE, C.D., 2008. Deja vu in proteomics. A hit parade of repeatedly identified differentially expressed proteins. *Proteomics*, 8(9), pp. 1744-1749.
- PIRKMAJER, S. and CHIBALIN, A.V., 2011. Serum starvation: caveat emptor. *American journal of physiology - cell physiology*, 301(2), pp. c272-c279.
- POPAT, K.C., CHATVANICHKUL, K., BARNES, G.L., LATEMPA, T.J., GRIMES, C.A. and DESAI, T.A., 2007. Osteogenic differentiation of marrow stromal cells cultured on nanoporous alumina surfaces. *Journal of biomedical materials research part A*, 80A(4), pp. 955-964.
- PORTO, I.C., ANDRADE, A.K. and MONTES, M.A., 2009. Diagnosis and treatment of dentinal hypersensitivity. *Journal of oral science*, 51(3), pp. 323-332.
- PREIBISCH, S., SAALFELD, S. and TOMANCAK, P., 2009. Globally optimal stitching of tiled 3D microscopic image acquisitions. *Bioinformatics*, 25(11), pp. 1463-1465.
- QIAN, W.J., KALETA, D.T., PETRITIS, B.O., JIANG, H., LIU, T., ZHANG, X., MOTTAZ, H.M., VARNUM, S.M., CAMP, D.G., 2ND, HUANG, L., FANG, X., ZHANG, W.W. and SMITH, R.D., 2008. Enhanced detection of low abundance human plasma proteins using a tandem IgY12-SuperMix immunoaffinity separation strategy. *Molecular & cellular proteomics: MCP*, 7(10), pp. 1963-1973.
- QIN, C., BABA, O. and BUTLER, W.T., 2004. Post-translational modifications of sibling proteins and their roles in osteogenesis and dentinogenesis. *Critical reviews in oral biology and medicine: an official publication of the american association of oral biologists*, 15(3), pp. 126-136.
- QIN, C., D'SOUZA, R. and FENG, J.Q., 2007. Dentin matrix protein 1 (DMP1): new and important roles for biomineralization and phosphate homeostasis. *Journal of dental research*, 86(12), pp. 1134-1141.
- RADIN, S., DUCHEYNE, P., ROTHMAN, B. and CONTI, A., 1997. The effect of in vitro modeling conditions on the surface reactions of bioactive glass. *Journal of biomedical materials research*, 37(3), pp. 363-375.

- REES, J.S. and ADDY, M., 2002. A cross-sectional study of dentine hypersensitivity. *Journal of clinical periodontology*, 29(11), pp. 997-1003.
- REFFITT, D.M., OGSTON, N., JUGDAOHSINGH, R., CHEUNG, H.F., EVANS, B.A., THOMPSON, R.P., POWELL, J.J. and HAMPSON, G.N., 2003. Orthosilicic acid stimulates collagen type 1 synthesis and osteoblastic differentiation in human osteoblast-like cells in vitro. *Bone*, 32(2), pp. 127-135.
- RICHARDSON, D.D., SADI, B.B.M. and CARUSO, J.A., 2006. Reversed phase ion-pairing HPLC-ICP-MS for analysis of organophosphorus chemical warfare agent degradation products. *Journal of analytical atomic spectrometry*, 21(4), pp. 396-403.
- RITCHIE, H.H., PINERO, G.J., HOU, H. and BUTLER, W.T., 1995. Molecular analysis of rat dentin sialoprotein. *Connective tissue research*, 33(1-3), pp. 73-79.
- ROBERTS-CLARK, D.J. and SMITH, A.J., 2000. Angiogenic growth factors in human dentine matrix. *Archives of oral biology*, 45(11), pp. 1013-1016.
- ROEHM, N.W., RODGERS, G.H., HATFIELD, S.M. and GLASEBROOK, A.L., 1991. An improved colorimetric assay for cell proliferation and viability utilizing the tetrazolium salt XTT. *Journal of immunological methods*, 142(2), pp. 257-265.
- RUCH, J.V., LESOT, H. and BEGUE-KIRN, C., 1995. Odontoblast differentiation. *The International journal of developmental biology*, 39(1), pp. 51-68.
- RUTHERFORD, R.B., SPANGBERG, L., TUCKER, M., RUEGER, D. and CHARETTE, M., 1994. The time-course of the induction of reparative dentine formation in monkeys by recombinant human osteogenic protein-1. *Archives of oral biology*, 39(10), pp. 833-838.
- RUTHERFORD, R.B., WAHLE, J., TUCKER, M., RUEGER, D. and CHARETTE, M., 1993. Induction of reparative dentine formation in monkeys by recombinant human osteogenic Protein-1. *Archives of oral biology*, 38(7), pp. 571-576.
- SALIAN, S., THAKUR, S., KULKARNI, S. and LATORRE, G., 2010. A randomized controlled clinical study evaluating the efficacy of two desensitizing dentifrices. *The Journal of clinical dentistry*, 21(3), pp. 82-87.
- SANDY, J., DAVIES, M., PRIME, S. and FARNDAL, R., 1998. Signal pathways that transduce growth factor-stimulated mitogenesis in bone cells. *Bone*, 23(1), pp. 17-26.
- SARAVANAPAVAN, P., JONES, J.R., VERRIER, S., BEILBY, R., SHIRTLIFF, V.J., HENCH, L.L. and POLAK, J.M., 2004. Binary CaO-SiO<sub>2</sub> gel-glasses for biomedical applications. *Bio-medical materials and engineering*, 14(4), pp. 467-486.
- SARIKAYA, A., RECORD, R., WU, C.C., TULLIUS, B., BADYLAK, S. and LADISCH, M., 2002. Antimicrobial activity associated with extracellular matrices. *Tissue engineering*, 8(1), pp. 63-71.
- SASAKI, T. and GARANT, P.R., 1996. Structure and organization of odontoblasts. *The anatomical record*, 245(2), pp. 235-249.
- SAWA, Y., HORIE, Y., YAMAOKA, Y., EBATA, N., KIM, T. and YOSHIDA, S., 2003. Production of Colony-stimulating Factor in Human Dental Pulp Fibroblasts. *Journal of dental research*, 82(2), pp. 96-100.

- SCHILKE, R., LISSON, J.A., BAUSS, O. and GEURTSSEN, W., 2000. Comparison of the number and diameter of dentinal tubules in human and bovine dentine by scanning electron microscopic investigation. *Archives of oral biology*, 45(5), pp. 355-361.
- SCHMALZ, G., SCHUSTER, U., THONEMANN, B., BARTH, M. and ESTERBAUER, S., 2001. Dentin barrier test with transfected bovine pulp-derived cells. *Journal of endodontics*, 27(2), pp. 96-102.
- SCHOUR, I. and HOFFMAN, M.M., 1939. Studies in Tooth Development: II. the Rate of Apposition of Enamel and Dentin in Man and Other Mammals. *Journal of dental research*, 18(2), pp. 161-175.
- SCHROEDER, L. and FRANK, R.M., 1985. High-resolution transmission electron microscopy of adult human peritubular dentine. *Cell and tissue research*, 242(2), pp. 449-451.
- SHAO, M.Y., FU, Z.S., CHENG, R., YANG, H., CHENG, L., WANG, F.M. and HU, T., 2011. The presence of open dentinal tubules affects the biological properties of dental pulp cells ex vivo. *Molecules and cells*, 31(1), pp. 65-71.
- SHARMA, N., ROY, S., KAKAR, A., GREENSPAN, D.C. and SCOTT, R., 2010. A clinical study comparing oral formulations containing 7.5% calcium sodium phosphosilicate (NovaMin), 5% potassium nitrate, and 0.4% stannous fluoride for the management of dentin hypersensitivity. *The Journal of clinical dentistry*, 21(3), pp. 88-92.
- SHAW, L., AL-DLAIGAN, Y.H. and SMITH, A., 2000. Childhood asthma and dental erosion. *ASDC journal of dentistry for children*, 67(2), pp. 102-6, 82.
- SHIBA, H., FUJITA, T., DOI, N., NAKAMURA, S., NAKANISHI, K., TAKEMOTO, T., HINO, T., NOSHIRO, M., KAWAMOTO, T., KURIHARA, H. and KATO, Y., 1998. Differential effects of various growth factors and cytokines on the syntheses of DNA, type I collagen, laminin, fibronectin, osteonectin/secreted protein, acidic and rich in cysteine (SPARC), and alkaline phosphatase by human pulp cells in culture. *Journal of cellular physiology*, 174(2), pp. 194-205.
- SHIRAKAWA, M., SHIBA, H., NAKANISHI, K., OGAWA, T., OKAMOTO, H., NAKASHIMA, K., NOSHIRO, M. and KATO, Y., 1994. Transforming growth factor-beta-1 reduces alkaline phosphatase mRNA and activity and stimulates cell proliferation in cultures of human pulp cells. *Journal of dental research*, 73(9), pp. 1509-1514.
- SIGAL, M.J., AUBIN, J.E., TEN CATE, A.R. and PITARU, S., 1984a. The odontoblast process extends to the dentinoenamel junction: an immunocytochemical study of rat dentine. *The journal of histochemistry and cytochemistry : official journal of the histochemistry society*, 32(8), pp. 872-877.
- SIGAL, M.J., PITARU, S., AUBIN, J.E. and TEN CATE, A.R., 1984b. A combined scanning electron microscopy and immunofluorescence study demonstrating that the odontoblast process extends to the dentinoenamel junction in human teeth. *The anatomical record*, 210(3), pp. 453-462.
- SILVA, T.A., LARA, V.S., SILVA, J.S., GARLET, G.P., BUTLER, W.T. and CUNHA, F.Q., 2004. Dentin sialoprotein and phosphoprotein induce neutrophil recruitment: a mechanism dependent on IL-1beta, TNF-beta, and CXC chemokines. *Calcified tissue international*, 74(6), pp. 532-541.
- SIMON, S., SMITH, A.J., LUMLEY, P.J., BERDAL, A., SMITH, G., FINNEY, S. and COOPER, P.R., 2009. Molecular characterization of young and mature odontoblasts. *Bone*, 45(4), pp. 693-703.
- SIQUEIRA, J.F. and LOPES, H.P., 1999. Mechanisms of antimicrobial activity of calcium hydroxide: a critical review. *International endodontic journal*, 32(5), pp. 361-369.

- SLOAN, A.J., MOSELEY, R., DOBIE, K., WADDINGTON, R.J. and SMITH, A.J., 2002. TGF-beta latency-associated peptides (LAPs) in human dentin matrix and pulp. *Connective tissue research*, 43(2-3), pp. 381-386.
- SLOAN, A.J., PERRY, H., MATTHEWS, J.B. and SMITH, A.J., 2000. Transforming growth factor-beta isoform expression in mature human healthy and carious molar teeth. *The Histochemical journal*, 32(4), pp. 247-252.
- SLOAN, A.J. and SMITH, A.J., 1999. Stimulation of the dentine-pulp complex of rat incisor teeth by transforming growth factor-beta isoforms 1-3 in vitro. *Archives of oral biology*, 44(2), pp. 149-156.
- SMITH, A., PATEL, M., GRAHAM, L., SLOAN, A. and COOPER, P., 2005. Dentine Regeneration: Key Roles for Stem Cells and Molecular Signalling. *Oral biosciences & medicine*, 2(2), pp. 127 - 132.
- SMITH, A.J., 2003. Vitality of the dentin-pulp complex in health and disease: growth factors as key mediators. *Journal of dental education*, 67(6), pp. 678-689.
- SMITH, A.J., CASSIDY, N., PERRY, H., BEGUE-KIRN, C., RUCH, J.V. and LESOT, H., 1995. Reactionary dentinogenesis. *The International journal of developmental biology*, 39(1), pp. 273-280.
- SMITH, A.J. and LEAVER, A.G., 1979. Non-collagenous components of the organic matrix of rabbit incisor dentine. *Archives of oral biology*, 24(6), pp. 449-454.
- SMITH, A.J. and LESOT, H., 2001. Induction and regulation of crown dentinogenesis: embryonic events as a template for dental tissue repair *Critical reviews in oral biology and medicine: an official publication of the american association of oral biologists*, 12(5), pp. 425-437.
- SMITH, A.J., MATTHEWS, J.B. and HALL, R.C., 1998. Transforming growth factor-beta1 (TGF-beta1) in dentine matrix. Ligand activation and receptor expression. *European journal of oral sciences*, 106 Suppl 1, pp. 179-184.
- SMITH, A.J., MATTHEWS, J.B., WILSON, C. and SEWELL, H.F., 1985. Plasma proteins in human cortical bone: In vitro binding studies. *Calcified tissue international*, 37(2), pp. 208-210.
- SMITH, A.J., TOBIAS, R.S., CASSIDY, N., PLANT, C.G., BROWNE, R.M., BEGUE-KIRN, C., RUCH, J.V. and LESOT, H., 1994. Odontoblast stimulation in ferrets by dentine matrix components. *Archives of oral biology*, 39(1), pp. 13-22.
- SMITH, A.J., TOBIAS, R.S. and MURRAY, P.E., 2001. Transdental stimulation of reactionary dentinogenesis in ferrets by dentine matrix components. *Journal of dentistry*, 29(5), pp. 341-346.
- SMITH, A.J., TOBIAS, R.S., PLANT, C.G., BROWNE, R.M., LESOT, H. and RUCH, J.V., 1990. In vivo morphogenetic activity of dentine matrix proteins. *Journal de biologie buccale*, 18(2), pp. 123-129.
- SMITH, J.G., SMITH, A.J., SHELTON, R.M. and COOPER, P.R., 2012a. Antibacterial activity of dentine and pulp extracellular matrix extracts. *International endodontic journal*, 45(8), pp. 749-755.
- SMITH, A.J., SCHEVEN, B.A., TAKAHASHI, Y., FERRACANE, J.L., SHELTON, R.M. and COOPER, P.R., 2012b. Dentine as a bioactive extracellular matrix. *Archives of oral biology*, 57(2), pp. 109-121.
- SMITH, J.G., SMITH, A.J., SHELTON, R.M. and COOPER, P.R., 2012c. Recruitment of dental pulp cells by dentine and pulp extracellular matrix components. *Experimental cell research*, 318(18), pp. 2397-2406.

- SONOYAMA, W., LIU, Y., YAMAZA, T., TUAN, R.S., WANG, S., SHI, S. and HUANG, G.T., 2008. Characterization of the apical papilla and its residing stem cells from human immature permanent teeth: a pilot study. *Journal of endodontics*, 34(2), pp. 166-171.
- STANLEY, H.R., PEREIRA, J.C., SPIEGEL, E., BROOM, C. and SCHULTZ, M., 1983. The detection and prevalence of reactive and physiologic sclerotic dentin, reparative dentin and dead tracts beneath various types of dental lesions according to tooth surface and age. *Journal of oral pathology*, 12(4), pp. 257-289.
- SUN, J.Y., YANG, Y.S., ZHONG, J. and GREENSPAN, D.C., 2007. The effect of the ionic products of Bioglass dissolution on human osteoblasts growth cycle in vitro. *Journal of tissue engineering and regenerative medicine*, 1(4), pp. 281-286.
- TAGAMI, J., HOSODA, H., BURROW, M.F. and NAKAJIMA, M., 1992. Effect of aging and caries on dentin permeability. *Proceedings of the finnish dental society. Suomen hammaslaakariseuran toimituksia*, 88 Suppl 1, pp. 149-154.
- TAI, B.J., BIAN, Z., JIANG, H., GREENSPAN, D.C., ZHONG, J., CLARK, A.E. and DU, M.Q., 2006. Anti-gingivitis effect of a dentifrice containing bioactive glass (NovaMin) particulate. *Journal of clinical periodontology*, 33(2), pp. 86-91.
- TAKAGI, Y., SHIMOKAWA, H., SUZUKI, M., NAGAI, H. and SASAKI, S., 1990. Immunohistochemical localization of alpha 2HS glycoprotein in dentin. *Calcified tissue international*, 47(1), pp. 40-45.
- TAKITA T, HAYASHI M, TAKEICHI O, OGISO B, SUZUKI N, OTSUKA K, ITO K., 2006. Effect of mineral trioxide aggregate on proliferation of cultured human dental pulp cells. *International endodontic journal*, 39(5):415-22.
- THEODOROU, G., GOUDOURI, M., KONTONASAKI, E., CHATZISTAVROU, X., PAPADOPOULOU, L., KANTIRANIS, N. and PARASKEVOPOULOS, K., 2011. Comparative Bioactivity Study of 45S5 and 58S Bioglasses in Organic and Inorganic Environment. *Bioceramics development and applications*, 1, pp. 1-4.
- THOMAS, H.F. and CARELLA, P., 1984. Correlation of scanning and transmission electron microscopy of human dentinal tubules. *Archives of oral biology*, 29(8), pp. 641-646.
- TILOCCA, A. and CORMACK, A.N., 2011. The initial stages of bioglass dissolution: a Car-Parrinello molecular-dynamics study of the glass-water interface. *Proceedings of the royal society a: mathematical, physical and engineering science*, 467(2131) pp. 2102-2111.
- TJÄDERHANE, L., CARRILHO, M.R., BRESCHI, L., TAY, F.R. and PASHLEY, D.H., 2009. Dentin basic structure and composition, an overview. *Endodontic topics*, 20(1), pp. 3-29.
- TOKIWA, O., PARK, B.K., TAKEZAWA, Y., TAKAHASHI, Y., SASAGURI, K. and SATO, S., 2008. Relationship of tooth grinding pattern during sleep bruxism and dental status. *Cranio: the journal of craniomandibular practice*, 26(4), pp. 287-293.
- TOMSON, P.L., 2013. Dentine Extracellular Matrix Components Liberated By Calcium Silicate Cements and Their Effects on Dental Pulp Cells. PhD thesis submitted to the University of Birmingham.
- TOMSON, P.L., GROVER, L.M., LUMLEY, P.J., SLOAN, A.J., SMITH, A.J. and COOPER, P.R., 2007. Dissolution of bio-active dentine matrix components by mineral trioxide aggregate. *Journal of dentistry*, 35(8), pp. 636-642.
- TOYOSAWA, S., OKABAYASHI, K., KOMORI, T. and IJUHIN, N., 2004. mRNA expression and protein localization of dentin matrix protein 1 during dental root formation. *Bone*, 34(1), pp. 124-133.

- TZIAFAS, D., ALVANOU, A., PANAGIOTAKOPOULOS, N., SMITH, A.J., LESOT, H., KOMNENOU, A. and RUCH, J.V., 1995. Induction of odontoblast-like cell differentiation in dog dental pulps after in vivo implantation of dentine matrix components. *Archives of oral biology*, 40(10), pp. 883-893.
- TZIAFAS, D., ALVANOU, A., PAPADIMITRIOU, S., GASIC, J. and KOMNENOU, A., 1998. Effects of recombinant basic fibroblast growth factor, insulin-like growth factor-II and transforming growth factor-beta 1 on dog dental pulp cells in vivo. *Archives of oral biology*, 43(6), pp. 431-444.
- TZIAFAS, D., AMAR, S., STAUBLI, A., MEYER, J.M. and RUCH, J.V., 1988. Effects of glycosaminoglycans on in vitro mouse dental cells. *Archives of oral biology*, 33(10), pp. 735-740.
- TZIAFAS, D. and KOLOKURIS, I., 1990. Inductive influences of demineralized dentin and bone matrix on pulp cells: an approach of secondary dentinogenesis. *Journal of dental research*, 69(1), pp. 75-81.
- TZIAFAS, D., SMITH, A.J. and LESOT, H., 2000. Designing new treatment strategies in vital pulp therapy. *Journal of dentistry*, 28(2), pp. 77-92.
- VALERIO, P., PEREIRA, M.M., GOES, A.M. and LEITE, M.F., 2009. Effects of extracellular calcium concentration on the glutamate release by bioactive glass (BG60S) preincubated osteoblasts. *Biomedical materials*, 4(4), pp. 5011-6041.
- VALERIO, P., PEREIRA, M.M., GOES, A.M. and LEITE, M.F., 2007. BG60S dissolution interferes with osteoblast calcium signals. *Journal of materials science. Materials in medicine*, 18(2), pp. 265-271.
- VANHAECKE, F., DAMS, R. and VANDECASTEELE, C., 1993. 'Zone model' as an explanation for signal behaviour and non-spectral interferences in inductively coupled plasma mass spectrometry. *Journal of analytical atomic spectrometry*, 8(3), pp. 433-438.
- WAKEFIELD, P.E., JAMES, W.D., SAMLASKA, C.P. and MELTZER, M.S., 1990. Colony-stimulating factors. *Journal of the american academy of dermatology*, 23(5, Part 1), pp. 903-912.
- WALTIMO, T., BRUNNER, T.J., VOLLENWEIDER, M., STARK, W.J. and ZEHNDER, M., 2007. Antimicrobial effect of nanometric bioactive glass 45S5. *Journal of dental research*, 86(8), pp. 754-757.
- WANG, J. and HUME, W.R., 1988. Diffusion of hydrogen ion and hydroxyl ion from various sources through dentine. *International endodontic journal*, 21(1), pp. 17-26.
- WANG, P., CLEMENTS, L.R., THISSEN, H., TSAI, W. and VOELCKER, N.H., 2013. High-throughput characterisation of osteogenic differentiation of human mesenchymal stem cells using pore size gradients on porous alumina. *Biomaterials science*, 1(9), pp. 924-932.
- WATT, F.M., 1988. Effect of seeding density on stability of the differentiated phenotype of pig articular chondrocytes in culture. *Journal of cell science*, 89(3), pp. 373-378.
- WEBER, G.H., O'BRIEN, J.K. and BENDER, F.G., 2004. Control of Escherichia coli O157:H7 with sodium metasilicate. *Journal of food protection*, 67(7), pp. 1501-1506.
- WEINER, S., VEIS, A., BENIASH, E., ARAD, T., DILLON, J.W., SABSAY, B. and SIDDIQUI, F., 1999. Peritubular Dentine Formation: Crystal Organization and the Macromolecular Constituents in Human Teeth. *Journal of structural biology*, 126(1), pp. 27-41.



- WEINSTOCK, M. and LEBLOND, C.P., 1973. Radioautographic visualization of the deposition of a phosphoprotein at the mineralization front in the dentin of the rat incisor. *The Journal of cell biology*, 56(3), pp. 838-845.
- WEST, N.X., ADDY, M., JACKSON, R.J. and RIDGE, D.B., 1997. Dentine hypersensitivity and the placebo response. *Journal of clinical periodontology*, 24(4), pp. 209-215.
- WEST, N.X., MACDONALD, E.L., JONES, S.B., CLAYDON, N.C., HUGHES, N. and JEFFERY, P., 2011. Randomized in situ clinical study comparing the ability of two new desensitizing toothpaste technologies to occlude patent dentin tubules. *The Journal of clinical dentistry*, 22(3), pp. 82-89.
- WISITHPHROM, K., MURRAY, P.E. and WINDSOR, L.J., 2006. Interleukin-1 alpha alters the expression of matrix metalloproteinases and collagen degradation by pulp fibroblasts. *Journal of endodontics*, 32(3), pp. 186-192.
- WISSOZKY, N., 1877. Ueber das Eosin als Reagens auf Hämoglobin und die Bildung von Blutgefäßen und Blutkörperchen bei Säugethier- und Hühnerembryonen. *Archiv für mikroskopische anatomie*, 13(1), pp. 479-496.
- XIAO, S., YU, C., CHOU, X., YUAN, W., WANG, Y., BU, L., FU, G., QIAN, M., YANG, J., SHI, Y., HU, L., HAN, B., WANG, Z., HUANG, W., LIU, J., CHEN, Z., ZHAO, G. and KONG, X., 2001. Dentinogenesis imperfecta 1 with or without progressive hearing loss is associated with distinct mutations in DSPP. *Nature genetics*, 27(2), pp. 201-204.
- XU, T., BIANCO, P., FISHER, L.W., LONGENECKER, G., SMITH, E., GOLDSTEIN, S., BONADIO, J., BOSKEY, A., HEEGAARD, A.M., SOMMER, B., SATOMURA, K., DOMINGUEZ, P., ZHAO, C., KULKARNI, A.B., ROBEY, P.G. and YOUNG, M.F., 1998. Targeted disruption of the biglycan gene leads to an osteoporosis-like phenotype in mice. *Nature genetics*, 20(1), pp. 78-82.
- XYNOS, I.D., EDGAR, A.J., BUTTERY, L.D., HENCH, L.L. and POLAK, J.M., 2001. Gene-expression profiling of human osteoblasts following treatment with the ionic products of Bioglass 45S5 dissolution. *Journal of Biomedical Materials Research*, 55(2), pp. 151-157.
- XYNOS, I.D., HUKKANEN, M.V., BATTEN, J.J., BUTTERY, L.D., HENCH, L.L. and POLAK, J.M., 2000a. Bioglass 45S5 stimulates osteoblast turnover and enhances bone formation In vitro: implications and applications for bone tissue engineering. *Calcified tissue international*, 67(4), pp. 321-329.
- XYNOS, I.D., EDGAR, A.J., BUTTERY, L.D., HENCH, L.L. and POLAK, J.M., 2000b. Ionic products of bioactive glass dissolution increase proliferation of human osteoblasts and induce insulin-like growth factor II mRNA expression and protein synthesis. *Biochemical and biophysical research communications*, 276(2), pp. 461-465.
- YAMAKOSHI, Y., HU, J.C., IWATA, T., KOBAYASHI, K., FUKAE, M. and SIMMER, J.P., 2006. Dentin sialophosphoprotein is processed by MMP-2 and MMP-20 in vitro and in vivo. *The Journal of biological chemistry*, 281(50), pp. 38235-38243.
- YE, L., MACDOUGALL, M., ZHANG, S., XIE, Y., ZHANG, J., LI, Z., LU, Y., MISHINA, Y. and FENG, J.Q., 2004. Deletion of dentin matrix protein-1 leads to a partial failure of maturation of predentin into dentin, hypomineralization, and expanded cavities of pulp and root canal during postnatal tooth development. *The Journal of biological chemistry*, 279(18), pp. 19141-19148.
- YOSHIDA, S., OSHIMA, K. and TANNE, K., 1996. Biologic responses of the pulp to single-tooth dento-osseous osteotomy. *Oral surgery, oral medicine, oral pathology, oral radiology, and endodontics*, 82(2), pp. 152-160.

- ZASLANSKY, P., FRIESEM, A.A. and WEINER, S., 2006. Structure and mechanical properties of the soft zone separating bulk dentin and enamel in crowns of human teeth: insight into tooth function. *Journal of structural biology*, 153(2), pp. 188-199.
- ZEHNDER, M., LUDER, H.U., SCHATZLE, M., KEROSUO, E. and WALTIMO, T., 2006. A comparative study on the disinfection potentials of bioactive glass S53P4 and calcium hydroxide in contra-lateral human premolars ex vivo. *International endodontic journal*, 39(12), pp. 952-958.
- ZHANG, R., COOPER, P.R., SMITH, G., NORS, J.E. and SMITH, A.J., 2011. *Angiogenic activity of dentin matrix components*. *Journal of endodontics*, 37, pp. 26-30.
- ZHAO, S., SLOAN, A.J., MURRAY, P.E., LUMLEY, P.J. and SMITH, A.J., 2000. Ultrastructural localisation of TGF-beta exposure in dentine by chemical treatment. *The Histochemical journal*, 32(8), pp. 489-494.
- ZHONG J.P., LATORRE G.P., and HENCH L.L., The kinetics of bioactive ceramics Part VII: Binding of collagen to hydroxyapatite and bioactive glass. *Proceedings of the 7th international symposium on ceramics in medicine, Turku, Finland.*, 1994.
- ZOU, S., IRELAND, D., BROOKS, R.A., RUSHTON, N. and BEST, S., 2009. The effects of silicate ions on human osteoblast adhesion, proliferation, and differentiation. *Journal of biomedical materials research. Part B, Applied biomaterials*, 90(1), pp. 123-130.